Fonctionnement biogéochimique d'un barrage tropical : application au système turbide de Cointzio (Mexique)

Thuy Kim Phuong Doan

UNIVERSITÉ DE GRENOBLE

THÈSE

Pour obtenir le grade de

DOCTEUR DE L'UNIVERSITÉ DE GRENOBLE

Spécialité : **Sciences de la Terre, de l'Univers et de l'Environnement**

Arrêté ministériel : 7 août 2006

Présentée par

Thuy Kim Phuong DOAN

Thèse dirigée par **Nicolas Gratiot** et **Julien Némery**

préparée au sein du **Laboratoire d'Etude des Transferts en Hydrologie et Environnement (LTHE)**
dans **l'École Doctorale TERRE ET UNIVERS, ENVIRONNEMENT**

BIOGEOCHEMICAL FUNCTIONING OF TURBID TROPICAL RESERVOIRS: THE CASE STUDY OF COINTZIO, MEXICO

Thèse soutenue publiquement l**e 7Juillet 2014**
devant le jury composé de :

Bruno Tassin
DR, Ecole des Ponts Paris-Tech (Rapporteur)
Florentina Moatar
Professeur, Université de Tours (Rapporteur)
Martin Schmid
Chercheur senior, EAWAG (Examinateur)
Phuoc Dan Nguyen
Professeur, Ho Chi Minh University of Technology (Examinateur)
Eric Barthélemy
Professeur, G-INP/ENSE3 (Président du jury)
Nicolas Gratiot
CR1, HDR, IRD (Directeur de thèse)
Julien Némery
Maître de conférences, G-INP/ENSE3 (Co-directeur de thèse)

TABLE OF CONTENTS

INTRODUCTION....1
1. Background....1
2. Objectives of this study....3
3. Approach and outline....4
Chapter 1. LITERATURE REVIEW....6
A) Eutrophication of reservoirs in tropical areas....6
1. Water problems in tropical countries....6
2. Why do we need to study reservoirs in tropical areas?....8
3. General sources of pollution....10
4. Main concerns of reservoirs in tropical areas....10
4.1 Gas emissions in tropical reservoirs....10
4.2 Climate effects on behaviour of tropical reservoirs....11
4.3 Siltation, erosion of tropical reservoirs and their consequences on turbidity....11
4.4 Eutrophication caused by excess of nutrients....13
4.5 Downstream deficit of sediments and nutrients....14
B) Problematics in Mexico....14
1. Limnology in Mexico....14
2. Global situation in Trans-Mexican Volcanic Belt, central Mexico....17
3. Erosion within the watershed....19
4. Water scarcity and water pollution....20
5. The case of the Cointzio reservoir....22
Conclusions of chapter 1....22
Chapter 2. STUDY AREA AND FIELD DATA ANALYSIS....24
1. Study area....24
2. Field monitoring strategy....31
2.1 Survey in the watershed....31
2.2 Sampling within the Cointzio reservoir....32
2.3 Samples of sediments....35
2.4 Analytical methods of waters and sediments....35
3. Hydrodynamic and Biogeochemical functioning from field data....36
3.1 Hydrodynamic functioning....36
3.1.1 Inlet and outlet of the reservoir....36
3.2 Biogeochemical functioning....43
3.2.1 Input and output of the reservoir....43
3.2.2 Reservoir internal functioning....46
Conclusions of chapter 2....49
Chapter 3. NUMERICAL MODELLING OF THE COINTZIO RESERVOIR....51
1. Introduction....51
2. The physical models applied....52
2.1 Aquasim model....52
2.2 k- ε model....63
3. Biogeochemical model (Aquasim)....68
3.1 Overview....68
3.2 State variables....69
3.3 Mass balance equations....70
3.4 Model processes....71
3.5 Modelling approach....72
3.6 Model calibration....92

Conclusions of chapter 3 93
CHAPTER 4. CARBON, PHOSPHORUS, NITROGEN AND SEDIMENT RETENTION IN A SMALL TROPICAL RESERVOIR 94
Abstract: 95
Introduction 96
Material and methods 97
Study area 97
Survey in the watershed 98
Reservoir inflow and outflow 99
Sampling within the reservoir 99
Analysis of water and sediment 100
Accumulation rates in reservoir 101
Load calculations and uncertainties 102
Results 103
Hydrology 103
Pollution levels within the watershed 104
River input and reservoir output 104
Internal reservoir behavior 106
C, N and P content in sediment 108
Discussion 109
Nutrient sources within the watershed and reservoir trophic state 109
Effect of floods on the reservoir functioning 111
Sediment trapping efficiency 113
Organic carbon origin and C, N, P trapping efficiency 115
Conclusions 118
Acknowledgments 119
Conclusions of chapter 4 147
CHAPTER 5. EUTROPHICATION OF THE TURBID TROPICAL COINTZIO RESERVOIR: TRENDS AND PROJECTIONS BY THE END OF THE CENTURY 148
A) Scenarios and projections 148
1. Effect of water level regulation 148
2. Effect of air temperature increase 148
3. Effect of nutrients reduction 149
4. Description of modelling scenarios 149
B) Eutrophication of turbid tropical reservoirs: Modelling for the case of Cointzio, Mexico 150
Abstract 152
1. Introduction 153
2. Study site 154
3. Data and modelling approach 155
    3.1 Model input data 156
    3.2 Model output 156
    3.3 Modelling approach 157
    3.4 Modelling scenarios 158
4. Results 159
    4.1 Physical k-ε model 159
    4.2 Biogeochemical model 160
5. Discussion 163
    5.2 Effect of hydrology and global warming on trophic status 164
    5.3 Evaluation of the restoration process of the water quality in the reservoir 165
6. Conclusions 166

Acknowledgements 167
References 168
C) Biogeochemical mass balance in the turbid tropical reservoir of Cointzio, Mexico: Field data and modelling approach 183
1. Introduction 183
2. Results 183
2.1 Mineralization rates in the Cointzio reservoir 183
2.2 Temporal variability of benthic mineralization processes 184
2.3 Nutrients releases and N_2 removal 184
2.4 The mass balance of C, N, P in the Cointzio reservoir 186
3. Conclusions 188
Conclusions of chapter 5 189
CONCLUSIONS & PERSPECTIVES 190
REFERENCES 196
APPENDIX 216
ABSTRACT 223

LIST OF FIGURES

Figure 1.1 Tropical zone map....7
Figure 1.2 Geography of Mexico with main mountainous features. Adapted from SRH, 1976.16
Figure 1.3 Map of Trans-Mexican Volcanic Belt (Ferrari et al., 2012)....17
Figure 1.4 a) Desertification in Mexico and b) Landscape of degraded soils in Mexico....19
Figure 1.5 The Cointzio and Cuitzeo watersheds in Michoácan....20
Figure 1.6 Cointzio dam with the reservoir in dry season....22
Figure 2.1 Map of the Cointzio watershed, within the state of Michoácan, and location of sampling sites in the watershed, geographical position in UTM....25
Figure 2.2 Seasonal variation in regional precipitation and water temperature patterns (from http://es.climate-data.org/location/3382/)....25
Figure 2.3 Time series of (a) precipitation at Undameo & in the Cointzio reservoir and b) the water inflow at Undameo from the year 1955 to 2005....26
Figure 2.4 Aerial photograph of the Cointzio reservoir which supplies water to Morelia city (Adapted from http://paralelo19n.blogspot.fr/2011/03/toluca-guadalajara.html)....27
Figure 2.5 Rating curves between the volume and the depth in the Cointzio reservoir (years 1940, 1985, 2005)....27
Figure 2.6 Time series of the water depths in the Cointzio reservoir (from 1990 to 2009)....28
Figure 2.7 Cointzio sub watershed and its hydrological network (STREAMS 2008, P. Bonté) .28
Figure 2.8 Maps of land cover and land use change processes by period in the Cointzio watershed (Mendoza et al, 2013)....30
Figure 2.9 Cointzio reservoir catchment topography. The black line represents the Rio Grande de Morelia River (Susperregui, 2008)....31
Figure 2.10 Map of the Cointzio reservoir, and localization of measurement points in the reservoir. 16 vertical profiles were realized along the longitudinal axis (dashed line)....33
Figure 2.11 Seasonal time-series of inflow & outflow....36
Figure 2.12 Measured river water temperature....37
Figure 2.13 Measured and interpolated river water temperature....37
Figure 2.14 Vertical profiles of temperature at P27 in 2009....38
Figure 2.15 Hydro-meteorological response of the Cointzio reservoir....39
(September 2007 to January 2010)....39
Figure 2.16 Longitudinal evolution of TSS (a), DO (b) and temperature (c) from the Rio Grande mouth (left side) to the dam (right side) on September, 13th 2007.Vertical dotted lines represent the location of individual hydrolab measurements....42
Figure 2.17 Seasonal variations in TSS (a, b), TP, PO_4^{3-} (c, d), TN, NO_3^- (e, f), NH_4^+ (g, h), POC (i, j), DOC (k, l) and chlorophyll a (m, n) at the inlet and outlet of the Cointzio reservoir....45
Figure 2.18 Seasonal variations in TSS....46
Figure 2.19 Seasonal variations in DO....46
Figure 2.20 Seasonal variations in pH....46
Figure 2.21 Vertical profile of PO_4^{3-}....47
Figure 2.22 Vertical profile of NH_4^+....47
Figure 2.23 Seasonal variations in Secchi depth....48
Figure 2.24 Seasonal variations in chlorophyll a....48
Figure 2.25 Seasonal variations in zooplankton....48
Figure 3.1 Schematic overview of the Cointzio reservoir simulation model....54
Figure 3.2 Heat flux terms of the reservoir in 2009, calculated according to eqn. (3.1)....58
Figure 3.3 Sensivity function of some parameters in Aquasim model....59
Figure 3.4 Measured and simulated temperature profile during the year 2009....61
Figure 3.5 Simulated temperature profile after changing the input conditions....61
Figure 3.6 Turbulent diffusivity at some different depths during the year 2009....62

Figure 3.7 Relationship between the main state variables in Aquasim, shown in boxes, and the biogeochemical processes represented in the model. Note that physical processes of inflow, outflow and settling are not included (adapted from Hamilton & Schladow, 1997) 71

List of Figures in the paper Aquatic Sciences (chapter 4)

Figure 1: Map of the Cointzio watershed and reservoir: location of sampling sites (geographical position in UTM).....132
Figure 2: Seasonal time-series of a) water discharge (m^3 s^{-1}) and TSS inflow (mg L^{-1}), b) water discharge and TSS outflow (mg L^{-1}), and c) the volume of the Cointzio reservoir for 2007, 2008 and 2009 133
Figure 3: Seasonal variation of TSS, P-tot (including P-PO_4^{3-}), N-tot (including N-NO_3^-, N-NH_4^+), POC and DOC inputs to the reservoir of Cointzio (t day^{-1}) 134
Figure 4: Horizontal transects of temperature, DO and TSS at four dates covering the entire 2009 year. Dotted lines indicate date of vertical profiles.....135
Figure 5: Seasonal variation of a) temperature b) TSS c) DO and d) Chlorophyll a at the deepest point P27 in 2009 136
Figure 6: Comparison of the seasonal variations in a) Secchi depth, b) chlorophyll a (surface and bottom), and c) POC in suspended sediment (surface and bottom) in the water column at the two sampling points P6 and P27 137
Figure 7: Comparison of the seasonal variations in a) P-PO_4^{3-}, b) N-NO_3^-, and c) N-NH_4^+ in the water column at the two sampling points P6 and P27 (surface and bottom) in the Cointzio reservoir.....138
Figure 8: TSS, C, N, P inputs, outputs and accumulation in the Cointzio reservoir (loads are given in t y^{-1} with uncertainties).....139

List of Figures in the paper Ecological Modelling (section B/chapter 5)

Figure 1: Map of the Cointzio reservoir, and localization of sampling sites. 16 vertical profiles were realized along the longitudinal axis (dashed line) 173
Figure 2: Time series of the water depths in the Cointzio reservoir 173
Figure 3: Time evolution of the temperature in 2009 (left panels) and 2008 (right panels). The top map is obtained with the measured temperature, the middle one with the simulated one. The bottom one depicts the residues Tmea-Tsim.....174
Figure 4: Vertical profiles of measured (left panels) and simulated (right panels) DO, chlorophyll a, PO_4^{3-}, NH_4^+ at P27 of the Cointzio reservoir in 2009 175
Figure 5: The residues between measurement and simulation of DO and chlorophyll a in 2009 176
Figure 6: Simulation of DO and chlorophyll a under the dry year conditions (P1 scenario).....177
Figure 7: Simulation of DO and chlorophyll a under the wet year conditions (P2 scenario) 178
Figure 8: DO and chlorophyll a in increasing air temperature of 2.5°C and 4.4°C (P3 and P4 scenarios).....179
Figure 9: The results of DO and chlorophyll a for the case P1 180
Figure 5.1 Temporal variability of a) benthic aerobic mineralization b) benthic anaerobic mineralization and c) benthic anoxic mineralization rates at the deepest point of the Cointzio reservoir in 2009.....184
Figure 5.2 C, N, P mass balance in the Cointzio reservoir (fluxes are in t y^{-1}).....186

LIST OF TABLES

Table 3.1 Notations and units for meteorological data 55
Table 3.2 List of constant values used in the k-ε Lake model 66
Table 3.3 State variables in the Cointzio reservoir adopted from Omlin et al, (2001a).....69
Table 3.4 Process rates (in order of appearance).....72
Table 3.5 Biogeochemical processes.....74
List of Tables in the paper Aquatic Sciences (chapter 4)
Table 1: Water and TSS input and output for 2007, 2008 and 2009.....140
Table 2: Mean annual discharge (Q), DO and nutrient concentrations in the Cointzio watershed in 2009 (in bold min DO and maximum discharge and nutrient concentrations, in parenthesis standard deviation) 141
Table 3: Seasonal variations and annual mean of discharge (Q), TSS and water quality parameters at Undameo sampling site 8 (in bold maximum values) 142
Table 4: Seasonal variations and annual mean of discharge (Q), TSS and water quality parameters at the outlet of Cointzio reservoir (in bold maximum values).....143
Table 5: Input and output C, N, P loads in the Cointzio reservoir for 2009 (loads are given in $t\ y^{-1}$ with 95% confidence intervals).....144
Table 6: C, N, P content in deposited sediments.....145
Table 7: Accumulation rate of C, N, P in the Cointzio reservoir compared with other tropical reservoirs 146
Table 5.1 Summary of scenarios for water quality assessment of the Cointzio reservoir.....149
List of Tables in the paper Ecological Modelling (section B/chapter 5)
Table 1: Literature values and main parameters of the biogeochemical model compared to other published applications of the same model. See supplementary data for definitions of parameters. 180
Table 2: Summary of scenarios for water and ecological quality assessment of the Cointzio reservoir.....181
Table 3: P release in the global warming scenario for the last year of the simulation with the nutrient-reduction scenarios P8 and P9. 182
Table 5.2 Mineralization rates in the water column and in the sediments for the target year 2009 183
Table 5.3 The model estimations of nutrient releases and N2 and carbon removal in the Cointzio reservoir for the target year 2009 185

LIST OF APPENDIX

Appendix 1. Investigation results of priorities of municipalities in Michoacán, Mexico 216
Appendix 2. Instrumentations and strategy of monitoring data in the Cointzio reservoir 217
Appendix 3. Interpolated (pink colour) and measured (blue colour) surface temperature in 2009 218
Appendix 4. Linear regression between MES (mg L^{-1}) and Turbidity (NTU) from measurements data in the Cointzio reservoir 219
Appendix 5. Regression equations between chlorophyll a (μg L^{-1}) and chlorophyll a (volts) ..220
Appendix 6. The ratio between C and chlorophyll a in the Cointzio reservoir.....221
Appendix 7. The resulting time series of vertical turbulent diffusivity obtained from the physical k-epsilon model 222

INTRODUCTION

1. Background

With the onset of the XXIst century, the quantity and quality of water resources is declining significantly, especially in the "tropical world" (Tundisi, 2003). The biogeochemical functioning of reservoirs is strongly influenced by anthropological activities such as urban development, agricultural activity and waste water inputs (Kennedy et al, 2003). The sediments, organic matters and nutrients coming from watersheds are efficiently trapped in reservoirs, which can lead to eutrophication (Donohue & Molinos 2009), a loss of storage capacity (Vörösmarty et al, 2003; Syvitski et al, 2005; Dang et al, 2010), and have important consequences for water treatment and downstream ecosystems. The eutrophication has been a main issue in epicontinental waters, progressively extending to tropical water bodies (Alcocer & Bernal-Brooks, 2010). The eutrophication in tropical systems is reflected by algal growth, turbidity of water and oxygen depletion in the hypolimnion (Thomaz & Bini, 2003). The process of eutrophication in the tropics has many specific characteristics that have led to some key questions that are still unanswered: (1) *Is the control of eutrophication more difficult in tropical areas?* (Tundisi 2003) *(2) How much do we need to reduce nutrient inputs to mitigate eutrophication?*

Our understanding about how subtropical and tropical systems will process high nutrient loads and high turbidity is restricted due to the lack of publications and the limitation of biogeochemical studies on these systems (Seitzinger et al, 2010). Besides that, the main issues of water pollution, siltation of river and reservoir systems, and lack of management of rivers and reservoirs in tropical zones are more severe and widespread in developing countries than in developed ones. This is due to poverty, rapid population growth, ineffective institutions and policies for water resources management, and lack of funds in developing nations. The need for water quality modelling has arisen essentially because of increased eutrophication of reservoirs throughout the world (Canfield & Hoyer, 1988). Many sources of limnological knowledge on temperate systems and biogeochemical models are better constrained, and have greater predictive ability in developed countries (Seitzinger et al, 2010). As a result, the study of tropical reservoirs is a great interest for scientists today in order to improve the understanding of biogeochemical processes and enhance the water quality management in these systems (Dumont et al, 2005).

It should be noted that the water quality management needs to expand in line with the economic development; otherwise the environmental issues may limit the economic growth. A specific example would be the building of a reservoir for drinking water supply and

irrigation. If this reservoir is not well protected from pollutions such as agricultural runoff or domestic wastewater, its water quality will deteriorate with time. Such water quality deterioration will in turn affect the economic activities such as irrigation and drinking water supply.

In recent years, several studies have been carried out to tackle the problems of water quality deterioration in tropical reservoirs (e.g. Araujo et al, 2008; Kunz et al, 2011). Numerical modelling is a relevant tool to assess responses of complex systems, for its ability to integrate different factors and to best describe the complex relationships between waste load inputs, and resulting water quality in water columns. For this reason, many lake models have been developed during the past thirty years to evaluate the lake management strategies, improve the understanding of lake ecosystems, synthesize and communicate quantitative knowledge about important processes in reservoirs (Mieleitner & Reichert, 2006). The challenges of using mathematical models in developing countries are requirements for considerable investments in collecting reliable data, weakness of scientific capacity development and water quality management policies and strategies (Deksissa et al, 2004).

Water quality management has become an increasingly important issue in developing countries and newly industrialized countries, including Mexico. According to various studies, the overall water quality of lakes and reservoirs in many regions of Mexico is degrading (Olvera -Viascán et al, 1998; Lind et al, 1992; Bravo - Inclan et al, 2008). Approximately 593 wastewater treatment plants operate in Mexico, treating only 26% of the total wastewater flow produced nationwide (Conagua, 2007). The remaining 74% usually end up in aquatic ecosystems, causing eutrophication. Consequently, most of the Mexican reservoirs located within or close to urban areas are heavily polluted, with direct consequences for the aquatic ecosystems as well as potential risks to human health (Welch & Jacoby, 2004). This is generating great concern as the volume of wastewater produced is increasing because of further urbanization and economic growth. It is admitted by Mexican stakeholders that water pollution is one of the most serious challenges for sustainable water resource management, and it also represents one of the most important concerns for local populations (Berrera Camacho & Bravo Espinosa, 2009).

In Mexico, few ecological and biological studies of inland waters have been published in the past. Alcocer & Bernal-Brooks (2010) recently provided an overview of the state of lakes and reservoirs in Mexico, particularly within the Trans –Mexican Volcanic Belt (TMVB), where our study site is located. The authors highlighted the lack of data on Mexican rivers and streams, indicating that few integrated studies focus on the linkages between sediments

and nutrient sources within upstream watersheds and the biogeochemical functioning of downstream reservoirs.

The present study focuses on the Cointzio reservoir (state of Michoacán), which is used for drinking water supply to the city of Morelia, capital of the state, and for irrigation purposes. The Cointzio reservoir is a perfect example of a human-impacted system since its watershed is mainly composed of volcanic degraded soils and is subjected to high erosion processes and agricultural land loss (Duvert et al, 2010). Moreover, the reservoir receives high domestic loads since wastewaters are not treated in the municipalities located upstream. In order to protect the ecosystem and wildlife in the watershed of Cointzio, it would be important to rapidly adopt some mitigation strategies to treat wastewaters and reduce nutrients input to the waterbodies. This study focuses on the examination of the impact of fine sediment, nutrient and organic matter loads on the annual functioning of the very turbid tropical Cointzio reservoir.

2. Objectives of this study

The first objective of this study is to give an overview of the functioning of the turbid tropical Cointzio reservoir. Based on a one year-long intensive field survey, the main objectives are: (i) to identify and quantify the nitrogen (N) and phosphorus (P) inputs from the watershed to the reservoir, and (ii) to characterize the internal biogeochemical functioning of the reservoir (nutrient cycling, sediment, and chlorophyll *a* dynamics) in relation with the climatic conditions, hydrology, nutrients, sediment and organic loads from the watershed and the general functioning of the reservoir for water uses. This analyze will lead to the evaluation of the total suspended sediments (TSS), C, N and P accumulation rate in the reservoir.

The secondary objective is to reproduce the main biogeochemical cycles in the reservoir and assess the trophic state of the reservoir by application of numerical models. The physical models were used to calibrate temperature profiles for the year 2009 and they were validated for the year 2008. The biogeochemical model was calibrated to reproduce the main patterns of DO, nutrients and chlorophyll *a* concentrations within the Cointzio reservoir for the target year 2009.

The third objective is to examine the ability of the models to assess scenarios of nutrients and eutrophication reduction in the coming decades and complete the entire mass balance of nutrients and carbon in the reservoir. Various simulations were conducted (i) to define which factors controlled the water quality in the Cointzio reservoir and (ii) to assess the long term evolution of the water quality in the reservoir under the influence of water level regulation

and air temperature increase (iii) to establish a management strategy to mitigate the negative effects of air temperature increase and (iv) to calculate the main processes involved in nutrients release and carbon removal. Some solutions of rehabilitation are proposed to restore the quality of the water. This study points out the advantages and limitations of the models and will help stakeholders to adopt appropriate strategies for the management of very turbid tropical reservoirs. It does end with some perspectives that could be applied to other similar reservoirs of the region or in different tropical countries.

3. Approach and outline

This study was undertaken in the framework of the European Research project DESIRE (2007-2011) and the French ANR Research project STREAMS (2008-2010).

Our approach included a critical analysis of data acquired during two and a half years (mid 2007-2009) for physical data and one year (2009) for biogeochemical data to provide a database for further water quality modelling. The contents of the thesis are divided into five chapters. Chapters 4 and 5 include individual manuscripts that have been targeted for publications in Aquatic sciences (submitted) and Ecological modelling (under review).

Chapter 1: Literature review

The first chapter presents the global overview of water problems in tropical countries and the specific problematics in Mexico with a focus on the Trans - Mexican Volcanic Belt.

Chapter 2: Study area and field data analysis

This chapter presents the study area, the field monitoring strategy and the laboratory analysis that have been gathered into the hydrological and biogeochemical database used for the present work. The analysis of two and a half years of hydrodynamic data and one year of biogeochemical measurements data is also presented.

Chapter 3: Numerical modelling of the Cointzio reservoir

This chapter describes the models used to simulate the hydrodynamics and the biogeochemistry of the Cointzio reservoir. It presents the advantages and limitations of each model considered, and try to evaluate the appropriate balance between model complexity and data availability. These models were then used to perform comparison of simulations with historical data series.

Chapter 4: Carbon, phosphorus, nitrogen and sediment retention in a small tropical reservoir

The main objectives of this chapter are i) to identify and quantify the N and P inputs from the watershed to the reservoir, ii) to characterize the internal biogeochemical processes of the reservoir and relate them with the seasonality of the inputs, and iii) to evaluate the TSS, C, N and P annual accumulation rate in the reservoir and assess its trapping efficiency.

Chapter 5: Eutrophication of the turbid tropical Cointzio reservoir: Trends and projections by the end of the century

The models presented in chapter 3 were used to calibrate and validate the hydrodynamics and the water quality in the reservoir of Cointzio for the years 2008 and 2009. The completed entire mass balance of nutrients and carbon in the reservoir was calculated by estimating the main processes involved in nutrients release and carbon removal from the model. The models allowed for investigating the long term evolution of the water quality in the reservoir under the influence of water level regulation and air temperature increase and assessing scenarios of nutrients (P and N) and eutrophication reduction in the coming decades. This exercise was conducted with targeted years in 2060 and 2090.

Conclusions and perspectives: This section summarizes the main results obtained in this study and discusses some perspectives of research that could be addressed in the future for a better understanding of turbid tropical reservoirs.

Chapter 1. LITERATURE REVIEW

This chapter presents the global overview of water problems in tropical countries and the main concerns of reservoirs in tropical areas. It highlights on the specific problematics in Mexico with a focus on the Trans - Mexican Volcanic Belt.

A) Eutrophication of reservoirs in tropical areas

1. Water problems in tropical countries

Tropical countries are those that lie between the Tropic of Cancer and the Tropic of Capricorn corresponding with the parallels of latitude at 23° 26' 16" North and 23° 26' 16" South (Figure 1.1). There are more than 3.3 billion people living in the tropics, mostly in developing countries, whilst the world's population is about 7.2 billion people (Beattie P., 2010).

In the Western Hemisphere, tropical countries include Mexico, all of Central America, all of the Caribbean islands. Eastward, it includes most of African, India and all countries of Southeast Asia. Most of the other island nations of Oceania in the South Pacific are also part of tropical countries (synthesized from/ source: http://www.wisegeek.com/what-are-tropical-countries.htm). Many countries of tropical belt are experiencing demographic and economic booms that will pursue during the century; they are also directly concerned by climatic changes that may have some higher consequences in tropical areas than elsewhere.

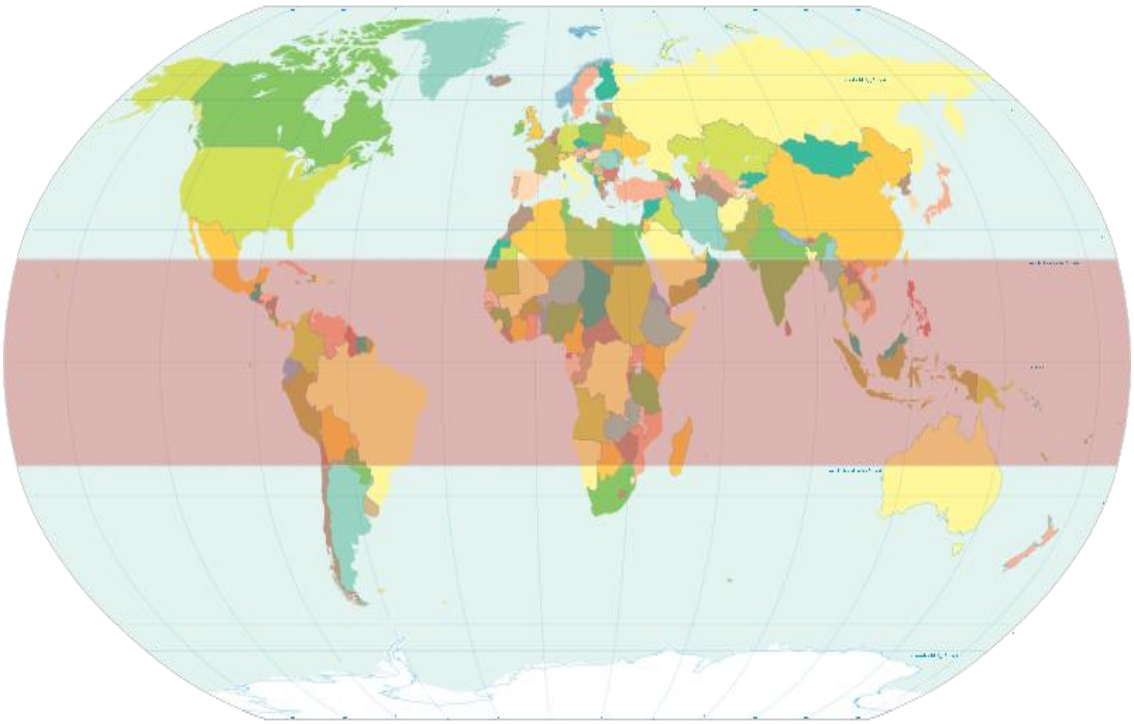

Figure 1.1 Tropical zone map

The issues and problems that experience tropical zones comprise of water pollution, inadequate drinking-water supply and sanitation facilities, floods, siltation of waterbodies, and lack of managements of rivers and reservoirs. These problems are more serious and extensive in developing countries than in developed ones. The difficulties to address these water problems in developing nations include poverty, rapid population growth, ineffective policies for water resources management, and lack of funds. The issues that should be considered when evaluating water resources problems in developing nations are as follows:

i) Water Pollution

Water pollution in developing countries is mainly caused by animal and anthropological sewage, overuse of fertilizers, industrial chemicals, urban runoff, and a lack of water pollution control policies and their implementation. Access to adequate wastewater treatment facilities is generally very limited in these countries.

ii) Inadequate drinking-water supply and sanitation facilities

Nearly one billion of the world's population do not have an "adequate" water supply, and approximately two billion do not have "adequate" sanitation facilities. Most of these people live in developing nations. The lack of adequate water facilities is the cause of much disease and illness in these countries.

iii) Floods

Floods convey some risks but also some benefits to people. Floods are responsible of about 40 percent of all deaths caused by natural disasters, most of them being in developing nations. However, floods also bring environmental and social benefits, for example, floods carry sediments and nutrients downstream. This natural process is important for water ecology and for agricultural production. Therefore, programs for floods management should consider to balance their risky and beneficial aspects.

iv) Siltation of rivers, reservoirs

Soil erosion is a natural process that transports sediments and nutrients to rivers or reservoirs. Deforestation and other human activities (overpopulation, unsuitable land use and inappropriate land management practices, and inadequate environmental regulations) have caused a five-fold increase in the average levels of sediments in the world's rivers. This will undoubtedly have some impacts on natural ecosystems over decades with feedback on human activity itself. As example, an excess of sediments in rivers or reservoirs can damage aquatic ecosystems and fisheries, affecting people who depend on them (synthesized from/ source: http://www.waterencyclopedia.com/Da-En/Developing-Countries-Issues-in.html).

v) Dams (reservoirs)

Thousands of dams have been constructed in developing countries in order to reduce flood damages, to generate hydroelectricity, and to increase and stabilize water supplies. These dams have provided noteworthy benefits to people but have also caused significant dynamic modifications and social changes.

Taking into account these five principal issues and in order to balance these negative and positive aspects on water resources, water planning programs and policies should be better integrated than during the past; for example, water projects must consider ecological and human factors along with hydrologic and engineering principles. This requires appropriate environmental regulations and assessment tools (synthesized from/ source: http://www.waterencyclopedia.com/Da-En/Developing-Countries-Issues-in.html).

2. Why do we need to study reservoirs in tropical areas?

Reservoirs are usually found in areas of water scarcity or water excess, or where there are agricultural, domestic, or industrial needs to regulate water supply. When water is scarce, reservoirs are mainly used to regulate the water supply for irrigation or domestic purposes. In low lying areas suffering heavy precipitation and storms, reservoirs are crucial to regulate floods and prevent downstream areas from being inundated. Besides that, other activities such as power generation, fish-farming, etc., are also responsed by building reservoirs. In the world, between 30 % and 40 % of 268 million ha of irrigation lands are reliant on water

supply of reservoirs. Although the developments of reservoirs are usually economically beneficial to communities, they can have negative impacts, such as encouraging accumulation of pollution, water-borne diseases spread, etc.,. The building of dams on rivers to create water storage reservoirs results in considerable modifications in nutrient dynamics, as well as plant and animal species composition (Bosch & Allan, 2008). This is due to changes in geomorphology, water depth, water residence time and resulting vertical stratification. Besides that, the creation of a reservoir submerges some downstream areas and often requires the resettlement of a large number of people.

For all these reasons, a particular need for managers and policy-makers is to understand the physics, chemistry and biology of reservoirs. The objectives of monitoring and assessment strategies should be governed by specific water quality requirements. For example, the location and depth of water withdrawal within reservoirs may affect significantly the water quality and is thus essential to achieve optimum water quality for intended uses. In addition, it is necessary to determine and understand the relationships between reservoirs and their watersheds. The effects of inflows and outflows, retention time, and morphometry of reservoirs imply to get an integrated understanding of physical and biogeochemical cycles in these terrestrial ecosystems.

Historically and on a worldwide basis, reservoirs of temperate latitudes have been taken as the main source of limnological knowledge. However, in the past 20 years, an increasing number of limnologists have paid attention on tropical reservoirs. Although some literatures on tropical lakes exist, it is diffuse and difficult to use (Lewis, 1987; Torres-Orozco et al, 1996). Some features of tropical reservoirs are similar to those of temperate reservoirs in summer, but contrasts are greater during other periods of the year (Kalff & Watson, 1986; Lewis, 1996). Information on nutrient cycling from temperate reservoirs cannot be extrapolated to tropical reservoirs, due to the basic differences in the physical and biological dynamics of these two types of systems (Gardner et al, 1998). Accordingly, management of reservoirs for the protection of water quality, aquatic life and other uses in the tropics must be approached differently from that of temperate latitudes.

In the world, there are more than half of all tropical lakes and reservoirs built on natural rivers. Therefore, degradation of water quality in rivers will have direct negative effects on the majority of reservoirs in the tropics. Also, regulation of rivers, which is one result of river impoundment, is a potential cause of damage to reservoirs (Lewis, 2000). A particular attention should be paid to tropical reservoirs built in poor developing countries. In these countries, the population can face a decline of the economic activities, a poor political

stability, and a rapid degradation of environment with some critical consequences on water resources quantity and quality (Ujang & Buckley, 2002). Sometimes, water pollution issues are not the main concern in these nations because other issues such as national security, food availability and epidemic control are more urgent.

3. General sources of pollution

The main components of the continental water cycle are rivers and reservoirs, and they need to be protected from all sources of pollution. This is because the survival of human depends on their sustainable usage. However, these rivers and reservoirs are threatening progressively from different pollutants such as high organic and nutritive pollutions and eutrophication (Chuco, 2003). Although the natural phenomena such as climate and geology can affect the water quality of rivers and reservoirs (Boorman, 2003), human activities are the major sources of pollution: urbanization, cattle farming, agriculture, forestry, etc. One can distinguish two main categories of water pollution sources: direct and indirect contaminant sources (point and non-point sources). Point source pollution is water pollution that comes from a single source, typically a pipe whilst non-point (diffuse) sources include polluted runoff from agricultural areas, fertilizer manufacturing process or stormwater runoff from deforestation, etc. Both of these two sources of pollution lead to two important water quality issues, namely eutrophication and high turbidity. While the impacts of point source pollution can be minimized by proper wastewater managements and land use activities, controlling the influences of non-point pollution sources to water quality deterioration is more difficult (Jiashal, 2013) and implies to get a good understanding of the relationship between watershed and its corresponding reservoirs.

4. Main concerns of reservoirs in tropical areas

4.1 Gas emissions in tropical reservoirs

The conversion of terrestrial land to an aquatic area modifies significantly the carbon cycle and is a main issue in the production of greenhouse gas (GHG) (St Louis et al, 2000, Chanudet et al, 2011). Flood events and ensuing degradation of organic carbon initially exist in soils and plants jointly with the flux of carbon from upstream watersheds cause variations in carbon dioxide (CO_2) and methane (CH_4) emissions (Abril et al, 2006; St Louis et al, 2000). GHGs are emitted to the atmosphere either at the surface of reservoirs (diffusion and ebullition), or from the downstream rivers (degasing and diffusion) (Guérin et al, 2006; Kemenes et al, 2007). Emissions were described in both boreal (Demarty et al, 2009; Teodoru et al, 2011) and tropical reservoirs (Guérin et al, 2008; Roland et al, 2010). These studies pointed out that processes leading to GHG productions and emissions in the tropics

are clearly higher than in the boreal regions (Barros et al, 2011). The comparison of emissions between tropical reservoirs and thermal alternatives shows that some reservoirs are expected to emit more GHGs than thermal power plants for similar power production (Dos Santos et al, 2006; Chanudet et al, 2011). The uncertainty and inconsistency in the collected data could be the main reasons on the issue of net GHG emissions by reservoirs. In tropical systems, this phenomenon is very important since the biomass is often abundant (FAO 2006). Additionally, the lack of biogeochemical data in developing regions makes it difficult to evaluate the ecological impacts of existing and planned reservoirs.

4.2 Climate effects on behaviour of tropical reservoirs

In order to assess the trophic state of reservoirs, we should consider the effect of climatic conditions. This is because the ratio of evaporation versus precipitation controls whether a reservoir will become more concentrated with time, and also become more saline and eutrophic. Not all tropical countries have the same climate, but the amplitude of seasonal variations in temperature and solar radiation is smaller in the tropics than in the temperate zones. Their climate is distinguished mainly by wet and dry seasons (source: http://www.wisegeek.com/what-are-tropical-countries.htm). In most of tropical lakes, temporal fluctuations in rainfall, runoff and/or vertical mixing imply some patterns in annual variations which are reflected on richness of phytoplankton (Wetzel, 2001). Moreover, the other processes such as sudden storms and periods of strong wind contribute to the mixing of the upper water layers increasing the phytoplankton diversity. These processes have been interpreted as intermediate perturbations (Padisak, 1994; Hambrigth & Zohary, 2000). The hydrodynamic condition of mixed layer in tropical reservoirs accelerates recycling of nutrients. In temperate reservoirs, the mixed layer is quite stable, nutrients lost from the epilimnion can almost not be used again by primary producers until the autumn mixing. Meanwhile in tropical reservoirs, a large quantity of nutrients lost from the mixed layer can recapture through the mixed layer thickness (Lewis 2000). Therefore, the potency for phytoplankton production on a given nutrient in tropical reservoirs is higher than in temperate reservoirs (Lewis 1974). This means that tropical reservoirs may be more reactive to eutrophication than temperate reservoirs (Lewis 2000).

4.3 Siltation, erosion of tropical reservoirs and their consequences on turbidity

In the context of climate and human-induced changes, soil erosion and sediment load are increasing worldwide (Syvitsky et al, 2005), with considerable implications for the management of water resources and the ecological health of aquatic ecosystems. De Boer et al, (2003) recently reminded that "[…] in many parts of the world, erosion rates and sediment

yields are not, or only poorly monitored. This problem is particularly evident in developing countries, where this information is most urgently required […]".

As highlighted by the review of Donohue & Molinos, (2009), the impact of increased sediment load on the ecology of lakes and reservoirs is principally driven by fine particles. The decreased transmission of light through the water column is generally recognized as the main physical effect of increased sediment load on aquatic ecosystems (Donohue & Molinos, 2009). The absorption and scattering of light by suspended particles reduce the compensation depth, below which light intensity is insufficient to sustain photosynthesis, thus diminishing the volume of water supporting primary production (Whalen et al, 2006). Furthermore, fine particles also actively contribute to the bio-geochemical equilibrium by adsorbing, transporting and releasing some pollutants and nutrients, with major effects on global nutrient cycles (Regnier et al, 2013). Sediment load can also actively modify the hydrodynamics of reservoirs through the generation (or not) of various particle-laden density currents (Mulder & Alexander, 2001). In addition to on-site effects, fine sediments supply leads to severe off-site impacts: sediments can accumulate on river beds, increase flooding potential, and degrade aquatic ecosystems by increasing water turbidity and by mobilizing associated contaminants (Newcombe & McDonald, 1991). This can reduce the density, growth rates and production of lake phytoplankton considerably (Dokulil, 1994; Guenther & Bozelli, 2004).

At large scales, human-induced soil erosion has resulted in an increase of 2.3 billion metric tons of sediments being transported by rivers globally every year (Syvitski et al, 2005) but only 1.4 billion metric tons of these sediments actually reaches coastal waters, owing to the retention of sediments in reservoirs, rivers and their floodplains (Walling et al, 2003; Syvitski et al, 2005). Although the delivery of sediments to reservoirs has diminished in some regions owing to the introduction of sediments control programs and the improvement of land management practices (Lal, 2001), excessive sediment loading remains one of the primary forms of anthropogenic disturbance of aquatic ecosystems in both tropical and temperate regions (USEPA, 2000). Globally, the retention of eroded sediments in reservoirs is a major environmental, social and economic concern. For instance, high sedimentation rate reduces hydropower efficiency and viability. It also increases costs of dam maintenance and water treatment and has important consequences for water supply, fisheries and tourism (Clarke et al, 1985; Robertson & Colletti, 1994; Pimentel et al, 1995).

In summary, sediments delivery to water bodies needs to be controlled to prevent these problems. Firstly, the main sources of erosion need to be determined and the transit times of

sediments within rivers need to be evaluated to implement appropriate and effective erosion control measures. In tropical areas where hydrology is controlled mainly by a dry and a rainy season, characterization of seasonal cycles of sediment (and associated contaminant) input is essential to address an appropriate evaluation of physical and biogeochemical cycles taking place in waterbodies ecosystems. This is particularly true in the case study that will be presented in this thesis.

4.4 Eutrophication caused by excess of nutrients

In the last three decades there has been great concern about the increased eutrophication of aquatic systems worldwide from excess nitrogen (N) and phosphorus (P) loading (Lewis 2000; Conley et al, 2009). Human activity is accelerating rapidly in tropical watersheds, where eutrophication is becoming the main water quality issue (Downing et al, 1999), with some consequences on the uses of reservoirs downstream (Salas & Martino 1991). The eutrophication in tropical areas is reflected by increase of algal growth, decrease of water transparency and appearance of a stable oxygen depletion in the hypolimnion (Thomaz & Bini, 2003). It is the result of nutrient enrichment in surface waters. Although it is a natural process, eutrophication can often be accelerated by human activities. Hence, it is sometimes called cultural eutrophication (Laws, 1993). This cultural eutrophication results from a direct discharge of organic wastes or nutrients into rivers and/or indirect nutrient loads via runoff from agricultural sites. The degree of eutrophication or nutrient enrichment has been classified according to the relative extent of nutrient enrichment (Laws, 1993): oligotrophic, mesotrophic and eutrophic. Oligotrophic systems are undernourished, i.e. biological production is limited by nutrient additions. At the opposite, eutrophic systems are over-fertilized. The mesotrophic status of water lies somewhere in between the two.

By adsorbing nutrients, sediments transported in suspension and deposited on the river bed participate actively to the eutrophication of waterbodies; phytoplankton and cyanobacteria can form blooms, causing the release of cyanotoxins. Most lakes, rivers and wetlands are suffering from the input of sediments and nutrients such as nitrogen and phosphorus. Nutrients enrichment in rivers or reservoirs promotes excessive algal blooms, which can result in large fluctuations of dissolved oxygen concentration. In some extreme cases, the rapid drop in oxygen concentration during the night due to algal respiration can kill fish (Chuco, 2003). For those reasons, external and internal nutrient loads are major concerns for water quality management in reservoirs. An excessive concentration of P is the most common cause of eutrophication in freshwater lakes, reservoirs, streams, and headwaters of estuarine systems.

4.5 Downstream deficit of sediments and nutrients

Building of dams on rivers modifies natural sediment dynamics. Regardless of purposes of these constructions, all dams and their reservoirs trap sediments and lead to physical and ecological changes downstream of reservoirs, as well as in the reservoirs themselves (Kantoush et al, 2010). This is the main cause for the decline in sediment fluxes in downstream areas (Gupta et al, 2012). Besides modifying flow regimes and sediment load of dams, they can produce adjustments in alluvial channels (Kondolf, 1997).

The impacts of sediments deficit downstream of dams are classified into three groups, causing morphological, hydrological, and ecological effects. Morphological effects on river channels consist of riverbed incision, riverbank instability, upstream erosion in tributaries, damage to embankments and levees (Kondolf, 1997; Batalla, 2003), and changes in channel width (Williams & Wolman, 1984; Wilcock et al, 1996). Hydrological effects caused by dams include changes in flood frequency and magnitude, reduction in overall flows, changes in seasonal flows, and alteration of time of releases (Petts, 1984; Ligon et al, 1995). In addition, by altering the downstream flow regime of rivers (Williams & Wolman, 1984), dams control many physical and ecological aspects of rivers forms and processes, including sediment transport and nutrient exchange, e.g., loss of aquatic and riparian habitants (Poff et al, 1997).

Besides that, reservoirs are often sinks for P and N due to higher residence times and more increased sedimentation and burial rates than rivers (Sherman et al, 2001, Friedl & Wüest, 2002, Bosch & Allan 2008). As a result, there is an increasing global shortage of P fertilizer reserves for agricultural purposes at downstream (Vaccari, 2009) and the accumulation of P in reservoirs leads to excessive algal production in systems (Schindler, 1977).

In summary, reducing nutrients accumulation in reservoir sediments is important both in maintaining nutrients and sediments in downstream for agricultural production, and preventing eutrophication of water supplies (Burford et al, 2012). The above listed issues are of a great interest in tropical areas, where the climatic and anthropic conditions lead to rapid changes that clearly need complementary studies.

B) Problematics in Mexico

1. Limnology in Mexico

Mexico's geographic position overlaps tropical and subtropical areas between two oceans (Pacific and Atlantic), including mountainous topographies with a wide variety of climatic conditions. Mexico's topography includes seven main mountain systems (SRH, 1976): Sierra Madre Oriental, Sierra Madre Occidental, Trans-Mexican Volcanic Belt, Sierra Madre de

Oaxaca, Sierra Madre del Sur, Sierra Madre de Chiapas, and the Baja California (Figure 1.2). Since the meteorological conditions of this global belt are semiarid, Lind et al, (1992) suggested that the behaviour of continental waterbodies may be different from equatorial and temperate systems.

Approximately 45000 water reservoirs exist worldwide, most of them constructed for irrigation purposes (Cosgrove & Rijsberman, 2000). In Mexico, there are more than 4000 lakes and reservoirs, 667 of them are classified as large dams (CNA, 2006). Mexico's 52 largest lakes and reservoirs hold 60% of the country's total water storage capacity (CONAGUA, 2007). Epicontinental waters in Mexico provide multiple benefits to humans: drinking water, irrigation, power generation, recreation, tourism, navigation, fisheries, aquaculture, etc. (Alcocer & Bernal-Brooks, 2010).

In Mexico, the spatial disparities in water resources interrelate with temporal and altitudinal variations. The hydrological balance of Mexico depends mainly on atmospheric precipitation; a substantial difference in comparison to northern countries where some water is stored in solid phases in mountains (snow and glaciers). For example, the contribution of rains to most Mexican rivers during the wet season occupies 90% of the total annual discharge, which extends 4–6 months from May to October. Short periods of rains associated with cold winds coming from the north Pacific and the Gulf of Mexico sometime happen during the time of low ambient temperature (December–January) (García, 1982, 1988; INEGI, 1995) but these rains generally have a strong erosive capacity and do not contribute positively to refill the underground aquifers. As a consequence, the densely populated region is particularly vulnerable to time-limited water supplies. A negative water budget predominates in more than half of Mexico's territory (52.7%). In contrast, a positive water balance is observed in the other 47.3% (Bassols, 1977). Both areas finally cope with problems associated with water availability: droughts in the former, floods in the latter (SEDESOL, 1993; INEGI, 1995).

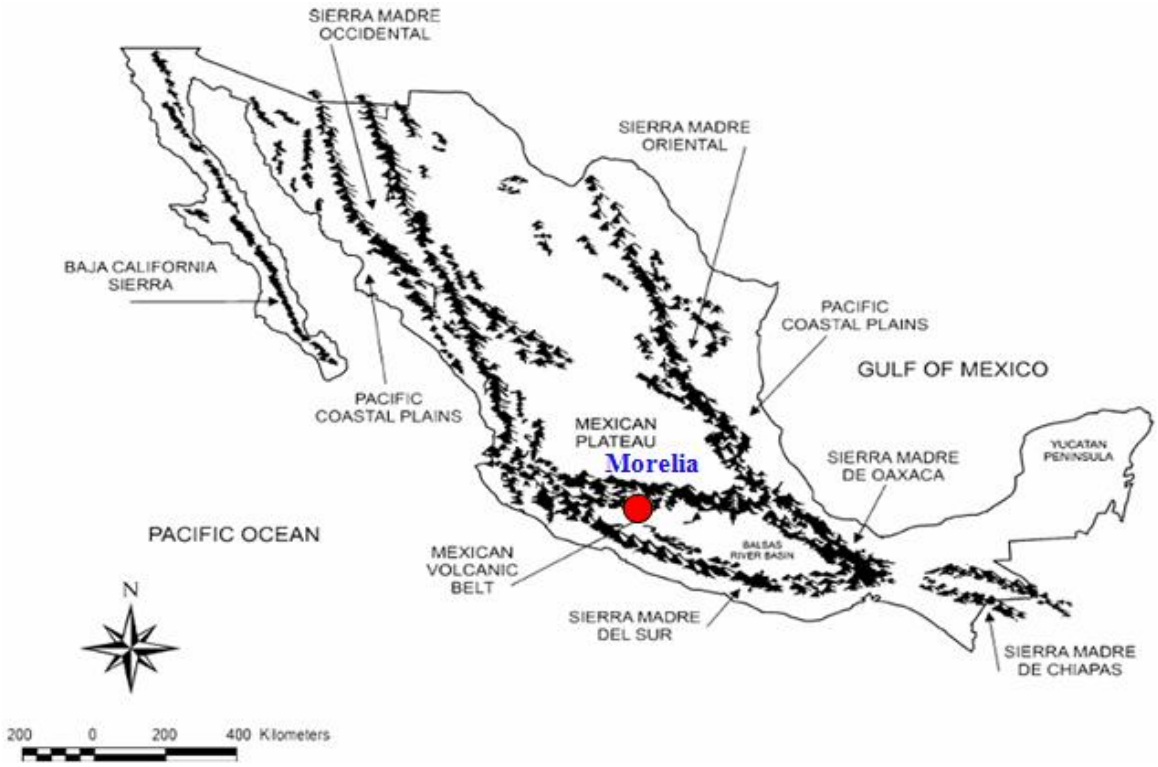

Figure 1.2 Geography of Mexico with main mountainous features. Adapted from SRH, 1976

A nationwide survey undertaken in Mexico revealed that 68% of surface waters were contaminated, and 18% were heavily contaminated (INEGI, 1996). There are about 80% of freshwater lies in impoundments below 500 masl, and only 5% above 2000 masl because of the differences in altitude. Conversely, 76% of the Mexican population reside in the highlands (e.g., the Mexican Plateau; INEGI, 1995), as well as two-thirds of the manufacturing industry and agricultural lands. Therefore, water quality problems can complicate the distribution of limited water resources in Central and Northern Mexico because of uneven distribution of precipitation and population (CNA, 2008). As we know, agricultural lands, aside from their huge water requirements, are also a large source of water pollutants, such as fertilizers and pesticides. Agricultural runoffs carry fertilizers that cause eutrophication; pesticides can be poisonous to humans as well as other organisms. As a result, most of the Mexican reservoirs located within or close to urban areas are heavily polluted, with direct consequences for the aquatic ecosystems as well as potential risks to the human health (Welch & Jacoby, 2004). This is generating great concern as the volume of wastewater produced is increasing because of further urbanization and economic growth. Moreover, the demands of multi-purpose reservoirs such as municipal drinking water, industrial water supply, irrigation, hydroelectric power generation, and recreation dictate

scientific communities to pay more attention to this kind of water bodies for a better understanding of ecosystem functioning and management (Thornton et al, 1990).

Despite this observation, studies on Mexican freshwater are still very limited since most limnological research covers only general hydrobiological aspects. The lack of limnological studies is troublesome considering the large number of lakes and reservoirs existing in Mexico (Arredondo -Figueroa & Aguilar, 1987).

2. Global situation in Trans-Mexican Volcanic Belt, central Mexico

The Trans-Mexican Volcanic Belt (TMVB) is a 1000 km long Neogene continental arc describing a large variation in composition and volcanic style (Ferrari et al., 2012). It is a unique volcanic belt running from west to east in the central portion of Mexico (Figure 1.3). The TMVB covers an area of 91685 square kilometers. It is composed of more than 20 volcanoes, some of which are among the highest peaks in Mexico, e.g. the Pico de Orizaba (5747 m) and the Popocatépetl (5452 m). Three main basins encompass the highlands of the TMVB: Lerma-Santiago river basin at the west, Valley of Mexico basin in the middle, and the eastern basin (Alcocer & Bernal-Brooks, 2010).

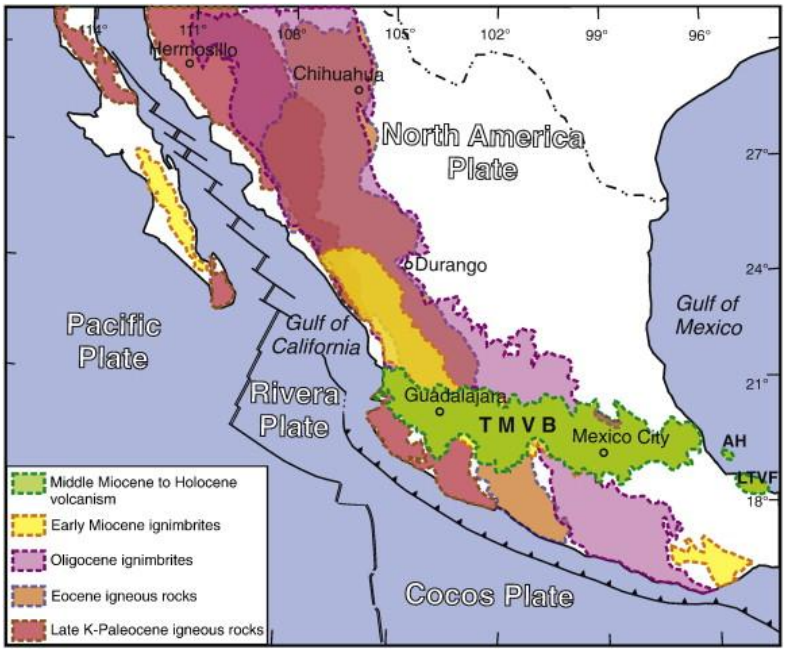

Figure 1.3 Map of Trans-Mexican Volcanic Belt (Ferrari et al., 2012)

Intense volcanic activities have allowed the formation of many fluvial deposits; the soils in this region have a strong propensity to retain water. The forests play an important role as a "rain trap"; they can contribute to refill the underground aquifers for water supply of adjacent towns (López-García et al, 1996). Almost half of the total Mexican population lives in the

states of the TMVB, including Mexico City (Toledo et al, 1989), thus forests in this region have suffered the effects of urbanization (synthesized from /source http://worldwildlife.org/ecoregions/nt0310). Degradation of the natural resources is alarmingly aggravated in the catchments of the TMVB, which provide water for nearly one third of Mexico's population. It was estimated that 60 percent of the TMVB presents problems due to soil erosion (SEMARNAT, 2002). This in turn leads the degradation of surface water bodies and the increase of water treatment costs (Vidal et al, 1985; Alcocer & Escobar, 1993). This situation is particularly severe in the volcanic region located around Morelia (capital of Michoacán state, ca. 700 000 inhabitants) (Duvert et al, 2010).

The lakes and reservoirs present within the TMVB originate from the regional tectonism and volcanism, which is a representative feature of this area (Alcocer & Bernal-Brooks, 2010). Besides its tectonic and/or volcanic origin, the TMVB holds the ''largest'' Mexican lakes, together with a cluster of small water bodies. The large lakes produced by tectonic activity or lava flow, differ largely from small volcanic water bodies. The first ones are characterized by remarkable shallowness, turbid waters, and meso- to eutrophic conditions. Meanwhile, the latter ones are more likely ''deep'', transparent and oligotrophic, even if the turbidity is generally increasing in all systems. Turbidity in Mexican lakes relates to biogenic (e.g., phytoplankton) or inorganic sources (e.g., suspended clays in Lake Chapalaas described by Lind et al, 1992). In this climatic region, the water temperature generally ranges from 15 °C to 25 °C. There are two major lake types in Mexico: (i) warm monomictic in small deep lakes and (ii) warm polymictic in large shallow ones (Alcocer et al, 2000). The deeper water bodies (roughly more than 10 m depth) are generally thermally stratify between March and October or even longer. The hypolimnion of the warm monomictic lakes frequently becomes anoxic during the stratification period. The Cointzio reservoir is a typical example of this type of water body. It fulfils the definition of a warm monomictic tropical reservoir, which has a minimum temperature of 14°C with a period of stratification from February to October followed by a period of mixing during the rest of the year (Doan et al, 2012).

An overview of the state of lakes and reservoirs in Mexico, particularly within the TMVB was provided and the lack of data on Mexico's rivers and reservoirs was highlighted (Alcocer & Bernal-Brooks, 2010). Moreover the development of wastewater treatment infrastructure remains insufficient, both in large cities and in small rural settlements in Mexico. A recent study on the main reservoir of Valle de Bravo, which provides water supply to the Mexico City, recommended the implementation of monitoring networks of discharge and nutrients as well as the establishment of policy and mitigation strategies of point and non-point sources of

pollution (Ramírez-Zierold et al, 2010). Therefore, Mexican governments became particularly concerned with improving the environmental conditions of cities and proposed many measures dealing with water usage and managements that were based on European technological innovations.

3. Erosion within the watershed

Mexico is faced with a serious problem of soil erosion: 80% of the land is subject to erosion. The topographic characteristics and rain intensity of the country promote a high risk of erosion, especially on hillside land. Up to 61% of the area devoted to annual crops is located on slopes greater than 4% (source from http://www.desire-his.eu/es/descargas/doc_view/333-highlight-conclusions-cointzio-study-site). The Michoacán state is located in the center west of the Mexican Republic, on the southern coast of the Pacific Ocean, between 17º54`34" and 20º23`37" north latitude and 100º03`23" and 103º44`09" west longitude (source: http://www.sre.gob.mx/coordinacionpolitica/images/stories/documentos_gobiernos/pmichoing.pdf). It has one of the largest levels of soil erosion, with more than 2 million hectares affected, 70% of the surface area (source: http://en.ird.fr/layout/set/popup/the-media-centre/scientific-newssheets/396-rehabilitation-of-eroded-land-in-mexico).

Figure 1.4 a) Desertification in Mexico and b) Landscape of degraded soils in Mexico

Aggressive climate, rugged topography and fragile soils in Mexico indicate that nature is an important element of erosion. However, the main cause is human activity due to overgrazing with overpopulation of animals. Since prices of agricultural products are low in Mexico (e.g. low corn prices), crop cultivation becomes a secondary source for farmers. As a result, many farmers have turned to livestock farming or abandoned their land in order to migrate to the cities or the United States for living. Thus, we can see the animals go nearly everywhere,

from the forest to the fields when they have been harvested. This is the major cause of land degradation in watersheds of Mexico.

The watersheds of Morelia, the capital of Michoacán, are emblematic of the situation. It is surrounded by chains of volcanoes up to 3,500 m in height, with steep slopes accelerating the runoff and the hydraulic erosion. The watersheds are located in the hydrological region of Lerma-Chapala, within the central Trans-Mexican Volcanic Belt, in the state of Michoacán. The Cointzio watershed is located at the south western part of the Cuitzeo lake watershed of 4000 km^2 (Figure 1.5). The catchment is representative of the region since it experiences all the problems such as soil erosion, deforestation, grazing, etc., which also affect water quantity and quality.

Figure 1.5 The Cointzio and Cuitzeo watersheds in Michoácan

(Source: http://www.desire-his.eu/es/descargas/doc_view/333-highlight-conclusions-cointzio-study-site)

4. Water scarcity and water pollution

Mexican water resources are commonly considered poor in quality and sparse in quantity, particularly in Michoacán state (Vidal et al, 1985). Over the past years, the explosive human population growth affected many lakes and reservoirs in the region which have suffered the consequences of the eutrophication process. In the Mexican territory, which represents 0.39% of earth's land area, water is scarce. It is only equivalent to 0.1% of the world's freshwater reserves, reflecting its low rain input (0.00003% of the world's input) (García-Calderón & De la Lanza, 2002). Therein, the Michoacán state has been facing a decrease of about 70% in its

surface water resources over the last century (Morales, 2007). This evolution correlates with the high migration rate in Michoacán (63% of total population), which contributed to the impact of land-use changes on water resources (Lopez Granados et al, 2006). Obviously, as the urban area is expanded, demand and competition for urban and industrial water need to be intensified.

The poor water quality of Morelia city was stemmed from high sediment load and high organic material content of the Chiquito and the Rio Grande de Morelia rivers, and contaminants in the infrastructures themselves. Among them, the Rio Grande is Morelia's most problematic river where some sections are so full of sediments that its natural course has changed in places. As a result, problems of salinity and deteriorating water quality in the region became worse as farmers irrigated fields with water contaminated from urban wastewater. This affected not only agricultural productivity but also farmers' health (e.g. gastrointestinal illness, skin diseases and fungal infections). Therefore, it becomes necessary to treat water and construct new piped supply networks. A recent study given by various local institutions stressed that water contamination, solid residuals management and drinkable water supply are three main priorities of environmental issues in the Michoacán settlements (Ortiz Ávila, 2009). According to the government, most of the surface waters in Mexico range from polluted to excessively polluted, and only a few places remain non- or slightly polluted. Even if we could instantaneously prevent any further contamination, it would take at least 10 years and perhaps more than 30 years (and enormous operating costs) to recover the ‘‘original’’ conditions (Alcocer & Bernal-Brooks, 2010). In addition, the waste of water resources through leakage and inefficient usage, and lack of wastewater treatment plants leading to water problems becoming more and more serious. It has been estimated that the amount of water lost in Mexico City's supply system is sufficient to meet the needs of a city the size of Rome (Falkenmark & Lindh, 1993).

In summary, water is limited both in quantity and quality in Mexico. As available fresh water is limited (only 1% of the total water reserve), its good quality must be maintained and polluted water must be restored. The problem of water scarcity can be addressed by efficient water use, whereas the problem of water pollution requires the implementation of an appropriate water quality regulation (Al-Kharabsheh & Táany, 2003). In order to protect all water bodies from all sources of pollution, Mexico therefore needs to have appropriate environmental regulations and assessment tools.

5. The case of the Cointzio reservoir

The Cointzio reservoir (state of Michoacán), located in the southern part of the Mexican Central Plateau on the TMVB, is used for domestic water supply to the city of Morelia, situated 13 km downstream, and for irrigation purposes. Besides that, it is also used to control flood for Morelia (Figure 1.6). The Cointzio dam controls the flow of the Rio Grande de Morelia River and irrigates more than 20000 hectares of farmland. Water demand of the city has been growing over the last decades because of increasing individual water consumption coupled with a severe urban growth: Morelia experienced an augmentation of its population of 600% during the period 1975–2000 (López-Granados et al, 2001) and counts now over 700000 inhabitants (INEGI, 2006).

Figure 1.6 Cointzio dam with the reservoir in dry season

Conclusions of chapter 1

The general issues of tropical countries (e.g. poverty, rapid population growth, ineffective policies for water resources management, and lack of funds), the limitation of knowledge about tropical waterbodies, and the significant increase in the eutrophication of tropical reservoirs during recent decades required information and studies on the processes taking place in tropical reservoirs, particularly in Mexico where our study site is located.

The overall water quality of reservoirs in many regions of Mexico is deteriorating. The Cointzio reservoir, located in the Trans-Mexican Volcanic Belt, is no exception. Alcocer & Bernal-Brooks, (2010) recently provided an overview of the state of reservoirs in Mexico and

highlighted the lack of data on Mexican rivers, indicating that few knowledge about the linkages between sediments and nutrients sources within upstream watersheds and the biogeochemical functioning of downstream reservoirs. The implementation of monitoring networks of discharge and nutrients as well as the establishment of policy and mitigation strategies of pollution sources are important actions that need to be undertaken to solve water quality problems in tropical systems, including Mexico. In the case of the Cointzio reservoir, this issue is critical since part of the water stored is used for drinking water supply. This turbid tropical reservoir has been studied from 2007 to 2009 to better understand its hydrodynamics and its biogeochemical functioning and try to define some common behaviors of various turbid tropical reservoirs.

Chapter 2. STUDY AREA AND FIELD DATA ANALYSIS

Chapter 2 describes the study area, the field monitoring strategy and the laboratory analysis that have been realized to generate the hydrological and biogeochemical database. The results of two and a half years of hydrodynamic data and one year of biogeochemical measurements data are also presented.

1. Study area

The Cointzio reservoir itself (19.622°N, -101.256°W) is located in the southern part of the Mexican Central Plateau on the TMVB, at an altitude of 1990 metre above sea level (masl) (Figure 2.1). The region, which is located in the state of Michoácan, is subjected to high soil erosion of clay particles. It has a temperate sub-humid climate with a mean annual rainfall nearby the reservoir of 810 mm, mainly concentrated during the wet season from June to October. The dry season occurs the rest of the year (period 1956-2001; Gratiot et al, 2010). The rainfall is characterized by a high sub-daily variability, with localized convective storms generally promoting intense precipitation over a few km^2 in the late afternoon through early night (Duvert et al, 2010). The amplitude of seasonal variations in water temperature in the region varies from about 14°C to 23°C (Figure 2.2). Figure 2.3a shows the time series of precipitation from the year 1955 to 2005 at Undameo (the inlet of the Cointzio reservoir) and in the Cointzio reservoir. The water inflow at Undameo during this period are also presented in Figure 2.3b. The trend of the inflow increased a bit in the last years as a potential response of run-off to land use change over the decades in the region (Gratiot et al., 2010). Precipitations showed in Figure 2.3a, do not exhibit any statistical trends.

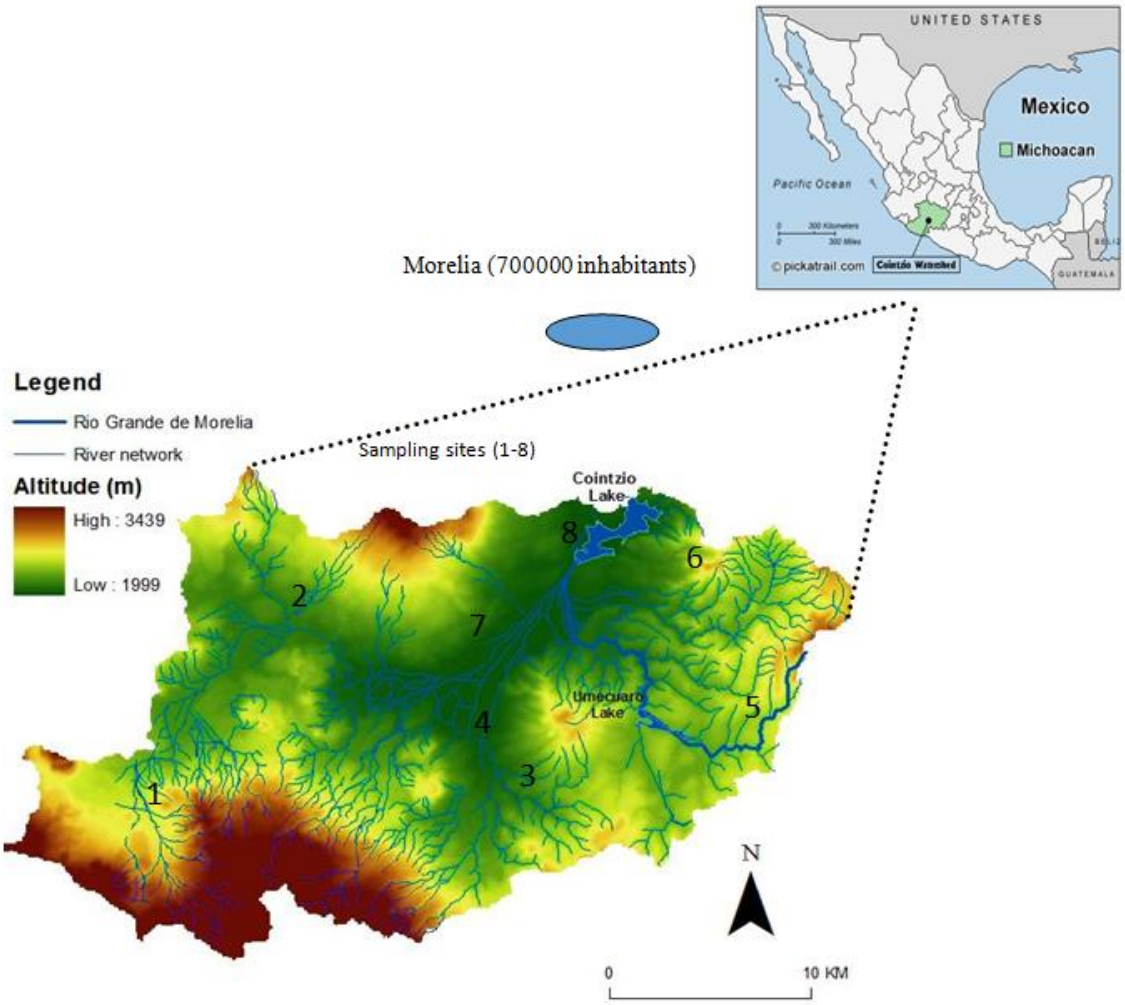

Figure 2.1 Map of the Cointzio watershed, within the state of Michoácan, and location of sampling sites in the watershed, geographical position in UTM

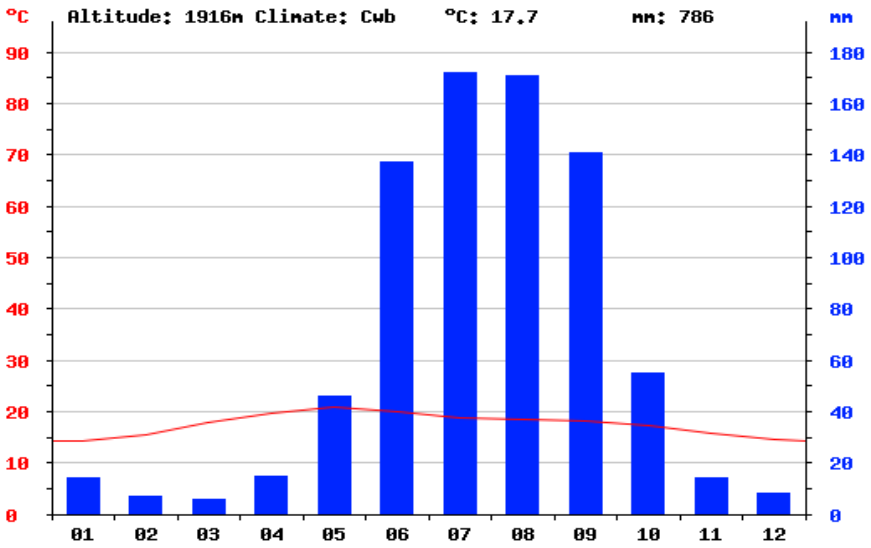

Figure 2.2 Seasonal variation in regional precipitation and water temperature patterns (from http://es.climate-data.org/location/3382/)

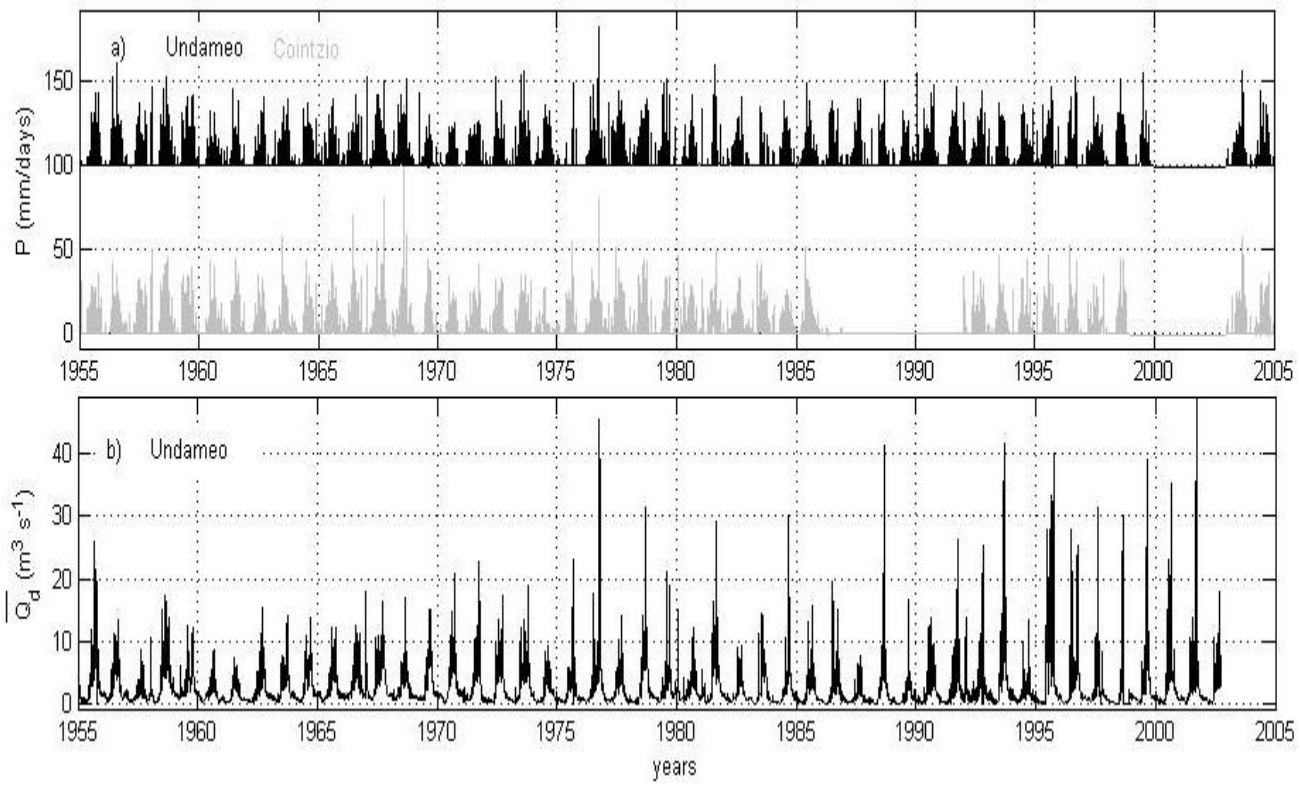

Figure 2.3 Time series of (a) precipitation at Undameo & in the Cointzio reservoir and b) the water inflow at Undameo from the year 1955 to 2005

An aerial photography of the Cointzio reservoir is shown in Figure 2.4. It was built in 1940 to supply water for domestic purpose (15-20 % of the need of the city of Morelia, 700 000 inhabitants, i.e. 0.67 m^3 s^{-1} all year long) and for downstream irrigation during the dry season, from January to June with the maximum discharge up to 8 m^3 s^{-1}. Besides that, it is also used as flood control for Morelia. The outflow of the dam is located at about 20 m depth from the surface. The morphometry of the reservoir is described by the rating curve between the volume and the depth in the reservoir (Figure 2.5). The water depth in the reservoir varies from year to year (Figure 2.6). The Cointzio reservoir drains a volcanic watershed, where domestic waters are rejected without any treatment. It has a storage capacity of 66 Mm^3 and a surface area of 6 km^2 for a maximum depth of 29 m. As the reservoir is filled and emptied each year, the residence time of the water within the reservoir is about one year (Némery et al, submitted). Increasing siltation of this reservoir is a major concern as it supplies a significant part of the distributed water in Morelia city.

Figure 2.4 Aerial photograph of the Cointzio reservoir which supplies water to Morelia city (Adapted from http://paralelo19n.blogspot.fr/2011/03/toluca-guadalajara.html)

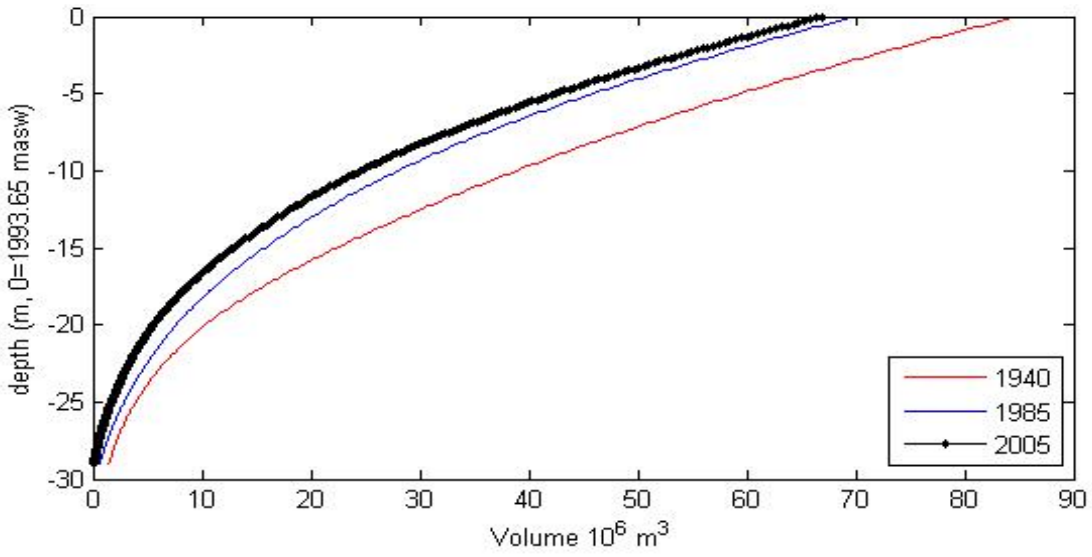

Figure 2.5 Rating curves between the volume and the depth in the Cointzio reservoir (years 1940, 1985, 2005)

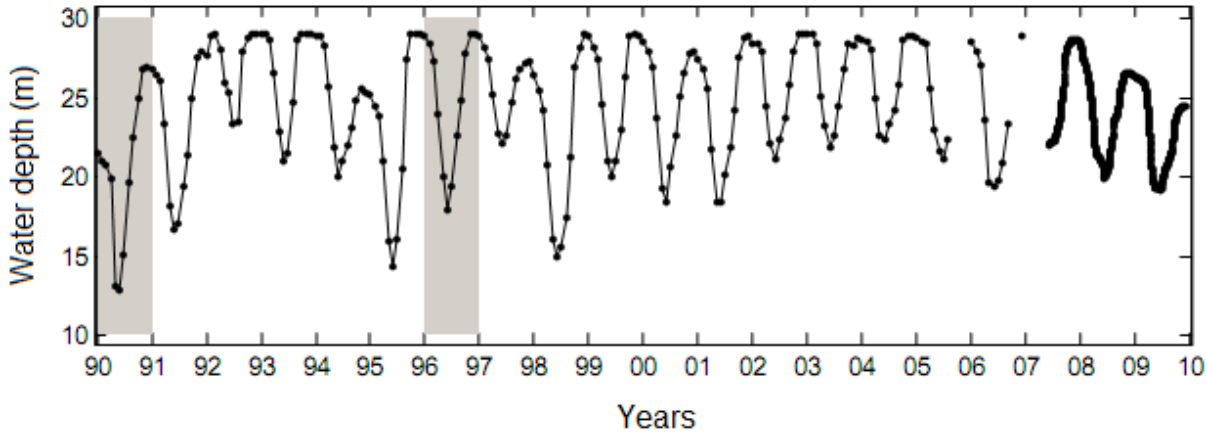

Figure 2.6 Time series of the water depths in the Cointzio reservoir (from 1990 to 2009)

Figure 2.7 shows the watershed of Cointzio, its subdivision into 17 sub watersheds and its hydrological network. This watershed includes small cities such as Lagunillas (5136 people) and Acuitzio del Canje (9366 people) (Mendoza & Lopez-Granados, 2007). These sub watersheds contain hills, high valleys and plains developed over volcanic materials aged from Miocene to recent time. The topography shows a ridged area with slopes between 0 to 70 %.

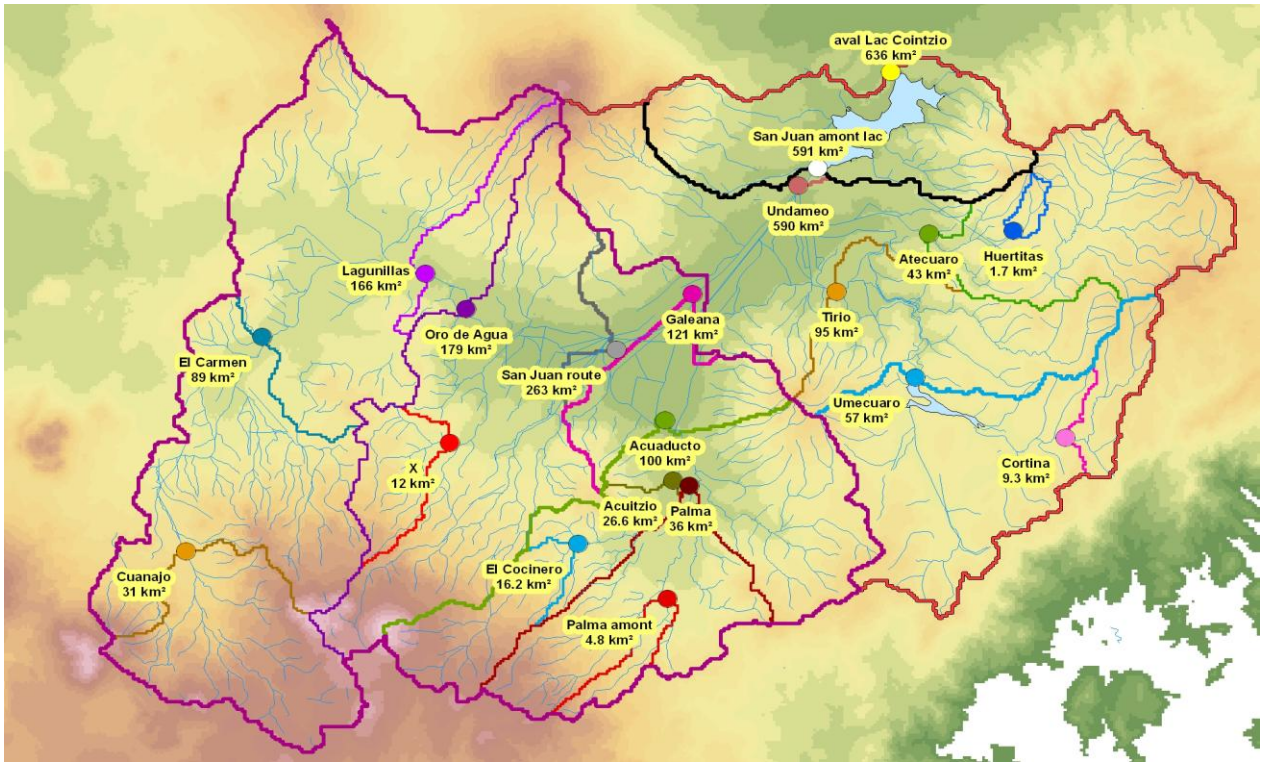

Figure 2.7 Cointzio sub watershed and its hydrological network (STREAMS 2008, P. Bonté)

The Cointzio catchment covers an area of 630 km^2 with altitudes ranging from 3440 masl at the summit to 1990 masl at the outlet. This watershed consists of a combination of cropland (40%), forests (37%) and grassland (23%) (Duvert et al, 2010). In 2005, the mean population density was 68 inh. km^{-2} for a total of 43 000 inhabitants (López-Granados et al, 2013). The watershed of Cointzio behaves similarly to a small plain surrounded by mountains. It has a semi-humid climate with a rainy season from June to October. There are three types of soils and land uses distributed among the different landscapes: Luvisols are in the plains of irrigated and highly mechanized agriculture, Acrisols are distributed for survival agriculture on the hills and Andosols are mainly covered by forests over ±2300 m. These types of soils are known to be poorly resistant to water erosion when they suffer land use changes (Poulenard et al, 2001; Bravo-Espinosa et al, 2009). The outflow of the basin is controlled by a dam, built 74 years ago. One of the consequences of erosion is siltation of the reservoir. Besides that, the contaminants are adsorbed on suspended particles and eventually settle as sediments leading to further water quality deterioration (synthesized from/source http://www.desire-his.eu/es/descargas/doc_view/333-highlight-conclusions-cointzio-study-site)**.** As there is no waste water treatment plants in the upstream villages the water inflow contains high levels of nutrients which lead to high levels of organic and nutritive pollution downstream (Némery et al, submitted).

Land use has changed over the period 1975-2003 in the watershed with an increase in deforestation especially on steep slopes but also with some reforestation and progression of scrublands in some areas (López-Granados et al, 2013) (Figure 2.8). These changes are nearly equilibrated. The catchment bedrock consists of igneous rocks generated by Quaternary volcanic activities. According to the World Reference Base for soil resources (FAO, 2006), the main soils within the catchment (Acrisols, Andisols, and Luvisols) are highly degraded in some parts of the watershed where important processes of erosion occur during the wet season (Duvert et al, 2010). As a result, the reservoir presents a high turbidity level all year long and has partially lost its storage capacity because of siltation (Susperregui et al, 2009).

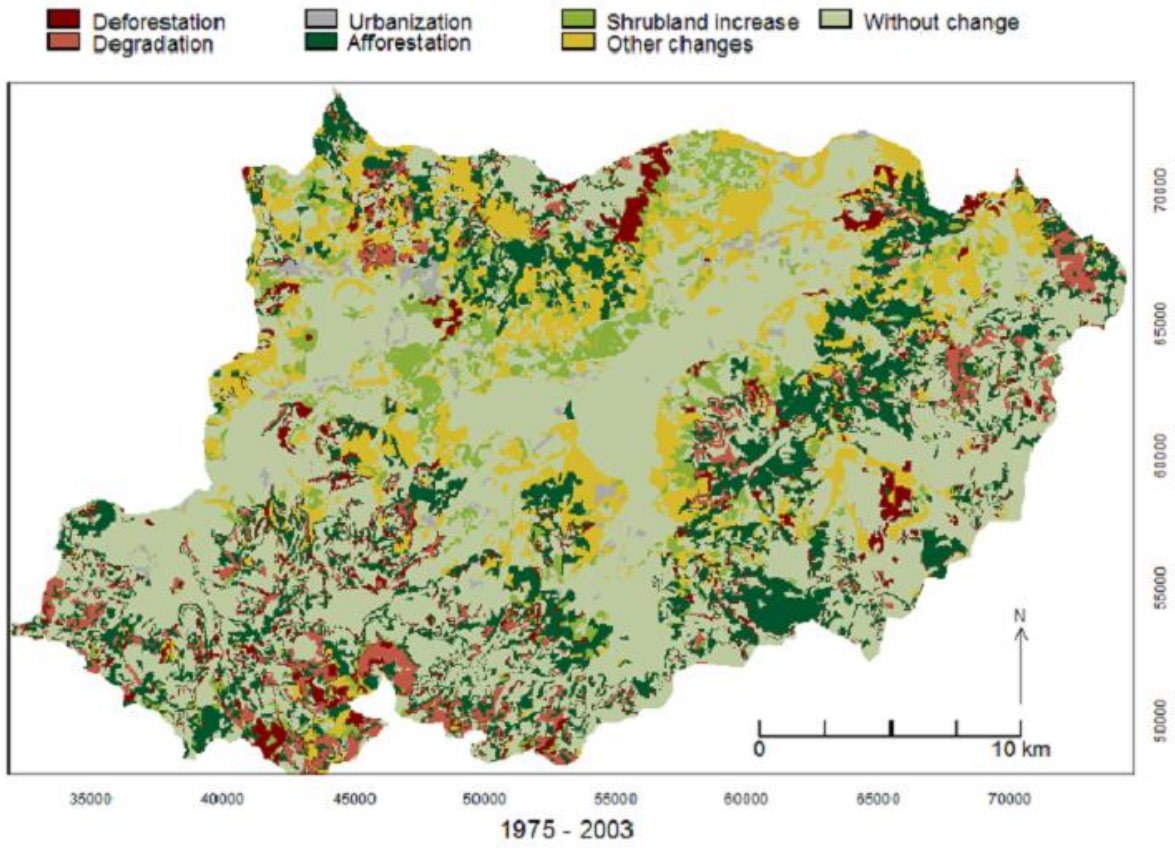

Figure 2.8 Maps of land cover and land use change processes by period in the Cointzio watershed (Mendoza et al, 2013)

The main permanent watercourse is the Rio Grande de Morelia River whose source lies about 25 km upstream of the Cointzio reservoir (Figure 2.9). The dam is located at the outlet of the catchment, 13 km upstream of Morelia city. Water and sediment inflows come almost exclusively from the Rio Grande de Morelia River, whereas the outflow is done through gates opening at a dam. The water inflow (floods) mainly occurs during five months of the rainy season (May-September), representing 77% of the water input and 98% of the sediment load (Duvert et al, 2011). The water outflow is concentrated mainly during the end of the dry season, when the agricultural water demand is high and also all throughout the year for drinkable water production.

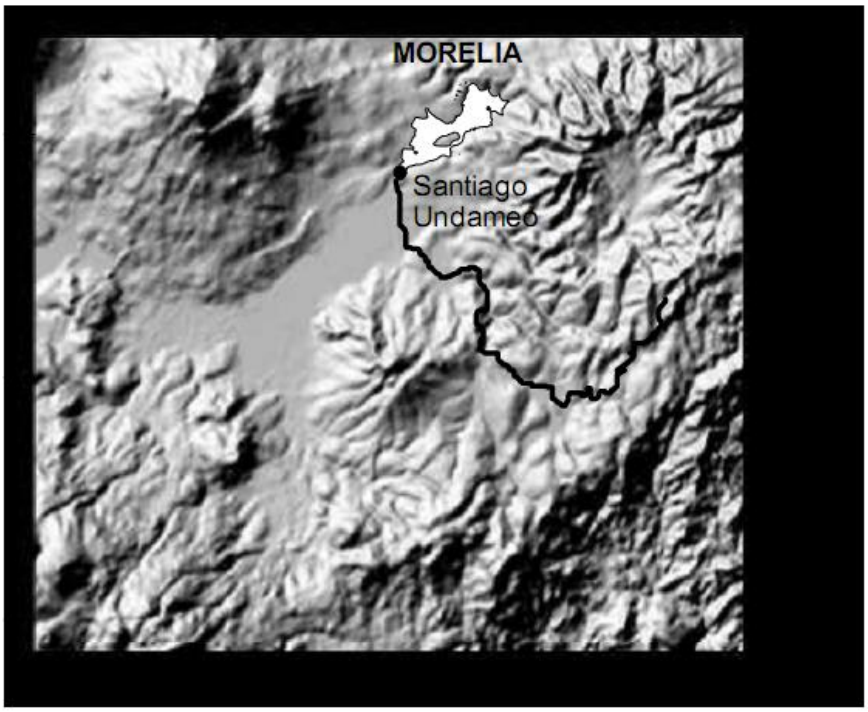

Figure 2.9 Cointzio reservoir catchment topography. The black line represents the Rio Grande de Morelia River (Susperregui, 2008)

2. Field monitoring strategy

2.1 Survey in the watershed

2.1.1 Watershed area

To localize the origin of nutritive pollution upstream of the reservoir, eight sampling sites were identified in the watershed according to land use, population density and location in the river network (Figure 2.1). Their characteristics are described in Table 1 of chapter 4. Water samples were taken on a monthly basis in 2009. Discharge (Q), pH and dissolved oxygen (DO) were measured at the same time. The site n°8 in Figure 2.1, located in the Santiago Undameo township, corresponds to the outlet of the Cointzio watershed and to the inlet of the Cointzio reservoir. At this site, a gauging station was built in 1940 by the Comisión Nacional Del Agua (CONAGUA) (Gratiot et al, 2010). Water discharge was monitored by the commission at a subdaily frequency (2 to 3 times) from 1940 to 2005. From 2007 to 2010, as part of our investigations, some automatic instruments were installed to measure water and sediment discharge every 10 minutes. This in order to quantify rigorously the reservoir water and total suspended sediments (TSS) inputs (Duvert et al, 2011).

2.1.2 Inlet and outlet data

In order to establish biogeochemical mass balances of carbon (C), nitrogen (N), phosphorus (P) and TSS, daily samples were taken at the reservoir inlet (i.e. Undameo gauging station, sampling site 8) and outlet during 2009 (Figure 2.1). Given the low population density around the reservoir banks and the absence of other rivers, the Rio Grande de Morelia River was considered to be the predominant source of C, N, P and TSS. This was confirmed by two preliminary field surveys realized in December 2005 and May 2006 (Susperregui et al, 2009).

For all sites, a similar methodology was considered. Sampling was conducted in the middle of the river using a bucket and samples were stored at 4°C. Weekly composites were obtained by a discharge-averaged mix of daily samples at each site for further analysis. At the reservoir inlet, ten minutes time step of discharges were measured using a continuous water level record and a rating curve (Duvert et al, 2011). The river water temperature has been measured or estimated from correlations with air temperature. At the outlet daily discharges and additional daily TSS data were obtained from the CONAGUA for the period 2007-2009. Annual fluxes entering and exiting the reservoir were calculated as the product of water discharge and sample concentration over time.

2.2 Sampling within the Cointzio reservoir

2.2.1 Physical data

At the beginning of the project, two extensive campaigns of measurements were conducted in December 2005 and May 2006 at high and low water levels, respectively in order to check whether lateral effects were playing a role in the hydrodynamics. Temperature, DO, turbidity, and conductivity were measured along thirty three vertical profiles, distributed along the longitudinal axis and along five cross sections. The results of these two campaigns did not reveal significant lateral heterogeneities (data not shown here) and it was decided to focus the monitoring effort on the temporal variations along the longitudinal axis. The spatial distribution of profiles is presented in Figure 2.10.

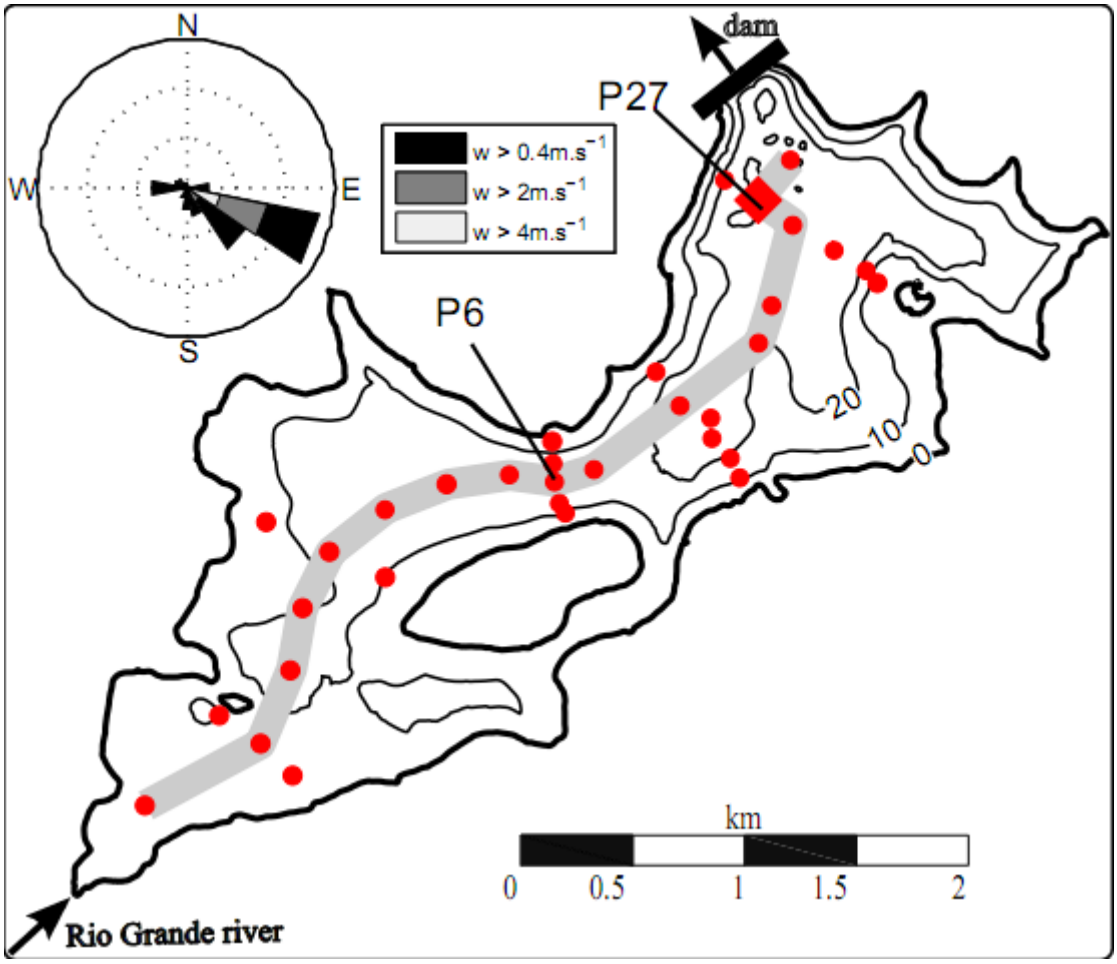

Figure 2.10 Map of the Cointzio reservoir, and localization of measurement points in the reservoir. 16 vertical profiles were realized along the longitudinal axis (dashed line)

From September 2007 to January 2010, field measurements were carried out at a fortnightly to monthly basis. The measurements were systematically done from the dam to the Rio Grande de Morelia River with a small boat, propelled by an electrical engine. The mean duration of a survey was of about 6 hours, beginning in the morning (at about 9:00 AM) and lasting until mid afternoon (at about 15:00 PM). A multiparameter Hydrolab MS5 probe (Hach Company, Loveland, CO, USA) was used to determine the vertical profiles of temperature, turbidity, conductivity and DO, at 16 field stations regularly distributed along the longitudinal axis (Figure 2.10). The probe included: (i) an optical self-cleaning sensor for turbidity measurement (accuracy = 0.1 nephelometric turbidity units (NTU); (ii) a pressure sensor to determine depth (accuracy = 0.05 m); (iii) a 30-ohm thermistor to measure temperature (accuracy = 0.1°C). At each sampling station, the probe was immersed manually and plunged at a mean rate of 0.3 m s^{-1}. With a measurement frequency of 1 Hz, hydrodynamic parameters were acquired two to three times per vertical meter. At each station, Secchi depth was measured to evaluate the attenuation of light by turbidity using a

Secchi disk. Thirty two longitudinal profiles were acquired from 2007 to 2009 are available online[1]. In total, about ten thousands individual measurements done with the multiparameter probe.

To assess the intraday fluctuations, a thermal chain composed of 12 sensors with wide interval of one meter between each from water surface to 8 m depth, and with 5 m wide interval below, was anchored at the deepest point P27 of the reservoir (diamond symbol on Figure 2.10). It measured the temperature with Vemco minilog sensors (accuracy=0.2°C) every 10 minutes. After a complete year of monitoring, it has been decided to reduce the temporal frequency of measurements to 30 minutes in October 2008. This in order to prevent the loss of data (limited storage capacity of sensor) without affecting notably our estimation of the intraday fluctuations. The thermal chain disappeared the 15th April 2009 due to human disturbance and the only surface sensor was found again the 5th of May. After this date, the thermal chain was reinstalled with other Vemco sensors available at our laboratory. Their number and specificities were not optimal (with only five sensors that did saturate at temperature above 20.6°C). When necessary, the temporal series were interpolated with the Hydrolab datasets measured every two to three weeks. When the water surface temperature was not properly recorded in the reservoir from mid-June to September due to saturated sensor (see appendix 3), the reservoir surface temperature was estimated from a linear regression to the air temperature time series ($T_{surf} = 0.52*T_{air}+9.8$, r2=0.84).

The monitoring of the hydrodynamics was completed with the measurements of the main meteorological forcings. A Davis anemometer was mounted at the Cointzio dam station to monitor the wind speed and direction every 10 minutes (Figure 2.10). The instrument was located at about 20 meters above the water surface at the roof of a dam monitoring building. The wind direction and velocity are potentially affected by local venturi effects of the valley. In this work, wind series were thus examined qualitatively rather than quantitatively. Minimal and maximal daily air temperatures were collected manually by technical agents. The solar radiations were obtained from the official meteorological station of Morelia city, located at 10 km downstream. A time series of measurements of rainfall, evaporation above the reservoir was collected and analyzed statistically. Raw data were provided by the Comisión Nacional del Agua. The daily database covers the period between 1941 and 1985.

[1] www.lthe.fr/PagePerso/gratiot/Cointzio_serie.htm

2.2.2 Biogeochemical data

To assess the spatial and temporal dynamics of biogeochemical parameters within the reservoir, the biogeochemical survey was focused on a shorter temporal window from the beginning of 2009 to the beginning of 2010. The water samples were taken at the deepest point of the reservoir (P27) and at a middle position between the river input and the dam (P6) (Figure 2.10). At these two locations, additional vertical water samples were retrieved from different depths (0, 1, 2, 5, 10, 15, 20 m) and from near the bottom. A 2L Niskin bottle was used for TSS, chlorophyll *a*, zooplankton, Dissolved Organic Carbon (DOC), Particular Organic Carbon (POC), pH, and nutrients (TP, TN, PO_4^{3-}, NH_4^+, and NO_3^-) analysis.

2.3 Samples of sediments

Samples of bottom sediments were also taken using a Van Veen grab sampler at two periods, during the dry season (19th May 2009) and at the end of the wet season (13th October 2009). Six points (P27, P13, P11, P6, 47 and P3) were chosen along the longitudinal profile to assess the C, P, and N stocks in deposited sediments. We assume that sampling is representative of the top 2 cm corresponding to sediment surface layer.

2.4 Analytical methods of waters and sediments

After sampling, water samples were stored in polypropylene flasks at 4 °C before analysis. TSS was weighed on GF/F Whatman filters after drying at 105 °C. Chlorophyll *a* was analyzed after filtering on GF/C Whatman filter using methanol extraction according to Holm-Hansen and Rieman (1978). POC analyses were performed after filtering on GF/F Whatman filter (ignited at 500 °C). Filters were treated with HCl (2 N) to remove carbonates and dried at 60 °C for one night (Etcheber et al, 2007). POC was then determined on dry filters by combustion in a LECO CS 125 analyzer at EPOC laboratory (France) (Etcheber et al, 2007). DOC was analyzed on filtered water using a TOC-V Shimadzu analyzer (Sugimura and Suzuki 1998). Analytical accuracy of carbon analysis was higher than 5 % (Coynel et al, 2005). Nutrients (PO_4^{3-}, NH_4^+, and NO_3^-) were analyzed with Hach DR/2010 spectrophotometric equipment. Accuracy with standardized methods was evaluated at 10 %. Data on (TSS; g L^{-1}) were obtained using an automatic water sampler (ISCO 3700) triggered by water-level variations. During floods, water samples were collected after each 5-cm water-level variation. TSS (generally $\geq$ 2 g L^{-1}) was estimated at the laboratory after drying the entire sample for 24 h at 60 ^{o}C. Total particulate P (TPP) content was determined using a high temperature/HCl extraction technique (Aspila et al, 1976; Némery & Garnier, 2007) before phosphate measurement by colorimetric method (Murphy and Riley, 1962). To estimate particulate inorganic P (PIP), the analysis was similar to that for TPP, except that

the high temperature organic P mineralization was omitted. Particulate organic P (POP) was determined by calculating the difference between TPP and PIP (Svendsen et al., 1993). Bulk carbon (C) and nitrogen (N) content were measured by CHN analysis using a CN-analyzer FlashEA 1112 (Thermo Fisher Sci., MA, USA). Carbonates was analyzed at the INRA soil analysis laboratory in Arras (France) using classical calcimetric method (Robertson et al, 1999) according to the normative procedure NF ISO 10693.

3. Hydrodynamic and Biogeochemical functioning from field data

3.1 Hydrodynamic functioning

3.1.1 Inlet and outlet of the reservoir

The inflow data were measured by a continuous water level record and a rating curve and the data were obtained from the CONAGUA. The inflow data were high during the wet season and they were low in the rest of the year. As a result, the Cointzio dam was built in 1940 to retain water during high flow period in order to provide water for domestic purpose all year long and to deliver water for irrigation in dry season (Figure 2.11).

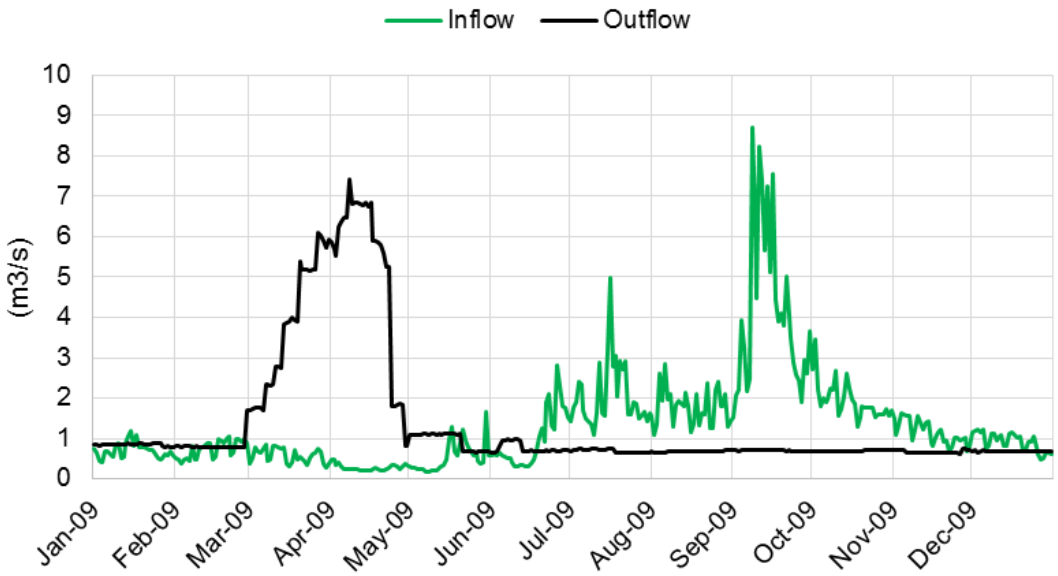

Figure 2.11 Seasonal time-series of inflow & outflow

The river water temperature was measured with a Vemco minilog TR8k sensor (+0.2°C), it had some periods of missing data in 2009 due to malfunctioning (Figure 2.12).

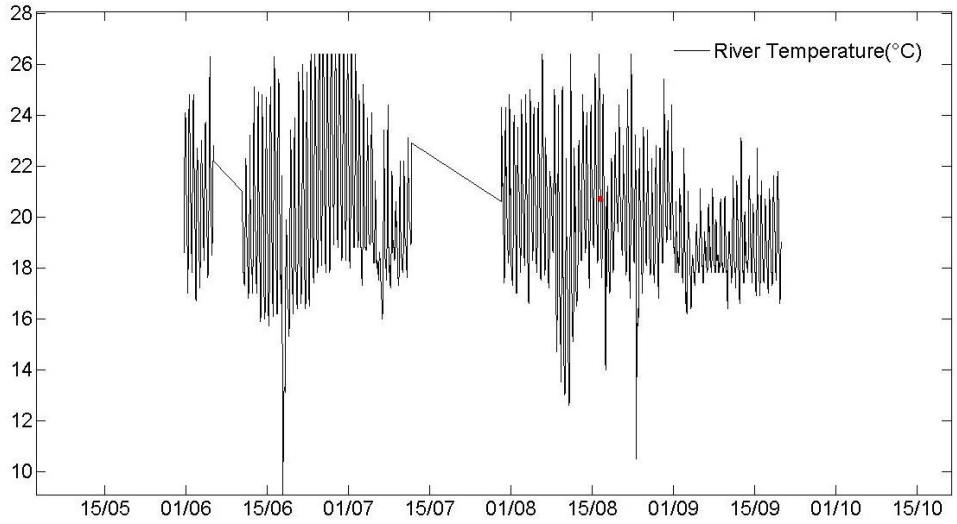

Figure 2.12 Measured river water temperature

The missing river water temperature was estimated from correlations with air temperature (Figure 2.13). During the high flow period (May-September), it was measured with a Vemco minilog TR8k sensor (+0.2°C). The data were collected every week to limit the risk of unrecorded periods. When malfunctioning occurred, a linear regression was fitted to air temperature (T_{river}=0.45*T_{air}+11, r^2=0.79) to replace missing data. During the low flow period, the river water depth never exceeded a few centimeters at the outlet of the Cointzio watershed. This led to a good heat exchange between air and water, as revealed by short period of monitoring of air and water temperature. Based on this specific surveys, the river water temperature was deduced from the adjustment of a linear regression with the air temperature (T_{river}=0.28*T_{air}+13, r^2=0.82).

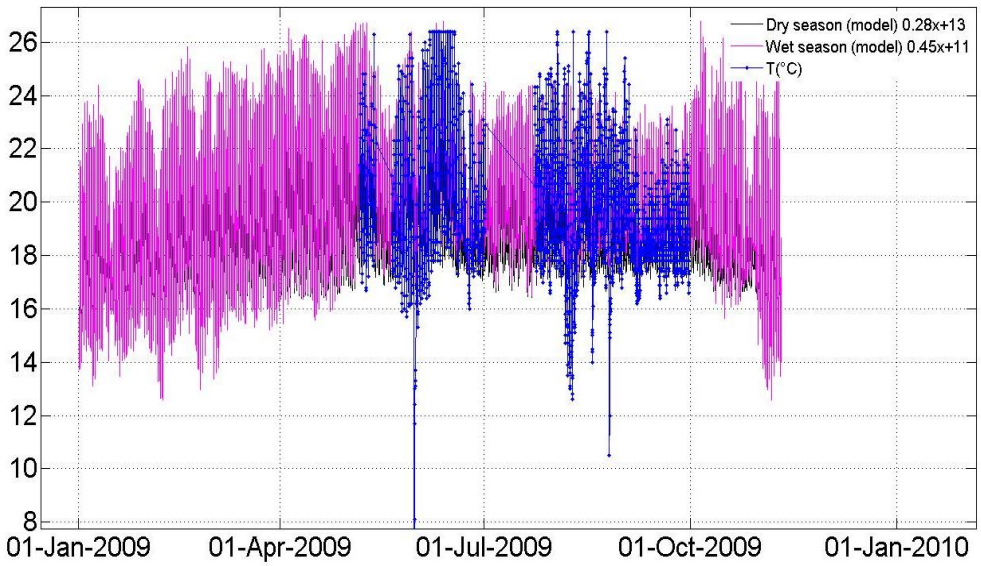

Figure 2.13 Measured and interpolated river water temperature

3.1.2 Hydrodynamics of the water column

First of all, the time series of the vertical temperature profiles at the deepest point P27 of the Cointzio reservoir with the same data in 2009 are shown in Figure 2.14. The point P27 corresponds to the most complete set of data of the reservoir. The panel 2.14a is defined with the vertical axis oriented upward, the origin is at the bottom, and the elevation is defined by meter above sea level. In contrast, in order to be suitable with the structure of the model used in this study, the axis of the panel 2.14b is oriented downward, and the origin is at the water surface. The profiles show an important water level fluctuation of the reservoir with a minimum water depth in June (18.9 m), and a maximum in January (24.3 m). The water level of the reservoir decreases from January to June, and then increases from June to December. The temperature values are presented by colorbar. The reservoir was stratified during eight months, from February to October; it was mixed by the end of October and destratified from November until January. Temperature is homogeneous during November, December, and January due to night time cooling (Figure 2.14).

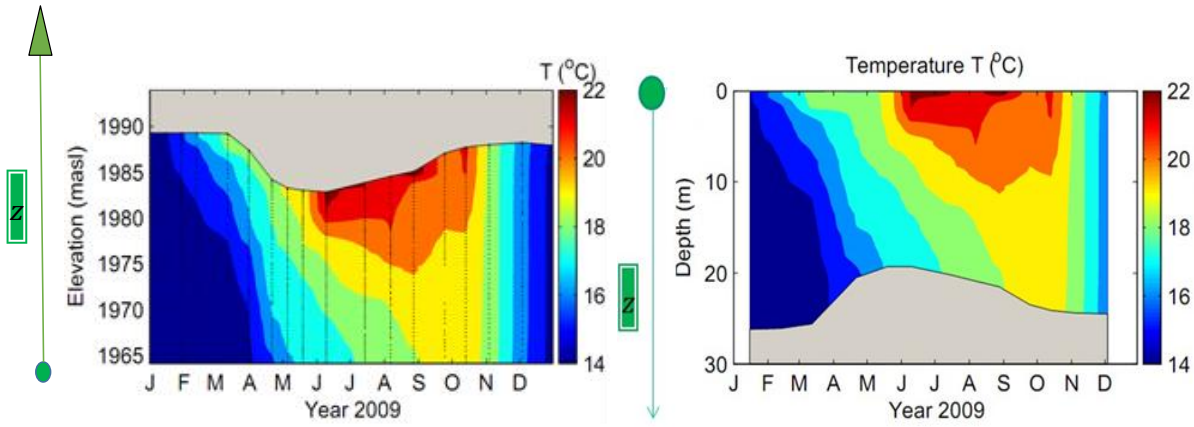

Figure 2.14 Vertical profiles of temperature at P27 in 2009

In the panel 2.14a, the vertical axis has its origin at the bottom and is oriented upward; the grey mask reduces down when the water depth decreases and reversely. The panel 2.14b represents the same data series with another referential. The horizontal axis represents the months of the year 2009.

Figure 2.15 presents the multi-year evolution of the hydrometeorological parameters and the main biogeochemical characteristics of the reservoir. In the light of these time series and of their correlated seasonal evolution, one can distinguish three contrasted periods, namely the "dry season-mixing period", the "dry season-stratified period" and the "rainy stratified period" (respectively the cyan, the white and the grey backgrounds in Figure 2.15). The two and a half years of survey underline the same behavior from year to year. The analysis of

hydrological data in the Cointzio reservoir was done jointly with Valentin Wendling during his master's thesis (2011).

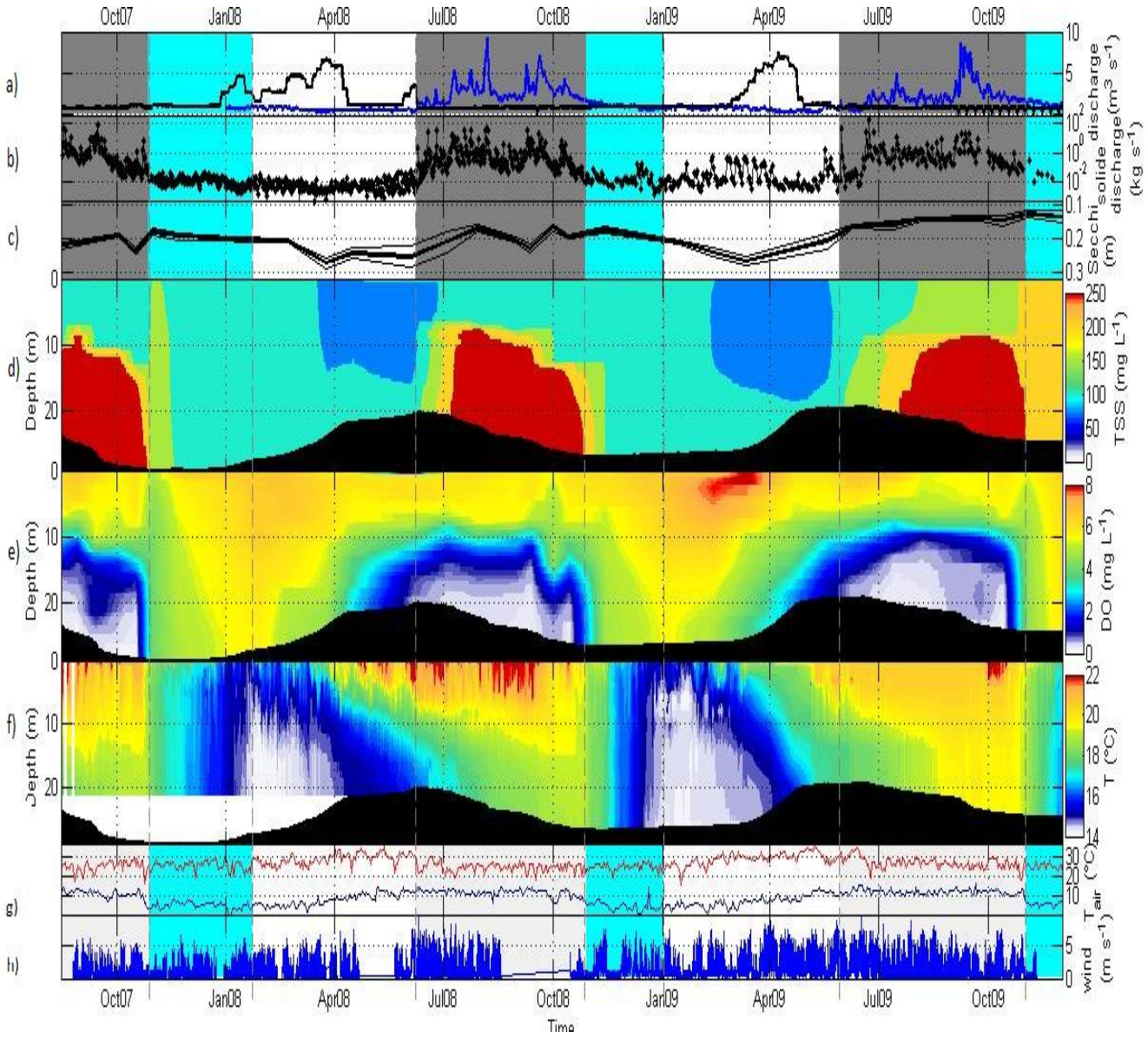

Figure 2.15 Hydro-meteorological response of the Cointzio reservoir (September 2007 to January 2010)

The background colors represents dry season-mixing (cyan), dry season-stratified (white), rainy stratified period (grey).
a) Rio Grande de Morelia River inflow (blue) and dam outflow (black), b) Rio Grande de Morelia River suspended solid load, c) Secchi depth (mean and standard deviation) from all the measurement stations, d) TSS (mg L^{-1}) was estimated from a linear regression to the fortnightly measurements of turbidity (NTU) (see detail in appendix), e) Dissolved oxygen as a function of depth and time, interpolated from fortnightly measurements, f) Temperature as a function of depth and time, measured at 10 (or 30) minutes from the thermal chain, g) Minimal (blue) and maximal daily air temperature (red) measured at the dam, h) Wind speed measured at the dam. The horizontal axis represents the months of the years.

(i) The dry season-mixing period (cyan background in Figure 2.15) extends from the end of October to January. It is characterized by a vertical homogeneous distribution of turbidity (Figure 2.15d), DO (Figure 2.15e) and temperature (Figure 2.15f), which highlights the existence of an efficient physical mixing of the water column. During this period, the water column is cooling, from ~19°C to ~14°C. For operational purposes, it is interesting to note that the mixing is nicely correlated with a drop in the minimum air temperature below a pivot temperature of 10°C (Figure 2.15f). This pivot temperature can be considered as a broad indicator of the transition between periods. This drop in air temperature remains quite stable with a daily minimum value of around 5°C and a maximum value of about 15°C (Figure 2.15g). This drop of air temperature leads to an efficient vertical homogenisation of TSS, DO and water temperature (Figure 2.15d, e and f). The night mixing stops during January and the water column is stratifying until the next fall. The reservoir of Cointzio experiences a single full mixing per year and can thus be classified as a warm monomictic lake, like the majority of Mexican hollow lakes (Alcocer and Bernal-Brooks, 2010).

(ii) The dry season-stratified period (white background in Figure 2.15) extends from January to May. During this period, air daily minimum temperature and solar radiations (not presented) increase (Figure 2.15g). The waterbody is warming up: the water temperature rises from ~15°C to ~21°C at the surface and from ~15°C to ~17°C near the bottom. A thermal stratification builds up, but we can already mention that the temperature gradient remains almost constant over the vertical, and no sharp thermocline is observed (Figure 2.15f). As soon as the stratification develops, the suspended particles are no longer re-homogenized by night-cooling, and sedimentation occurs. Consequently, the Secchi depth increases from ~0.15 m to ~0.25 m (Figure 2.15c) and the TSS of the water column decreases from ~ 40 mg L^{-1} to ~ 10-20 mg L^{-1} (Figure 2.15d). Despite this settling, the presence of very fine particles, colloids and dissolved material maintains a very high level of turbidity in the reservoir of Cointzio (Figure 2.15d). Stratification also affects considerably the biogeochemistry of the reservoir. Near the bottom, one can observe a progressive decrease in DO concentration from about 6 mg L^{-1} in January to anoxic conditions in June. Near the surface, DO remains nearly constant (~6 mg L^{-1}, Figure 2.15e). During this dry season period, a large amount of water is extracted from the reservoir for irrigation purposes. The water budget presented in Figure 2.15a shows that the patterns of riverine input into the reservoir were strongly influenced by the climatic regime of the region. From November to May during the dry season, the inflow was very low, it is almost negligible (0.2 to 1.2 $m^3 s^{-1}$) whereas the outflow was maximum due to irrigation demand, reaching its maximum (up to 7

m^3 s^{-1}). At the same period, the reservoir only provided water for the domestic water plant (base flow of 0,672 ± 0,088 m^3 s^{-1} all along the year; data CONAGUA). As a consequence, the water level decreases of about 10 m at a mean decreasing rate of about 8 cm per day. One can noticed that water consumption for irrigation was more distributed in 2008 (January to April) than in 2009 (March and April).

(iii) The rainy stratified period (grey background in Figure 2.15) starts with the first flood events, in early June. It lasts more than four months and ends in the mid October. The beginning of the rainy season leads to a five folds increase of the baseflow (from ~0.4 m^3 s^{-1} to ~2 m^3 s^{-1}). The maximum water discharge was ~18 m^3 s^{-1} in 2008 (2008/08/07) and was ~22 m^3 s^{-1} in 2009 (2009/09/08). Sediment load magnifies the trends observed on water discharge time series. Hence, sediment discharge increases over four folds during the wet season (Figure 2.15b). As shown on Figures 2.15c and d, the input of sediments in the reservoir is accompanied with an almost simultaneous increase of the turbidity. Secchi depth decreases from ~ 0.25 m to ~ 0.15 m. Near the bottom, the input of sediments is even higher, as highlighted by the TSS time series presented in Figure 2.15d. TSS increases by a seven folds factor, from 5 mg L^{-1} to 37 mg L^{-1}, at 5m depth; and by a ten folds factor, from 13 mg L^{-1} to 140 mg L^{-1}, at 15m depth. This bottom turbidity increase is a direct signature of the successive sediment-driven density currents, which propagate near the bottom after flood events. A nice illustration of these bottom density currents is presented in Figure 2.16a. This situation was observed on 13 September 2007, two days after a major flood event. This flood lasted two weeks, from 9 September 2007 to 23 September 2007. It brought about 10.5 Mm^3 of water and 8400 tons of sediments into the reservoir. Similar situations were observed very frequently during the three rainy stratified period of 2007, 2008 and 2009 (see the complete database in appendix).

The sediment-driven density currents have a clear impact on the annual evolution of the water column temperature profile. As shown in Figure 2.15f, the daily mean water temperature stabilises at about 22°C in the 10 m thick surface layer as a result of the relatively stable air temperature (Figure 2.15g, daily minimum of ~14°C and maximum of ~22°C). Near the bottom, water temperature warms significantly from ~16.5°C to ~19°C during the rainy season. This heating is not due to a heat flux from the surface but corresponds to the progressive injection of hotter water by the density currents. As observed in Figure 2.15e and Figure 2.16b, the successive density currents do not affect significantly the vertical gradient of oxygen. It means that the oxygen consumption rate is significantly higher than the oxygen flux advected by the density currents.

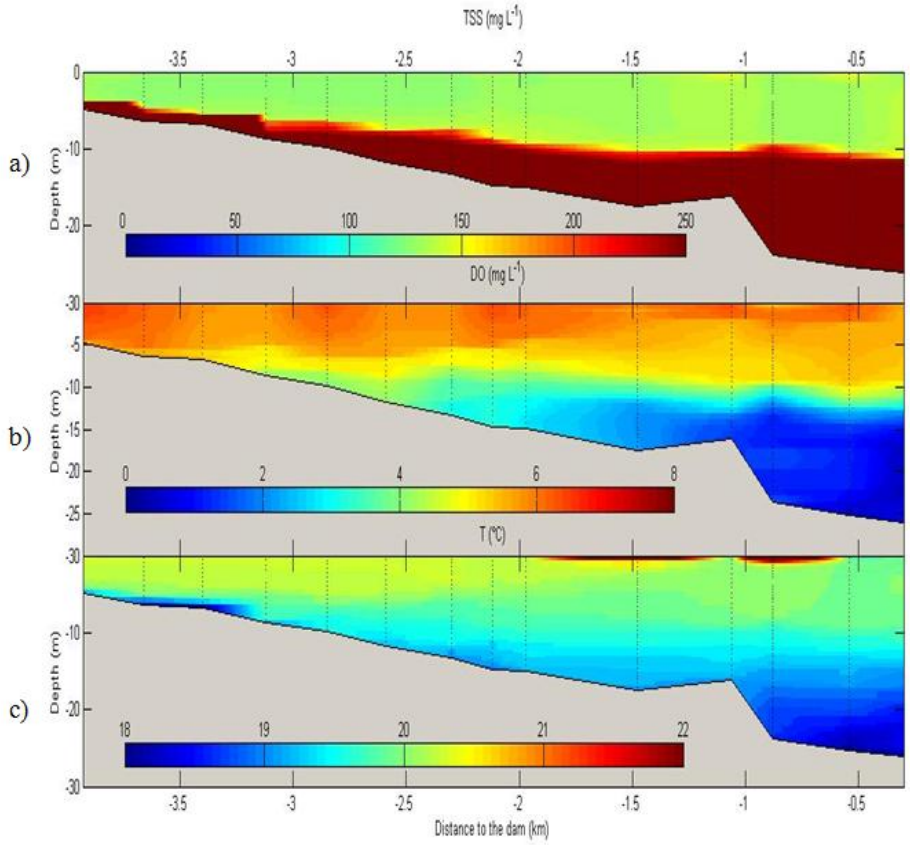

Figure 2.16 Longitudinal evolution of TSS (a), DO (b) and temperature (c) from the Rio Grande mouth (left side) to the dam (right side) on September, 13th 2007.Vertical dotted lines represent the location of individual hydrolab measurements.

Based on the analysis of the field measurements, some preliminary conclusions can be addressed concerning the functioning of the wind-swept tropical turbid reservoir of Cointzio. During the mixing period (from October to January), the strong turbidity (Secchi depth < 0.3 m) does not affect the hydrodynamics and the reservoir is well mixed as any monomictic system is. During the stratified period (from February to September), the functioning differs from the one of typical hollow waterbodies as follows: The majority of the incoming river water is plunging in such a way that the reservoir is filled up from the bottom. The successive sediment-driven currents are even sufficiently developed to advect a significant quantity of heat at the bottom of the reservoir.

It is worth noting that the vertical gradients of TSS and oxygen concentration exhibit a maximum stratification at 10 m depth during the rainy season. Below this water depth, suspended solid increases greatly (~ 40 mg L^{-1} above and ~ 140 mg L^{-1} below) and oxygen concentration drops drastically (~6 mg L^{-1} above and ~0 mg L^{-1} below). This drop is not observed in the temperature profiles, which points out that the thermal stratification does not

act as a physical barrier to the vertical gradients. This level seems to be representative of the upper limit of the hyperpycnal density currents.

3.2 Biogeochemical functioning

3.2.1 Input and output of the reservoir

The analytical results for the samples taken from the inlet of the Cointzio reservoir indicate that the water is of poor quality in the Rio Grande de Morelia River with a degradation that mainly originated from point sources (see discussion in chapter 4, Table 2). The water taken from this river gives high values especially for total P (0.38 ± 0.23 mg L^{-1}), P-PO_4^{3-} (0.11 ± 0.07 mg L^{-1}), NH_4^+ (0.15 ± 0.10 mg L^{-1}) and TSS (2220 ± 1559 mg L^{-1}), which indicates an important input of nutrients to the reservoir.

Figure 2.17 shows temporal variations in TSS, P, N, C and chlorophyll *a* at the inlet and outlet of the Cointzio reservoir. The input P, N and C concentrations were strongly influenced by discharge especially the particulate concentrations inputs linked to TSS dynamics (POC and TP). On average, input concentrations of all substances were higher than their output concentrations (Figure 2.17), indicating that there are some dispersal and dilution, and the internal biological processes taking place in the reservoir partially transform the inputs. For instance, maximum TSS was observed during the wet season with peaks > 10 000 mg L^{-1}. Output TSS concentrations never exceeded 600 mg L^{-1} (Figure 2.17 a, b). Less total phosphorus (TP) and orthophosphate (PO_4^{3-}) exit through the outflow than enters through the inflow. The reservoir could retain phosphorus (i.e. P sediment) (Figure 2.17 c, d). The concentrations of total nitrogen (TN) and nitrate (NO_3^-) through the outflow are less than from the inflow (Figure 2.17 e, f). The inputs of POC and DOC are higher than their outputs. More chlorophyll *a* enters through the inflow than exits through the outflow; this means that concentrations in the river are higher than in the reservoir. This could be due to the deposition at the bottom of the reservoir or consumption by zooplankton (Figure 2.17 m, n). This data set will be used for the calculation of inputs and outputs loads in chapter 4.

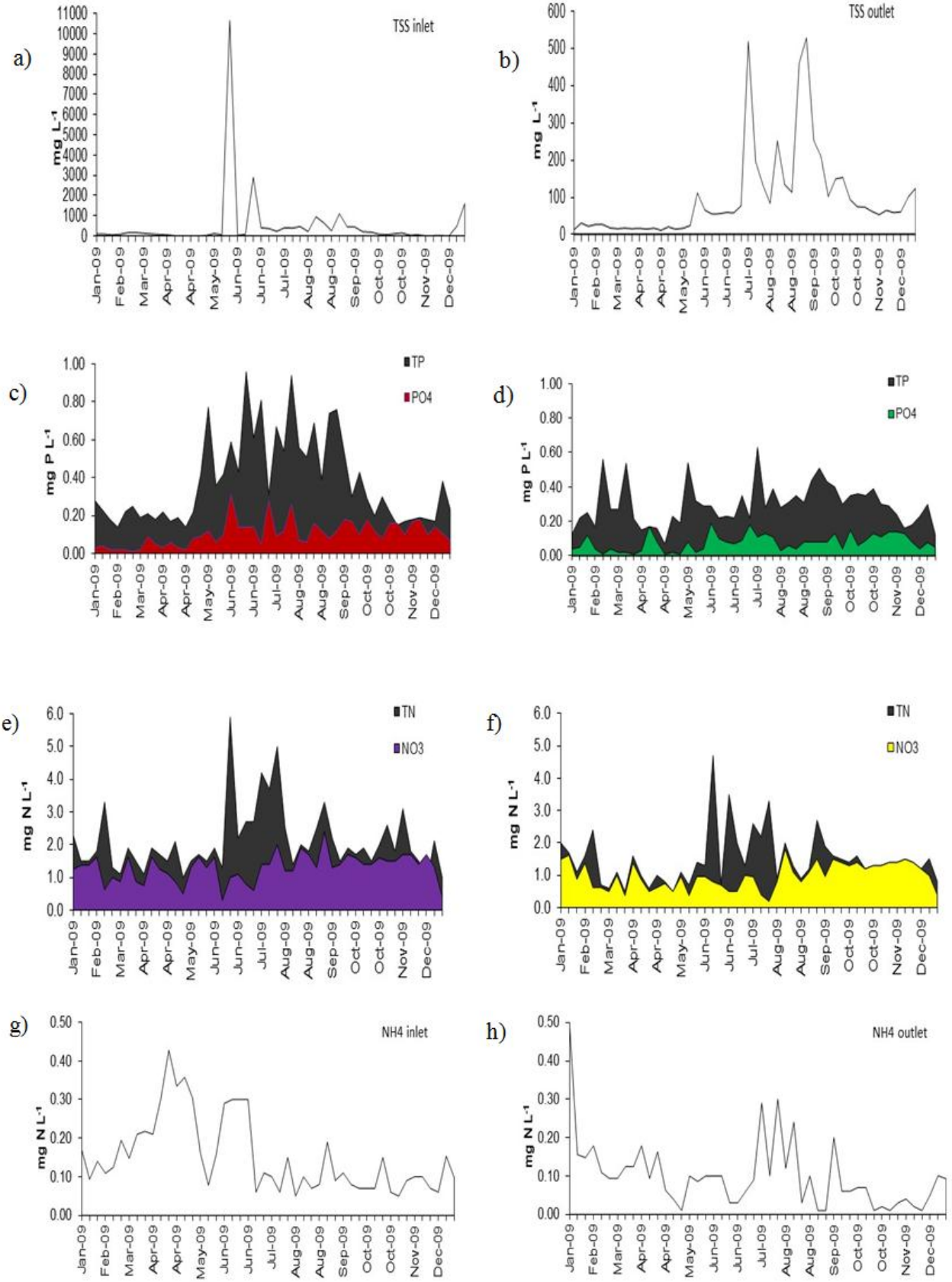
a)
TSS inlet
mg L-1
b)
TSS outlet
mg L-1
c)
TP
PO4
mg P L-1
d)
TP
PO4
mg P L-1
e)
TN
NO3
mg N L-1
f)
TN
NO3
mg N L-1
g)
NH4 inlet
mg N L-1
h)
NH4 outlet
mg N L-1
Jan-09
Feb-09
Mar-09
Apr-09
Apr-09
May-09
Jun-09
Jun-09
Jul-09
Aug-09
Aug-09
Sep-09
Oct-09
Oct-09
Nov-09
Dec-09

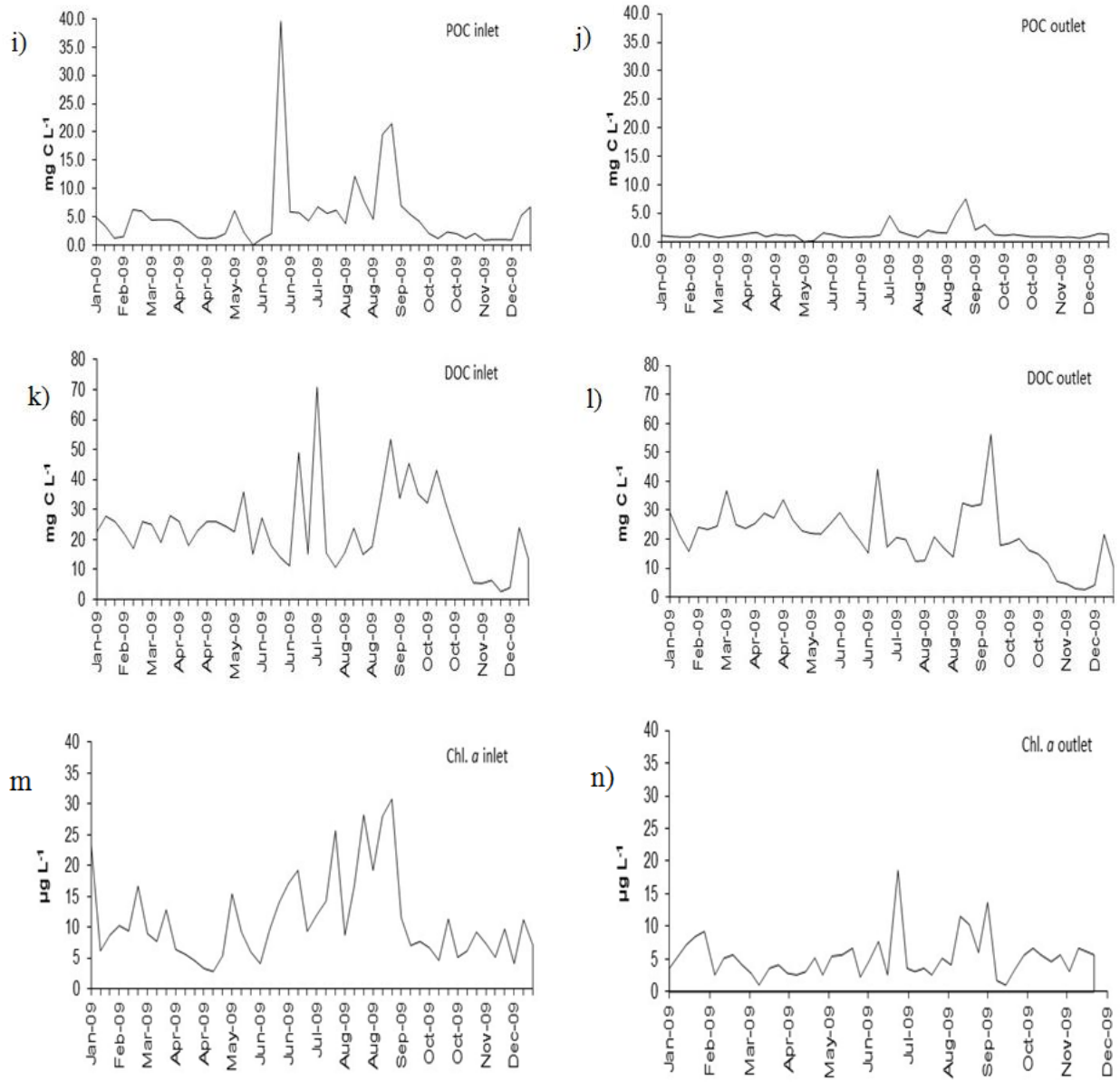

Figure 2.17 Seasonal variations in TSS (a, b), TP, PO_4^{3-} (c, d), TN, NO_3^- (e, f), NH_4^+ (g, h), POC (i, j), DOC (k, l) and chlorophyll a (m, n) at the inlet and outlet of the Cointzio reservoir

3.2.2 Reservoir internal functioning

The Figures 2.18 to 2.25 present the spatio-temporal variations of biogeochemical parameters in the Cointzio reservoir.

During the high flow periods (June to October), suspended solid increased because a large quantity of sediments eroded in the watershed were transported to the reservoir. Sediment concentration was high enough to generate the hyperpycnal flow at the bottom of the reservoir. The bottom turbidity increase is a direct signature of the successive sediment-driven density currents, which propagate near the bottom after flood events (Figure 2.18 and Figure 2.16a).

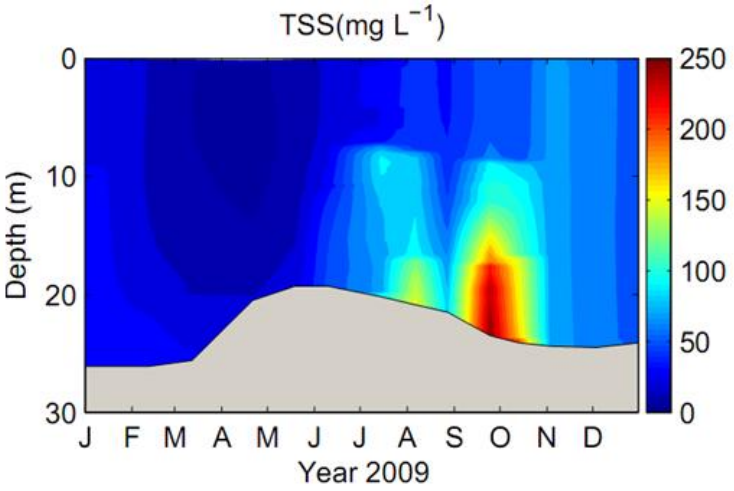

Figure 2.18 Seasonal variations in TSS

From May to the end of October, DO decreased below 1.0 mg L^{-1} at the bottom and extended to the whole hypolimnion (Figure 2.19). This depletion of oxygen could be the result of nitrification and of the benthic mineralization leading to anoxic conditions at the bottom reservoir. Two main sources of bottom organic matters are:

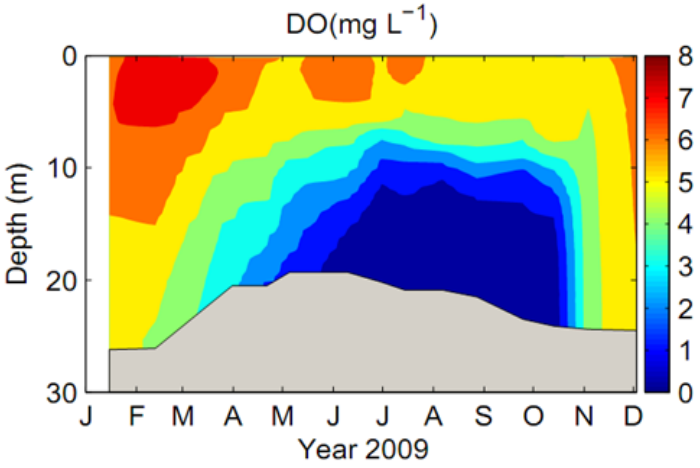

Figure 2.19 Seasonal variations in DO

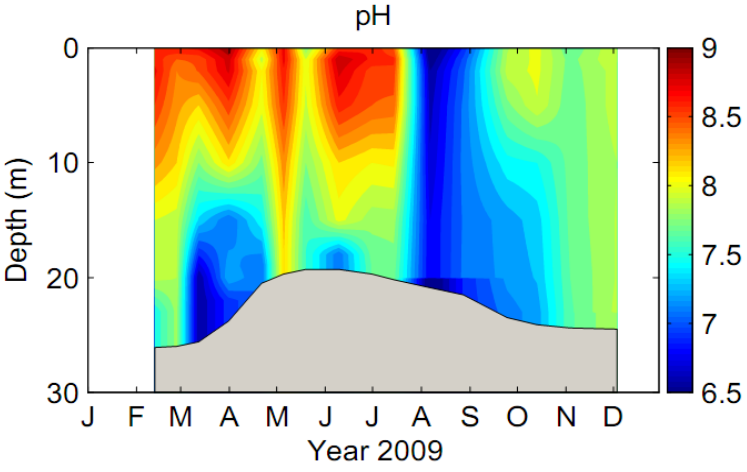

Figure 2.20 Seasonal variations in pH

(i) The production of phytoplankton and its sedimentation, which are dominant during the first period of the year,

(ii) The input of organic matters with the arrival of hyperpycnal sediment flows, which prevail from June to October (Doan et al, 2012).

At the surface, DO remained high (>6.0 mg L^{-1}) because of oxygen production by photosynthesis and an efficient air - water exchange.

Stratification also affected pH in the reservoir (Figure 2.20). The epilimnion water layer towards to alkaline conditions, with a maximum pH value of 9.0 from February to July as a result of the photosynthetic activity at the surface. The pH at the bottom towards to neutrality over time as a result of hypolimnetic anoxia. At the end of August, the pH was at its lowest level with a value of 6.5. During destratification, the pH got back to neutral conditions in the water column (Doan et al, 2012).

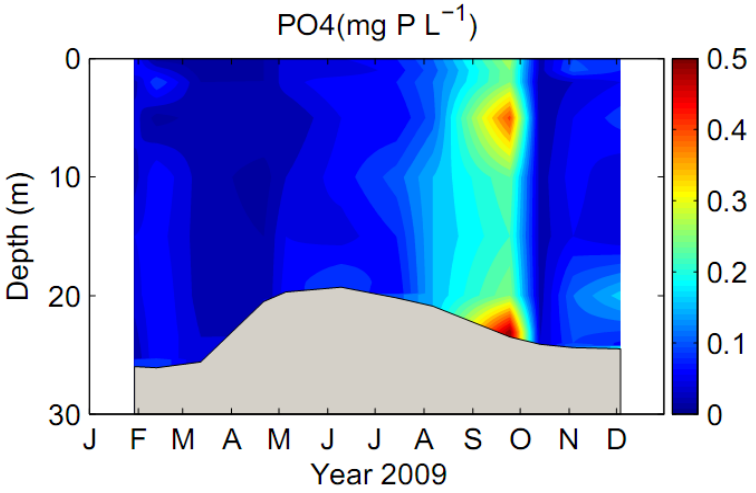

Figure 2.21 Vertical profile of PO_4^{3-}

The results of PO_4^{3-} profile in Figure 2.21 show clearly the significant upward flux of PO_4^{3-} in September - October released by mineralization from sediments thus increasing concentrations in the water column. From January to July, PO_4^{3-} concentrations were not only low in the epilimnion, where they were consumed by primary production of algae but also below in the metalimnion. Late destratification in the end of October led to a sharp decrease in PO_4^{3-} in the hypolimnion due to an increase of the reservoir volume.

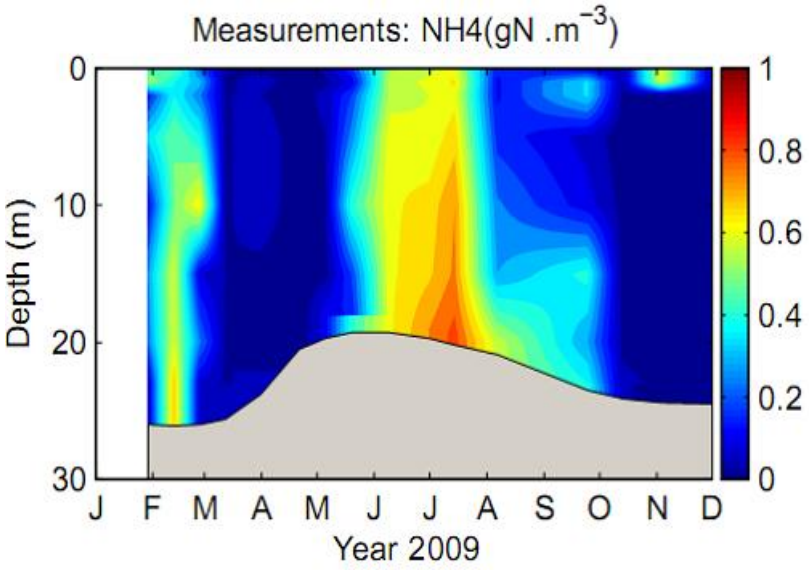

Figure 2.22 Vertical profile of NH_4^+

As a result, the NH_4^+ concentrations in the hypolimnion increased (> 0.6 mg N L^{-1}) (Doan et al, 2012). In general, NH_4^+ concentration in reservoirs may be influenced by atmospheric and riverine inputs, biological uptake, mineralization and nitrification (Dodds, 1993). In the Cointzio reservoir, the NH_4^+ concentrations were low in the epilimnion. The benthic mineralization prevailed from May over the course of stratification and the progressive DO depletion in the hypolimnion leading to release of NH_4^+ from sediments (Figure 2.22). These increasing trends coincided well with the anoxia period identified from May to October, but also with the incoming TSS peaks from the watershed. The benthic mineralization increases during this period resulted from the accumulation of organic matters from inputs and from dead algae sink.

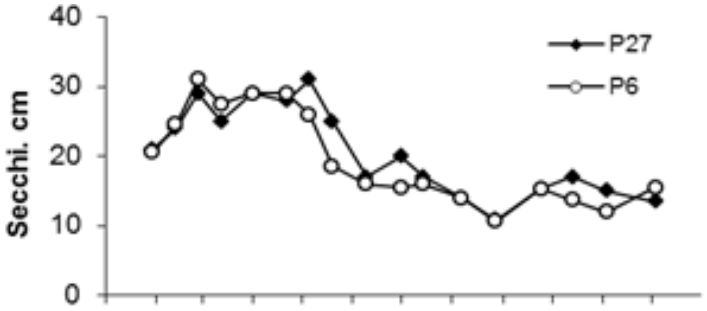

Figure 2.23 Seasonal variations in Secchi depth

Secchi depth presented a very good spatial homogeneity that is pointed out by the good fit between measurements at P6 and P27 (Figure 2.23). Maximum value was between 20 and 31 cm from January to May. With the beginning of the wet season (end of May) and the higher incoming TSS loads, Secchi depth decreased to reach a minimum of 11 cm in September and a mean of 15 cm ± 2 cm from June to December.

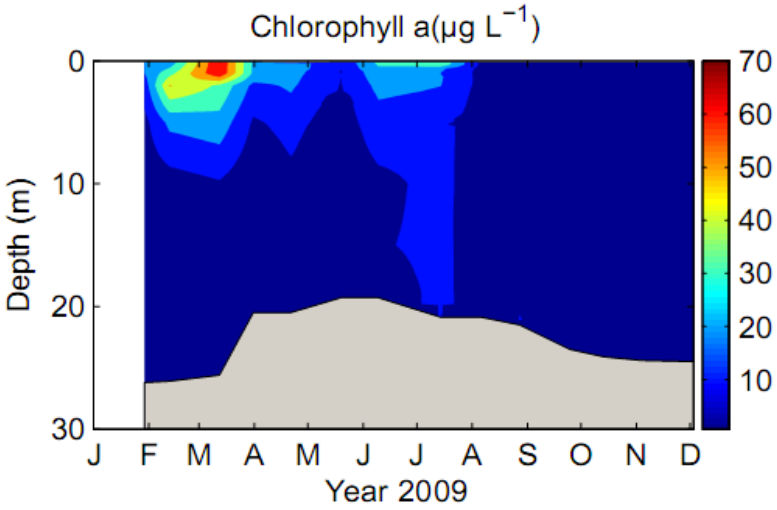

Figure 2.24 Seasonal variations in chlorophyll a

The overall distribution of chlorophyll *a* was well correlated with Secchi depth because of the direct influence of higher TSS values on light penetration. The chlorophyll *a* was high in the top 10 m from January to July, with an average concentration of 30 ± 19 µg L^{-1}. From January to April, the maximum chlorophyll *a*

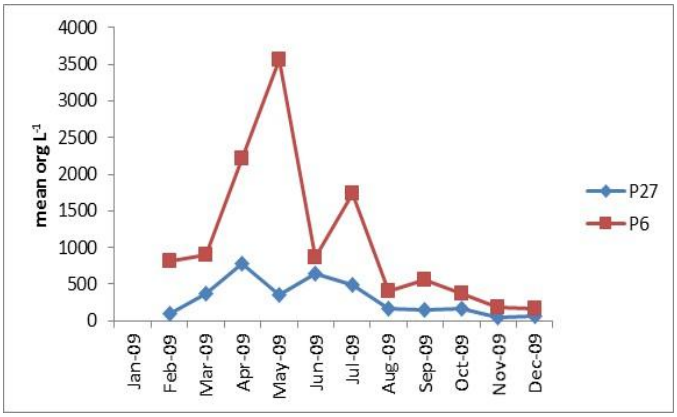

Figure 2.25 Seasonal variations in zooplankton

increased up to 70 μg L^{-1} due to higher light penetration and nutrient availability (Figure 2.24). After reaching the first maximum peak in March, the chlorophyll *a* was reduced drastically by grazing of zooplankton, especially at the beginning of June and then recovered during the following months (Figure 2.25). During the wet season, the successive flood events supplied a large quantity of TSS which reduced Secchi depth to less than 0.2 m. This hindered photosynthesis and chlorophyll *a* dropped below 10 μg L^{-1}.

Conclusions of chapter 2

The turbid tropical Cointzio reservoir, located in the Trans - Mexican Volcanic Belt, has been built since 1940 for the drinking water supply of the city of Morelia, and for downstream irrigation. In order to identify the origin of nutritive pollutions upstream of the Cointzio reservoir, eight water samples sites in the watershed were taken to measure discharge (Q), DO, and nutrients monthly during 2009. Moreover, daily samples were taken at the reservoir inlet and outlet to measure concentrations of C, N, P and TSS during 2009. In addition, at the reservoir inlet, discharges were measured at the time step of ten minutes (Duvert et al, 2011). These measurements were used to identify the boundary conditions of the reservoir. Two and a half years of measurements data (temperature, turbidity, conductivity and DO) from 2007 to 2009 were carried out at a fortnightly to monthly basis at 16 field stations regularly distributed along the longitudinal axis; and the water samples were taken at the deepest point of the reservoir and at the middle of the reservoir to measure biogeochemical parameters (TSS, chlorophyll *a*, DOC, POC, pH, and nutrients (TP, PO_4^{3-}, NH_4^+, and NO_3^-) during the intensively monitoring year 2009. This strategy of monitoring of the reservoir and its watershed was designed in order to evaluate the status of dynamics and water quality of the reservoir.

Based on the thermal classification proposed by previous studies (Hutchinson, 1975), the Cointzio reservoir can be classified as a warm - monomictic lake, like the majority of Mexican hollow lakes. The stratification takes place eight months from February to September and with complete mixing from October to January due to night time cooling. Photosynthetic activity of the phytoplankton was responsible for the basic pH values in the epilimnion during the productive period (January to May). With the first floods at the beginning of the rainy season, the turbidity of the water column increased at the same time as the phytoplankton dropped rapidly. During the second part of the year, the reservoir became anoxic in the hypolimnion as a result of the intense benthic respiration and decomposition processes leading to nutrients release. The analyses of two and a half years of hydrodynamic and one year of biogeochemical measurements data are presented to provide (i) a first

assessment of the dynamics of the reservoirs and (ii) some input data for further water quality modelling.

Chapter 3. NUMERICAL MODELLING OF THE COINTZIO RESERVOIR

This chapter describes the models used to simulate the hydrodynamics and the biogeochemistry of the Cointzio reservoir. The advantages and limitations of the models are also discussed. The model definition, model equations, all processes and modelling approach are presented in detail in this chapter. Some of the results of modelling simulations are showed in chapter 4 and most of them are developed in chapter 5.

1. Introduction

Numerical modelling is a relevant tool to assess response of complex systems, integrating different factors. Moreover, the application of mathematical modelling is necessary in order to design management strategy, test functional hypotheses and simulate future states for a system in response to environmental alteration. Many biogeochemical lake models have been developed during the last thirty years to evaluate the lake ecosystems, propose management strategies, improve the understanding of lake ecosystems, synthesize and communicate quantitative knowledge about important processes in reservoirs. Lake models can be used to test and improve our understanding of lake ecosystems functioning by comparing model results with measured data (Mieleitner & Reichert, 2006). Many models are assuming a one-dimensional vertical approach. They are able to describe vertical variations of physical and chemical parameters (Goudsmit et al, 2002).

An overview of several models of different levels of complexity is given by Jøgensen & Bendoricchio, (2001). In the hydrologic community, there have been some interesting discussions regarding the best way to use numerical models. According to Grayson & Bloschl, (2000), a balance between model complexity and data availability must be found to optimize the model performance. A model requiring many input parameters (at high spatial and temporal frequencies) may suffer from a lack of data acquisition. In such situation, the uncertainty resulting from the calibration of unmeasured parameters may be larger than the decrease in model structure uncertainty.

It may be questioned to what extent a one-dimensional model adequately represents a natural system such as a lake or a reservoir. The response is not unique and clearly depends on timescales and whether the study is conducted for research or operational purposes. The application of 2D or 3D models is usually limited by the capacity of operators to measure a full set of variables at an adequate resolution, both in time and space. The assumption of the one dimensionality is justified for lakes of small or medium size as horizontal variations of temperature and concentrations of substances are not significant in most cases. This is

because vertical transport in density stratified lakes is about 10^3-10^5 times smaller than the horizontal one (Imboden & Wüest, 1995). Furthermore, gradients in the horizontal direction are generally small when compared to the vertical gradients that exist, and are rapidly annihilated by gravitational adjustments. Based on these considerations, we decided to use one-dimensional models for our simulation. This choice was also sustained by two extensive 3D campaigns of measurements of temperature, turbidity and dissolved oxygen conducted in December 2005 and May 2006. During these surveys, thirty three vertical profiles, distributed regularly on the water surface, were acquired (Figure 2.10 in chapter 2). The field results of these two measurements did not reveal significant lateral heterogeneities. It has been thus decided to focus the long term monitoring effort on the temporal variations along the longitudinal axis. Along that line horizontal gradients are negligible, at the exception of short term periods of 3-5 days corresponding to flood related hyperpycnal flows (Susperregui et al, 2009). Besides that, the vertical profiles of water quality variables realized fortnightly at two distinct locations of the reservoir (points P27 and P6 see Figure 2.10 in chapter 2) confirmed that longitudinal gradients are negligible for long term applications. On the other hand, we did not have enough data to simulate a multi-dimensional model integrating all parameters. Indeed, given the difficulty of setting realistic initial conditions for all water quality variables in a multi-dimensional model and also the difficulty of knowing all of the input fluxes in the spatial scale of the model, a multi-dimensional approach would have a highly uncertain outcome in the case of the Cointzio reservoir.

2. The physical models applied

The physical modelling approach aims at identifying the physical factors that drive the hydrodynamics of the Cointzio reservoir in order to constitute a good basis for an ecological model to survey water quality. It was applied to predict the seasonal development of temperature stratification and destratification in the Cointzio reservoir during the years 2008 and 2009.

2.1 Aquasim model

2.1.1 Overview

Aquasim is a vertical 1D model used to reproduce physical and biogeochemical processes in natural and technical aquatic systems (Reichert, 1998). It is flexible due to an open structure that allows modifications and integration of new processes. Aquasim is organized into two parts, the first deals with the modelling of the thermal structure of the reservoir; the second is related to biogeochemical modelling that allows inclusion of phytoplankton, nutrients, organic matter and dissolved oxygen dynamics. It uses the DASSL (Differential Algebraic

System Solver) algorithm (Petzold, 1983); in which the time step and the integration order are constantly adapted following the evaluation of convergence criteria. The physical Aquasim model is based on turbulence closure schemes where the rates for vertical transport are related to the turbulent kinetic energy (k).

The Aquasim model performs the four tasks of simulation, identifiability analysis, parameter estimation and uncertainty analysis. Due to the similarity of the mathematical techniques involved, identifiability and uncertainty analyses are combined to yield sensitivity analysis (Reichert, 1998). The first task of Aquasim is to allow the user to perform model simulations. By comparing calculated results with field measurements, such simulations reveal whether certain model assumptions are compatible with measured data. The Aquasim's second task is to perform sensitivity analysis with respect to a set of selected variables. This feature allows the user to calculate linear sensitivity functions of arbitrary variables with respect to each of the parameters included in the analysis. The third important task of Aquasim is to perform parameter estimations automatically for a given model structure using measured data. This is not only important for obtaining neutral estimates of parameters, but is also a main prerequisite for efficiently comparing different models (Reichert, 1998).

2.1.2 Data inputs and model outputs

Figure 3.1 gives an overview of the main model processes. The simulation is driven by meteorological data, inflow and outflow data and heat flux. Output was compared with the field data collected at a mid-lake station P27 since they represent the most complete set of data for the reservoir. The output data include the vertical temperature profiles of the reservoir in relation with depth and time.

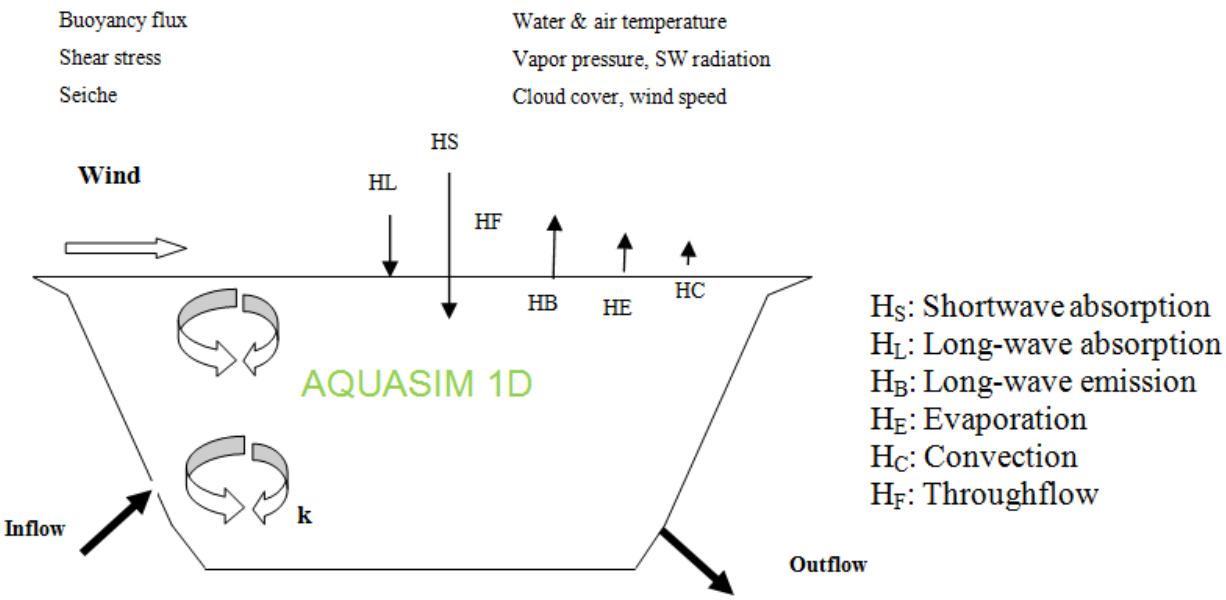

Figure 3.1 Schematic overview of the Cointzio reservoir simulation model

Vertical exchanges create the thermal structures of the reservoir as most of the heat transfer takes place at the reservoir surface, and then progressively affects all the layers downwards. The model discussed here takes into account the main mixing processes: The advection related to throughflow, the eddy diffusion induced by wind and internal seiches, the mixing due to surface waves and free convection. The simulation is driven by data of cloud cover, wind speed, vapor pressure, radiation, and water and air temperature. Our modelling approach required the following input data.

Meteorological data

The meteorological data were acquired from the report of Synoptics Raw Data provided by the Centre of Météo Morelia, Mexico. The air temperature, shortwave radiation and relative humidity were measured every 10 minutes; atmospheric pressure was measured every hour. The measurement of wind speed was recorded every 10 minutes with the maximum velocity of 8 m s^{-1}. The cloud cover was estimated from shortwave radiation data during the day, and it was interpolated for the night. The light absorption coefficient was calculated from secchi depth that was measured every month at P27.

Inflow and outflow data

In the case of the Cointzio reservoir, the water input in the model was placed at the level of the hypolimnion layer. This is because the inflow, which comes almost exclusively from the Rio Grande de Morelia River, is driven by sediment load and sink to generate a hyperpycnal flow. The outflow occurs through the gates located at about 20 m depth of the reservoir. In

addition, the temperature for the inflow is required while that of the outflow is not necessary for the simulation. Inflow temperature was measured for several months or when the data was not available, it was deduced from the adjustment of a linear regression with the air temperature (see Fig. 2.11).

Heat flux

The net heat flux between water and atmosphere at the surface is expressed as indicated below. The notations, units and parameter values of heat flux are summarized in Table 3.1.

Table 3.1 Notations and units for meteorological data

Parameters	Definition	Units or assigned values
Bowen	Bowen ratio, corrected for altitude	0.52 mbar K^{-1}
C	Cloud cover	[0 ÷1]
ea	Vapor pressure	mbar
es	Saturated vapor pressure at lake surface temperature	mbar
B	buoyancy flux	W kg^{-1}
p1, p2	Sensitivity parameters for H_L and H_E	estimate parameters
ra	Reflection of infrared radiation at lake surface	0.03
rs	Reflection of solar radiation at lake surface	0.08
T	Temperature	°C
$\hat{T}_{air}$	Absolute air temperature	°K
$\hat{T}_{surf}$	Absolute temperature of lake surface	°K
u10	Wind speed 10 m above lake surface	m s^{-1}
z	Vertical coordinate	m
Z	Water surface	m
γ	Coefficient for seiche energy decay	$6.2*10^{-11}$ $kg^{-1/2}$ m^{-1}
λ	Light absorption coefficient	m^{-1}
ρ	Water density	kg m^{-3}
б	Stefan-Boltzmann constant	$5.67*10^{-8}$ W m^{-2} K^{-4}
Q	Lake outflow	m^3 s^{-1}
Cp	Specific heat of water	4200 J kg^{-1} K^{-1}
Tz	Mean inflow temperature	°C
Ao	Lake surface area	m^2
Secchi	Secchi depth	m

The net heat flux into a reservoir can be expressed as follows:

$$H_{net} = H_S + H_L + H_B + H_E + H_C + H_F \qquad (3.1)$$

Where the six terms on the right-hand side of the equation (3.1) represent the heat fluxes associated with the processes of absorption of direct and diffuse global radiation (shortwave) from sun and atmosphere (H_S), the absorption of infra-red radiation (long-wave) from atmosphere (H_L), the emission of infra-red radiation (long-wave) from lake surface (H_B), the exchange of latent heat between lake surface and atmosphere due to evaporation (H_E), the convective exchange of sensible heat between lake surface and atmosphere (H_C) and through flow (H_F) (Livingstone D. M., et al, 1989). The influence of other heat exchange processes, such as the reflection of infra-red radiation by mountains surrounding the lake or the heat exchange between water body and sediments, has been assumed to be negligible and will not be considered further in this work. The radiative absorption terms (H_S and H_L) are always positive and the radiative emission term (H_B) is always negative, whereas the terms representing non-radiative heat exchange (H_E, H_C, H_F) can take either positive or negative values.

Short wave absorption H_S

Short wave radiation originates from the sun. Some of the solar radiation is reflected at the water surface and the remainder penetrates into the lake. Most of the radiation that penetrates is absorbed in the water column and converted to heat. According to Henderson–Sellers 1986, forty percent of the solar radiation is absorbed at the lake surface; the rest penetrates into the epilimnion with an attenuation light absorption coefficient λ. The absorption coefficient λ is estimated using the Beer - Lambert law.

$$H_S = H_{SO} \cdot (1 - rs) \cdot e^{-\lambda z} \qquad (3.2)$$

Where H_{so} is the measured solar radiation above the water surface that is obtained by meteorological data every 10 minutes, rs and λ are the reflection and extinction coefficient of the lake water. The latter can be approximated by $\lambda = 1.84/Secchi^{0.61}$.

Long-wave absorption H_L

The long-wave absorption term H_L is the most difficult of the six terms to assess and is also the most prone to computational error. The atmosphere is treated as an infrared radiator with an emission coefficient E_L (Anderson, 1954).

$$H_L = p1 * (1 - ra) * E_L * б * \hat{T}air^4 \qquad (3.3)$$

$$E_L = 1.24 * (1 + 0.17 * C^2) * (\frac{ea}{\hat{T}air})^{1/7} \qquad (3.4)$$

H_L was found to vary between 320 W m^{-2} (February) and 417 W m^{-2} (March) and has an annual mean of 367 W m^{-2} (Figure 3.2).

Long-wave emission H_B

Long-wave radiation is emitted from the surface of a lake according to the Stefan-Boltzmann law for a "grey body" with an emission coefficient of 0.97 (Sweers, 1976).

$$H_B = -0.97 * \sigma * \bar{T}surf^4 \quad (3.5)$$

H_B is not only the most accurately determinable term of H_{net}, but also the term with the greatest absolute magnitude. H_B varies between -378 W m^{-2} in December and -413 W m^{-2} in October and has an annual mean of -397 W m^{-2} (Figure 3.2).

Evaporation and condensation H_E

Evaporation is the conversion of liquid water to water vapor; condensation is the conversion of water vapor to liquid water. Both of these reactions are accompanied by a flux of heat. Evaporation from the lake surface extracts heat from the lake and results in cooling of the water surface. Condensation extracts heat from the atmosphere and adds it to the water surface, resulting in heating at the water surface. Thus, evaporation cools the lake surface, and condensation heats the lake surface. Evaporation and condensation are also accompanied by a flux of water; thus they affect the total water budget of the lake.

The heat loss of a lake occurring as the result of evaporation at the lake surface is described by the following empirical formula.

$$H_E = -p2 * (es - ea) * [4.4 + 1.82 * u10 + 0.26 * (\bar{T}surf - \bar{T}air)] \quad (3.6)$$

Where es is saturated vapor pressure at lake surface temperature

es= fw*10*(0.7859+0.03477*(T*Z+273))/(1+0.00412*(T*Z+273))

fw= 0.61*(1+1e-006*patm*(4.5+6*1e-005*(T*Z+273)^2)): Transfer function

ea = Rh*ew/100: Vapor pressure

Rh is measured relative humidity

ew=fw*10*(0.7859+0.03477*(T*Z+273))/(1+0.00412*(T*Z+273))

p2 is sensitivity parameter for longwave absorption

H_E lies between -4 W m^{-2} in November and -90 W m^{-2} in February and has an annual mean of -47 W m^{-2} (Figure 3.2).

Convection H_C

The ratio of H_C to H_E is proportional to the ratio of ($\bar{T}surf - \bar{T}air$) to (es - ea). The constant of proportionality is called the Bowen coefficient (Bowen, 1926). Hence, from the equation (3.6):

$$Hc = Bowen * H_E * \frac{(\hat{T}surf - \hat{T}air)}{(es - ea)} \qquad (3.7)$$

H_C varies from -24 W m^{-2} in December to 15 W m^{-2} in April and has an annual mean of -5 W m^{-2} (Figure 3.2).

Throughflow H_F

It is assumed here that the influence of groundwater on the heat balance is negligible. It is also assumed that the temperature of the outflow is identical to that of the reservoir (T), H_F is computed as follows:

$$H_F = Q * Cp * \rho * \frac{Tz - T}{Ao} \qquad (3.8)$$

H_F, which varies between 0 W m^{-2} and 16 W m^{-2} and has an annual mean of 2 W m^{-2}, is small in magnitude compared to the other terms and can be neglected in most cases (Figure 3.2).

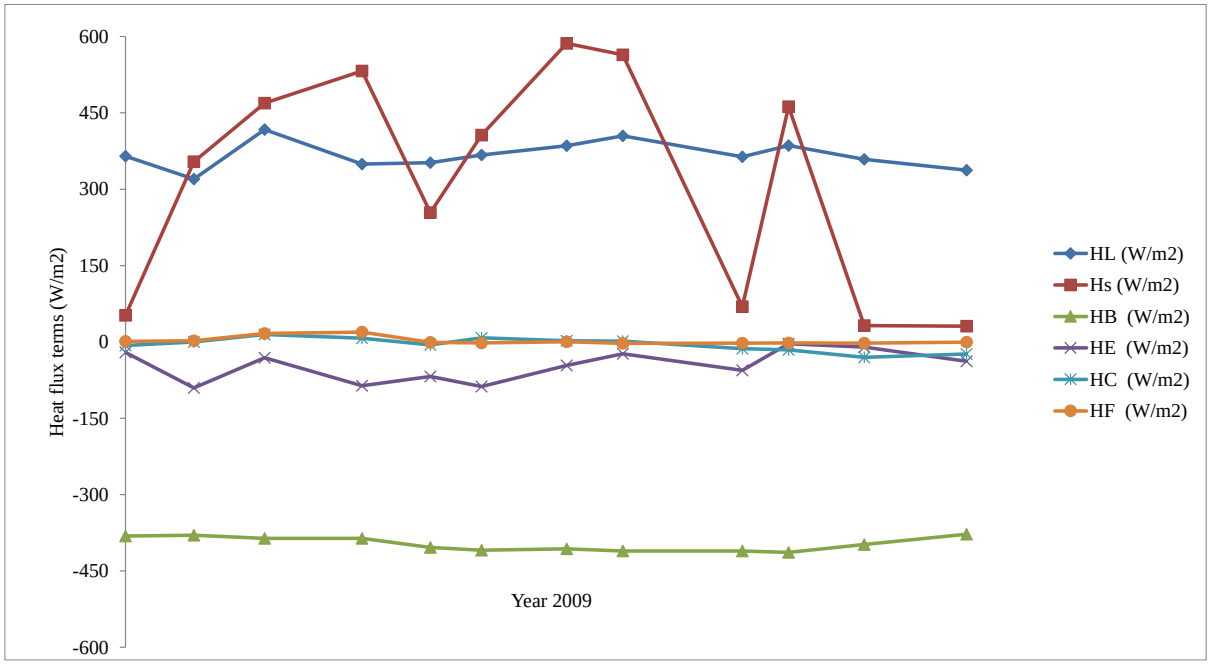

Figure 3.2 Heat flux terms of the reservoir in 2009, calculated according to eqn. (3.1)

The contributions of the various heat exchange processes to the heat balance are illustrated in Figure 3.2. Their magnitudes differ greatly. The two processes involving the absorption and emission of long wave radiation by the lake play the greatest role in determining the heat balance. The mean value of H_L is 367 W m^{-2} and that of H_B is -397 W m^{-2}.

Turbulent diffusivity in Aquasim model

Two equations are used in Aquasim model giving the vertical diffusivity coefficient Kz in lakes or reservoirs.

(i) The turbulent diffusion coefficient Kz=max(cmu*$(tke)^2$/eps/Pr, Kz_min) from turbulent kinetic energy (tke) in Aquasim model is the first option to be used for simulating.

Where cmu =0.09: Coeffiecient of turbument model

tke: Turbulent kinetic energy

eps: dissipation

Pr: Prantl number

Kz_min= 0.05 m2/d

(ii) The second formula of vertical turbulent diffusion coefficient Kz_N2 is a function of Brunt Vaisala frequency N2; If N2>0 then min (Kz_max,a_Kz/(N2)$^{b\_Kz}$) else Kz_max endif;

Where Kz_max=10m^2/day

N2 $= \frac{-g\partial\rho}{\rho\,\partial z}$: Brunt Vaisala frequency

a_Kz, b_Kz are calibration parameters for diffusivity

Density of water

There are two main factors that make lake water more or less dense than about 999.843 kg/m3. The first is water temperature and the other is sediments. This is important for the case of the Cointzio reservoir due to high input of suspend sediments from the watershed.

$\rho = 999.843+0.001*(65.4891*T-8.56272*T^2+0.059385*T^3) + 0.63*TSS$

Where ρ is water density, T is temperature, and TSS is concentration of suspended sediments

2.1.3 Sensitivity analysis

The most useful sensivity function which is distinguished by Aquasim is the absolute – relative sensivity function, $\sigma_{y,p} = \frac{1}{y}\frac{\partial y}{\partial p}$ (SensAR)

Where y is a variable calculated by Aquasim and p is a model parameter represented by a constant variable or by a real list variable. This function measures the absolute change in y for a 100% change in p.

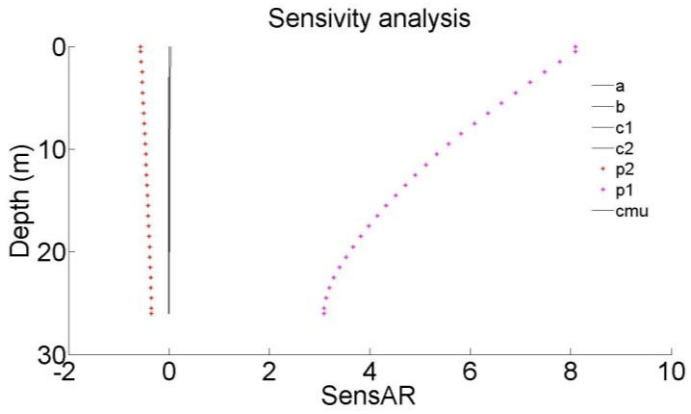

Figure 3.3 Sensivity function of some parameters in Aquasim model

In this model, the sensitivity has been tested for seven model parameters with the sensitivity analysis tool of AQUASIM (Reichert 1994). The Figure 3.3 shows the dependence of the

sensitivity function (SensAR) of a calculated temperature with respect to the model parameters (a, b, c1, c2, c3, p1, p2, cmu).

It becomes evident from the Figure 3.3 that the parameters (a, b, c1, c2, cmu) are insensitive with calculated temperatures since $\sigma_{y,p} \approx 0$. The sensitivity of calculated temperature with respect to p1 has its maximum at a depth of zero and decreases exponentially. The dependence of temperature on the parameters such as p2 leads to a shape of the changes in temperature, with negative signs. The positive signs indicate that the calculated temperatures increase with increasing values of model parameters. The negative signs indicate that the calculated temperatures decrease with increasing values of model parameters. This leads to a correlation between the estimates of these parameters.

2.1.4 Model calibration

For the prediction of the stratification and destratification of the Cointzio reservoir during the year 2009, the simulation should start in January. A vertical resolution of 1 m and a time step of 30 minutes were chosen to simulate the thermal structure in the Cointzio reservoir. The maximum water depth of the reservoir in 2009 was fixed at 26 m. The data set collected at the deepest point P27 was used to calibrate the model. All simulations were implemented within the lake module of the software Aquasim 2.1 (Reichert 1994, 1998).

Initial conditions

Initial values for all solved variables need to be set before any computation. They included data for the first day of the simulation.

Boundary conditions

The predictive ability of one – dimensional lake water temperature models is highly dependent on the treatment of boundary conditions (i.e., the heat exchange between water and the atmosphere) and the determination of mixing dynamics in the epilimnion and the hypolimnion (Fang & Stefan, 1996). Therefore, boundary conditions are important in determining the mathematical solutions for many physical problems.

In this study, at the surface the net heat flux H_{net} can be used as a boundary condition (Neumann type) for the temperature equation. Long-wave absorption H_L and emission H_B, evaporation H_e, convection H_C, and through flow H_F are assumed to operate only at the surface layer. Furthermore, about 40% of the incoming shortwave radiation is kept in the upper few centimeters of the water column. The remaining fraction decays through the water column following the standard Beer–Lambert law (Octavio et al., 1977). The factor 86400

converts the time units of "s" used for the formulation of heat flux to the time units of "d" used for the simulation. These equations are described below:

$$H_{\_toplayer} = \left((1 - rs) * H_S + H_L + H_B + H_C + H_E + H_F\right) * Z * \frac{86400}{(Cp * \rho)} \text{ for the top layer} \quad (3.9)$$

$$H_{\_layersbelow} = 0.6 * (1 - rs) * Hs * \exp(-\lambda * z) * \frac{86400}{(Cp * \rho)} \text{ below} \quad (3.10)$$

2.1.5 Technical results: Limitation of the physical Aquasim model to reproduce the hydrodynamics in the Cointzio reservoir

After calibration of the physical Aquasim model with the data set of 2009, it is possible to simulate the temperature profile in the Cointzio reservoir. In the figures below, we compare the model results with the measured temperature profiles for the same year.

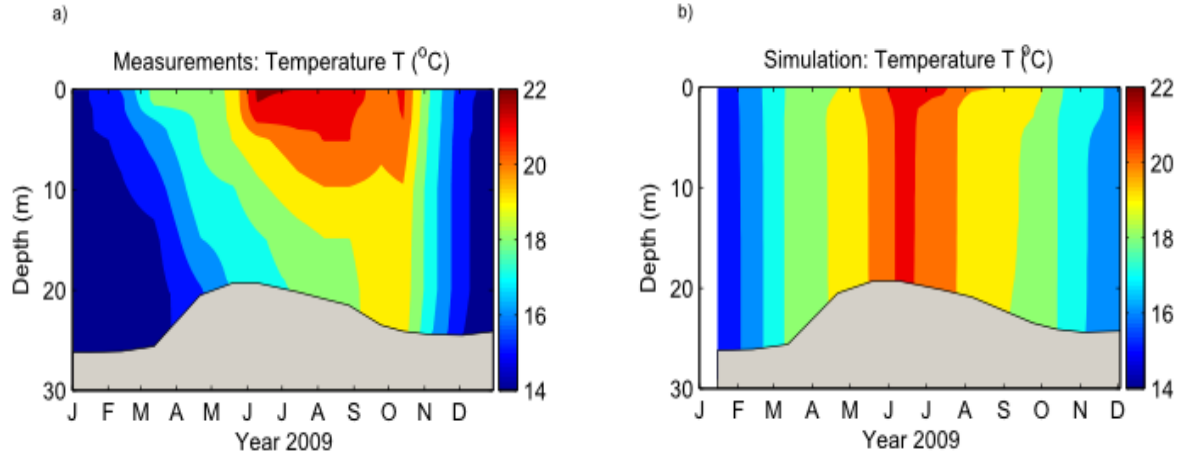

Figure 3.4 Measured and simulated temperature profile during the year 2009

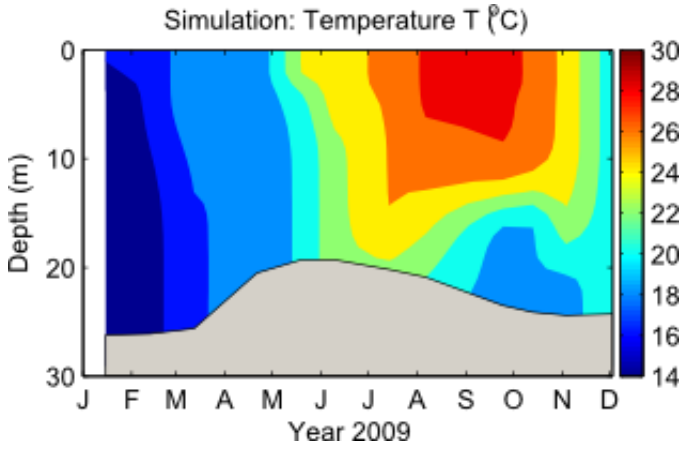

Figure 3.5 Simulated temperature profile after changing the input conditions

Figure 3.4b shows the simulated temperature results of the reservoir in 2009. They are in the range of the values of the measured temperature (from 14 °C to 23 °C). However, the vertical mixing does not fit with the measurements; simulated temperature profiles are almost

homogeneous, which clearly overestimates the vertical mixing. This is probably due to very high water turbidity as well as high winds from the Cointzio reservoir. The input of turbulent kinetic energy is indeed proportional to third power of wind speed and it is difficult to create a stratification since sunlight does not penetrate in depth because of the very high turbidity (Wendling, 2011). In order to verify these assumptions, we tried changing the conditions of turbidity and wind speed, for instance we increase secchi depth 5-fold, and decrease wind speed 2-fold. As a result of this new simulation using Aquasim, the model could now reproduce some stratified conditions as shown in Figure 3.5. Although in this virtual case stratification was obtained, the simulated temperature profile was not meaningful since the input conditions were not realistic.

Below, the results of turbulent diffusivity from turbulent kinetic energy submodel in Aquasim model at some different depths during the calibration year 2009 are presented in Figure 3.6. The values of turbulent diffusivity are quite strange, most of them got zero all year long, except at the end of the year.

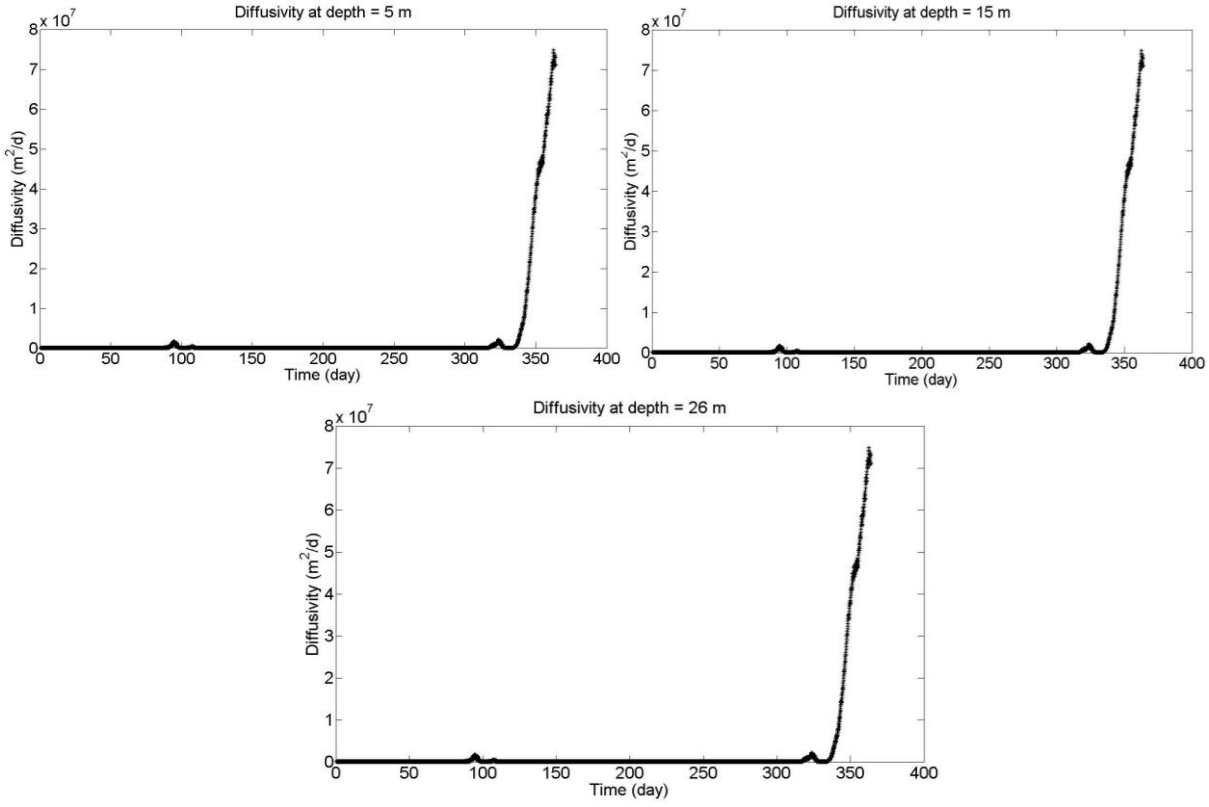

Figure 3.6 Turbulent diffusivity at some different depths during the year 2009

2.1.6 Conclusions and discussion

The turbulent kinetic energy submodel in Aquasim cannot deal properly with the case study of the Cointzio reservoir which is subjected to very high water turbidity and high wind. These physical features actually induce water mixing all year around.

With the current version of the Aquasim model, only one velocity direction is considered (except if we artificially change directions by adding negative signs); therefore wind speeds can accumulate to unreasonable high values. Under these circumstances, the wind stress which is always in the same direction could explain why turbulent kinetic energy simulated in Aquasim overestimates mixing even though the model is able to create stratification in the Cointzio reservoir if we reduce wind by two and increase secchi depth to at least 1.0 m - 1.5 m. As the physical section of Aquasim model revealed to be inappropriate, we applied a k-ε model to predict the seasonal development of temperature stratification and turbulent diffusivity for the wind swept turbid Cointzio reservoir. Actually, the mixing model implemented in Aquasim is a modified version of the k-epsilon model.

2.2 k- ε model

2.2.1 Overview

The k-ε model by Goudsmit et al, 2002, which is based on the buoyancy–extended k-ε model (Rodi, 1984), describes the vertical density structure and mixing in the water column. It was applied for the simulation of physical lake processes. The basic idea behind the k-ε approach, the most popular two-equation turbulence model, is the combination of the budget of turbulent kinetic energy (k), representing the source of turbulent mixing, with the budget of the dissipation rate (ε). Turbulent mixing is driven by the energy introduced into the system by surface shear stress from wind forcing, and by buoyancy due to heat loss to the atmosphere or heat input to the monimolimnion[2] (Schmid et al, 2003). Turbulence dissipation is the rate at which turbulence kinetic energy is converted into thermal internal energy.

Apart from the classical k sources, shear and buoyancy, Goudsmit et al, (2002) introduced an additional term to account for boundary mixing from internal seiches (Wüest & Lorke, 2003). The vertical diffusivities are then calculated from k, ε and stratification (N2) (see detail in section 2.2.2). The resulting time series of vertical turbulent diffusivity were then used as the input data for the Aquasim biogeochemical model.

In the present version, there are four different types of forcing files that can be used in the k-ε model. They are (i) wind speed, water surface temperature and solar radiation; (ii) wind

[2] Monimolimnion is the lower, dense stratum of a meromictic lake that does not mix with the waters above

speed, air temperature, solar radiation and vapor pressure; (iii) wind speed, air temperature, solar radiation, vapor pressure and cloud coverage; (iv) wind speed, water surface temperature, heat flux and solar radiation. Based on our field measurements, the second option was applied for this simulation. As a result, the model inputs of water inflow (Qin), outflow (Qout), temperature of inflow, light absorption, wind data, solar radiation, and water surface temperature were considered in this study. After simulation, the physical k-ε model gave the results of vertical mixing that was calculated as turbulent diffusivities ($m^2\ s^{-1}$). The resulting turbulent diffusivities profiles were then used as input for the biogeochemical Aquasim model in order to simulate DO, chlorophyll *a* and nutrients.

2.2.2 Model equations (Goudsmit et al, 2002)

The k-ε one dimensional model equations are based on the assumption that horizontal gradients are negligible, which is usually fulfilled for small or medium-sized basins. The basic set of equations in the one dimensional vertical k-ε model is described below and a list of model constant values used in the equations is given in Table 3.2.

List of equations in the one dimensional vertical k-ε model

$$\frac{\partial T}{\partial t} = \frac{1}{A}\frac{\partial}{\partial z}\left(A(v'_t + v')\frac{\partial T}{\partial z}\right) + \frac{1}{\rho_0 c_p}\frac{\partial H_{sol}}{\partial z} + \frac{dA}{dz}\frac{H_{geo}}{A\rho_0 c_p} \qquad (3.11)$$

$$\frac{\partial u}{\partial t} = \frac{1}{A}\frac{\partial}{\partial z}\left(A(v_t + v)\frac{\partial u}{\partial z}\right) + fv \qquad (3.12)$$

$$\frac{\partial v}{\partial t} = \frac{1}{A}\frac{\partial}{\partial z}\left(A(v_t + v)\frac{\partial v}{\partial z}\right) - fu \qquad (3.13)$$

$$\frac{\partial k}{\partial t} = \frac{1}{A}\frac{\partial}{\partial z}\left(Av_k\frac{\partial k}{\partial z}\right) + P + P_{seiche} + B - \epsilon \qquad (3.14)$$

$$\frac{\partial \varepsilon}{\partial t} = \frac{1}{A}\frac{\partial}{\partial z}\left(Av_\epsilon\frac{\partial \epsilon}{\partial z}\right) + \frac{\epsilon}{k}\left(c_{\epsilon 1}(P + P_{seiche}) + c_{\epsilon 3}B - c_{\epsilon 2}\epsilon\right) \qquad (3.15)$$

The shear stress production P ($W\ kg^{-1}$) and the buoyancy production B ($W\ kg^{-1}$) are given by

$$P = v_t\left(\left(\frac{\partial u}{\partial z}\right)^2 + \left(\frac{\partial u}{\partial z}\right)^2\right) \qquad (3.16)$$

$$B = -v'_t(N^2) \qquad (3.17)$$

Where N is the Brunt Väisälä frequency defined by

$$N^2 = -\frac{g}{\rho_0}\frac{\partial \rho}{\partial z} \qquad (3.18)$$

The turbulent viscosity and diffusivity can be calculated using the relation of Kolmogorov and Prandtl

$$v_t = c_\mu \frac{k^2}{\epsilon} \quad (3.19)$$

$$v'_t = c'_\mu \frac{k^2}{\epsilon} \quad (3.20)$$

The turbulent diffusivities for turbulent kinetic energy (k), and for dissipation rate (ε) are

$$v_k = \frac{c_\mu}{\delta_k} \frac{k^2}{\epsilon} \quad (3.21)$$

$$v_\epsilon = \frac{c_\mu}{\delta_\epsilon} \frac{k^2}{\epsilon} \quad (3.22)$$

The production of TKE due to internal seiche P_{seiche} (W kg^{-1}) was expressed by Schmid et al, (2003).

$$P_{seiche} = \frac{1}{A} . \frac{\partial A}{\partial z} . \frac{\gamma}{\rho_o A_B} . E_{seiche}{}^{3/2} \left(1 - 10. \sqrt{C_D}\right) \quad (3.23)$$

The energy balance for the internal seiche motion was described based on the ideas of Gloor et al, (2000).

$$\frac{dE_{seiche}}{dt} = PW - LS \quad (3.24)$$

PW (W) is the production of seiche energy by wind forcing

$$PW = \alpha . A . \rho_{air} . C_{10} . (u_{10}{}^2 + v_{10}{}^2)^{3/2} \quad (3.25)$$

LS (W) is the loss of internal seiche energy by friction

$$LS = -\gamma . E_{seiche}{}^{3/2} \quad (3.26)$$

Where:

z is the positive upwards axis, T (°C) is the temperature, u and v (m s^{-1}) are the mean horizontal velocity components with respect to x and y direction, k (J kg^{-1}) is the TKE per unit mass, and ε is the TKE dissipation rate (W kg^{-1}).

ρ_o (kg m^{-3}) and c_p (J kg^{-1} K^{-1}) represent the reference density and the specific heat of lake water respectively.

A (m^2) is the surface area of the lake at depth z, H_{sol} (W m^{-2}) is the shortwave solar radiation penetrating the water, H_{geo} (W m^{-2}) is the geothermal heat flux, and f (s^{-1}) is the Coriolis parameter.

ν and ν_t are the molecular and turbulent viscosity, ν' and ν'_t are the molecular and turbulent diffusivity of temperature, and ν_ε and ν_k (m^2 s^{-1}) are the turbulent diffusivities of energy dissipation and TKE, respectively.

A_B (m^2) is the area of the lake bottom boundary, C_D is the bottom friction coefficient (0.002), ρ_{air} (kg m^{-3}) is the density of air, u_{10} and v_{10} (m s^{-1}) are the East and North component of wind speed measured at 10 m height above the water surface.

The wind drag coefficient C10 depends not only on the wind speed U10 (measured at standard 10-m height above surface), but also on the presence and on the state of the surface waves. The constant of proportionality α is a model parameter which gives the fraction of the total wind energy introduced at the lake surface which is transferred to the seiche motion. In general, these two model parameters are subject to model calibration.

Table 3.2 List of constant values used in the k-ε Lake model

Model constants	$c_{\epsilon 1}$	$c_{\epsilon 2}$	$c_{\epsilon 3}$ (B<0)	$c_{\epsilon 3}$ (B>0)	δ_ϵ	δ_k	c_μ	c'_μ	v'(m^2 s^{-1})	v (m^2 s^{-1})	H_{geo} (W m^{-2})
Values	1.44	1.92	-0.4	1.0	1.3	1.0	0.09	0.072	$1.5*10^{-7}$	$1.5*10^{-6}$	0.1

2.2.3 Model calibration and validation

Calibration and validation are required for both the physical and biogeochemical parts of the model. Once calibration is achieved, validation is always required to get a picture of the model reliability (Jørgensen et al, 1995). In practice, validation is achieved when predictions from a model that has been calibrated and verified with one data set, give a good approximation of the behavior of a second data set (Beck, 1987). This means that a calibrated model must be compared to data not used in the calibration to determine whether the model is applicable to cases outside the calibration data set. Once complete, validation indicates that the model can be used as a tool to make prospects about the system for which it was calibrated.

We chose to calibrate the model using the data collected in 2009 at station P27, where the reservoir was deepest, because it corresponds to the most complete set of data. The model was validated using the set of data gathered at the same point for the year 2008. In the validation year 2008, the turbidity was lower and the water level was higher than that of the calibration year 2009. All other processes evaluated simultaneously at the same time step of 30 minutes and the same vertical resolution of 1 m in this study.

In most cases, the parameters p1, p2, α, C10, and/or qNN were used for parameter estimations (Goudsmit et al, 2002), where p1 and p2 are scaling the heat fluxes, qNN determines the vertical distribution of the seiche energy dissipation. However, in our case the water surface temperature was used as the boundary condition for temperature at the water atmosphere interface so it does not make any sense to do a parameter estimation for p1 and

p2. The other three parameters would be possible but qNN did not vary a lot so the default value was used as qNN=0.75. This led to two model specific parameters that needed to be fitted to reproduce the monthly measured temperature profiles for the calibration year 2009 and these were validated for the year 2008; they are the scaling factor for the wind energy transfer to the internal seiches (α), and the coefficient defining wind drag (C10). The wind drag coefficient C10 depends not only on the wind speed u10, but also on the presence and on the state of the surface waves. The typical values of C10 range from 0.0011 to 0.0021 (Wüest & Lorke, 2003). The constant of proportionality α is a model parameter which gives the fraction of the total wind energy introduced at the lake surface which is transferred to the seiche motion. These were then used to do model calibration and validation for the Cointzio reservoir.

Simulation for the calibration year 2009 with the real flow data Qin # Qout.

The k-ε model was calibrated on the basis of data collected with the inflow and the outflow data of 2009. In principle we could include reservoir level fluctuations in the k-ε model, but this variable can not be implemented in Aquasim model. In Aquasim, the software automatically generates additional inflow when the outflow is larger than the inflow, and vice versa. Therefore, we have to use an average lake level.

Simulation for the calibration year 2009 with the assumption Qin = Qout.

In order to perform a simulation using the k-ε model, it was assumed that the outflow data of the Cointzio reservoir is equal to the inflow data in 2009. The lake surface elevation is assumed to be constant in the model by closing the water balance with the surface outflow.

Simulation for the validation year 2008 in case of Qin = Qout.

The model was validated using the set of data at the same point P27 of the year 2008 but the estimated parameters used were taken from calibration of the year 2009.

The variation of measured and simulated temperature with time and the difference between observed and simulated results for the years 2009 and 2008 are presented in Figure 3 of the paper Ecological Modelling (see chapter 5).

2.2.4 Conclusions and discussion

The physical approach was deployed to simulate the thermal structure of a reservoir in order to build a basis for the biogeochemical model to survey water quality in the Cointzio reservoir. The physical Aquasim model described here was based on the solution of advective – diffusive transport equation by finite differences. A thirty minutes time step and one-meter space step were used to quantify the large scale vertical exchanges in the reservoir and were well suited to study the seasonal behavior of the reservoir using a reasonable

amount of computing time. However unfortunately, the physical part of the Aquasim model cannot deal with the case of the Cointzio reservoir which suffers from very high water turbidity and high wind. This caused mixing all year long. The reason could be that the wind stress is always considered to be in the same direction by Aquasim; therefore wind speeds can result in buildup of unrealistically strong currents.

The k-ε model accurately reproduced mixing and stratification in the Cointzio reservoir (see the results in Figure 3 of chapter 5). The parameters of k-ε model were well estimated with the most numerous data to ensure a precise calibration in 2009. The validation of the model was then successfully applied to the year 2008, which ensures a reasonable predictability making this numerical model useful in water management. Water temperatures closely followed the measured profiles, which was of particular interest in order to simulate water quality. The time series of turbulent diffusivities obtained from the k-ε model were added as a function of depth and time for the biogeochemical Aquasim model. The results from physical k-ε model, after coupling with the biogeochemical model, will be useful to assess the impact on water quality and to perform projection scenarios. However, there are some restrictions.

The first restriction is no feedback between biogeochemistry and stratification/mixing since we first simulate the mixing and then the biogeochemistry. We cannot simulate any potential influences that biogeochemistry could have on mixing, for example, the change in stratification because of increased or decreased light absorption due to phytoplankton. The second restriction is that the influence of particles on density can not be included. Finally, the last limitation comes from the fact that in principle we could include lake level fluctuations in the k-ε model, but then it can not define later in the Aquasim model; therefore, we have to use an average lake level.

3. Biogeochemical model (Aquasim)

3.1 Overview

A biogeochemical advection-diffusion-reaction model (Omlin et al, 2001a, 2001b) based on the Aquasim software (Reichert, 1994) was adapted to simulate the biogeochemical cycling in the reservoir. The lake compartment of Aquasim can be used to describe the stratification of the water column, vertical mixing and advection of substances dissolved or suspended in the water column, sedimentation, and resuspension of particles, exchange of dissolved substances between water column, and pore water of the top sediment layer, advective and diffusive exchange between an arbitrary number of sediment layers, and transformation processes in the water column as well as in the sediment layers (Reichert, 1994).

Aquasim, was first developed to model mesotrophic lake Zürich, and was then applied to oligotrophic Ohrid lake (Matzinger et al, 2007) and to various lake types (Mieleitner and Reichert, 2006), also in a tropical region (tropical Itezhi –Tezhi reservoir, Kunz et al, 2011). In this study, the Aquasim biogeochemical model was calibrated to measured DO, chlorophyll *a*, and nutrients. The water balance, solar radiation, water surface temperature, mixing, as well as the initial conditions were directly adapted from the k-ε model. Vertical grids of 1 m and input data with the time step of 30 minutes were used in the model. The time step of output data was adjusted by the software depending on stability criteria for the solution of the differential equation system.

3.2 State variables

The Aquasim biogeochemical model describes the dissolved species: Phosphate, ammonium, nitrate and oxygen; and the particulate species: Zooplankton, algae, inert and degradable organic particles.

The biological part of the model is represented by algae and zooplankton. Biodegradable and inert organic matters include organic particles resulting from inputs, from death of algae and zooplankton and also from zooplankton excretion as fecal pellets. The phosphorus contents of algae, and organic matter are separate state variables because the variable stoichiometry of primary production leads to a variable phosphorus content of these particles. On the other hand, zooplankton is described with a constant phosphorus content according to the Redfield stoichiometric ratio (Redfield et al, 1966). In addition, the phosphorus content resulting from phosphate adsorption by sinking particles is considered as a state variable. According to the explanation of this process given by Hupfer et al, 1995, this state variable is denoted inorganic phosphorus. Phosphate, ammonium and nitrate are the most relevant nutrients and together with dissolved oxygen represent the dissolved state variables of the model.

Table 3.3 State variables in the Cointzio reservoir adopted from Omlin et al, (2001a)

State variables	**Unit**	**Description (concentration of…)**
Dissolved species		
S_HPO4	gP m^{-3}	Phosphate-P
S_NH4	gN m^{-3}	Ammonium-N
S_NO3	gN m^{-3}	Nitrate-N
S_O2	gO m^{-3}	Dissolved oxygen
Particulate species		
X_ALG	gDM m^{-3}	Algal biomass (excluding algal P)

X_P_ALG	gP m^{-3}	Organic phosphorus in algae
X_ZOO	gDM m^{-3}	Zooplankton biomass
X_S	gDM m^{-3}	Biodegradable dead organic material
X_I	gDM m^{-3}	Inert dead organic material (OM)
X_P_S	gP m^{-3}	Organic P in biodegradable dead OM
X_P_I_S	gP m^{-3}	Organic P in inert dead organic material
X_P_I	gP m^{-3}	Phosphates adsorbed to X_S

3.3 Mass balance equations

The reservoir equations solved by Aquasim consist of a combination of a conventional advection –diffusion equation for the water column (Ulrich et al, 1995) with a sediment model describing an arbitrary number of sediment layers, and with a k-ε model turbulence model (Rodi, 1984; Burchard and Baumert, 1995) that has been extended by a simple model of energy storage in seiche motion in the lake basin. The user can specify the coefficient of vertical turbulent diffusion as a given function of time and space, but it is also possible to use a parameterization depending on the stability of the water column and on turbulent kinetic energy and dissipation. In this subsection, the full set of equations is described (Finger et al, 2007).

For each dissolved state variable, the model numerically solves the equation:

$$\frac{\partial C}{\partial t} = \frac{1}{A}\frac{\partial}{\partial z}\left(AK_z\frac{\partial C}{\partial z} - QC\right) + r_C \qquad (3.27)$$

For particulate state variables, a sedimentation term is added to the equation, which accounts for vertical transport due to sedimentation and for the loss of the particles to the sediment.

$$\frac{\partial C}{\partial t} = \frac{1}{A}\frac{\partial}{\partial z}\left(AK_z\frac{\partial C}{\partial z} - QC\right) + r_C + v_{sed,C}\left(\frac{\partial C}{\partial z} - \frac{C}{A}\frac{\partial A}{\partial z}\right) \qquad (3.28)$$

Where C is the concentration of the substance, A (m^2) is the lake area as a function of depth, K_Z (m^2/s) is the vertical diffusivity, Q (m^3/s) is the vertical water flow due to the deep water intrusions, r_C is a term including all sources and sinks of the substance, t is the time (s) and z (m) is the vertical dimension positive upwards.

$v_{sed,C}$ (m/s) is the (positive downwards) sedimentation velocity, and the two parts of the last term are the settling of particles and the removal of particles from the water column when they reach the sediment surface.

3.4 Model processes

The biogeochemical model comprises subroutines for phytoplankton production and loss, nutrient cycling and dissolved oxygen dynamics. Algae biomass is represented in the model as the concentration of chlorophyll *a*. At each time step and in each model layer, the set of equations that describe these processes are solved. Figure 3.5 shows the interrelationships between the main ecological state variables in the model.

Lake water quality models often describe the processes occurring in the sediments in less detail than the ones occurring in the water column. Usually, only the mineralization process is considered in the sediments (Omlin et al, 2001a) as is the case for the present model.

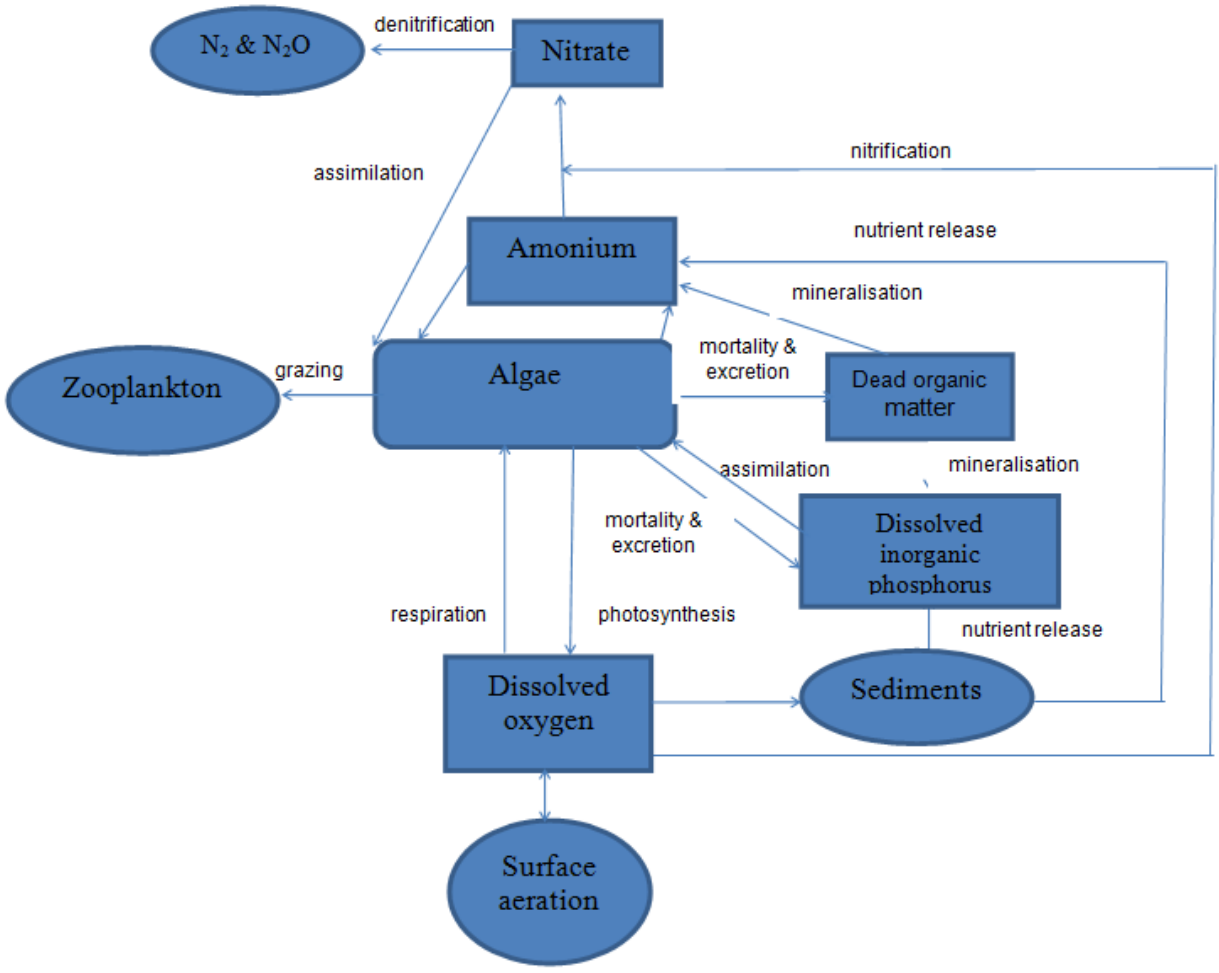

Figure 3.7 Relationship between the main state variables in Aquasim, shown in boxes, and the biogeochemical processes represented in the model. Note that physical processes of inflow, outflow and settling are not included (adapted from Hamilton & Schladow, 1997)

Table 3.4 Process rates (in order of appearance)

State variable	Unit	Description
growth_ALG	gDM/m^3/d	Growth of algae
resp_ALG	gDM/m^3/d	Respiration of algae
death_ALG	gDM/m^3/d	Death of algae
growth_ZOO	gDM/m^3/d	Growth of zooplankton
resp_ZOO	gDM/m^3/d	Respiration of zooplankton
death_ZOO	gDM/m^3/d	Death of zooplankton
P_uptake	gP/m^3/d	Adsorption of orthophosphates to organic particles
nitrification	gN/m^3/d	Nitrification
mineral_aero	gDM/m^3/d	Aerobic mineralization in water column
mineral_anox	gDM/m^3/d	Anoxic mineralization in water column (denitrification)
mineral_anaero	gDM/m^3/d	Anaerobic mineralization in water column
mineral_aero_sed	gDM/m^3/d	Aerobic mineralization at sediment surface
mineral_anox_sed	gDM/m^3/d	Anoxic mineralization at sediment surface (denitrification)
mineral_anaero_sed	gDM/m^3/d	Anaerobic mineralization at sediment surface
miner_bg	gDM/m^3/d	Background mineralization (oxidation of reduce substances)

3.5 Modelling approach

A two steps procedure was chosen for the evaluation of the water quality model. Vertical mixing was calculated as turbulent diffusivities Kz ($m^2\ s^{-1}$) based on the physical k-ε model. The resulting Kz profiles were then used as input for the Aquasim biogeochemical model in order to simulate biogeochemical cycling in the reservoir.

To model reservoir internal biogeochemical cycles, we modified the existing biogeochemical model established by Omlin et al, (2001a) and Mieleitner & Reichert, (2008). Our study (hereafter called ‘‘COINTZIO’’) was run using a one-dimensional reaction-advection-diffusion model, implemented in the software package Aquasim (Reichert 1994). The changes from the model by Omlin et al, (2001a) are summarized below.

+ The description of algae was simplified. To obtain a model with the highest degree of aggregation for this first transferability study, P. rubescens and other algae were combined into a single group (chlorophyll *a*). In the study by Omlin, P. rubescens was modelled as a separate algal group because this species is of specific interest to the water supply authority of Zürich and so P. rubescens was not necessary for describing the biogeochemical cycles in this study. Moreover, this species only can grow when there is enough light in the metalimnion of the lake in summer (Mieleitner & Reichert, 2006). This is not the case for the turbid Cointzio reservoir that contains six main species of Cyanophyta, Chrysophyta, Euglenophyta, Pyrrophyta, Bacilliariophyta, and Chlorophyta.

+ In the model of Omlin et al, 2001a, only growth of algae on nitrate as the nitrogen source was considered, because in Lake Zürich growth on ammonium is not relevant. In the Cointzio reservoir, the ammonium concentrations are much higher than those in Lake Zürich. Therefore, growth of algae on ammonium was added. An additional parameter is required for describing preference of growth on ammonium over growth on nitrate. The parameterization of this extended process description was taken from Reichert et al, 2001.

+ Ryding & Rast (1989) stated: “It is generally believed that nitrogen is the primary nutrient which limits the maximum algal biomass levels in tropical/subtropical systems”. Moreover, it is notable that the majority of the tropical studies in Mexican lakes and reservoirs were determined to be nitrogen limited (Bravo-Inclán et al, 2010). One of the reasons is that the nutrient inputs of treated or untreated waste water discharges and agricultural losses to the lake are sources of soluble phosphate. As a result, Nitrogen (N) fixation is likely to become important under N limiting conditions. Therefore, in this study, we adopted the process described by (Kiirkki et al, 2001) that simulates atmospheric N_2 fixation by allowing phytoplankton growth independent of a N input (Kunz et al, 2011).

+ To consider mineralization in the absence of dissolved oxygen and nitrate, anaerobic mineralization processes in water column and at sediment surface were introduced. These processes are of quantitative importance for the modelled compounds only in the eutrophic lake with very small oxygen concentration in the deep water (Omlin et al, 2001a; Kunz et al, 2011). And also according to RES1 (Kunz et al, 2011), an additional process for the

oxidation of reduced substance by consuming DO (hereafter referred to as ‘‘background mineralization’’) need to be accounted.

+ Following the approach by Matzinger et al, (2007b), we excluded an explicit sediment compartment as described by Omlin et al, 2001a, but limited mineralization processes to the sediment-water interface (process mineral_sed) was replaced.

+ To make the sediment composition more realistic, an additional state variable X_I was introduced to describe inorganic particles constituting the bulk of the sediment. We applied constant ratios for organic matter becoming inert. As this new compound does not interact with the other substances, omission of the accumulation process does not cause a problem for the model concept. The main effect is the reduction of the concentrations of organic material in the sediment (Mieleitner & Reichert, 2006).

Table 3 gives an overview of the biogeochemical processes mentioned above used in the model. The top cell indicates the respective process rate. The contribution of a process to the transformation rate of state variables is calculated by multiplying the rate with the corresponding stoichiometric coefficient. Formulas for stoichiometric and process rate variables are indicated in the suitable “equations”. Finally constant variables are given at the end of each table. The explanation of the processes was presented in details in Omlin et al, 2001a.

Table 3.5 Biogeochemical processes

a. Growth processes (assimilation): Chlorophyll *a* and Zooplankton

Algae (chlorophyll *a*):

In the reservoir of Cointzio, as mentioned before, growths of algae on nitrate (growth_ALG_NO3), ammonia (growth_ALG_NH4) and nitrogen (growth_ALG_N2) were considered in this study. Light and nutrient limitations are described with Monod-type rate reduction factors.

growth_ALG_NO3=k_gro_ALG*monod_I*min(monod_NO3_ALG,monod_HPO4_ALG)*X_ALG		
Bio-geochemical conversion processes		
State variables	**Stoichiometric coefficients**	**Description**
X_ALG	1	Algal growth
X_P_ALG	b_P	Algal uptake of orthophosphate
S_O2	1.24	According to the Redfield ratio
S_NO3	-a_N	Reduction of nitrate in water
S_HPO4	-b_P	Reduction of orthophosphate in water

Equations			
k_gro_ALG =k_gro_ALG_20*exp(beta_ALG*(T-20))		Temperature dependence of bacterial activity (d^{-1})	
monod_NO3_ALG = S_NO3/(K_NO3_ALG+S_NO3)		Effect of dissolved nitrate concentrations on growth rate (-)	
monod_HPO4_ALG = S_HPO4/(K_HPO4_ALG+S_HPO4)		Effect of dissolved orthophosphate concentrations on growth rate (-)	
monod_I = Iz/(K_I_ALG+Iz)		Effect of light intensity (I) on growth rate (-)	
I z= I × exp (-k_extinct × z)		In-situ light intensity (Wm^{-2})	
I= (1-rs)*phi_s			
phi_s		Shortwave radiation (Wm^{-2}) from measurement	
k_extinct = lamda +k_2 × w_ALG × X_ORG_withoutzoo		Light attenuation coefficient (m^{-1})	
X_ORG_withoutzoo = X_ALG+X_S+X_I		Organic particles without living zooplankton ($gDMm^{-3}$)	
b_P = (b_P_min+b_P_max)/2+(b_P_max-b_P_min)/2 × tanh((S_HPO4-S_HPO4_crit)/DeltaS_HPO4)		P incorporation as a function of phosphate concentration $gP(gDM)^{-1}$	
Constant variables	**Unit**	**Value**	**Description**
k_gro_ALG_20	d^{-1}	**1.2**	Maximum specific growth rate at 20 °C; fitted parameter
β_ALG	$°C^{-1}$	0.046	Coefficient for temperature dependency
K_I_ALG	Wm^{-2}	34.3	Light intensity at half saturation rate (Monod)
K_HPO4_ALG	gPm^{-3}	0.0007	Concentration of orthophosphate at half saturation rate (Monod)
rs	-	0.08	Reflection coefficient of shortwave radiance, as in k-ε model by Goudsmit et al, 2002
b_P_min b_P_max	$gP(gDM)^{-1}$	0.0014 0.0087	Minimum and maximum P content of newly produced algae
lamda	m^{-1}		Light extinction (1.84/secchi^0.61)
k_2	$g\ m^2(WM)^{-1}$	0.026	Coefficient for light extinction with particles
w_ALG	$gWM(gDM)^{-1}$	5	Factor for converting dry mass to wet mass (Jørgensen et al, 1991)
S_HPO4_crit	gPm^{-3}	0.004	Orthophosphate concentration at which algal growth switches to

			reduced P content
DeltaS_HPO4	gPm^{-3}	0.0013	Parameter for switching to production with reduced P content

growth_ALG_NH4=k_gro_ALG*monod_I*min(monod_NH4_ALG,monod_HPO4_ALG)*X_ALG			
Bio-geochemical conversion processes			
State variables	**Stoichiometric coefficients**	**Description**	
X_ALG	1	Algal growth	
X_P_ALG	b_P	Algal uptake of orthophosphate (stoichiometry is dependent on S_HPO4)	
S_O2	1.24	According to the Redfield ratio	
S_NH4	-a_N	Reduction of ammonium in water	
S_HPO4	-b_P	Reduction of orthophosphate in water	
Equations			
k_gro_ALG=k_gro_ALG_20*exp(beta_ALG *(T-20))	Temperature dependence of bacterial activity (d^{-1})		
monod_I = Iz/(K_I_ALG+Iz)	Effect of light intensity (I) on growth rate (-)		
monod_HPO4_ALG= S_HPO4/(K_HPO4_ALG+S_HPO4)	Effect of dissolved orthophosphate concentrations on growth rate (-)		
monod_NH4_ALG= S_NH4/(K_NH4_ALG+S_NH4)	Effect of dissolved ammonium concentrations on growth rate (-)		
I z= I × exp (-k_extinct × z)	In-situ light intensity (Wm^{-2})		
I= (1-rs)*phi_s			
phi_s	Shortwave radiation (Wm^{-2}) from measurement		
k_extinct=lamda+k_2× w_ALG× X_ORG_withoutzoo	Light attenuation coefficient (m^{-1})		
X_ORG_withoutzoo = X_ALG+X_S+X_I	Organic particles without living zooplankton ($gDMm^{-3}$)		
b_P = (b_P_min+b_P_max)/2+(b_P_max-b_P_min)/2 × tanh((S_HPO4-S_HPO4_crit)/DeltaS_HPO4)	P incorporation as a function of phosphate concentration ($gP(gDM)^{-1}$)		
Constant variables	**Unit**	**Value**	**Description**
k_gro_ALG_20	d^{-1}	**1.2**	Maximum specific growth rate at 20°C; fitted parameter
β_ALG	$°C^{-1}$	0.046	Coefficient for temperature dependency
K_I_ALG	Wm^{-2}	34.3	Light intensity at half saturation rate (Monod)
K_HPO4_ALG	gPm^{-3}	0.0007	Concentration of orthophosphate at

			half saturation rate (Monod)
rs	-	0.08	Reflection coefficient of shortwave radiance, as in k-ε model by Goudsmit et al, 2002.
b_P_min b_P_max	$gP(gDM)^{-1}$	0.0014 0.0087	Minimum and maximum P content of newly produced algae
lamda	m^{-1}		Light extinction in the absence of particles
k_2	$gm^2(WM)^{-1}$	0.026	Coefficient for light extinction with particles
w_ALG	$gWM(gDM)^{-1}$	5	Factor for converting dry mass to wet mass
S_HPO4_crit	gPm^{-3}	0.004	Orthophosphate concentration at which algal growth switches to reduced P content
DeltaS_HPO4	gPm^{-3}	0.0013	Parameter for switching to production with reduced P content

growth_ALG_N2=k_gro_ALG_N2*monod_I*min(monod_N2_ALG,monod_HPO4_ALG)*X_ALG		
Bio-geochemical conversion processes		
State variables	**Stoichiometric coefficients**	**Description**
X_ALG	1	Algal growth
X_P_ALG	b_P	Algal uptake of orthophosphate (stoichiometry is dependent on S_HPO4)
S_O2	1.24	According to the Redfield ratio
S_HPO4	-b_P	Reduction of orthophosphate in water
Equations		
k_gro_ALG_N2=k_gro_ALG_N2_20*exp(beta_ALG*(T-20))	Temperature dependence of bacterial activity (d^{-1})	
monod_I = Iz/(K_I_ALG+Iz)	Effect of light intensity (I) on growth rate (-)	
monod_HPO4_ALG= S_HPO4/(K_HPO4_ALG+S_HPO4)	Effect of dissolved orthophosphate concentrations on growth rate (-)	
monod_N2_ALG= (S_NH4+S_NO3)/(K_NH4_ALG+S_NO3+S_NH4)	Effect of dissolved ammonium concentrations on growth rate (-)	
I z= I × exp (-k_extinct × z)	In-situ light intensity (Wm^{-2})	
I= (1-rs)*phi_s		
phi_s	Shortwave radiation (Wm^{-2}) from measurement	

k_extinct=lamda+k_2× w_ALG× X_ORG_withoutzoo		Light attenuation coefficient (m^{-1})	
X_ORG_withoutzoo = X_ALG+X_S+X_I		Organic particles without living zooplankton ($gDMm^{-3}$)	
b_P = (b_P_min+b_P_max)/2+(b_P_max-b_P_min)/2 × tanh((S_HPO4-S_HPO4_crit)/DeltaS_HPO4)		P incorporation as a function of phosphate concentration ($gP(gDM)^{-1}$)	
Constant variables	**Unit**	**Value**	**Description**
k_gro_ALG_N2_20	d^{-1}	**0.85**	Maximum specific growth rate at 20 °C; fitted parameter
β_ALG	$°C^{-1}$	0.046	Coefficient for temperature dependency
K_I_ALG	Wm^{-2}	34.3	Light intensity at half saturation rate (Monod)
K_HPO4_ALG	gPm^{-3}	0.0007	Concentration of orthophosphate at half saturation rate (Monod)
rs	-	0.08	Reflection coefficient of shortwave radiance, as in k-ε model by Goudsmit et al, 2002
b_P_min b_P_max	$gP(gDM)^{-1}$	0.0014 0.0087	Minimum and maximum P content of newly produced algae
lamda	m^{-1}		Light extinction in the absence of particles
k_2	$gm^2(WM)^{-1}$	0.026	Coefficient for light extinction with particles
w_ALG	$gWM(gDM)^{-1}$	5	Factor for converting dry mass to wet mass
S_HPO4_crit	gPm^{-3}	0.004	Orthophosphate concentration at which algal growth switches to reduced P content
DeltaS_HPO4	gPm^{-3}	0.0013	Parameter for switching to production with reduced P content

Zooplankton

The simplest possible zooplankton model is used which includes all organisms in one class that feeds on algae.

growth_ZOO= k_gro_ZOO × X_ALG × X_ZOO × LimitAlgP		
Bio-geochemical conversion processes		
State variables	**Stoichiometric coefficients**	**Description**
X_ZOO	1	Zooplankton growth

X_ALG	-1 / Y_ZOO	Zooplankton feeding on algae
X_P_ALG	-a_P_ALG / Y_ZOO	P transfer from phytoplankton to zooplankton
X_S	c_e × (1-Y_ZOO) / Y_ZOO	Increase of dead organic material due to fecal pellets
X_P_S	0	Fecal contains no P
S_O2	-0.93 × (1-c_e) × (1 - Y_ZOO) / Y_ZOO	Oxidation of food not excreted and not used for zoo plankton biomass; factor according to Redfield ratio
S_NH4	(1- c_e × (1-Y_ZOO))/Y_ZOO-1)*a_N	
S_HPO4	a_P_ALG / Y_ZOO-a_P_red	P release due to inefficient zooplankton feeding

Equations	
k_gro_ZOO = k_gro_ZOO_20 × exp (β_ZOO × (T-20))	Temperature dependence of growth (d^{-1})
LimitAlgP = min(1, a_P_ALG / a_P_red)	The greater the algal P content, the greater the growth; P content of zooplankton is according to Redfield ratio (-)
a_P_ALG = X_P_ALG / X_ALG	Average algal P content ($gP(gDM)^{-1}$)
Y_ZOO = Y_ZOO_max × min(1, a_P_ALG / a_P_red)	Yield for zooplankton growth; the smaller the algal P content, the more algae must be eaten for zooplankton growth (-)

Constant variables	**Unit**	**Value**	**Description**
k_gro_ZOO_20	$gDM^{-1}m^3d^{-1}$	**0.001**	Max. specific growth rate of zooplankton at 20°C ; fitted parameter
β_ZOO	$°C^{-1}$	0.08	Coefficient for temperature dependency
c_e		0.7	Fraction of food not used for zoopl. biomass that is excreted as fecal pellets
a_P_red	$gP(gDM)^{-1}$	0.0087	P content of organic material according to Redfield ratio
Y_ZOO_max		0.5	Maximum yield for zooplankton growth

b. Respiration processes: Chlorophyll *a* and Zooplankton

Algae (chlorophyll *a*)

The stoichiometry of algae, and zooplankton respiration are described in the tables below. The two processes are similar with the minor difference, that phosphate release by respiring algae depends on its current phosphorus content, a_P_ALG, whereas phosphate release by respiring zooplankton is constant (a_P_red) because of the constant elemental composition of zooplankton.

resp_ALG=k_resp_ALG*monod_O2_resp*X_ALG			
Bio-geochemical conversion processes			
State variables	**Stoichiometric coefficients**	**Description**	
X_ALG	-1	"Feeding" of algae on their biomass	
X_P_ALG	-a_P_ALG	P release to water column	
S_O2	-0.94	DO consumption; according to Redfield ratio	
S_HPO4	a_P_ALG	P release to water column	
S_NH4	a_N	N release to water column	
Equations			
k_resp_ALG = k_resp_ALG_20 × exp (β_ALG × (T-20))		Temperature dependence of respiration (d^{-1})	
monod_O2_resp = S_O2/(K_O2_resp+S_O2)		Effect of dissolved oxygen on respiration (-)	
a_P_ALG = X_P_ALG / X_ALG		Average algal P content ($gP(gDM)^{-1}$)	
Constant variables	**Unit**	**Value**	**Description**
k_resp_ALG_20	d-1	0.05	Maximum specific respiration rate at 20°C
β_ALG	°C-1	0.046	Coefficient for temperature dependency
K_O2_resp	g-DOm-3	0.5	DO concentration at half saturation rate (Monod)

Zooplankton

resp_ZOO=k_resp_ZOO*monod_O2_resp*X_ZOO		
Bio-geochemical conversion processes		
State variables	**Stoichiometric coefficients**	**Description**
X_ZOO	-1	"Feeding" on own biomass
S_O2	-0.94	DO consumption; according to Redfield ratio
S_HPO4	a_P_red	P release to water column
S_NH4	a_N	N release to water column
Equations		
k_resp_ZOO = k_resp_ZOO_20 × exp	Temperature dependence of respiration (d -1)	

(β_ZOO × (T-20))			
monod_O2_resp = S_O2/(K_O2_resp+S_O2)		Effect of dissolved oxygen on respiration (-)	
Constant variables	**Unit**	**Value**	**Description**
k_resp_ZOO_20	d^{-1}	0.003	Maximum specific respiration rate at 20 °C
β_ZOO	$°C^{-1}$	0.08	Coefficient for temperature dependency
K_O2_resp	$gDOm^{-3}$	0.5	DO concentration at half saturation rate (Monod)

c. Death processes (mortality & excretion): Chlorophyll *a* and Zooplankton

Algae (chlorophyll *a*)

Death processes transform algae and zooplankton into degradable and inert organic material.

death_ALG=k_death_ALG*X_ALG			
Bio-geochemical conversion processes			
State variables	**Stoichiometric coefficients**		**Description**
X_ALG	-1		Algae death
X_P_ALG	-a_P_ALG		P transfer to dead organic matter
X_S	1-f_p		Increase in dead organic matter
X_P_S	(1-f_p)*a_P_ALG		P transfer to dead organic matter
X_I_S	f_p		Increase in inert organic matter
X_P_I_S	f_p *a_P_ALG		P transfer to inert organic matter
Equations			
k_death_ALG = k_death_ALG_20 × exp (β_ALG × (T-20))		Temperature dependence of respiration (d^{-1})	
a_P_ALG = X_P_ALG / X_ALG		Average algal P content ($gPg(DM)^{-1}$)	
Constant variables	**Unit**	**Value**	**Description**
k_death_ALG_20	d^{-1}	**0.03**	Maximum specific death rate at 20°C, fitted parameter
β_ALG	$°C^{-1}$	0.046	Coefficient for temperature dependency
f_p		0.1	Fraction of organisms that becomes inert during death

Zooplankton

death_ZOO=k_death_ZOO*X_ZOO			
Bio-geochemical conversion processes			
State variables	**Stoichiometric coefficients**	**Description**	
X_ZOO	-1	Algae death	
X_S	1-f_p	Increase in dead organic matter	
X_P_S	(1-f_p)*a_P_red	P transfer to dead organic matter	
X_I_S	f_p	Increase in inert organic matter	
X_P_I_S	f_p *a_P_red	P transfer to inert organic matter	
Equations			
k_death_ZOO = k_death_ZOO_20 × exp (β_ZOO × (T-20))		Temperature dependence of respiration (d^{-1})	
Constant variables	**Unit**	**Value**	**Description**
k_death_ZOO_20	d^{-1}	**0.1**	Maximum specific death rate at

			20°C, fitted parameter
β_ZOO	$°C^{-1}$	0.08	Coefficient for temperature dependency
f_p		0.1	Fraction of organisms that becomes inert during death
a_P_red		0.0087	Phosphorus content of organic material according to Redfield

d. Mineralization processes

Mineralization processes account for bacterially mediated oxidation of degradable organic matter. The aerobic mineralization using dissolved oxygen, the anoxic mineralization using nitrate as the oxidant (denitrification) and the anaerobic mineralization (summarizing other electron acceptors than oxygen and nitrate) are used in the model. These two first processes are known to be very important for the lakes. The first process leads to a significant reduction of oxygen concentrations in the deep hypolimnion, the second leads to a large nitrogen elimination in the lake (Mengis et al, 1997). The third process is relevant in highly eutrophic lakes with very small oxygen concentration in the deep water like the Cointzio reservoir.

Aerobic mineralization of organic material in open water (Aero_miner):

The process rate of aerobic mineralization has a Monod-type limitation factor with respect to oxygen.

mineral_aero = k_miner_aero × monod_O2_miner × X_S		
Bio-geochemical conversion processes		
State variables	**Stoichiometric coefficients**	**Description**
X_S	-1	Mineralization of organic matter
X_P_S	-a_P_S	Release to water column of incorporated P
X_P_I_S	-a_PI_S	Release to water column of adsorbed P
S_O2	-0.94	Consumption of DO; according to Redfield ratio
S_NH4	a_N	N release by mineralization
S_HPO4	a_P_S + a_PI_S	P release to water column
Equations		
k_miner_aero = k_miner_aero_20 × exp (β_BAC × (T - 20))	Temperature dependence of bacterial activity (d^{-1})	
monod_O2_miner = S_O2 / (K_O2_miner + S_O2)	Effect of dissolved oxygen (-)	
a_P_S = X_P_S / X _S	Average P-content in organic matter ($gP(gDM)^{-1}$)	

a_PI_S = X_PI_S / X_S		Average P adsorbed to organic matter (gP(gDM)$^{-1}$)	
Constant variables	**Unit**	**Value**	**Description**
k_miner_aero_20	d^{-1}	**0.1**	Aerobic specific mineralization rate at 20°C in open water for eutrophic lake, fitted parameter
β_BAC	$°C^{-1}$	0.046	Temperature dependence coefficient for bacteria
K_O2_miner	g DOm^{-3}	0.05	Half saturation rate for mineralization with respect to oxy

Anoxic mineralization of organic material in open water = denitrification (Anox_miner)

The rate of anoxic mineralization has an inhibition factor with respect to oxygen and a limitation factor with respect to nitrate.

mineral_anox = k_miner_anox × monod_NO3_miner × (1-monod_O2_miner) × X_S			
Bio-geochemical conversion processes			
State variables	**Stoichiometric coefficients**	**Description**	
X_S	-1	Mineralization of organic matter	
X_P_S	-a_P_S	Release to water column of incorporated P	
X_P_I_S	-a_PI_S	Release to water column of adsorbed P	
S_NO3	-0.33	Consumption of NO3	
S_NH4	a_N	N release by mineralization	
S_HPO4	a_P_S + a_PI_S	P release to water column	
Equations			
k_miner_anox = k_miner_anox_20 × exp (β_BAC × (T - 20))		Temperature dependence of bacterial activity (d^{-1})	
monod_O2_miner = S_O2 / (K_O2_miner + S_O2)		Effect of dissolved oxygen (-)	
monod_NO3_miner = S_NO3/(K_NO3_miner + S_NO3)		Effect of NO3 (-)	
a_P_S = X_P_S / X _S		Average P-content in organic matter (gP(gDM)$^{-1}$)	
a_PI_S = X_PI_S / X_S		Average P adsorbed to organic matter (gP(gDM)$^{-1}$)	
Constant variables	**Unit**	**Value**	**Description**
k_miner_anox_20	d^{-1}	**0.01**	Anoxia specific mineralization rate at 20°C in open water; fitted parameter
β_BAC	$°C^{-1}$	0.046	Temperature dependence coefficient for bacteria
K_O2_miner	gDOm^{-3}	2	Half saturation rate
K_NO3_miner	gNm^{-3}	0.1	Half saturation rate (Mieleitner and

			Reichert, 2006)

Anaerobic mineralization of organic material in open water (Anaero_miner)

In highly eutrophic lakes with very small oxygen concentration in the deep water, anaerobic mineralization process can become relevant.

mineral_anaero = k_miner_anaero × (1-monod_NO3_miner) × (1-monod_O2_miner) × X_S			
Bio-geochemical conversion processes			
State variables	**Stoichiometric coefficients**	**Description**	
X_S	-1	Mineralization of organic matter	
X_P_S	-a_P_S	Release to water column of incorporated P	
X_P_I_S	-a_PI_S	Release to water column of adsorbed P	
S_NH4	a_N	N release by mineralization	
S_HPO4	a_P_S + a_PI_S	P release to water column	
Equations			
k_miner_anaero = k_miner_anaero_20 × exp (β_BAC × (T - 20))		Temperature dependence of bacterial activity (d-1)	
monod_O2_miner = S_O2 / (K_O2_miner + S_O2)		Effect of dissolved oxygen (-)	
monod_NO3_miner = S_NO3/(K_NO3_miner + S_NO3)		Effect of NO3 (-)	
a_P_S = X_P_S / X _S		Average P-content in organic matter (g-P g-DM -1)	
a_PI_S = X_PI_S / X_S		Average P adsorbed to organic matter (g-P g-DM -1)	
Constant variables	**Unit**	**Value**	**Description**
k_miner_anaero_20	d^{-1}	**0.001**	Anaerobic specific mineralization rate at 20 °C in open water; fitted parameter
β_BAC	$°C^{-1}$	0.046	Temperature dependence coefficient for bacteria
K_O2_miner	$gDOm^{-3}$	2	Half saturation rate
K_NO3_miner	gNm^{-3}	0.1	Half saturation rate

Aerobic mineralization of organic material at sediment surface (mineral_aero_sed)

mineral_aero_sed = v_sed_ORG × abs(AreaGradient/Area) × X_S × a_miner_sed × monod_O2_miner		
Bio-geochemical conversion processes		
State variables	**Stoichiometric coefficients**	**Description**
S_O2	-0.94	Consumption of DO during mineralization

S_HPO4	a_P_S + a_PI_S		Production of bioavailable P during mineralization
S_NH4	a_N		Production of N during mineralization
Equations			
monod_O2_miner = S_O2 / (K_O2_miner + S_O2)		Effect of dissolved oxygen (-)	
a_P_S = X_P_S / X _S		Average P-content in organic matter (g-P g-DM -1)	
a_PI_S = X_PI_S / X_S		Average P adsorbed to organic matter (g-P g-DM -1)	
Constant variables	**Unit**	**Value**	**Description**
abs(AreaGradient/Area)	m^{-1}		Sediment area per lake volume
v_sed_ORG	md^{-1}	0.5	Settling velocity of OM (Matzinger et al, 2007b)
K_O2_miner	$gDOm^{-3}$	2	Half saturation rate
a_miner_sed		0.62	Fraction of sedimented org. material, which is mineralized at sediment surface (1-a_miner_sed, enters sediment permanently).

Anoxic mineralization of organic material at sediment surface (mineral_anox_sed)

mineral_anox_sed=v_sed_ORG×abs(AreaGradient/Area)×X_S×a_miner_sed×(1-monod_O2_miner) ×monod_NO3_miner)			
Bio-geochemical conversion processes			
State variables	**Stoichiometric coefficients**		**Description**
S_HPO4	a_P_S + a_PI_S		Production of bioavailable P during mineralization
S_NO3	-0.33		Consumption of N during mineralization
S_NH4	a_N		Production of N during mineralization
Equations			
monod_O2_miner = S_O2 / (K_O2_miner + S_O2)		Effect of dissolved oxygen (-)	
monod_NO3_miner = S_NO3 / (K_NO3_miner + S_NO3)		Effect of NO3 (-)	
a_P_S = X_P_S / X _S		Average P-content in organic matter (g-P g-DM -1)	
a_PI_S = X_PI_S / X_S		Average P adsorbed to organic matter (g-P g-DM -1)	
Constant variables	**Unit**	**Value**	**Description**
abs(AreaGradient/Area)	m^{-1}		Sediment area per lake volume
v_sed_ORG	md^{-1}	0.5	Settling velocity of organic material

K_O2_miner	$gDOm^{-3}$	0.05	Half saturation rate
K_NO3_miner	gNm^{-3}	0.1	Half saturation rate
a_miner_sed		0.62	Fraction of sedimented org. material, which is mineralized at sediment surface (1-a_miner_sed, enters sediment permanently).

Anaerobic mineralization of organic material at sediment surface (mineral_anaero_sed)

mineral_anaero_sed = v_sed_ORG×abs(AreaGradient/Area)×X_S×a_miner_sed×(1-monod_O2_miner)×(1-monod_NO3_miner)			
Bio-geochemical conversion processes			
State variables	**Stoichiometric coefficients**		**Description**
S_HPO4	a_P_S + a_PI_S		Production of bioavailable P during mineralization
S_NH4	a_N		Production of N during mineralization
Equations			
a_P_S = X_P_S / X _S		Average P-content in organic matter (g-P g-DM -1)	
a_PI_S = X_PI_S / X_S		Average P adsorbed to organic matter (g-P g-DM -1)	
monod_O2_miner = S_O2 / (K_O2_miner + S_O2)		Effect of dissolved oxygen (-)	
monod_NO3_miner = S_NO3 / (K_NO3_miner + S_NO3)		Effect of NO3 (-)	
Constant variables	**Unit**	**Value**	**Description**
abs(AreaGradient/Area)	m^{-1}		Sediment area per lake volume
v_sed_ORG	md^{-1}	0.5	Settling velocity of organic material
K_O2_miner	$gDOm^{-3}$	0.05	Half saturation rate
K_NO3_miner	gNm^{-3}	0.1	Half saturation rate
a_miner_sed		0.62	Fraction of sedimented org. material, which is mineralized at sediment surface (1-a_miner_sed, enters sediment permanently).

Background mineralization (mineral_bg)

After having optimized mineralization rates of organic matters for PO_4^{3-}, NH_4^+, and NO_3^- release, these processes did not fully account for the observed depletion. This mismatch could not be resolved by increasing the respective mineralization rates because the aerobic mineralization rate in COINTZIO (0.1 d^{-1}), which is an order of magnitude higher than the mineralization rate of OM by Omlin et al, (2001a), but compare well simulated mineralization rate of OM in eutrophic Itezhi –Tezhi reservoir (Kunz et al, 2011). Therefore, we assumed that the observed DO demand originates from the oxidation of reduced

substances (i.e., CH_4 and reduces metals). These substances most likely results from mineralization of older deposits of OM (Kunz et al, 2011). As a result, in COINTZIO, the process "Background mineralization" for the oxidation of reduced substances by consuming DO was added.

mineral_bg = k_miner_bg × monod_O2_bg			
Bio-geochemical conversion processes			
State variables	**Stoichiometric coefficients**		**Description**
S_O2	-1		Consumption of DO
Equations			
monod_O2_bg = S_O2 / (K_O2_bg + S_O2)		Effect of dissolved oxygen (-)	
Constant variables	**Unit**	**Value**	**Description**
k_miner_bg	d^{-1}	**0.1**	Background mineralization rate, fitted parameter
K_O2_bg	$gDOm^{-3}$	**0.25**	Half saturation rate, fitted parameter

e. Nitrification

Nitrification influences the dissolved inorganic nitrogen fraction, which includes ammonium and nitrate as state variables. Nitrification is the biological oxidation of ammonia with oxygen into nitrite followed by the oxidation of these nitrites into nitrates.

nitrification = k_nitri_wat × min(monod_O2_nitri, monod_NH4_nitri)			
Biogeochemical conversion processes			
State variables	**Stoichiometric coefficients**	**Description**	
S_O2	-4.55	Consumption of DO	
S_NO3	1	Production of NO3	
S_NH4	-1	Consumption of NH4	
Equations			
k_nitri_wat = k_nitri_wat_20 × exp (β_BAC × (T - 20))		Temperature dependence of bacterial activity (d^{-1})	
monod_O2_nitri = S_O2 / (K_O2_nitri + S_O2)		Effect of dissolved oxygen (-)	
monod_NH4_nitri = S_NH4 / (K_NH4_nitri + S_NH4)		Effect of NH4(-)	
Constant variables	**Unit**	**Value**	**Description**
k_nitri_wat_20	$gN^{-1}m^3d^{-1}$	**0.05**	Nitrification rate at 20 degrees; fitted parameter
β_BAC	$°C^{-1}$	0.046	Temperature dependence

			coefficient for bacteria
K_O2_nitri	$gDOm^{-3}$	2	Half saturation rate
K_NH4_nitri	$g\ Nm^{-3}$	2	Half saturation rate

f. Uptake and release of phosphate (nutrient release)

In many lakes, it can be observed that phosphate concentrations are very low during the summer not only within the photic zone, where it is consumed by growing algae, but also below. This can be explained with a phosphate adsorption process on sinking particles.

P_uptake = abs(AreaGradient/Area) × k_upt × (a_P_max-a_PI_S) × monod_O2_ads × S_HPO4 ×X_S			
Bio-geochemical conversion processes			
State variables	**Stoichiometric coefficients**		**Description**
X_PI_S	1		Adsorption of P to organic matter
S_HPO4	-1		Reduction in phosphates
Equations			
a_PI_S = X_PI_S / X_S		Mass of adsorbed phosphate per mass of X_S ($gP(gDM)^{-1}$)	
monod_O2_ads = S_O2/(K_O2_ads+S_O2)		Effect of dissolved oxygen on adsorption (-)	
Constant variables	**Unit**	**Value**	**Description**
abs(AreaGradient/Area)	m^{-1}		Sediment area per lake volume
k_upt	$gDM^{-1}m^4d^{-1}$	1200	Phosphate uptake rate constant
a_P_max	$gP(gDM)^{-1}$	0.007	Maximum mass fraction of phosphate adsorbed to organic matter (Mieleitner et al, 2006)
K_O2_ads	$gDOm^{-3}$	0.5	DO concentration at half saturation rate (Kunz et al, 2011)

h. Heat exchange by surface temperatures as boundary condition

T_relax = (T-surf-T)*20			
Bio-geochemical conversion processes			
State variables	**Stoichiometric coefficients**		**Description**
T	1		Adaptation of T to measured surface temperature to mimic heat budget
Constant variables	**Unit**	**Value**	**Description**
k_relax	d^{-1}	20	Rate of temperature adaptation
T_meas	°C		Measured or interpolated surface temperatures

Table 3.6 Synthesis table of parameters in the Aquasim biogeochemical model

Parameters from literature	**Description**	**Parameters fitted**	**Description**
K_HPO4_ALG	Concentration of orthophosphate at half saturation rate (Monod)	k_gro_ALG_20	Maximum specific growth rate at 20 °C
S_HPO4_crit	Orthophosphate concentration at which algal growth switches to reduced P content	k_gro_ALG_N2_20	Maximum specific growth rate at 20 °C
DeltaS_HPO4	Parameter for switching to production with reduced P content	k_gro_ZOO_20	Max. specific growth rate of zooplankton at 20°C
β_ZOO	Coefficient for temperature dependency	k_death_ALG_20	Maximum specific death rate at 20°C
K_O2_resp	DO concentration at half saturation rate	k_death_ZOO_20	Maximum specific death rate at 20°C
k_resp_ZOO_20	Maximum specific respiration rate at 20 °C	k_nitri_wat_20	Nitrification rate at 20 degrees
k_resp_ALG_20	Maximum specific respiration rate at 20°C	K_O2_bg	Half saturation rate
K_O2_ads	DO concentration at half saturation rate	k_miner_bg	Background mineralization rate
a_P_max	Maximum mass fraction of phosphate adsorbed to organic matter	k_miner_anaero_20	Anaerobic specific mineralization rate at 20 °C in open water
K_NH4_nitri	Half saturation rate	k_miner_anox_20	Anoxia specific

			mineralization rate at 20°C in open water
K_O2_nitri	Half saturation rate	k_miner_aero_20	Aerobic specific mineralization rate at 20°C in open water
β_BAC	Temperature dependence		
K_O2_miner	Half saturation rate		
K_NO3_miner	Half saturation rate		

Rivers inputs and reservoir outputs

Rio Grande de Morelia River is the main source of the Cointzio reservoir. The outflow is discharged through the gates. Patterns of riverine inputs were strongly influenced by the climatic regime of the region. During the wet season water discharges were very low while reservoir outputs were maximum with the irrigation demand. In the dry season, riverine inputs were maximum and allowed the annual filling of the reservoir. In mean the concentrations of all substances (TP, TN, PO_4^{3-}, NO_3^-, NH_4^+, and chlorophyll *a*) were higher in the inputs than in the outputs (see detail in chapter 4).

Other fluxes

O2 - gas exchange at the lake surface

Dissolved oxygen exchange is considered as a boundary condition at the lake surface with a flux proportional to the difference of the current oxygen concentration and saturation. The gas exchange velocity, v_{O2atm} is approximated to be constant. The oxygen concentration is evaluated as the sum of the following oxygen sources and sinks: Surface transfer, inflows and outflows, phytoplankton photosynthesis and respiration, biogeochemical and sediment oxygen demand, and nitrification. Surface transfer acts as a source of oxygen when surface water concentrations are below saturation and as a sink when they exceed saturation. The saturation concentration of dissolved oxygen is determined from the equation given by Bauer et al, (1979).

$S\_O2\_sat = (14.652-0.41022T+0.007910T^2-7.7774*10\text{-}5\ T^3)\ (BP/29.92)$

Where T: Water temperature (°C)

BP: Barometric pressure (in.Hg)

Light absorption

Light intensity is assumed to decrease with water depth. The light extinction coefficient, k_extinct (L^{-1}), is assumed to depend linearly on the concentration of suspended particles.

$k\_extinct = k\_1 + k\_2 \times w\_ALG \times X\_ORG\_withoutzoo$

Where k_1 (L^{-1}) is light extinction in the absence of particles which was estimated from secchi depth.

k_2 ($M^{-1}L^{-2}$) is coefficient for light extinction with particles, k_2=0.026 (Omlin et al, 2001a).

X_ORG_withoutzoo is the sum of all particulate state variables except zooplankton.

w_ALG is a factor for converting dry mass to wet mass; w_ALG=5 (Jørgensen et al, 1991).

With these light extinction coefficients, the decrease of light intensity is: I(z) =I*exp(-k_extinct*z); I denotes the light intensity at the water surface.

Vertical mixing

The diffusion coefficient profiles Kz was gained from the calibration of k-ε model (Goudsmit et al, 2002) with the time step of every 30 minutes.

3.6 Model calibration

We chose to calibrate the model using the data collected at deepest point P27 on the target year 2009. All the processes are advanced in parallel at the same time step of 30 minutes and the same vertical resolution of 1 m. The time series of Kz(z) estimated with 30 minutes resolution from the physical k-ε model were then used as input data for the Aquasim biogeochemical model.

Our model calibration was carried out using a heuristic method. Aquasim model performs parameter estimations automatically. The set of calibrated parameters was then carefully compared with values reported in the literature to prevent unrealistic estimates. The half saturation rate for algae growth with respect to phosphate (K_HPO4_ALG) was calibrated to PO_4^{3-}; nitrification rate (k_nitri_wat_20) was fitted to NH_4^+ and NO_3^-; aerobic (k_miner_aero_20), anoxia (k_miner_anox_20), anaerobic (k_miner_anaero_20) specific mineralization rate at 20°C, and background mineralization rate (k_miner_bg) were fitted to DO. Maximal growth rate of algae (k_gro_ALG_20, k_gro_ALG_N2_20), and maximal growth rate of zooplankton (k_gro_ZOO_20) were fitted to observed X_{ALG}. These were then used to do modelling scenarios for the Cointzio reservoir.

Simulation for the calibration year 2009 with the assumption Qin = Qout.

In order to perform a simulation using Aquasim model, it was assumed that the outflow data of the Cointzio reservoir is equal to the inflow data in 2009. This is because the main limitation of Aquasim is that it automatically generates additional inflow when the outflow is larger than the inflow, and vice versa. Globally, the average water depth over years (dry or wet years) did not vary a lot (see the time series of volume with depth in Figure 2.6).

Therefore, the assumption of constant water level in Aquasim could be acceptable for the case of Cointzio reservoir. The measured and simulated results of the main variables in the Cointzio reservoir for the target year 2009 are presented in Figure 4 of the paper Ecological Modelling (see chapter 5).

Conclusions of chapter 3

The modelling simulations were performed in the Cointzio reservoir using two independent models: i) The physical lake k-ε model developed by Goudsmit et al, 2002 was used to determine vertical diffusion coefficient. It was calibrated using temperature measurements in 2009 and validated from the data in 2008 and ii) The Aquasim biogeochemical advection-diffusion-reaction model (Reichert, 1994) was used to simulate the biogeochemical cycling in the reservoir. The time series of diffusion coefficients obtained from the physical k-ε model were added as a function of depth and time for the biogeochemical Aquasim model. All the detailed results are developed in chapter 5.

CHAPTER 4. CARBON, PHOSPHORUS, NITROGEN AND SEDIMENT RETENTION IN A SMALL TROPICAL RESERVOIR

This section is copied from the paper that was submitted to Aquatic Sciences. Results of the field survey were first used to discuss the origin of pollution within the watershed and to estimate the internal biogeochemical functioning of the reservoir and discuss its retention capacity.

Carbon, phosphorus, nitrogen and sediment retention in a small tropical reservoir

Némery J[1], Gratiot N[1], Doan TKP[1], Duvert C[1,2], Alvarado-Villanueva R[3], Duwig C[1]
[1] Université Grenoble Alpes /CNRS/IRD, LTHE UMR 5564, Grenoble, 38000, France
[2] EEBS, Queensland University of Technology, *Brisbane,* Australia
[3] Laboratorio de Biología Acuática, UMSNH, Morelia (Michoacán), Mexico
Corresponding author:
Julien Némery
LTHE – UMR 5564, BP 53, 38 041 GRENOBLE Cedex 09
tél : (0)4 76 63 55 39
fax : (0)4 76 82 50 14
email : Julien.nemery@grenoble-inp.fr or Julien.nemery@ujf-grenoble.fr

Abstract:
As a result of rapid urbanization and absence of efficient water management policies, tropical reservoirs in developing countries are increasingly facing water quality degradation. The small tropical reservoir of Cointzio, located in the Trans Mexican Volcanic Belt, behaves as a warm monomictic water body (surface area = 6 km^2 and water residence time < one year). The Cointzio reservoir is strategic for the drinking water supply of the city of Morelia and for downstream irrigation during the dry season (6 months of the year). It is threatened by sediment accumulation and nutrients originating from untreated waters in the upstream watershed. Intensive field measurements were carried out in 2009 (sampling in the watershed, deposited sediment and water vertical profiles in the reservoir, reservoir input and output) for the estimation of total suspended sediment (TSS), carbon (C), nitrogen (N) and phosphorus (P) loads and accumulation in the reservoir. We found that point sources represent the majority of P and N inputs to the reservoir. The trophic state is clearly eutrophic with high chlorophyll *a* peaks (up to 70 µg L^{-1}) and a long period of anoxia (from May to October). Internal biogeochemical processes in the reservoir were strongly influenced by the incoming floods. Most of the TSS, C, N and P were conveyed to the reservoir between June and October during the wet season. The TSS yield from the watershed was estimated at 35 ± 19 t km^2 y^{-1} of which more than 90 % was trapped in the reservoir (sediment accumulation rate = 7 800 ± 3 300 g m^{-2} y^{-1}). Incoming loads of P and N were reduced by 30 % and 46 % respectively through the transfer into the reservoir. Carbon accumulation rate was 83 ± 35 g C m^{-2} y^{-1} with a large proportion of allochthonous C (75 %) brought in during floods. This study reveals the effect of climatic seasonality on the processes occurring in tropical reservoirs, and points out the need to reduce nutrient input to preserve water resources in tropical areas.

Keywords: tropical reservoir; TSS, C, N, P retention; eutrophication; Mexico

Introduction

The biogeochemical functioning of reservoirs is strongly influenced by the human activities that occur upstream (Kennedy et al. 2003). Large amounts of sediments, organic matter and nutrients are efficiently trapped in reservoirs, which can in turn lead to eutrophication (Garnier et al. 1999; Donohue and Molinos 2009) and to a loss of the storage capacity (Maneux et al. 2001; Vörösmarty et al. 2003; Rãdoane and Rãdoane 2005; Dang et al. 2010). On a global scale, reservoirs have been identified as the most significant sink of suspended sediment (TSS), carbon (C), nitrogen (N), phosphorus (P) in inland waters, reducing nutrient fluxes from upland to downstream ecosystems and coastal regions (Cole et al. 2007; Frield and Wüest 2002; Bosh and Allan 2008; Seitzinger et al. 2010). However, these studies showed large disparities between regions of the world and sizes of reservoirs. Although most studies have focused on large reservoirs, small reservoirs are also of great interest on a global scale (Syvitski et al. 2005). Based on the global database of inland waters developed by Lehner and Döll (2004), the total surface area of reservoirs was estimated at 2.5×10^5 km^2 (Harrison et al. 2009). The area of small reservoirs (< 50 km^2) accounted for 40% of this total area. The authors showed the importance of small reservoirs that could retain, for instance, up to 45% of the total N retention by all reservoirs on a global scale. Furthermore, the number of reservoirs in tropical areas is increasingly important due to the numerous impoundment projects that are currently being carried out in developing countries (Tranvik et al, 2009). Tropical regions are characterized by contrasted wet and dry seasons, with important consequences on the hydrological processes taking place in small reservoirs. These systems develop a high vulnerability to eutrophication, especially during the extended dry and warm season when nutrients accumulate, increasing algal blooms (Burford et al. 2012). Furthermore, the warmer temperatures characterizing tropical regions may lead to substantial greenhouse gas emissions (CO_2 and CH_4) through intense mineralization of the carbon present in reservoirs (Guérin et al. 2008, Chanudet et al. 2012). However, the literature on tropical reservoirs remains limited (Kunz et al. 2011). There is therefore a clear need to provide further knowledge on the biogeochemical processes in small tropical reservoirs influenced by the strong seasonality of incoming water, TSS and nutrient fluxes.

In tropical areas, water quality management has become an increasingly important issue in developing countries such as Mexico. The release of untreated wastewater into aquatic ecosystems is a common practice in many tropical countries. This is of great concern as the

volume of wastewater produced is increasing together with rapid urbanization and economic growth (Le et al. 2014).

According to various studies in Mexico, most of the Mexican lakes and reservoirs continue to deteriorate, with ecological consequences for the aquatic ecosystems such as eutrophication (Bravo-Inclán et al. 2011). It is admitted by Mexican stakeholders that water pollution is one of the most serious challenges for sustainable water resources management, and it also represents one of the most important concerns for local populations (Berrera Camacho and Bravo Espinosa 2009). In Mexico the development of wastewater treatment infrastructure remains insufficient, both in large cities and in smaller rural settlements (Ramírez-Zierold et al. 2010). Alcocer and Bernal-Brooks (2010) recently provided an overview of the state of lakes and reservoirs in Mexico, particularly within the Trans-Mexican Volcanic Belt (TMVB), where our study site is located. The authors highlighted the lack of data on Mexican rivers, indicating that the knowledge about the linkages between sediment and nutrient sources within upstream watersheds and the biogeochemical functioning of downstream reservoirs is limited in Mexico. Hence, the implementation of monitoring networks of discharge and nutrients, as well as the establishment of policy and mitigation strategies of point and non-point sources of pollution are necessary to solve water quality problems in the country.

The present study focuses on the small tropical reservoir of Cointzio (state of Michoacán), which is used for supplying drinking water to the city of Morelia and for irrigation purposes. This reservoir is threatened by sediment accumulation and eutrophication that may increase the water treatment costs and decrease the sustainability of the regional water resources. On the regional scale, the quality and quantity of water flowing out of the Cointzio reservoir also affects the downstream Cuitzeo endorheic laguna, which is the second largest Mexican lake and is of great hydrological and ecological interest (Alcocer and Bernal Brooks 2010). The main objectives of the present work are i) to identify and quantify the N and P inputs from the watershed to the reservoir, ii) to characterize the internal biogeochemical processes of the reservoir and relate them with the seasonality of the inputs, and iii) to evaluate the TSS, C, N and P annual accumulation rate in the reservoir and assess its trapping efficiency.

Material and methods

Study area

The Cointzio reservoir (19.622°N, -101.256°W) is located in the southern part of the Mexican Central Plateau on the Trans-Mexican Volcanic Belt (TMVB), at an altitude of 1990 masl (Figure 1). The region has a sub-humid climate with mean annual rainfall of 810 mm and air temperature fluctuation between 18 and 35 °C according to data taken at Morelia meteorological station (data from Servicio Nacional de Meteorología de México). Rainfall is concentrated during the wet season from June to October while the period between November and May is dry (period 1956-2001; Gratiot et al. 2010). The Cointzio reservoir was built in 1940. Its storage capacity is 66 Mm^3 (more recent bathymetry in 2005; Susperregui 2008) with a maximal surface area of 6 km^2 for a maximum depth of 29 m. The Cointzio reservoir is an essential component of the drinking water supply (20 % i.e. 21 10^6 m^3, Ooapas 2007) for the city of Morelia (700 000 inhabitants) and it is also used for agricultural irrigation during the dry season.

The Cointzio watershed drains an area of 630 km^2 with elevations between 1990 and 3440 masl. The only perennial river is the Rio Grande de Morelia. At the outlet of the reservoir this river continues its course downstream to the Cuitzeo endorheic laguna (375 km^2) (Allende et al. 2009). The Cointzio watershed is mainly forested (30 %) and cultivated (43 %) (López-Granados et al. 2013). The mean population density is 68 inh. km^2 for a total of 43 000 inhabitants (López-Granados et al. 2013). Soils are mostly volcanic (Andosols, Acrisols) and highly degraded in some parts of the watershed where important processes of erosion take place during the wet season (Duvert et al. 2010).

Figure 1

Survey in the watershed

To localize the origin of nutritive pollution upstream of the reservoir, eight sampling sites were selected in the watershed according to their land use, population density and location in the river network (Figure 1; Table 1). Sites 2 and 4 located downstream of the biggest villages were typical of domestic point sources, whereas sites 3 and 5 were characteristic of diffuse sources in low population density areas and mixed forest/agriculture land uses. Site 1 was intermediate. Site 6 was representative of degraded agricultural lands affected by severe erosion. Site 7 is located in the downstream part of the watershed, along the main course of the Rio Grande de Morelia. In 2009 monthly water samples were taken using a 2-L polypropylene recipient just below the surface in the middle reach of the river. Discharge

(salt dilution gauging method) and dissolved oxygen (DO) were measured at the same time using a multi-parameter Hydrolab MS5 probe. Water samples were kept refrigerated at 4 °C during transportation to the laboratory.

Reservoir inflow and outflow

Given the low population density around the reservoir banks and the absence of other rivers, we considered the Rio Grande de Morelia River to be the predominant source of C, N, P and TSS. Sampling site 8 is located at the outlet of the Cointzio watershed, downstream from the Santiago Undameo township (Figure 1). Monitoring at the gauging station of Undameo started in 1940 by the Comisión Nacional Del Agua (CONAGUA). At that time a Parshall flume was built to provide a control of the hydraulic section. A stage-discharge rating curve was also established and regularly adjusted. Since 2007 water levels have been measured at a 5-min time-step with a Thalimede OTT water level gauge and water discharge time series have then been determined via the CONAGUA rating curve (Duvert et al. 2011). The Undameo gauging station physically separates the outlet of the Cointzio watershed from the inlet of the Cointzio reservoir. In order to calculate (C, N, P, TSS) annual loads, surface sampling was conducted using a bucket in the middle of the river (4 m width) and samples were stored at 4 °C. The sampling frequency was daily for TSS measurements (since 2007) and weekly for C, N and P measurements (in 2009).

At the outlet of the reservoir, daily discharges were measured by CONAGUA immediately downstream of the reservoir in the water uptake pipe, and additionally in the irrigation canal downstream of the spillway during the dry period. A meteorological station on the roof of the building of the dam allowed the measurement of evaporation and precipitation. For this study discharge, evaporation and precipitation data corresponding to the period 2007-2009 were collected at CONAGUA. Daily TSS data were additionally obtained from the CONAGUA for the period 2007-2008. In 2009 our sampling frequency was daily for TSS measurements and weekly for C, N and P measurements. All water samples were taken using a bucket from the water uptake pipe and in the irrigation canal and stored at 4°C.

Sampling within the reservoir

To assess the spatial and temporal dynamics of biogeochemical parameters within the reservoir, the vertical distributions of temperature (°C), DO (mg L^{-1}), turbidity (NTU) were

measured using a multi-parameter Hydrolab MS5 probe. NTU measurements correlated well with TSS values (R^2 = 0.97 data not shown). Surveys were conducted in 2009 at a fortnightly to monthly frequency, at 15 longitudinal points along the reservoir (Figure 1). At each station, Secchi depth was measured using a Secchi disk. The deepest point P27 and the middle point P6 were additionally sampled along the vertical axis, at different depths (surface = 0.1, 1, 2, 5, 10, 15, 20 m and bottom = 0.3 m from the bottom) using a 2-L Niskin bottle. Each water sample was collected in a 2-L polypropylene recipient for TSS, C, N, P measurements and chlorophyll *a* analysis. Samples were kept at 4 °C in an icebox during transportation to the laboratory. Samples of bottom sediments were taken using a Van Veen grab sampler at two periods, i.e. during the dry season (19th May 2009) and at the end of the wet season (13th October 2009). Six points (P27, P13, P11, P6, P47 and P3) were chosen along the longitudinal profile to assess the C, N, P contents in deposited sediments. We assumed that sampling was representative of the first 2 cm corresponding to the sediment surface layer. Sediments were oven-dried at 60°C for 24 hours in the laboratory.

Analysis of water and sediment

After sampling, water was filtered within 3-6 hours in the laboratory through GF/F membrane filters (Whatman 0.7 µm porosity) and frozen before dissolved nutrient analysis. Unfiltered water samples were also frozen for further total nutrient analysis. Total suspended solid (TSS) was weighed on GF/F filters (dried 2h at 105°C) and expressed per volume unit filtered. Reproducibility for replicate was better than 3%. Chlorophyll *a* was analyzed after filtering on GF/C Whatman membrane filters using methanol extraction according to Holm-Hansen and Rieman (1978). Reproducibility for replicate was better than 3 %. Particulate organic carbon (POC) analyses were performed after filtering on GF/F Whatman membrane filters (ignited at 500°C). Filtrates were kept for dissolved organic carbon (DOC) analysis. Filters were treated with HCl (2N) to remove carbonates and dried at 60°C for one night (Etcheber et al., 2007). POC was then determined on dry filters by combustion in a LECO CS 125 analyzer (Etcheber et al., 2007). POC concentration (mg L^{-1}) was then obtained multiplying POC (mg g^{-1}) and TSS (mg L^{-1}). DOC was analyzed on filtered water using an OC-V Shimadzu analyzer (Sugimura and Suzuki 1998). Analytical accuracy and reproducibility of carbon analysis was better than 5 % (Coynel et al. 2005). P-tot and N-tot were analyzed on infiltrated water samples using a persulfate digestion process and standard colorimetric method (American Public Health Association; APHA, 1995). Dissolved

nutrients (PO_4^{3-}, NH_4^+, and $NO3^-$) were analyzed on filtrated water samples using standard colorimetric method (APHA, 1995). Reproducibility for replicate measurements was better than 5 % for all total and dissolved nutrient analysis.

The total particulate P (TPP) content of sediment was determined using a high temperature/HCl extraction technique (Aspila et al. 1976; Némery and Garnier 2007) before phosphate measurement by colorimetric method (Murphy and Riley 1962). To estimate particulate inorganic P (PIP), the analysis was similar to that for TPP, except that the high temperature organic P mineralization was omitted. Particulate organic P (POP) was determined by calculating the difference between TPP and PIP (Svendsen et al. 1993). Total carbon (TC) and total nitrogen (TN) content was measured by CHN analysis using a CN-analyzer FlashEA 1112 (Thermo Fisher Sci., MA, USA). Based on the catchment geology mainly composed of volcanic and acid soils, inorganic C (IC) in sediment was expected to be low (Covaleda et al. 2011). To confirm this hypothesis, carbonates were analyzed using the calcimetric method (Robertson et al, 1999) and all values were < 0.01 % C ($CaCO_3$) (data not shown). Hence measured TC was hereafter considered organic carbon (OC). Reproducibility for replicate measurement was better than 5 % for OC, TN, TPP and PIP.

Accumulation rates in reservoir

The sediment deposition rate was estimated in previous studies by using three sediment cores sampled in 2006 at P27, P11 and P47 (Susperregui 2008; Mendoza et al. 2013). Stratigraphy and chronology using radioisotopic datation (^{210}Pb) allowed reconstitution of the historical sediment deposition until 1974. Annual cycles of deposition were evidenced using RX intensity and particle sizing, and they fitted well with the seasonality of inflow discharge at Undameo (Susperregui 2008). During the wet season (June to October), a large quantity of sediment is transported towards the bottom of the reservoir by hyperpycnal flows after flood events. During the dry season, settling occurs on the whole water column. The comparison between cores showed homogeneous deposition within the reservoir (Susperregui 2008). This result was also consistent with the low variability of particle size distribution (D50 < 10 μm) for bottom sediments (Susperregui et al, 2009). The annual deposition rate was estimated at 2.5 ± 0.5 cm y^{-1} and the mean bulk density of sediment was 550 kg m^{-3}, leading to an annual sedimentation rate of 1.4 ± 0.6 g cm^{-2} y^{-1} (Susperregui 2008). A reasonable surface of deposition of 2 km^2 was then considered for the sediment accumulation (Sed_{acc}) calculation:

$$Sed_{acc} = \text{sedimentation rate} \times \text{surface} \times K \qquad \text{[Eq. 1]}$$

With Sed_{acc} in t y^{-1}, sedimentation rate = 1.4 ± 0.6 g cm^{-2} y^{-1}, surface = 2 km^2 and K is the unit conversion factor

Mean contents of C, N and P determined in deposited sediment during dry and wet periods were then assumed to be representative of the settling particles. The significance of differences between the two seasons was tested using statistical *U*-test (Mann-Whitney *U*-test using XLSTAT software). Annual C accumulation (C_{acc}), N accumulation (N_{acc}) and P accumulation (P_{acc}) were calculated by multiplying Sed_{acc} with mean OC, TN and TPP content (Table 6). Uncertainties of these estimations were evaluated based on the uncertainty of annual sediment accumulation rate.

Load calculations and uncertainties

Input and output TSS loads were calculated as the product of instantaneous TSS concentrations with the instantaneous discharge (for the output we considered that the daily discharge provided by CONAGUA was on average the same as instantaneous discharge). The TSS load (*HL* in t d^{-1}) is calculated as follows:

$$HL = Qi \times Ci \times 3600 \times 24 / 1000 \qquad \text{[Eq. 2]}$$

Where Qi is the instantaneous discharge (m^3 s^{-1}), Ci is the instantaneous TSS concentration (kg m^{-3})

The load (*L* in t) is the sum of daily loads during the time duration considered:

$$L = \sum_{duration} HL \qquad \text{[Eq. 3]}$$

In the Undameo monitoring station, Duvert et al. (2010) assessed the uncertainty of TSS load at ± 20 % according to the daily sampling strategy carried out in 2009. This uncertainty was assumed to be the same in 2007 and 2008 both at the Undameo station and at the reservoir outlet.

The instantaneous P-tot, N-tot and carbon loads resulted from the product of instantaneous concentrations in the water and the discharge measured at the same time. From the weekly sampling database, the P-tot, N-tot and carbon loads (L) expressed in t y^{-1} were calculated according to the load estimating procedure previously described by Verhoff et al. (1980) and recommended by Walling and Webb (1985):

$$L = \frac{K\sum_{i=1}^{n}(C_i Q_i)}{\sum_{i=1}^{n} Q_i} Q_m \qquad \text{[Eq. 4]}$$

Where K is a conversion factor for the time duration and unit conversion C_i is the instantaneous concentration in the water (g m^{-3}), Q_i is the instantaneous discharge (m^3 s^{-1}) and Q_m is the mean annual discharge for 2009 ($m^3 s^{-1}$). The P-tot, N-tot and carbon loads were presented with 95% confidence intervals (CI) calculated as described by Hope et al. (1997) and recommended when [Eq. 3] was used (Dawson et al. 2011; Némery et al. 2013). The total carbon (TOC) load was calculated as the sum of POC and DOC loads and uncertainty of TOC load was the square root of the sum of the square of uncertainties of POC and DOC loads described above.

Results

Hydrology

Patterns of riverine input into the reservoir were strongly influenced by the climatic regime of the region. Two periods could be distinguished based on the 2007-2009 observations. From November to May during the dry season, water input was very low (minimum Q was between 0.18-0.31 m^3 s^{-1}) while the reservoir output was maximum due to the irrigation demand (maximum Q was 7-8 m^3 s^{-1} Figure 2a and 2b). From June to October during the wet season, riverine input was maximum (Q was 8-18 m^3 s^{-1}) and allowed the annual filling of the reservoir (Figure 2c). During the same period, the reservoir only provided water for the drinking water production (Q = 0.67 ± 0.09 m^3 s^{-1} all along the year). Water input from the watershed decreased from 49 x 10^6 m^3 in 2007 to 42 x 10^6 m^3 in 2009 mainly due to the decrease in precipitation (from 750 mm in 2007 to 690 mm in 2009). Reservoir output decreased from 60 x 10^6 to 43 x 10^6 m^3, indicating a progressive deficit of water year to year. Mean annual volume of the reservoir then decreased from 53.8 in 2007 to 40 Mm^3 in 2009. Between 2007 and 2009, evaporation (11-15.5 % of mean reservoir volume) was twice as

much higher than precipitation (6 % of mean reservoir volume) (Table 1). Therefore the residence time of water in Cointzio was estimated at 1.03-0.81 y in 2007 to 0.90-0.83 y in 2009 (Table 1). Hydrological conditions in the period 2007-2009 (precipitation and Qmax between 750-690 mm y^{-1} and 8-18 m^3 s^{-1} respectively, Table 1 and Figure 2a) were in the low range of the long-term time-series (1956-2001, 650-1200 mm y^{-1}, Qmax 10-40 m^3 s^{-1}) as shown in Gratiot et al. (2010). Years 2007, 2008 and 2009 were therefore typical of dry years. In 2009, the reservoir of Cointzio was characterized by a low water level (minimum of 21 m) as compared to 2007 and 2008 and to the water level fluctuations from 1991 to 2005 (Figure 2c).

Table 1

Pollution levels within the watershed

Maximum P-tot, PO_4^{3-}, NH_4^+ concentrations were observed downstream of highly populated villages (Table 2). The highest mean P-PO_4^{3-} (2.2 ± 1.6 mg L^{-1}), N-NH_4^+ (5.9 ± 3.8 mg L^{-1}) and N-NO_3^- (2.6 ± 1.2 mg L^{-1}) concentrations were observed at site 2 where we also measured the lowest DO (2.3 ± 1.2 mg L^{-1}). Site 4 presented the highest mean P-tot concentration (4.4 ± 5.4 mg L^{-1}) and also important concentrations of P-PO_4^{3-} (0.37 ± 0.23 mg L^{-1}) and N-NH_4^+ (1.23 ± 1.07 mg L^{-1}), which suggest pollution by domestic sewage. N-NO_3^- concentrations remained quite low (< 3 mg L^{-1}) at all sites. Site 5 presented the best water quality with very low concentrations of P-PO_4^{3-} (0.05 ± 0.03 mg L^{-1}), N-NH_4^+ (0.06 ± 0.11 mg L^{-1}) and N-NO_3^- (0.78 ± 0.41 mg L^{-1}) indicating a low contribution of diffuse sources. Sites 7 and 8 were quite similar in terms of nutrient concentrations. Mean concentrations at site 8 remained high especially for P-tot (0.38 ± 0.23 mg L^{-1}), P-PO_4^{3-} (0.11 ± 0.07 mg L^{-1}) and N-NH_4^+ (0.15 ± 0.10 mg L^{-1}), which indicated an important input of nutrients to the reservoir.

Table 2

Figure 2

River input and reservoir output

TSS input was nearly equivalent for the three years (≈ 22 200 ± 4 400 t, Table 1). Maximum TSS concentration was observed during the wet season with peaks > 10 000 mg L^{-1} (Figure 2a, Table 3). Consequently TSS input showed a strong seasonality. TSS input during the wet season (June to October) represented more than 95 % of annual TSS input for the three years (shown only for 2009, Figure 3a). TSS output was found to be comparable for the three years and one order of magnitude smaller than TSS input (1 800 – 2 500 ± 400 – 500 t, Table 1). Moreover, TSS output concentrations never exceeded 600 mg L^{-1} (Figure 2b; Table 4), which implies a high TSS retention in the reservoir. TSS output accounted for 10 % only of the TSS input. In 2009 mean input concentrations of P-tot (0.38 ± 0.23 mg L^{-1}), N-tot (2.1 ± 1.0 mg L^{-1}) and TOC (POC + DOC = 32.6 ± 26.5 mg L^{-1}) were one and a half times higher than their output concentrations (Tables 3 and 4). The input concentrations of P-tot, N-tot and TOC increased with the rising of the discharge and TSS concentration during the wet season (Table 3). For instance, maximum P-tot (0.94 mg L^{-1}) and N-tot (5.9 mg L^{-1}) were measured on the 24th June 2009 (Table 3) during the second most significant peak of TSS (Figure 2a). TOC was maximum (173.5 mg L^{-1}) during the extreme peak of TSS on the 2nd June 2009 (Figure 2a, Table 3). Therefore P-tot, N-tot and TOC inputs to the reservoir showed a strong seasonality concomitantly with floods and TSS inputs (Figure 3).

Figure 3

The input of P-tot was 20 ± 4 t y^{-1} (P-PO_4^{3-} accounted for 26 %, Table 5). The input of P-tot during the wet season (June to October) represented 84 % of the annual P-tot input and showed the same seasonal trend as the TSS input (Figure 3b). The input of P-tot was reduced by 30 % during the transfer through the reservoir (the output of P-tot was 12 ± 3 t y^{-1} with the same proportion of P-PO_4^{3-}, i.e 25 %). The input of N-tot was 98 ± 17 t y^{-1} (61 % as N-NO_3^- and 5.5 % as N-NH_4^+) and was reduced by 46 % in comparison to the output (53 ± 15 t y^{-1} 73.6 % as N-NO_3^- and 10 % N-NH_4^+) (Table 5). The input of NO_3^- was much more reduced (about 30 %) than the input of NH_4^+, which remained equivalent (very close values with uncertainties overlapping) (Table 5). TOC was reduced by 30 % between the input (1617 ± 340 t y^{-1}, 25 % as POC) and the output (1115 ± 167 t y^{-1}, 5 % as POC). For TOC, the difference between the input and output is mainly due to POC, which indicates an effective retention in the reservoir. As for P-tot, most of the N-tot (81 %) and TOC inputs (80 %) were concentrated on the wet season (Figure 3b and 3c).

Overall, the reservoir received most of the TSS, P-tot, N-tot and TOC inputs during 5 months from June to October. The rest of the year, inputs were very low. With the occurrence of high discharges and high TSS concentrations, September was the most exceptional period in terms of input (about 50 % of TSS, 30 % of P-tot and N-tot and 40 % of TOC annual inputs).

Table 3

Table 4

Table 5

Internal reservoir behavior

The tidal range was up to 7 m in 2009 between the maximum water level in January and the minimum in June (Figure 4, Figure 5) as a result of the output for irrigation during the dry season (Figure 2b). Temperature and DO exhibited a longitudinal homogeneity in the reservoir, as shown on the cross profiles presented for four dates in Figure 4. P27 was hereafter considered to be representative of the entire reservoir. The spatiotemporal dynamics of temperature, chlorophyll *a*, TSS and DO at P27 are presented in Figure 5. Temperature fluctuated between 14 and 22 °C. The reservoir behaved as a warm monomictic system with a progressive thermic stratification building up from April to October (Figure 5a). This was followed by a complete vertical mixing of the water column in early November. During the stratified period DO decreased drastically, from 4 mg L^{-1} to ~ 0 mg L^{-1} in the hypolimnion (Figure 5b) indicating an intensive benthic mineralization activity. The influence of hyperpycnal flows was observed between July and October when floods occurred in the watershed and filled the reservoir with very turbid water (Figure 5c). The signature of the high TSS inputs from the watershed was even more evident on the 24th September 2009 (Figure 4c). These latter led to an increase in TSS from 50 mg L^{-1} to 250 mg L^{-1} in the hypolimnion layer of the reservoir (Figure 5c). Consequently to the input of TSS, Secchi depth dropped from 31 cm in February to a minimum of 11 cm in September (Figure 6a).

Chlorophyll *a* was highly concentrated in the shallow layer of the reservoir (0-5 m) during the dry season (January-June) (Figure 5d). Lower values of chlorophyll *a* were found during the second period of the year (July-December), with a homogeneous distribution across the

vertical column. In the epilimnion, chlorophyll *a* was high from January to June (mean values of 30 ± 19 µg L^{-1} and maximum 70 µg L^{-1} observed in March, Figure 5d). Concentrations then drastically dropped to 4 µg L^{-1} from July until December, probably due to the decrease of Secchi depth at the same time (Figure 6a and 6b) that induced a reduction in light penetration.

The temporal variability of POC in TSS showed the same trend as for Chlorophyll *a* (Figure 6c). There was a good agreement in POC values in TSS between P6 and P27 (Figure 6c). POC followed the chlorophyll *a* dynamics with maximum values of 300-400 mg g^{-1} at the surface from January to June (mean 200 ± 100 mg g^{-1}, Figure 6c). The maximum POC content in TSS was close to the Redfield-typical algal organic matter of ~400 mg C g^{-1}, which indicated that during the dry season most of the POC was autochthonous in the epilimnion. With the arrival of the first flood waves in June, POC decreased simultaneously with the decrease in chlorophyll *a* to a minimum value of 10 mg g^{-1} in December (mean 29 ± 18 mg g^{-1} between July and December). Therefore, during the wet season POC was likely dominated by poor-allochthonous POC from the watershed rather than algae-autochthonous POC. POC in the hypolimnion was on average 100 ± 25 mg g^{-1} from January to June, indicating that dead algal sedimentation occurred. However POC was two times lower than the POC at the surface during the same period (200 ± 100 mg C g^{-1} respectively; Figure 6c), suggesting a possible mixing with settled sediment poorer in C originating from the watershed. Then, POC was almost ten times lower (12 ± 3 mg g^{-1}) from July to December. This result again highlights the dilution effect with the arrival of floods within the reservoir.

Figure 4

Figure 5

Figure 6

PO_4^{3-}, NO_3^-, NH_4^+ concentrations were similar at P6 and P27 and showed comparable seasonal trends (Figure 7). Concentrations were slightly higher in the hypolimnion than in the epilimnion, but remained in the same order of magnitude. P-PO_4^{3-} concentration was low during the dry period (0.05 ± 0.05 mg L^{-1} on average from January to May) (Figure 7a). N-NH_4^+ decreased rapidly from January to March and remained very low until May (0.04 ± 0.02 mg L^{-1} at minimum in May) (Figure 7c). The decrease in NH_4^+ and the low

concentration of PO_4^{3-} were likely due to algal uptake during the dry period when maximum chlorophyll *a* was observed (Figure 5d).

Before the arrival of flood waves, PO_4^{3-} and NH_4^+ had already started to increase from May over the course of stratification. This is consistent with a release from potential benthic mineralization activity that induced an important O_2 consumption, as observed in the hypolimnion from May to October (Figure 5c). Increase in PO_4^{3-} and NH_4^+ then intensified with incoming floods from the watershed and nutrient inputs during the wet season (Figure 3). Overall, PO_4^{3-} and NH_4^+ increased more than 10-fold from May and remained high until the destratification in late October where a sharp decrease in PO_4^{3-} and NH_4^+ was observed (Figures 7a and 7c). This decrease can be explained by the complete mixing of the water column, but also by the increase in the volume of the reservoir leading to a dilution effect (Figure 2c). NO_3^- increased slightly throughout the year (Figure 7b) probably due to nitrification and also inputs from floods during the wet season. Indeed, NO_3^- load was important from June to October (Figure 3). NO_3^- did not seem to accumulate that much and this may reflect the progressive elimination of NO_3^- by denitrification processes during the anoxic period (May to October).

C, N and P content in sediment

The OC, TN and TPP content of sediment showed minor variability along the longitudinal transect from the dam to the Rio Grande de Morelia River mouth (for all parameters, individual values were globally in the range of the standard deviation of the mean, Table 6). This result is coherent with the homogeneous sediment deposition within the reservoir. Sediments collected during the wet season had significantly lower mean content of TPP compared to sediments collected during the dry season (0.21 ± 0.03 against 0.12 ± 0.02 mg P g^{-1}, *p*-value < 0.001). This was explained by a decrease in POP (0.17 ± 0.03 against 0.07 ± 0.01 mg P g^{-1}) rather than PIP as the latter remained in the same order of magnitude (0.04 ± 0.01 against 0.05 ± 0.01 mg P g^{-1}). This result may indicate a mineralization of POP between both seasons but negligible PIP desorption. OC (11.1 ± 1.4 mg C g^{-1}) and TN (1.0 ± 0.1 mg N g^{-1}) in the dry season were similar to their concentrations in the wet season (10.2 ± 0.1 mg C g^{-1} and 0.09 ± 0.1 mg N g^{-1} respectively for OC and TN, *p*-value > 0.05) (Table 6). Resulting C:N ratio was 11 ± 1 at both dates. The low mean C:N ratio in deposited sediment (11 ± 1) indicates that deposited sediment contained a significant proportion of autochthonous C (Park et al. 2009). However, the low OC content in sediment was

comparable to the value of POC in TSS from the watershed during the wet season (11.4 ± 4.4 mg g^{-1} from June to October, data not shown but POC content on TSS can be calculated from Table 3). TN content in sediments remained very low (~ 1 mg g^{-1}). These low OC and TN content outline the probable dominance of allochthonous inputs in the OC and TN accumulation.

Figure 7

Table 6

Discussion

Nutrient sources within the watershed and reservoir trophic state

Field observations indicated that point sources from domestic wastewater clearly dominated in the Cointzio watershed. Nutrient emission mainly originated from the most populated villages located upstream. This conclusion is coherent with two studies published on the Cointzio reservoir (López-López and Dávalos-Lind 1998; Ramírez-Olvera and López-López 2004). Both studies identified wastewater discharge to be the major input of nutrients in this reservoir. It is also known that there are no wastewater treatment plants in the villages located upstream (Avila Garcia 2006).

Our results showed that P and N concentrations were low in agricultural sub-watersheds (sites 3 and 5, Table 2). Nitrate concentrations remained low within the whole watershed (mean NO_3^- of 1.5 ± 0.7 mg $N\text{-}NO_3^-$ L^{-1}) with regards to, for instance, the European standard of water quality (Water Framework Directive, 2000/60/EC; Bouraoui and Grizzetti, 2014). These results are in good agreement with the study of Bravo-Espinosa et al. (2009) conducted in the eastern part of the Cointzio watershed (site 6 Huertitas sub-basin, Table 2). These authors estimated very low nitrate loss in runoff waters under cultivated soils in the range of 0.1 – 0.6 mg $N\text{-}NO_3^-$ L^{-1}. Diffuse sources from agricultural soils are also usually linked to erosion processes that constitute a global concern (Quinton et al. 2010). A recent study using fingerprinting methods showed the prevailing contribution of degraded soils to the sediment load at the outlet of the Cointzio watershed (Evrard et al. 2013). Those soils (mainly Acrisols and Andosols) were very poor in C, N and P content (Bravo-Espinosa et al. 2009), indicating

once more the low contribution from diffuse sources in this study. Other sources such as N and P atmospheric deposition can also be neglected given the low contribution of precipitation to the mean annual volume of the reservoir (6%, Table 1). Rough estimation from a neighboring study in Valle de Bravo in central Mexico (16 kg P km^{-2} y^{-1} and 550 kg N km^{-2} y^{-1}, Ramírez-Zierold et al. 2010) confirms that N and P depositions were negligible in the case of the Cointzio reservoir (0.06 t P y^{-1} and 2 t N y^{-1} i.e. 0.3 % and 2 % of P-tot and N-tot inputs respectively, calculation was done with mean annual area of reservoir of 3.6 km^2).

To support the assumption of the predominance of point sources, we calculated the theoretical domestic load based on the physiological per capita production of P (1-1.5 g P day^{-1}, Billen et al. 2007). Given the total population of the watershed (43 000 inhabitants), direct point sources would represent an annual load of 15.5 to 23.5 t P. This is the same order of magnitude as the value at the outlet of the watershed (site 8), i.e. 20 ± 4 t P (Table 5). P domestic inputs from direct wastewater release would then explain the P-tot load reaching the reservoir.

To qualify the trophic state of the Cointzio reservoir, we applied the P trophic model for warm-water tropical lakes and reservoirs first proposed by Salas and Martino (1991). This approach allows estimating trophic state of reservoirs from annual P load and the water residence time in the reservoir. It was applied to the Cointzio reservoir and led to an annual P load of 0.5 ± 0.1 g m^{-3} y^{-1} (ratio between input P-tot load of 20 ± 4 t P and mean annual volume of reservoir 40 Mm^3 in 2009). Given the residence time of about one year (Table 1), the Cointzio reservoir was classified as eutrophic. According to the maximum chlorophyll *a* concentration (up to 70 µg L^{-1}, Figure 6b) and the maximum POC content in suspended sediment, (300-400 mg C g^{-1}) the Cointzio reservoir appeared to be a highly productive system. The measurements of POC and chlorophyll *a* allowed calculating the C:chl *a* ratio for the reservoir (51 ± SD = 19; R = 0.78). This ratio is the slope of the linear regression between POC concentrations and chlorophyll *a* (Garnier et al. 1989). Based on the algal growth rate (0.26 d^{-1}) measured in the Cointzio reservoir by López López & Dávalos-Lind (1998), mean chlorophyll *a* (30 ± 19 µg L^{-1}) converted in C from this C:chl *a* ratio and the layer 0-5 m (17 Mm^3) from January to July, algal C uptake would be estimated at 1400 ± 450 t C y^{-1}. The annual primary production rate would then be 390 ± 130 g C m^{-2} y^{-1} which once again categorizes the Cointzio reservoir as eutrophic given the classification of the lake trophic state (eutrophic > 365 g C m^{-2} y^{-1}; Wetzel 2001).

The Cointzio reservoir seemed to follow the same general trend as the one observed in neighboring eutrophic lakes and reservoirs located in the TMVB region, such as the Chapala lake (de Anda et al. 2001), the Lago de Guadalupe (Sepulveda-Jauregui et al. 2013) and many others (Bravo-Inclán et al. 2010). For instance, a recent study on the main reservoir of Valle de Bravo, which provides water to Mexico City, showed that N and P loads in the Valle de Bravo reservoir have increased two to three-fold between 1992 and 2005 (Ramírez-Zierold et al. 2010). The Valle de Bravo reservoir is eutrophic due to the local township sewage and agriculture diffuse sources from the watershed. Close to the Cointzio reservoir, the Pátzcuaro lake has been facing severe eutrophication problems for at least 20 years (Chacón Torres 1993; Rosas et al. 1993). Mijangos Caro et al. (2008) estimated the contribution of point and diffuse sources from 13 surrounding sub-watersheds (total surface of 933 km^2). They concluded that urban nutrient loads were of high concern in lake neighbouring towns, whereas diffuse sources predominated in eroded and agricultural catchments. The oligotrophic lake Zirahuen located in the same region has been spared from eutrophication so far, but the study of Chacón-Torres and Rosas Monge (2008) alerted on the urgency to collect and treat the incoming wastewater to preserve this ecosystem.

According to the above-cited studies related to the TMVB region, and due to the evident link between nutrient loads and eutrophication of reservoirs in tropical area, there is a crucial need to implement best management practices (BMPs) in upstream watersheds. Classical recommendations, as made by Ramírez-Zierold et al. (2010), are to reduce P and N inputs from wastewater (treating sewage) and also from agricultural diffuse sources (regulation of fertilizers uses and input from livestock). In the case of the Cointzio watershed, the main priority issue would be the drastic control of nutrient point sources from domestic effluents (collection and treatment) which would benefit the water quality of the Cointzio reservoir, as recently shown by the study of Doan et al. (2013, comm pers). This mitigation would also have positive effects on the downstream Cuitzeo laguna, which has been suffering from hypereutrophication and fish-Fauna ecological impacts for many years, particularly when it dried up during severe droughts in the early 1990s (Soto-Galera et al. 1999).

This regional context in Mexico can be generalized to many other developing countries in the inter-tropical area. Such countries are facing increasing population and lack of wastewater treatment, and the implementations of BMPs listed above were largely recommended in numerous studies worldwide (Brazil, India, Sri Lanka, China and others; Reddy 2005).

Effect of floods on the reservoir functioning

In the Cointzio reservoir, a large proportion (> 80 %) of the TSS, P-tot, N-tot and TOC annual inputs occurred during the wet season (June to October). The seasonality of the inputs had a strong effect on the internal functioning of the reservoir. The most important feature was the very high TSS input during the wet season that induced a rapid decrease of light penetration due to high turbidity. The range of Secchi depth in the Cointzio reservoir (0.11 to 0.30 m) was among the lowest of the tropical lakes and reservoirs of the region. For instance this value is 13 to 19 m in the clear lake Zirahuen (Martinez-Almeida and Tavera 2005) and 3.2 to 5.8 m in the eutrophic reservoir of Valle de Bravo (Merino-Ibarra et al. 2008). Consequently to this decrease in Secchi depth, a rapid drop of Chlorophyll *a* was observed. In the comparable eutrophic reservoir of Valle de Bravo, chlorophyll *a* remained high during all the stratified period (Merino-Iberra et al. 2008). Moreover, in eutrophic systems the decrease in Secchi depth is generally correlated with an increase in chlorophyll *a* (Wollenweider 1968). This is not the case in the Cointzio reservoir where floods have a strong effect on the seasonality of primary production.

Increase in nutrients in the reservoir was also largely driven by the large inputs of nutrients during floods. These inputs quickly and strongly enriched the reservoir to a high concentration level of PO_4^{3-} and NH_4^+, both in epilimnion and hypolimnion. During stratification in tropical systems, a depletion of nutrient in the epilimnion due to algal uptake is generally observed, together with enrichment in the hypolimnion due to benthic mineralization and benthic desorption under anoxic conditions (Kunz et al. 2011; Merino-Iberra et al. 2008, Burford et al. 2012). In most of the warm monomictic Mexican lakes and reservoirs listed by Alcocer and Bernal-Brooks (2010), the hypolimnion becomes anoxic during the stratification period, which then leads to PIP release from sediments and an increase in PO_4^{3-} in the hypolimnion. The long and intense anoxia was observed in the Cointzio reservoir, but there was little evidence of PIP desorption since PIP in deposited sediment did not vary between dry and wet season. This behavior can be the consequence of the Acrisol-origin of sediments brought during the floods (Evrard et al. 2013). These soils typically have an important P adsorption capacity caused by the presence of iron and aluminium (Parfitt and Clayden 1991). In lakes and reservoirs with high iron and aluminium concentrations, hypolimnic anoxia does not necessary lead to P release (Gächter and Müller 2003). In the Cointzio reservoir, aluminium and iron concentrations were high and regularly above the standard for drinking water production (unpublished data from Oaapas). Floods would then have a major effect on PO_4^{3-} concentration, whereas desorption of PIP from

sediments appeared to be a negligible process. The effect of floods on the increase of hypolimnic concentrations was also highlighted in the Itezhi-Tezhi reservoir in Zambia (Kunz et al. 2011), but in this study nutrient concentrations remained stratified in the water column while in our study the increase was not only observed in the hypolimnion but also in the epilimnion. This could be the consequence of a wind-swept effect that may have driven nutrient movement from hypolimnion to epilimnion through boundary mixing caused by internal waves (Merino-Iberra et al. 2008). This effect is likely to take place in the Cointzio reservoir given the high diurnal variability of wind (Susperregui 2008).

Regarding the high interannual variability of precipitation and discharge in the Cointzio watershed, the effect of floods was probably much more pronounced in wet years (Gratiot et al. 2010). This effect of floods is more important in tropical areas where the seasonality is highly marked (Burford et al. 2012; Syviski et al. 2014).

Sediment trapping efficiency

Table 7

The reservoir of Cointzio acted as a sink of TSS. The large difference between inputs and outputs was explained by a large amount of sediment accumulation (28 000 ± 12 000 t y^{-1} Table 7). Given the range of uncertainties, both estimations from input-output difference and Sed_{acc} were in the same order of magnitude (Figure 8a). This result leads to the assumption that external TSS input was dominant in the Cointzio reservoir in comparison to internal input such as dead algae sedimentation. With the level of accuracy of our calculations, sediment retention would be > 90 % of the incoming TSS. According to the classification proposed by Vörösmarty et al. (2003), the trapping efficiency of the Cointzio reservoir was within the highest range of anthropogenic sediment dam-retention (80-100 %). The sediment accumulation rate deduced from our study was 7 800 ± 3 300 g m^{-2} y^{-1} (Table 7). This value is very similar to that estimated on the global scale for small reservoirs (7 700 g m^{-2} y^{-1}) when large reservoirs presented slightly higher sediment accumulation rates (Syvitsky et al. 2005, Table 7). Compared to other tropical reservoirs listed in Table 7, sediment accumulation rates were higher in the Cointzio reservoir to those of the Itezhi-Tezhi reservoir (900 g m^{-2} y^{-1}, Kunz et al. 2011, Table 7) or the Pampulha reservoir in Brazil (320 g m^{-2} y^{-1}, Torres et al. 2007). Large differences in the trapping efficiency among reservoirs can be explained by the morphology of the reservoir (depth and surface area) and its water residence time (Cunha et

al. 2014). For instance, lower depths with high water residence times can favor the trapping efficiency. The geological context of the upstream watershed is also of importance, since the more upstream soil erosion there is, the higher the downstream TSS load is. Syvitsky et al. (2005) stated that whole areas of Central and North Mexico were affected by high sediment accumulation rates, which can be related to the high erosion rates prevalent in those regions (Descroix et al. 2008). The example of the lower sediment accumulation rate for the Pampulha reservoir can be explained by low water residence (0.2 y) and also a low specific TSS load (20 t km^{-2} y^{-1}). In the case of Cointzio, even with a low residence time (< 1 y) and large depth, the reservoir presented a very efficient retention. This is likely to be a consequence of the high seasonality of the TSS input, which caused very dense hyperpycnal flows and led to rapid trapping of the sediment.

Sediment trapping is a key issue for the management of the Cointzio reservoir since it has already lost 25 % (i.e. 22 Mm^3) of its initial storage capacity on its construction in 1940 (initial capacity was 88 Mm^3, Susperregui, 2008). Based on the sediment accumulation rate determined in this study, the reservoir may lose an additional 1 Mm^3 in the next 20 years (i.e. 1.5 % of its current capacity). This estimate appears low compared to the trapping of 22 Mm^3 since 1940. The three years studied presented similar TSS load and were characteristic of dry years. From our results we can estimate the specific TSS yield from the watershed to amount to 35 ± 19 t km^{-2} y^{-1}. The historical database of discharge and TSS at the watershed outlet (1973-1985, Oaapas, data not shown) allowed calculation of TSS loads of up to 150 000 t y^{-1} i.e. 240 t km^{-2} y^{-1} for some wet years (1976 and 1981 for instance, Susperregui 2008). This indicates a considerable interannual variability of the TSS input to the reservoir, which is driven by the hydrological conditions. This was also evidenced by Susperregui (2008) using sediment core data. Another factor possibly involved in the TSS input reduction is the land use changes that occurred in the Cointzio watershed over the last decades. López-Granados et al. (2013) identified significant land use changes between 1986-1996 in benefit to reforested areas and shrubland progression. Moreover, alternative agronomic practices such as the plantation of agave forestry and native species are being implemented locally in the Cointzio watershed to prevent severe soil erosion (Schwilch et al. 2012), which might have long-term positive effects on the TSS input to the reservoir. Modifying the morphology or the hydraulic processes occurring within reservoirs to reduce their sediment accumulation rates appears unachievable. The most promising way of mitigating the decrease in reservoir storage capacity would therefore be the reduction of incoming TSS inputs through limitation of upstream erosion.

Organic carbon origin and C, N, P trapping efficiency

The Cointzio reservoir reduced significantly the incoming TOC load (40 %), which modified somehow its internal biogeochemical functioning. The accumulation of C (C_{acc}) was estimated at 298 ± 128 t C y^{-1} (Table 7 and Figure 8b) and is likely composed of a fraction of the allochthonous C mainly brought in during the wet season and a fraction of new autochthonous C produced by algae during the dry season. The respective contribution of allochthonous C and autochthonous C has to be quantified to analyse the factors responsible for the high anoxia due to mineralization in the Cointzio reservoir. The signature of autochthonous C is assumed to be the mean POC in surface TSS during the production period in the dry season (200 ± 100 mg C g^{-1}). The signature of allochthonous C can be deduced from the mean POC content of bottom settled sediment that has been reduced 10-fold with the arrival of floods and hyperpycnal flow in July (decrease from 100 ± 90 mg C g^{-1} in the dry season to 12 ± 3 mg C g^{-1} in the wet season). The value of POC in bottom settled sediment during the wet season was very close to the mean OC content in deposited sediment (10.6 ± 1.1 mg C g^{-1}). We can then evaluate that, from July to December, OC in bottom settled sediment was nearly 100% of allochthonous origin. During the wet season a large amount of incoming sediment and allochthonous C did not completely settle and was resettled between November and January with the total mixing of the reservoir as evidenced with homogeneous distribution of TSS at this period. To estimate the contribution of autochthonous C ($\%C_{auto}$) in the C bottom settled sediment during the dry season, a simple mixing model comparable to the one presented in Kunz et al. (2011) was applied. Here we considered the allochthonous C signature (C_{allo}) to be 12 ± 3 mg C g^{-1} and the autochthonous signature (C_{auto}) to be 200 ± 100 mg C g^{-1} in the following equation:

$$C_{\text{bottom settled sediment}} = (1 - \%C_{auto}) \times C_{allo} + \%C_{auto} \times C_{auto} \qquad \text{[Eq. 5]}$$

Calculated $\%C_{auto}$ was 47 ± 23 %. Hence, the C bottom settled sediment was of about 50 % autochthonous origin during the dry season (half year) and of 100 % allochthonous origin during the rest of the year. Considering a continuous TSS and C deposition during the year, the allochthonous C contribution would then represent 74 ± 12% of the C_{acc} (i.e. 220 ± 36 t C y^{-1}). This proportion of allochthonous C was also found in the Itezhi Tehzi reservoir (84% of C_{acc}, Kunz et al. 2011), which received a major portion of allochthonous C during the flood

events. These authors also demonstrated a significant impact of allochthonous inputs in the deoxygenation of the hypolimnion. The rate of hypolimnic mineralization was maximal just after the deposition of allochthonous inputs. In the case of Cointzio we can also assume that the intense anoxia affecting the reservoir is due to the mineralization of allochthonous C inputs during the wet season. Based on our calculation, allochthonous C_{acc} would then account for 55 % of incoming POC (Figure 8b), indicating potential additional C removal by mineralization. Our field data did not allow quantifying C removal by mineralization. However, it is largely known that the aerobic and anaerobic mineralization in tropical reservoirs can saturate the water column in CO_2 and CH_4 likely to be degassed into the atmosphere (Guérin et al. 2006). The long and intense period of anoxia observed in the Cointzio reservoir was clearly an indicator of high aerobic mineralization and also favorable to methanization. Additional loss through CO_2 and CH_4 emission would most likely occur in the Cointzio reservoir. The methanization process has been largely demonstrated in tropical reservoirs and is of general concern for global warming on the global scale (Reigner et al. 2013). Further study is underway to assess these processes in the Cointzio reservoir using a modeling approach (Doan et al. 2014 comm.pers).

Our estimation of the C_{acc} rate was 83 ± 35 g C m^{-2} y^{-1} (Table 7) and appeared higher compared to the value estimated at the Itezhi-Tezhi reservoir for instance (62 g C m^{-2} y^{-1}, Kunz et al. 2011 Table 7). This can be explained by the higher sediment accumulation rate in the Cointzio reservoir and important POC inputs during the wet season. Other contrasted behavior was observed in the Pampulha reservoir in Brazil, which exported C rather than accumulated it (Torres et al. 2007, Table 7). Even if there was no estimation of contribution of autochthonous and allochthonous C in the study, the high productivity of this reservoir was identified as the main factor explaining the C exportation. C accumulation can therefore be highly variable among reservoirs and linked to the allochthonous C inputs and sediment trapping efficiency (Tranvik et al. 2009).

The difference between N-tot input and N-tot output indicated that N input was reduced by 46 % in the Cointzio reservoir. 60 % of this reduction can be explained by the N_{acc} which was estimated at 26 ± 11 t N y^{-1} (Table 7, Figure 8c). N accumulation rate (7.2 ± 3.1 g N m^{-2} y^{-1}) was in the same order of magnitude as the N accumulation rate estimated at the global scale (11 ± g N m^{-2} y^{-1}, Beusen et al. 2005, Table 7) and in the range of other reservoirs listed in Table 7. N accumulation can be highly variable among reservoirs because of the difference in

TSS trapping efficiency or water residence time, as highlighted previously for sediment accumulation (Cunha et al. 2014). Moreover, the estimation of total N removal in reservoirs is much more complex since the cycling of N is dynamic and involves not only accumulation but also numerous biological processes (i.e. denitrification, N fixation, nitrification, Wetzel 2001). Denitrification processes are particularly responsible for N removal, with the production of N_2 that is known to be an important process explaining the mass balance of nitrogen in aquatic tropical ecosystems (Lewis 2002). In the Cointzio reservoir, the reduction of 30 % that was observed between NO_3^- input and output suggest possible denitrification (Figure 8c). In the eutrophic reservoir of Valle de Bravo, for instance, N removal by denitrification was equivalent to N accumulation (Ramírez-Zierold et al. 2010). The long and intense anoxia in Cointzio was likely to favor denitrification. N removal by denitrification would then be of importance to close the N mass balance in the Cointzio reservoir. This assumption is consistent with the NiRReLa global model results of Harrison et al. (2009) who identified this central region of Mexico as having a high N removal rate potential. Further studies are needed to confirm our hypothesis. In addition, N fixation may also be an important process since N-fixing Cyanobacteria (*Oscillatoria lacustris*) were identified as the dominant group during the dry season in the Cointzio reservoir (Ramírez-Olvera et al. 2004).

The Cointzio reservoir acted as a sink of P with an estimation of 30 % reduction of incoming P-tot. P_{acc} was estimated at 5 ± 2 t P y^{-1} and, given the calculated uncertainties, this result allowed explaining a large proportion (>70 %) of the incoming P-tot reduction (Table 7, Figure 8d). Phosphorus is known to have a strong affinity with sediment (Némery and Garnier 2007). Therefore P trapping is commonly correlated with TSS retention and P is largely retained through sedimentation (Bensen et al. 2005). In the case of the Cointzio reservoir, despite TSS retention > 90 %, the proportion of P retained remained moderate. P retention in reservoirs is also influenced by their water residence time (Kõiv et al. 2011). The longer the residence time, the higher the internal P recycling is, which in turn leads to an increase in P retention. The large eutrophic tropical reservoir of Castanhão in Brazil has a residence time of about 10 y, and P retention was estimated at 98 % (Molisani et al. 2013). Therefore the low water residence time in the Cointzio reservoir may explain the moderate P trapping efficiency. However, the water residence time is not the only explicative factor to explain P trapping efficiency. For instance, Torres et al. (2007) calculated P retention to be 81 % in the Pampulha reservoir, which has a very low water residence time of 0.2 y and shallow waters. The latter feature can also favor the P trapping efficiency (Kõiv et al. 2011).

The P_{acc} rate for the Cointzio reservoir (1.4 ± 0.5 g P m^{-2} y^{-1}, Table 7) was close to the one of the Pampulha reservoir (1.2 g P m^{-2} y^{-1}) and also to the one of the Itezhi-Tezhi reservoir (0.8 g P m^{-2} y^{-1}). The latter has similar water residence time (0.7 y) and 60 % P trapping efficiency (Kunz et al. 2011, Table 7). P_{acc} was three-fold lower than the P accumulation in the neighboring Valle de Bravo reservoir (5.5 g P m^{-2} y^{-1}), which has a water residence time of 1.58 y and retained 85 % of P input (Ramírez-Zierold et al. 2010, Table 7). The difference can be explained by the P input to the Valle Bravo reservoir (121 t P y^{-1}), which was 10-fold higher than the P input to the Cointzio reservoir (20 t P y^{-1}) with a similar upstream watershed area. Apart from the morphologically induced characteristics of reservoirs discussed above, the P retention also depends on the watershed P inputs. Based on the analysis of 54 lakes and reservoirs in different climate regions around the world, Kõiv et al. (2011) found a strong correlation between the specific external P load and the reservoir P retention in P per m^2. The comparison between several reservoirs showed that, regardless of the wide variety of reservoirs, the level of P input is the main cause of high P retention. This is consistent with the 6-year study in the Wivenhoe reservoir (Australia) carried out by Burford et al. (2012), which concluded that the variability of annual P retention was largely driven by the level of P input during each year.

From the above discussion, the comparison of P trapping efficiency and P accumulation rate in tropical reservoirs is highly complicated because it depends on many factors such as water residence time, depth, TSS trapping and external P load.

Figure 8:

Conclusions

Our results illustrate the strong influence of watershed-emitted untreated point sources on the biogeochemistry of a small tropical reservoir. High nutrient inputs to the Cointzio reservoir were an essential driver of its eutrophication, as evidenced by the high chlorophyll *a* concentrations, high primary production and the long and intense hypolimnic anoxia observed. Eutrophication represents an issue of concern for most of the lakes and reservoirs in Central Mexico, and point source reduction should be the highest water management priority in Mexico in the upcoming years.

Our results indicate a pronounced seasonality in the upstream inputs to the reservoir. Alternating dry and wet seasons strongly influenced the functioning of the reservoir (high

turbidity, predominance of allochthonous carbon). Even with low water residence time, sediment trapping was very efficient and threatened the sustainability of its storage capacity. The reservoir was also a trap for incoming nutrients and carbon responsible for its eutrophic state. The accumulation of nutrients remained moderate relative to other eutrophic tropical reservoirs, which can be explained by different factors such as the residence time, importance of nutrient yields and internal biogeochemical transformations (mineralization, denitrification).

This study has important implications for reservoir managers when designing mitigation strategies to preserve siltation or to prevent eutrophication.

Acknowledgments

This work was undertaken in the framework of the European Research project DESIRE (2007-2011) and the French ANR Research project STREAMS (2008-2010). We thank the CIGA and CIECO, UNAM campus of Morelia, for giving access to their laboratory facilities. We are grateful to Jorge Schondube (UNAM) for kindly providing his wonderful electric boat and CONAGUA for their support in the project. We thank Alexandra Coynel and Henry Etcheber for help with POC analysis at the EPOC laboratory. We also thank students who helped us during field measurements from 2007 to 2009 (Florence Mahé, Natacha Salles, Antonio Munoz-Gaytan, Lila Collet and Anne-Sophie Susperregui). We are grateful to Marie-Paul Bonnet and Martin Schmid for fruitful discussions and comments.

References

Alcocer J, Bernal-Brooks FW (2010) Limnology in Mexico. Hydrobiol 644:15–68

Allende TC, Mendoza ME, López Granados EM, Morales Manilla LM (2009) Hydrogeographical Regionalisation: An Approach for Evaluating the Effects of Land Cover Change in Watersheds. A Case Study in the Cuitzeo Lake Watershed, Central Mexico. Water Res Manag 23:2587–2603

Alvarado-Villanueva R, Salles N, Ortega-Murillo MR, Némery J, Gratiot N, Hermandez-Morales R (2010) Distribucion vertical del fitoplancton, durante la epoca de secas en la presa

de Cointzio, Michoacan. SOMPAC 25 (XVI Reunión Nacional y IX Internacional de la Sociedad Mexicana de Planctología A. C. –SOMPAC-), 27-30 April 2010 Lapaz (Mexico)

American Public Health Association (APHA) (1995) Standard methods for the examination of water and wastewater. In: Greenburg AE, Clesceri LS, Eaton AD (eds) 20th ed. American Public Health Association, Washington, DC

de Anda J, Shear H, Maniak U, Riedel G (2011) Phosphates in Lake Chapala, Mexico. Lakes Reservoirs: Res Manag 6: 313–321

Aspila KI, Agemian H, Chau ASY (1976) A semi-automated method for the determination of inorganic, organic and total phosphate in sediments. Analyst 101:187–197

Avila Garcia P (2006) Water, society and environment in the history of one Mexican city. Environ Urban 8: 129 doi: 10.1177/0956247806063969

Berrera Camacho G, Bravo Espinosa M (2009) La planificación del territorio, gestión de recursos o gestión de conflictos. El Caso de Cointzio, Michoacán CONACYT report

Beusen AHW, Dekkers ALM, Bouwman AF, Ludwig W, Harrison J (2005) Estimation of global river transport of sediments and associated particulate C, N, and P. Glob Biogeochem Cycles 19: GB4S05, doi: 10.1029/2005GB002453

Bouraoui F, Grizzetti B (2014 Modelling mitigation options to reduce diffuse nitrogen water pollution from agriculture. Sci Tot Environ 468–469:1267–1277

Billen G, Garnier J, Némery J, Sebilo M, Sferratore A, Barles S, Benoit P, Benoît M (2007) A long-term view of nutrient transfers through the Seine river continuum. Sci Tot Environ 375:80–97

Bosch NS, Allan JD (2008) The influence of impoundments on nutrient budgets in two catchments of Southeastern Michigan. Biogeochem 87:325–338

Bravo-Inclán LA, Olvera-Viascán V, Sánchez-Chávez JJ, Saldaña-Fabela P, Tomasini-Ortiz AC (2011) Trophic state assessment in warm-water tropical lakes and reservoirs of the central region of Mexico in Van Bochove EPA, Vanrolleghem PA, Chambers G, Thériault B. Novotná and Burkart MR (eds.) Issues and Solutions to Diffuse Pollution: 14th International Conference of the IWA Diffuse Pollution Specialist Group, DIPCON 2010 Québec CANADA 495pp

Bravo-Espinosa M, Mendoza ME, Medina-Orozco L, Prat C, García-Oliva F, López-Granados E (2009) Runoff, soil loss, and nutrient depletion under traditional and alternative cropping systems in the Transmexican Volcanic Belt, Central Mexico. Land Degrad Develop 20(6):640–653

Burford MA, Green SA, Cook AJ, Johnson SA, Kerr JG, O'Brien KR (2012) Sources and fate of nutrients in a subtropical reservoir. Aquat Sci 74:179–190

Chacón Torres A (1993) Lake Pátzcuaro, Mexico: watershed and water quality deterioration in a tropical high-altitude Latin American lake. Lake and Reservoir Manag 8:37–47

Chacón-Torres A, Rosas-Monge C (2008) Water quality characteristics of a high altitude oligotrophic Mexican lake. Aquat Ecosy Health Manag 1:237–243

Chanudet V, Descloux S, Harby A, Sundt H, Brakstad BHHO, Serça D, Guérin F (2011) Gross CO_2 and CH_4 emissions from the Nam Ngum and Nam Leuk sub-tropical reservoirs in Lao PDR. Sci Total Environ 409:5382–5391

Cole JJ, Prairie YT, Caraco NF, McDowell WH, Tranvik LJ, Striegl RG, Duarte CM, Kortelainen P, Downing JA, Middelburg JJ (2007) Plumbing the global carbon cycle: Integrating inland waters into the terrestrial carbon budget. Ecosystems 10:172–185

Covaleda S, Gallardo JF, Garcıá-Oliva F, Kirchmann H, Prat C, Bravo M, Etchevers JD (2011) Land-use effects on the distribution of soil organic carbon within particle-size fractions of volcanic soils in the Transmexican Volcanic Belt (Mexico). Soil Use Manag 27:186–194

Coynel A, Etcheber H, Abril G, Maneux E, Dumas J, Hurtrez JE. (2005) Contribution of small mountainous rivers to particulate organic carbon input in the Bay of Biscay. Biogeochem 74:151–171

Cunha DGF, de Carmo Calijuri MC, Dodds WK (2014) Trends in nutrient and sediment retention in Great Plains reservoirs (USA). Environ Monit Assess 186:1143–1155

Dang TH, Coynel A, Orange D, Blanc G, Etcheber H, Le LA (2010) Long term monitoring (1960–2008) of the river-sediment transport in the Red River Watershed (Vietnam): temporal variability and dam-reservoir impact. Sci Total Environ 408:4654–4664

Descroix L, Gonzalez Barrios JL, Viramontes D, Poulenard J, Anaya E, Esteves M, Estraba J (2008) Gully and sheet erosion on subtropical mountain slopes: their respective roles and the scale effect. Catena 72(3):325–339

Doan TKP, Némery J, Schmid M, Gratiot N (2013) Eutrophication of turbid tropical reservoirs: Modelling for the case of Cointzio, Mexico. 19th ISEM Conference - Ecological Modelling for Ecosystem Sustainability, 28-31 october 2013 Toulouse (France)

Doan TKP, Némery J, Gratiot N, Schmid M (2014) Biogeochemical mass balances in a turbid tropical reservoir: field data and modelling approach. EGU General Assembly 27 April-2 May 2014 Vienne (Austria)

Donohue I, Molinos JG (2009) Impacts of increased sediment loads on the ecology of lakes. Biol Rev 84:517–531

Dawson JCC, Tetzlaff D, Speed M, Hrachowitz M, Soulsby C (2011) Seasonal controls on DOC dynamics in nested upland catchments in NE Scotland. Hydrol Proc 25:164–1658

Duvert C, Gratiot N, Evrard O, Navratil O, Némery J, Prat C, Esteves M (2010) Drivers of erosion and suspended sediment transport in three headwater catchments. Geomorph 123(3–4):243–256

Duvert C, Gratiot N, Némery J, Burgos A, Navratil, O (2011) Sub-daily variability of suspended sediment fluxes in small mountainous catchments-Implications for community-based river monitoring. Hydrol Earth Syst Sci 15:703–713

Etcheber H, Taillez A, Abril G, Garnier J, Servais P, Moatar F, and Commarieu M V (2007) Particulate organic carbon in the estuarine turbidity maxima of the Gironde, Loire and Seine estuaries: origin and lability. Hydrobiol 588: 245–259

Evrard O, Poulenard J, Némery J, Ayrault S, Gratiot N, Duvert C, Prat C, Lefèvre I, Bonté P, Esteves M (2013) Tracing sediment sources in a tropical highland catchment of central Mexico by using conventional and alternative fingerprinting methods. Hydrol Proc 27:911–922

Flipo N, Even S, Poulin M, Thery S, Ledoux E (2007) Modeling nitrate fluxes at the catchment scale using the integrated tool CAWAQS. Sci Tot Environ 375(1–3)69–79

Friedl G, Wüest A (2002) Disrupting biogeochemical cycles-consequences of damming. Aquatic Sc 64:55–65

Gächter R, & Müller B (2003) Why the phosphorus retention of lakes does not necessarily depend on the oxygen supply to their sediment surface. Limnol Ocean 48(2):929–933

Garnier J, Blanc P, Benest D (1989) Estimating a Carbon/Chlorophyll ratio in Nannoplankton (Creteil Lake, S-E Paris, France). Water Resour Bull 25:751–754

Garnier J, Leporcq B, Sanchez N & Philippon X (1999) Biogeochemical mass-balances (C, N, P, Si) in three large reservoirs of the Seine Basin (France). Biogeochem 47:119–146

Gratiot N, Duvert C, Collet L, Vinson D, Némery J, Saenz-Romero C (2010) Increase in surface runoff in the central mountains of Mexico: lessons from the past and predictive scenario for the next century. Hydrol Earth Syst Sci 14(2):291–300

Guérin F, Abril G, Richard S, Burban B, Reynouard C, Seyler P, Delmas R (2006) Methane and carbon dioxide emissions from tropical reservoirs: significance of downstream rivers. Geophys Res Lett 33:L21407, doi: 10.1029/2006GL027929

Guérin F, Abril G, de Junet A, Bonnet MP (2008) Anaerobic decomposition of tropical soils and plant material: implication for the CO_2 and CH_4 budget of the Petit Saut Reservoir. Appl Geochem 23:2272–83

Harrison JA, Maranger RJ, Alexander RB, Giblin AE, Jacinthe PA, Mayorga E, Seitzinger SP, Sobota DJ, Wollheim WM (2009) The regional and global significance of nitrogen removal in lakes and reservoirs. Biogeochem 93:143–157

Hope D, Billett MF, Cresser MS (1997) Exports of organic carbon in two river systems in NE Scotland. J Hydrol 193:61–82

Kennedy RH, Tundisi JG, Straškrábová V, Lind OT, Hejzlar J (2003) Reservoirs and the limnologist's growing role in sustainable water resource management. Hydrobiol 504:xi–xii

Kõiv T, Nõges T, Laas A (2011) Phosphorus retention as a function of external loading, hydraulic turnover time, area and relative depth in 54 lakes and reservoirs. Hydrobiol 660:105–115

Kunz MJ, Wüest A, Wehrli B, Landert J, Senn DB (2011) Impact of a large tropical reservoir on riverine transport of sediment, carbon, and nutrients to downstream wetlands. Water Resour Res 47:W12531, doi: 10.1029/2011WR010996

Kunz MJ, Anselmetti FS, Wüest A, Wehrli B, Vollenweider A, Thüring S, Senn DB (2011b) Sediment accumulation and carbon, nitrogen, and phosphorus deposition in the large tropical reservoir Lake Kariba (Zambia/Zimbabwe). JGR 116:G03003, doi: 10.1029/2010JG001538

Le TPQ, Billen G, Garnier J, Chau VM (2014) Long-term biogeochemical functioning of the Red River (Vietnam): past and present Situations. Reg Environ Change doi : 10.1007/s10113-014-0646-4

Lehner B, Döll P (2004) Development and validation of a global database of lakes reservoirs and wetlands. J Hydrol 296:1–22

Lewis WM (2002). Estimation of background nitrogen yields for North America by use of benchmark watersheds. Biogeochem 57–58:375–385

López López E, Dávalos-Lind L (1998) Algal growth potential and nutrient limitation in a tropical river-reservoir system of the Central Plateau, Mexico. Aquat Ecosyst Health Manag 1:345–351

López-Granados E, Mendoza ME, González DI (2013) Linking geomorphologic knowledge, RS and GIS techniques for analyzing land cover and land use change: a multitemporal study in the Cointzio watershed, Mexico. Ambi Água - Interdisci J App Sci 8(1):18-37 doi: 10.4136/ambi-agua.956

Maneux E, Probst JL, Veyssy E, Etcheber H (2001) Assessment of dam trapping efficiency from water residence time: application to fluvial sediment transport in the Adour, Dordogne and Garonne river basins (France). Water Resour Res 37:801–811

Martinez-Almeida V, Tavera R (2005) A hydrobiological study to interpret the presence of desmids in Lake Zirahuén, México. Limnologica 35:61–69

Mendoza M, Granado EL, Gratiot N, Arnaud F, Magand O, Prat C, Esteves M (2013) Relationships between land cover, land use change and erosion-sedimentation processes at the watershed level: A multitemporal study in the Cointzio watershed, Mexico. 8th IAG conf. on Geomorphology 27-31 August 2013. Paris (France)

Merina-Iberra M, Monroy-Ríos E, Vilaclara G, Castillo, FS, Gallegos, ME, Ramírez-Zierold J (2008) Physical and chemical limnology of a wind-swept tropical highland reservoir. Aquat Ecol 42:335–345

Mijangos Carro M, Izurieta Dávila J, Gómez Balandra A, López RH, Huerto Delgadillo R, Sánchez Chávez J, Bravo Inclán L (2008) Importance of diffuse pollution control in the

Patzcuaro Lake Basin in Mexico. Water Technol 58(11):2179–2186 doi:10.2166/wst.2008.820

Molisani MM, Becker H, Barroso H, Hijo CAG, Monte TM, Vasconcellos GH, Lacerda LD (2013) The influence of Castanhão reservoir on nutrient and suspended matter transport during rainy season in the ephemeral Jaguaribe river (CE, Brazil). Braz J Biol 73(1):115–123

Murphy J, Riley JP (1962) A modified single solution method for the determination of phosphate in natural waters. Anal Chim Acta 27:31–36

Némery J, Garnier J (2007) Origin and fate of phosphorus in the Seine watershed (France): The agricultural and hydrographic P budget. JGR-Biogeosci 112: G03012, doi: 10.1029/2006JG000331

Némery J, Mano V, Coynel A, Etcheber H, Moatar F, Meybeck M, Belleudy P & Poirel A (2013) Carbon and suspended sediment transport in an impounded alpine river (Isère, France). Hydrol Proc 27:2498–2508

Ooapas (2007) Organismo Operador de Agua Potable de Morelia. Evaluation socioeconomic del saneamiento de aguas residuals de Morelia (http://www.shcp.gob.mx/EGRESOS/ppi/Proyec_hidraulicos/saneamiento_morelia.pdf)

Parfitt RL, Clayden B (1991) Andisols - the development of a new order in Soil Taxonomy. Geoderma 49:181–198

Park HK, Byeon MS, Shin YN, Jung DI (2009) Sources and spatial and temporal characteristics of organic carbon in two large reservoirs with contrasting hydrologic characteristics. Water Resour Res 45:W11418, doi:10.1029/2009WR008043

Quinton JN, Govers G, Van Oost K, Bardgett R (2010) The impact of agricultural soil erosion on biogeochemical cycling. Nature Geosci 3:311–314

Rãdoane M, Rãdoane N (2005) Dams, sediment sources and reservoir silting in Romania. Sci Total Environ 71(1–2):112–125

Ramírez-Olvera MA, Díaz-Argüero M, López-López E (2004) Planktonic Crustacean Assemblages in a System of three reservoirs in the Mexican Central Plateau: Seasonal and Spatial Patterns. J Freshw Ecol 19(1):25–34

Ramírez-Zierold JA, Merino-Ibarra M, Monroy-Ríos E, Olson M, Castillo FS, Gallegos ME, Vilaclara G (2010) Changing water, phosphorus and nitrogen budgets for Valle de Bravo reservoir, water supply for Mexico City Metropolitan Area. Lake Reservoir Manag 26:23–34

Reddy MV (2005) Restoration and Management of Tropical Eutrophic Lakes. Science publisher Inc. Enfield (NH) USA, Plymouth, UK 543pp

Regnier P, Friedlingstein P, Ciais, P, Mackenzie FT, Gruber N, Janssens IA, Laruelle GG, Lauerwald R, Luyssaert S, Andersson AJ, Arndt S, Arnosti C, Borges AV, Dale AW, Gallego-Sala A, Goddéris Y, Goossens N, Hartmann J, Heinze C, Ilyina T, Joos F, LaRowe DE, Leifeld J, Meysman FJR, Munhoven G, Raymond PA, Spahni R, Suntharalingam P, Thullner M (2013) Anthropogenic perturbation of the carbon fluxes from land to ocean. Nature Geosci 6:597–607

Robertson GP, Coleman DC, Bledsoe CS, Sollins P (1999) Standard soil methods for long-term ecological research. Oxford University Press: New York Oxford, 480pp

Rosas I, Velasco A, Belmont R, Baez A, Martínez A (1993) The algal community as an indicator of trophic status in Lake Patzcuaro, Mexico. Environ Poll 80: 255–264

Salas HJ, Martino P (1991) A simplified phosphorus trophic state model for warm-water tropical lakes. Water Res 25(3):341–350

Schwilch G, Hessel R, Verzandvoort S (Eds) (2012) DESIRE for greener land. Options for sustainable land management in drylands. Publishers University of Bern - CDE, Alterra, Wageningen UR and ISRIC - World Soil Information WOCATFAO 250pp

Seitzinger SP, Mayorga E, Kroeze C, Bouwman AF, Beusen AHW, Billen G, Van Drecht G, Dumont E, Fekete B M, Garnier J, Harrison JA (2010) Global river nutrient export: A scenario analysis of past and future trend. Glob Biogeochem Cycles 24:1–16

Sepulveda-Jauregui A, Hoyos-Santillan J, Gutierrez-Mendieta FJ, Torres-Alvarado R, Dendooven L, Thalasso F (2013) The impact of anthropogenic pollution on limnological characteristics of a subtropical highland reservoir "Lago de Guadalupe", Mexico. Knowledge Manag Aquat Ecosyst 410:04, doi: 10.1051/kmae/2013059

Soto-Galera E, Paulo-Maya J, López-López E, Serna-Hernández JA, Lyons J (1999) Change in Fish Fauna as Indication of Aquatic Ecosystem Condition in Rio Grande de Morelia–Lago de Cuitzeo Basin, Mexico. Env Manag 24(1):133–140

Sugimura Y and Suzuki Y (1988) A high temperature catalytic oxidation method for non - volatile dissolved organic carbon in seawater by direct injection of a liquid sample. Mar Chem 24:105–131

Susperregui AS (2008) Caractérisation hydro-sédimentaire des retenues de Cointzio et d'Umécuaro (Michoacán, Mexique) comme indicateur du fonctionnement érosif du bassin versant. *Hydro-sedimentary characterization of the reservoirs of Cointzio and Umécuaro (Michoacán, Mexico) as an indicator of operating erosive watershed*. Phd Thesis Grenoble University 289pp

Susperregui AS, Gratiot N, Esteves M, Prat C (2009) A preliminary hydrosedimentary view of a highly turbid tropical, manmade lake: Cointzio Reservoir (Michoacán, Mexico). Lakes Reservoirs: Res Manag14:31–39

Svendsen LM, Redsdorf A, Nørnberg P (1993) Comparison of methods for analysis of organic and inorganic phosphorus in river sediment. Water Res 27:77– 83

Syvitski JPM, Vörösmarty JV, Kettner AJ, Green P (2005) Impacts of humans on the load of terrestrial sediments to the global coastal ocean. Science 308:376–380

Syvitski JPM, Cohen S, Kettner AJ, Brakenridge R (2014) How important and different are tropical rivers? An overview. Geomorph doi.org/10.1016/j.geomorph.2014.02.029

Thouvenot M, Billen G, Garnier J (2007) Modelling nutrient exchange at the sediment–water interface of river systems. J Hydrol 341:55–78

Torres IC, Resck RP, Pinto-Coelho RM (2007) Mass balance estimation of nitrogen, carbon, phosphorus and total suspended solids in the urban eutrophic, Pampulha reservoir, Brazil. Acta Limnol Brasiliensia 19:79–91

Tranvik LJ, Downing JA, Cotner JB, Loiselle SA, Striegl RG, Ballatore TJ, Dillon P, Finlay K, Fortino K, Knoll LB, Kortelainen PL, Kutser T, Larsen S, Laurion I, Leech DM, McCallister SL, McKnight DM, Melack JM, Overholt E, Porter JA, Prairie Y, Renwick WH, Roland F, Sherman BS, Schindler DW, Sobek S, Tremblay A, Vanni MJ, Verschoor AM, von Wachenfeldt E, Weyhenmeyera GA (2009) Lakes and reservoirs as regulators of carbon cycling and climate. Limnol Oceanogr 54(6):2298–2314

Verhoff FH, Yaksich SM, Mel fi DA (1980) River nutrient and chemical transport estimates. J Environ Engineer Division 10:591–608

Vörösmarty JV, Meybeck M, Fekete B, Sharma K, Green P, Syvitski JPM (2003) Anthropogenic sediment retention: major global impact from registered river impoundments. Glob Planet Ch 39(1–2):169–190

Walling DE, Webb W (1985) Estimating the discharge of contaminants to coastal waters by rivers: some cautionary comments. Mar Poll Bull 16(12): 488–492

Water Framework Directive, 2000/60/EC (2000) Establishing a framework for community action in the field of water policy (OJ (2000) L327/1)

Wetzel RG (2001) Limnology: Lake and River Ecosystems, 3rd ed., Academic, San Diego, Calif. 1006pp

Vollenweider RA (1968) Scientific fundamentals of the eutrophication of lakes and flowing waters, with particular reference to nitrogen and phosphorus as factors of eutrophication, Tech. Rep. DA 5/SCI/68.27, O.C.D.E., Paris 250pp

Figures caption:

Figure 1: Map of the Cointzio watershed and reservoir: location of sampling sites (geographical position in UTM).
Figure 2: Seasonal time-series of a) water discharge (m^3 s^{-1}) and TSS inflow (mg L^{-1}), b) water discharge and TSS outflow (mg L^{-1}), and c) the volume of the Cointzio reservoir for 2007, 2008 and 2009 (Mm^3, incomplete year in 2007, mean, minimum and maximum volumes are given for the period 1991-2005; data CONAGUA).

Figure 3: Seasonal variation of TSS, P-tot (including $P\text{-}PO_4^{3-}$), N-tot (including $N\text{-}NO_3^-$, $N\text{-}NH_4^+$), POC and DOC inputs to the reservoir of Cointzio (t day^{-1})

Figure 4: Horizontal transects of temperature, DO and TSS at four dates covering the entire 2009 year. Dotted lines indicate date of vertical profiles.

Figure 5: Seasonal variation of a) temperature b) TSS c) DO and d) Chlorophyll *a* at the deepest point P27 in 2009.

Figure 6: Comparison of the seasonal variations in a) Secchi depth, b) chlorophyll *a* (surface and bottom), and c) POC in suspended sediment (surface and bottom) in the water column at the two sampling points P6 and P27.
Figure 7: Comparison of the seasonal variations in a) $P\text{-}PO_4^{3-}$, b) $N\text{-}NO_3^-$, and c) $N\text{-}NH_4^+$ in the water column at the two sampling points P6 and P27 (surface and bottom) in the Cointzio reservoir.
Figure 8: TSS, C, N, P inputs, outputs and accumulation in the Cointzio reservoir (loads are given in t y^{-1} with uncertainties)

Figure 1: Map of the Cointzio watershed and reservoir: location of sampling sites (geographical position in UTM)

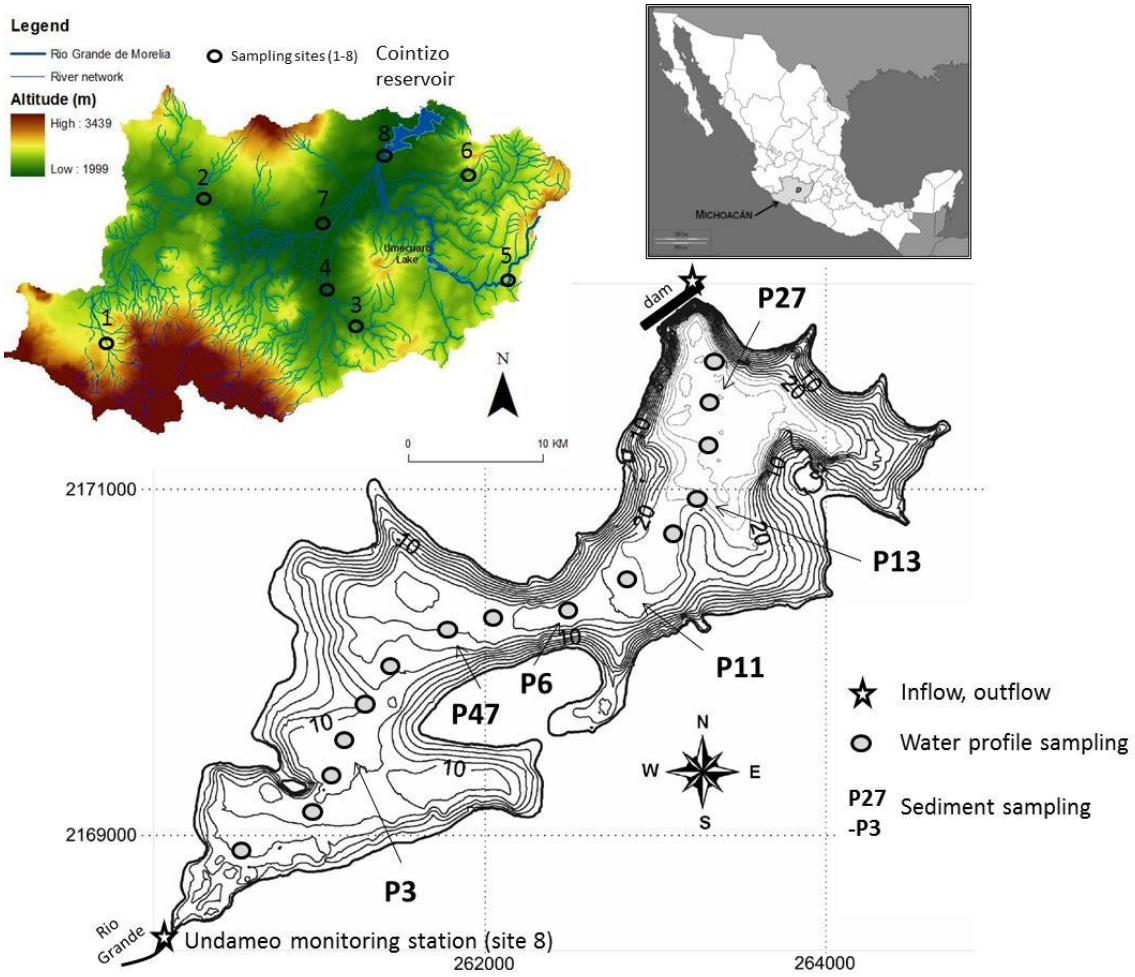

Figure 2: Seasonal time-series of a) water discharge (m^3 s^{-1}) and TSS inflow (mg L^{-1}), b) water discharge and TSS outflow (mg L^{-1}), and c) the volume of the Cointzio reservoir for 2007, 2008 and 2009

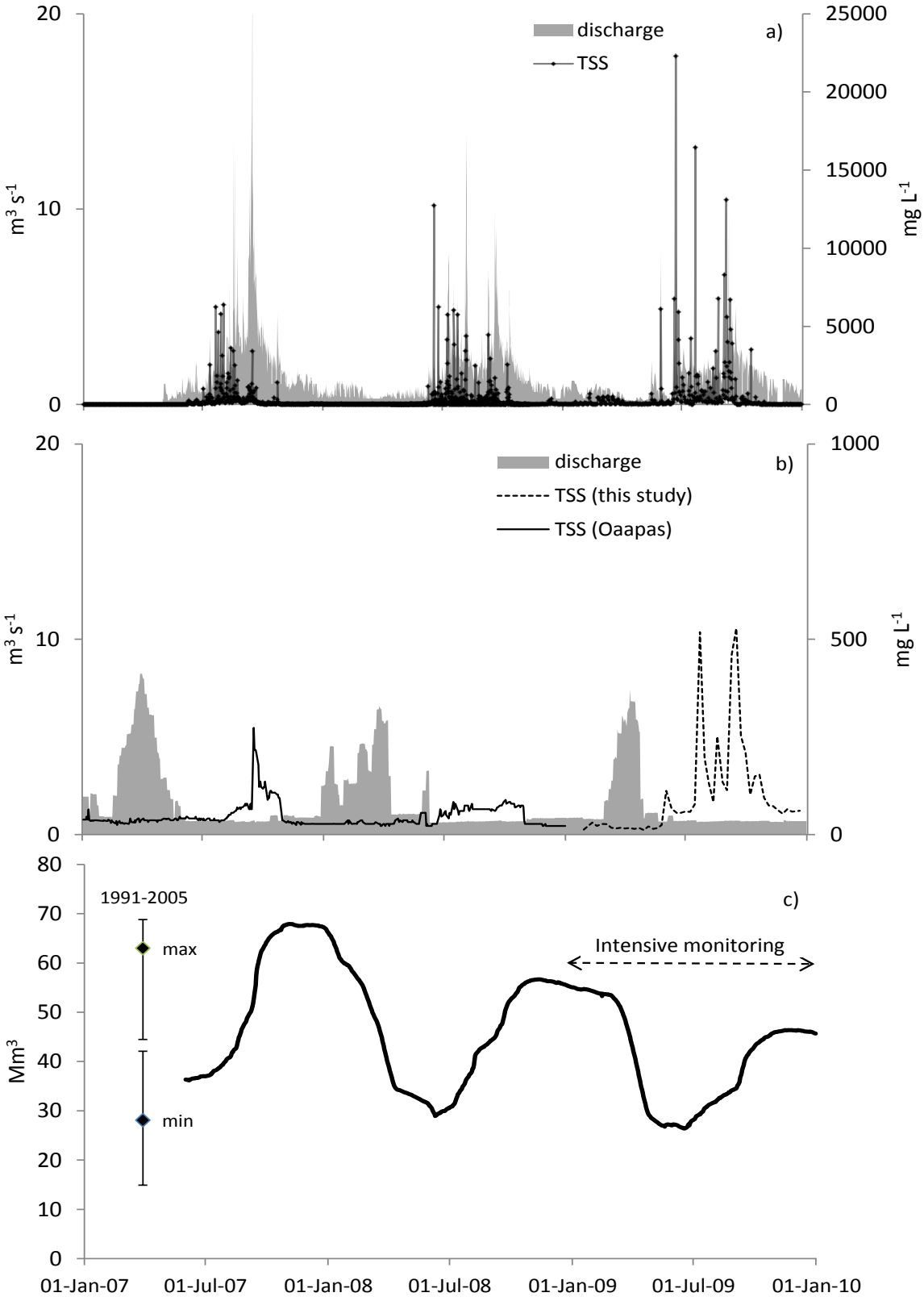

Figure 3: Seasonal variation of TSS, P-tot (including $P\text{-}PO_4^{3-}$), N-tot (including $N\text{-}NO_3^-$, $N\text{-}NH_4^+$), POC and DOC inputs to the reservoir of Cointzio (t day^{-1})

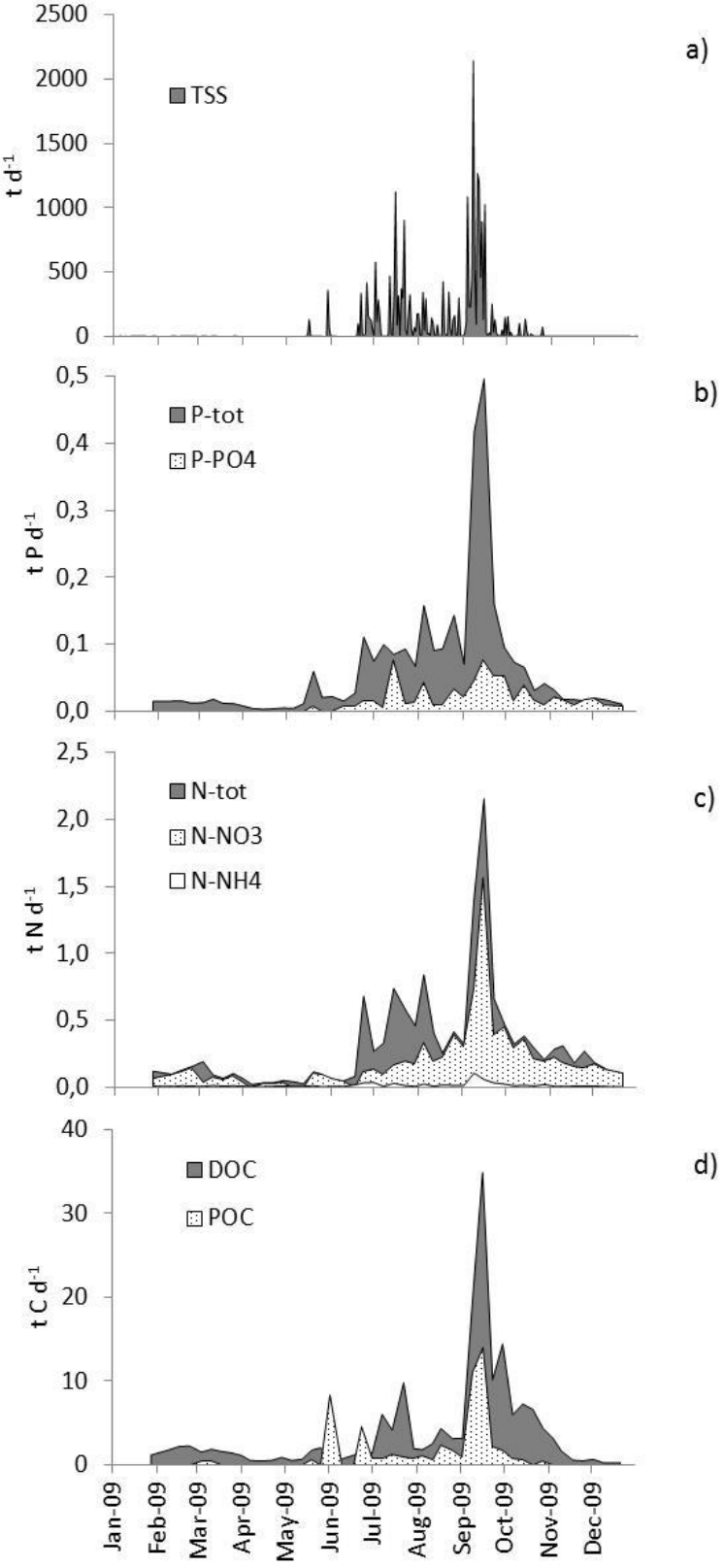

Figure 4: Horizontal transects of temperature, DO and TSS at four dates covering the entire 2009 year. Dotted lines indicate date of vertical profiles

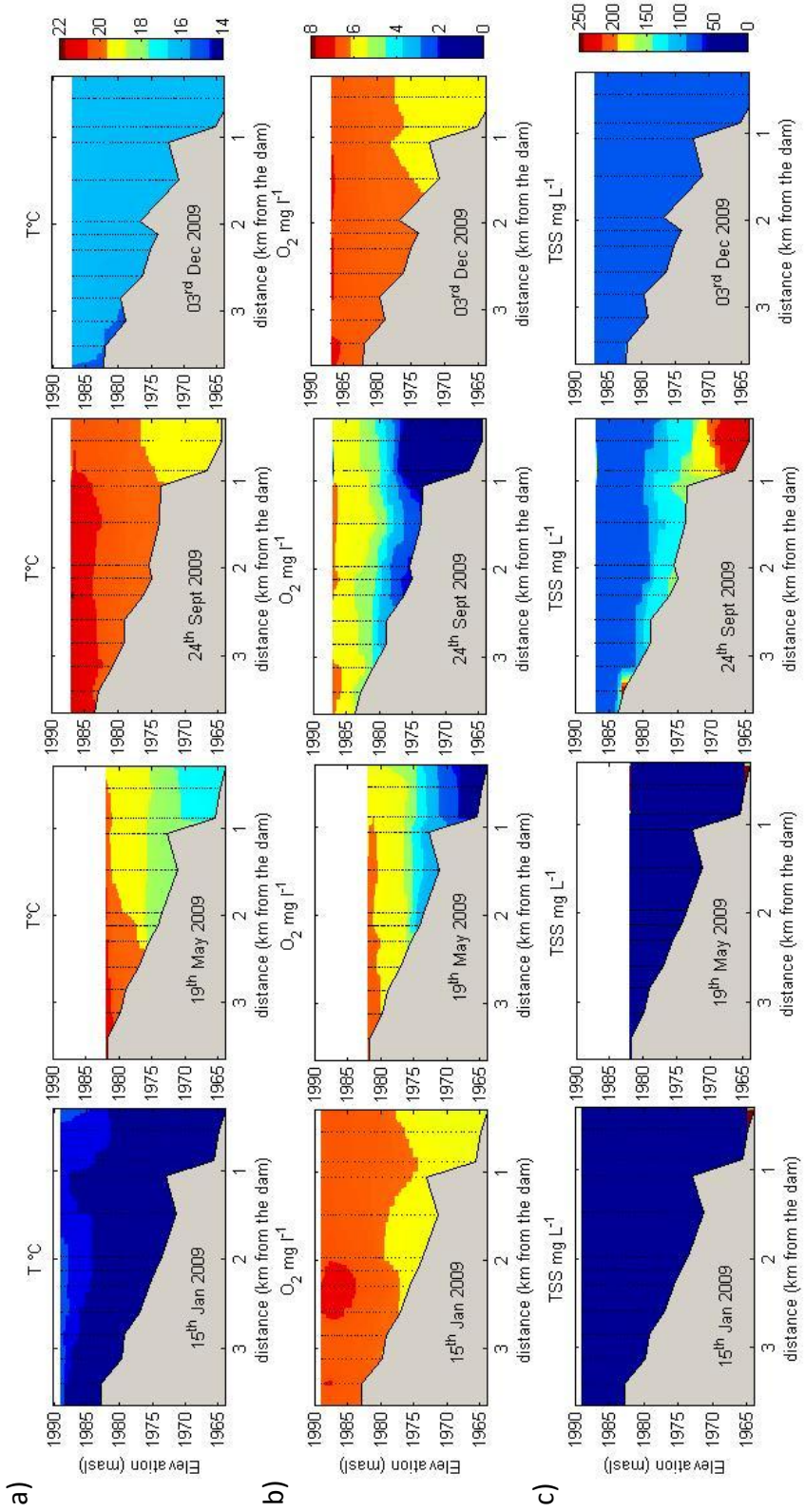

Figure 5: Seasonal variation of a) temperature b) TSS c) DO and d) Chlorophyll a at the deepest point P27 in 2009

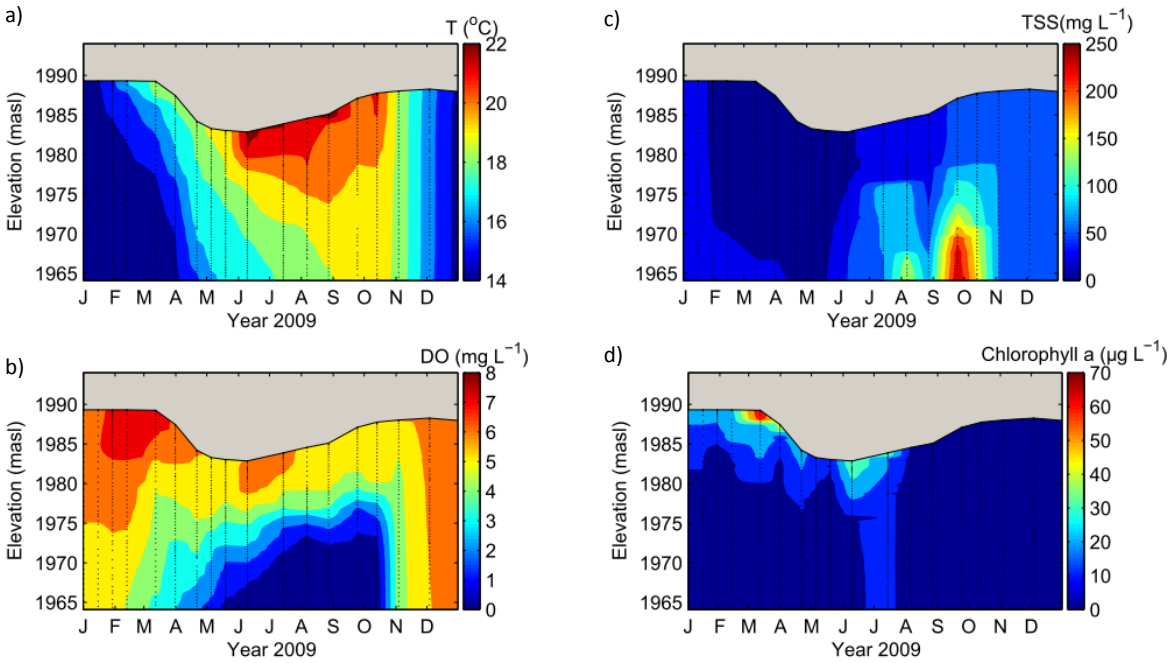

Figure 6: Comparison of the seasonal variations in a) Secchi depth, b) chlorophyll a (surface and bottom), and c) POC in suspended sediment (surface and bottom) in the water column at the two sampling points P6 and P27

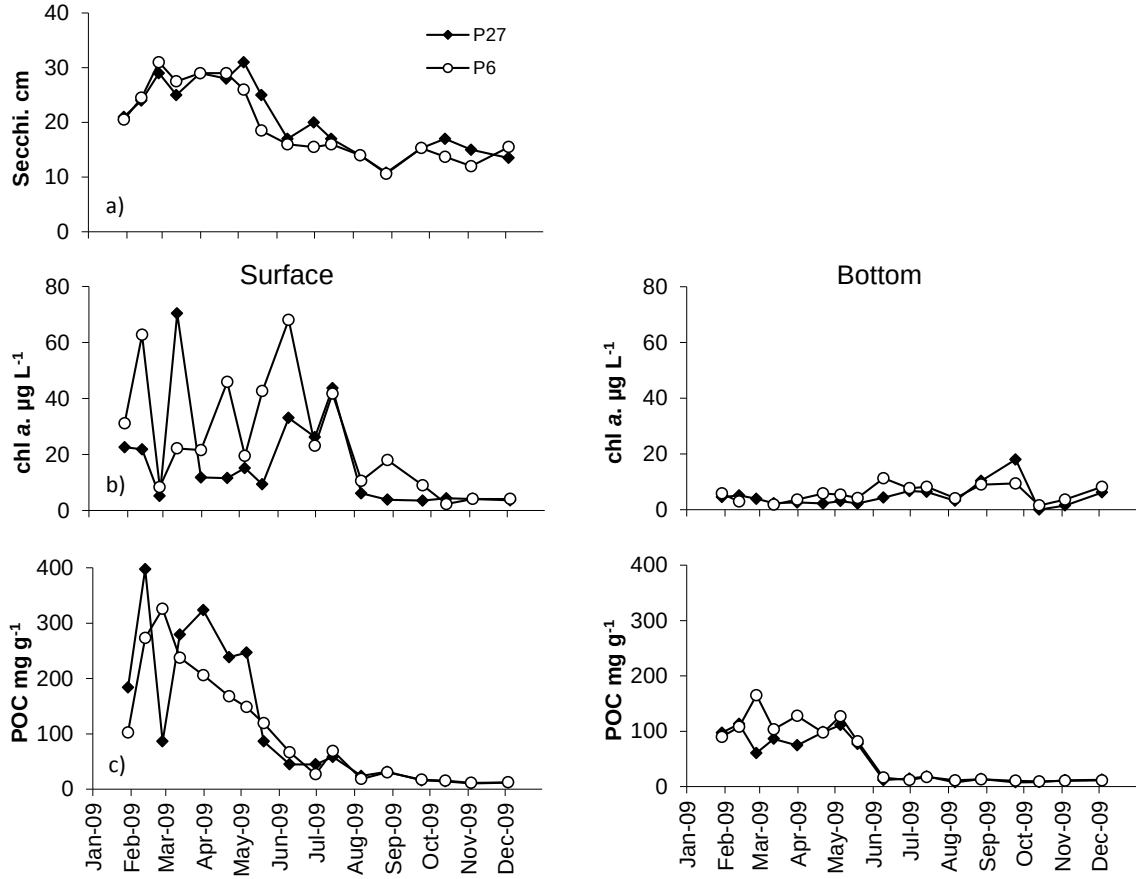

Figure 7: Comparison of the seasonal variations in a) P-PO_4^{3-}, b) N-NO_3^-, and c) N-NH_4^+ in the water column at the two sampling points P6 and P27 (surface and bottom) in the Cointzio reservoir.

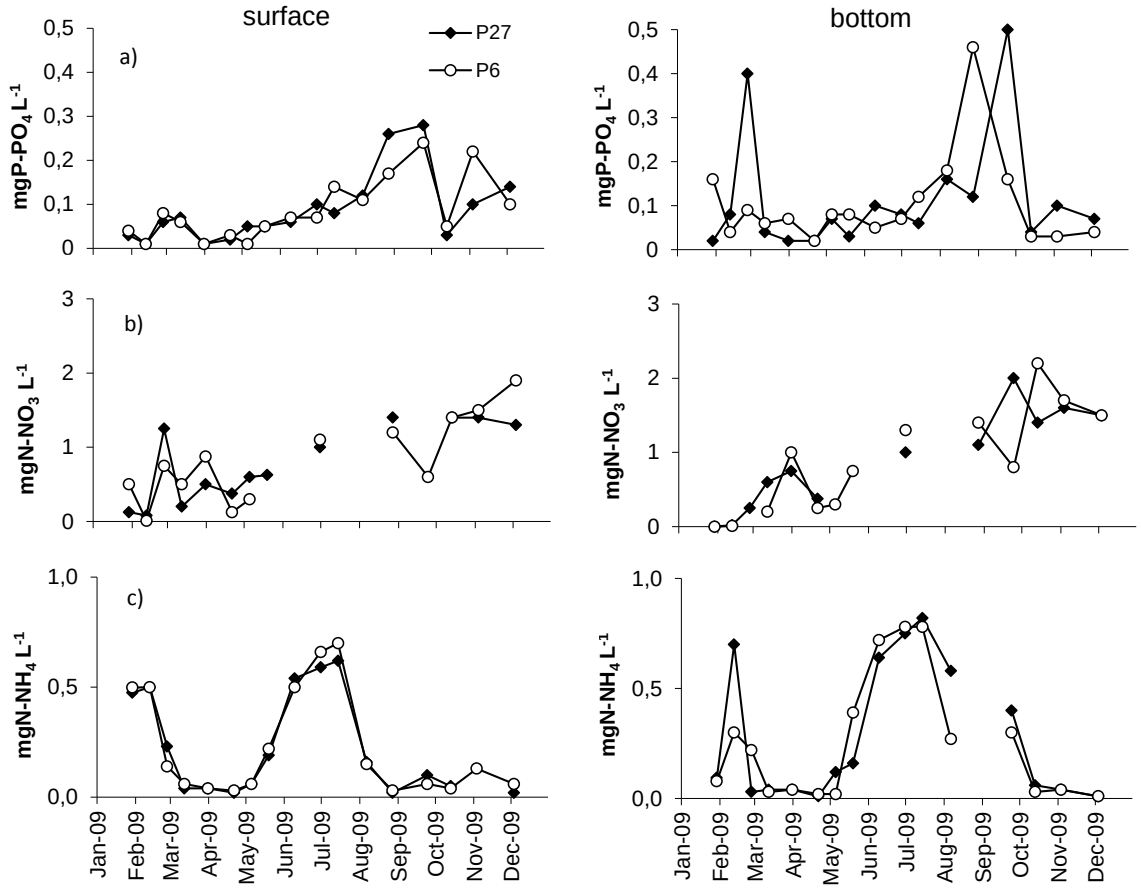

Figure 8: TSS, C, N, P inputs, outputs and accumulation in the Cointzio reservoir (loads are given in t y^{-1} with uncertainties)

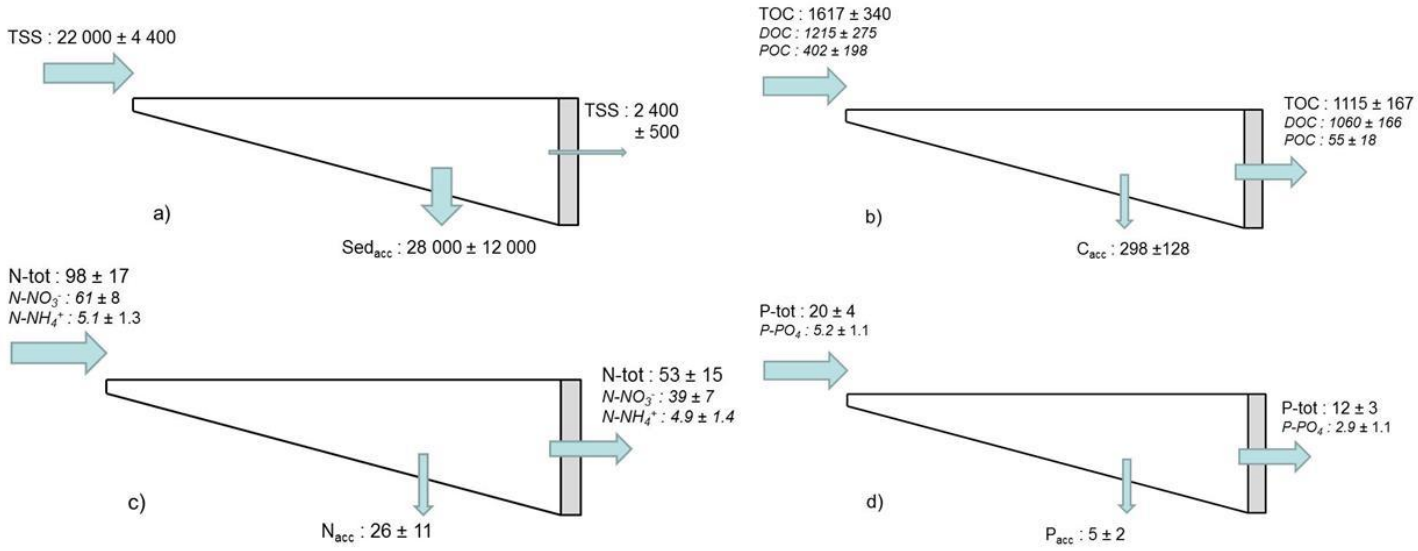

Table 1: Water and TSS input and output for 2007, 2008 and 2009

	2007		2008		2009	
	input	*output*	*input*	*output*	*input*	*output*
Water discharge (10^6 m^3)	49	60	44	53	42	43
TSS (10^3 tons)	22.4 ± 4.5	2.5 ± 0.5	22.2 ± 4.4	1.8 ± 0.4	22.2 ± 4.4	2.4 ± 0.5
Rainfall (mm)	750		710		690	
Rainfall[a] (10^6 m^3)	3.3		2.8		2.5	
Evaporation (mm)		1300-1500		1465		1450
Evaporation[a] (10^6 m^3)		6.1		5.8		6.2
Mean annual volume (10^6 m^3)	53.8		46		40	
Residence time[b] (y)	*1.02-0.81*		*0.98-0.78*		*0.90-0.83*	

[a]calculation based on mean annual surface of reservoir

[b]calculation based on mean annual volume of reservoir and on total input or output

Table 2: Mean annual discharge (Q), DO and nutrient concentrations in the Cointzio watershed in 2009 (in bold min DO and maximum discharge and nutrient concentrations, in parenthesis standard deviation)

Site	Description	Q L s^{-1}	DO mg L^{-1}	P-tot mg L^{-1}	$P\text{-}PO_4$ mg L^{-1}	$N\text{-}NH_4$ mg L^{-1}	$N\text{-}NO_3$ mg L^{-1}
1 El Carmen	Downstream of small	22	6.2	0.48	0.19	0.98	1.93
	village with pasture	(34)	(1.05)	NA	(0.24)	(2.36)	(1.44)
2 Lagunillas	Downstream of village of	194	**2.3**	3.6	**2.2**	**5.9**	**2.6**
	5100 Inh.	(439)	**(1.2)**	(2.3)	**(1.6)**	**(3.8)**	**(1.2)**
3 Villa	Upstream basin	23	6.3	0.3	0.11	0.05	0.92
Madero	Low population density	(19)	(0.6)	NA	(0.05)	(0.04)	(0.54)
4 Acuaducto	Downstream of village	235	5.3	**4.4**	0.37	1.23	1.93
	of 9400 inh.	(210)	(0.8)	**(5.4)**	(0.23)	(1.07)	(0.86)
5 Cortina	Forests/agricultural	45	6.7	NA	0.05	0.06	0.78
	Low population density	(33)	(0.6)	NA	(0.03)	(0.11)	(0.41)
6 Huertitas	Degraded	7	6.1	0.6	0.11	0.17	0.94
	lands/agricultural	(13)	(1.3)	NA	(0.12)	(0.27)	(0.50)
7 SAC	Main channel downstream	534	6.3	0.37	0.13	0.36	1.96
	(San Antonio Coapa)	(434)	(4)	(0.14)	(0.05)	(0.41)	(1.00)
8 Santiago	Outlet of the watershed	**1323**	7.3	0.38	0.11	0.15	1.32
Undameo	(see also table 3)	**(1241)**	(3.4)	(0.23)	(0.07)	(0.10)	(0.41)

NA : missing data

Table 3: Seasonal variations and annual mean of discharge (Q), TSS and water quality parameters at Undameo sampling site 8 (in bold maximum values)

date	**Q**	**TSS**	**Chl *a***	**P-tot**	**P-PO_4**	**N-tot**	**N-NO_3**	**N-NH_4**	**DOC**	**POC**
Inlet	$m^3 s^{-1}$	mg L^{-1}	µg L^{-1}	mgP L^{-1}	mgP L^{-1}	mgN L^{-1}	mgN L^{-1}	mgN L^{-1}	mgC L^{-1}	mgC L^{-1}
28/01/09	0,6	87	24	0,28	0,03	2,3	1,3	0,17	22	4,9
10/02/09	0,8	90	6	0,23	0,04	1,5	1,4	0,09	28	3,4
17/02/09	1,0	53	9	0,18	0,02	*1,5*	1,4	0,14	26	1,2
24/02/09	1,0	83	10	0,14	0,02	1,8	1,6	0,11	22	1,5
04/03/09	0,7	163	9	0,22	0,02	3,3	0,6	0,12	17	6,3
11/03/09	0,8	168	17	0,25	0,01	1,3	1,0	0,19	26	6,0
18/03/09	0,7	132	9	0,19	0,02	1,1	0,9	0,15	25	4,4
25/03/09	0,6	100	8	0,21	0,09	*1,9*	1,6	0,21	19	4,5
01/04/09	0,5	72	13	0,18	0,05	1,5	0,9	0,22	28	4,5
07/04/09	0,2	52	6	0,22	0,03	1,1	0,8	0,21	26	4,0
15/04/09	0,2	13	6	0,17	0,06	*1,9*	1,6	0,30	18	2,7
22/04/09	0,2	11	5	0,19	0,03	*1,7*	1,3	**0,43**	23	1,3
29/04/09	0,4	12	3	0,14	0,02	*1,5*	1,1	0,33	26	1,2
06/05/09	0,2	8	3	0,22	0,08	2,1	0,9	0,36	26	1,3
13/05/09	0,3	25	5	0,42	0,09	1,0	0,5	0,30	25	2,0
20/05/09	0,9	120	15	0,77	0,12	*1,5*	1,3	0,16	23	6,1
26/05/09	0,7	68	9	0,36	0,06	*1,7*	1,6	0,08	36	2,2
02/06/09	0,6	**10671**	6	0,42	0,10	1,5	1,3	0,16	15	**158,5**
10/06/09	0,3	28	4	0,59	**0,31**	1,9	1,6	0,29	27	1,2
18/06/09	0,7	80	10	0,43	0,14	1,3	0,3	0,30	18	2,0
24/06/09	1,3	2900	14	**0,96**	0,14	**5,9**	1,0	0,30	14	39,6
01/07/09	1,4	408	17	0,61	0,14	2,2	1,1	0,30	11	5,9
08/07/09	1,4	364	19	0,81	0,05	2,7	0,8	0,06	49	5,7
15/07/09	3,2	229	9	0,31	0,28	2,7	0,6	0,11	15	4,3
23/07/09	1,6	407	12	0,67	0,09	4,2	1,4	0,10	71	6,8
30/07/09	1,4	394	14	0,54	0,12	3,7	1,4	0,06	15	5,6
05/08/09	1,9	465	26	0,94	0,26	5,0	2,0	0,15	11	6,1
12/08/09	1,9	216	9	0,56	0,07	2,5	1,2	0,05	16	3,8
18/08/09	2,1	950	17	0,51	0,06	1,4	1,2	0,10	24	12,2
26/08/09	2,4	652	28	0,69	0,16	2,0	1,9	0,07	15	7,8
02/09/09	2,1	253	19	0,39	0,12	*1,8*	1,7	0,08	18	4,5
09/09/09	6,5	1112	28	0,74	0,08	2,5	1,3	0,19	35	19,6
16/09/09	**7,6**	438	**31**	0,76	0,12	3,3	**2,4**	0,09	**53**	21,5
23/09/09	3,5	438	12	0,53	0,18	2,2	1,3	0,11	34	7,0
30/09/09	3,7	202	7	0,30	0,17	1,5	1,4	0,08	45	5,4
07/10/09	2,0	194	8	0,43	0,10	1,9	1,7	0,07	35	4,2
14/10/09	2,6	91	7	0,29	0,18	*1,7*	1,6	0,07	32	2,1
21/10/09	1,8	58	5	0,20	0,12	1,9	1,4	0,07	43	1,2
28/10/09	1,6	107	11	0,30	0,08	*1,5*	1,4	0,15	32	2,3
04/11/09	1,6	147	5	0,22	0,16	2,0	1,6	0,06	23	2,0
10/11/09	1,4	37	6	0,15	0,16	2,6	1,5	0,05	14	1,2
18/11/09	1,2	52	9	0,17	0,10	1,8	1,5	0,09	6	2,1
25/11/09	1,0	8	7	0,18	0,17	3,1	1,7	0,10	5	0,9
02/12/09	1,2	17	5	0,19	0,18	*1,8*	1,7	0,10	6	1,0
09/12/09	1,1	21	10	0,18	0,10	*1,5*	1,4	0,07	3	0,9
21/12/09	0,7	11	4	0,17	0,14	0,8	1,7	0,06	4	0,9
Mean	*1,5*	*483*	*11*	*0,38*	*0,11*	*2,1*	*1,3*	*0,15*	*24*	*8,6*
SD	*1,5*	*1604*	*7*	*0,23*	*0,07*	*1,0*	*0,4*	*0,10*	*13*	*23,6*

NB : Italic for N-tot : N-tot = NO_3^- + NH_4^+

Table 4: Seasonal variations and annual mean of discharge (Q), TSS and water quality parameters at the outlet of Cointzio reservoir (in bold maximum values)

date	**Q**	**TSS**	**Chl *a***	**P-tot**	**P-PO_4**	**N-tot**	**N-NO_3**	**N-NH_4**	**DOC**	**POC**
Outlet	$m^3 s^{-1}$	$mg L^{-1}$	$\mu g L^{-1}$	$mgP L^{-1}$	$mgP L^{-1}$	$mgN L^{-1}$	$mgN L^{-1}$	$mgN L^{-1}$	$mgC L^{-1}$	$mgC L^{-1}$
28/01/09	0,8	13	4	0,13	0,04	*2,0*	1,5	**0,50**	29	1,1
10/02/09	0,8	31	7	0,22	0,05	*1,7*	1,6	0,16	21	0,9
17/02/09	0,8	22	8	0,25	0,12	*1,1*	0,9	0,15	16	0,8
24/02/09	0,8	27	9	0,17	0,04	*1,6*	1,4	0,18	24	0,8
04/03/09	1,8	27	3	0,56	0,01	2,4	0,6	0,11	23	1,4
11/03/09	2,8	18	5	0,27	0,04	0,7	0,6	0,09	25	1,0
18/03/09	3,9	16	6	0,27	0,02	*0,6*	0,5	0,09	37	0,7
25/03/09	5,2	17	4	0,54	0,02	*1,1*	1,0	0,12	25	0,9
01/04/09	5,9	16	3	0,22	0,01	*0,5*	0,4	0,12	24	1,1
07/04/09	6,5	17	1	0,15	0,03	*1,6*	1,4	0,18	25	1,4
15/04/09	**6,8**	15	4	0,17	0,17	*1,0*	0,9	0,09	29	1,6
22/04/09	5,3	17	4	0,16	0,08	0,6	0,5	0,16	27	0,9
29/04/09	0,8	12	3	0,07	0,01	1,0	0,6	0,06	34	1,3
06/05/09	1,1	21	3	0,23	0,02	*0,8*	0,8	0,04	27	1,1
13/05/09	1,1	14	3	0,19	0,01	*0,5*	0,5	0,01	23	1,1
20/05/09	1,1	17	5	0,54	0,08	1,1	1,0	0,10	22	/
26/05/09	0,7	24	3	0,32	0,02	0,7	0,4	0,09	22	0,2
02/06/09	0,7	112	5	0,29	0,04	1,4	1,0	0,10	25	1,5
10/06/09	1,0	66	6	0,29	0,19	1,3	1,0	0,10	29	1,3
18/06/09	0,7	55	7	0,22	0,1	**4,7**	0,8	0,10	24	0,8
24/06/09	0,7	56	2	0,23	0,08	0,7	0,7	0,03	20	0,8
01/07/09	0,7	60	5	0,22	0,07	3,5	0,5	0,03	15	0,8
08/07/09	0,7	58	8	0,35	0,09	2,0	0,5	0,06	44	0,9
15/07/09	0,7	78	3	0,22	**0,18**	1,3	1,0	0,09	17	1,2
23/07/09	0,7	518	**19**	**0,63**	0,11	2,6	1,0	0,29	21	4,6
30/07/09	0,7	196	4	0,28	0,13	2,2	0,4	0,10	20	1,8
05/08/09	0,7	133	3	0,39	0,11	3,3	0,2	0,30	12	1,2
12/08/09	0,7	84	4	0,28	0,03	*0,9*	0,8	0,12	13	0,8
18/08/09	0,7	251	3	0,31	0,06	*2,0*	1,8	0,24	21	2,0
26/08/09	0,7	134	5	0,35	0,04	1,3	1,1	0,03	17	1,6
02/09/09	0,7	114	4	0,31	0,08	*0,9*	0,8	0,10	14	1,5
09/09/09	0,7	460	12	0,44	0,08	1,2	1,1	0,01	32	5,0
16/09/09	0,7	**528**	10	0,51	0,08	2,7	1,5	0,01	31	**7,5**
23/09/09	0,6	253	6	0,43	0,08	1,9	1,0	0,20	32	2,1
30/09/09	0,7	209	14	0,40	0,13	*1,6*	1,5	0,06	**56**	3,0
07/10/09	0,7	102	2	0,30	0,04	*1,5*	1,4	0,06	18	1,3
14/10/09	0,7	149	1	0,35	0,15	1,4	1,3	0,07	19	1,1
21/10/09	0,7	153	3	0,36	0,06	*1,6*	1,4	0,07	20	1,3
28/10/09	0,7	94	6	0,35	0,09	*1,2*	1,2	0,01	16	1,1
04/11/09	0,7	75	7	0,39	0,13	1,3	1,3	0,02	15	0,8
10/11/09	0,6	74	6	0,3	0,11	1,3	1,3	0,01	12	0,8
18/11/09	0,6	62	5	0,29	0,14	1,4	1,4	0,03	5	0,9
25/11/09	0,6	53	6	0,24	0,14	1,4	1,4	0,04	5	0,8
02/12/09	0,7	65	3	0,16	0,13	1,5	1,5	0,02	3	0,8
09/12/09	0,7	59	7	0,18	0,08	1,4	1,4	0,01	3	0,6
21/12/09	0,7	61	6	0,23	0,04	1,2	1,2	0,05	4	0,9
Mean	*1,4*	*101*	*5*	*0,30*	*0,08*	*1,5*	*1,0*	*0,10*	*22*	*1,4*
SD	*1,7*	*124*	*3*	*0,12*	*0,05*	*0,8*	*0,4*	*0,09*	*10*	*1,3*

NB : Italic for N-tot : N-tot = NO_3^- + NH_4^+

Table 5: Input and output C, N, P loads in the Cointzio reservoir for 2009 (loads are given in t y^{-1} with 95% confidence intervals)

	Input (t y^{-1})	Output (t y^{-1})
P-tot	20 ± 4	12 ± 3
$P\text{-}PO_4$	*5.2 ± 1.1*	*2.9 ± 1.1*
N-tot	98 ± 17	53 ± 15
$N\text{-}NO_3$	*61 ± 8*	*39 ± 7*
$N\text{-}NH_4$	*5.1 ± 1.3*	*4.9 ± 1.4*
TOC	1617 ± 340	1115 ± 167
DOC	*1215* ± 275	*1060* ± 166
POC	*402* ± 198	*55* ± 18

Table 6: C, N, P content in deposited sediments

	Dry season (19th May 2009)					***Wet season (13th October 2009)***				
	TPP	PIP	OC	TN	C:N	TPP	PIP	OC	TN	C:N
Site		mg g^{-1}					mg g^{-1}			
P3	0.26	0,05	13,7	1,1	13	0.11	0,05	10,8	0,9	13
P47	0.23	0,05	10,6	0,9	12	0.13	0,05	11,1	0,9	12
P6	0.17	0,04	10,8	0,9	12	0.16	0,07	9,8	0,9	11
P11	0.21	0,04	11,2	1,0	11	0.12	0,05	10,3	0,9	11
P13	0.21	0,03	10,0	1,0	11	0.10	0,03	9,5	0,9	11
P27	0.19	0,03	10,1	1,0	10	0.10	0,04	9,8	0,9	10
Mean (±SD)	*0.21 (0.03)*	*0.04 (0.01)*	*11.1 (1.4)*	*1.0 (0.1)*	*11 (1.0)*	*0.12 (0.02)*	*0.05 (0.01)*	*10,2 (0.06)*	*0,9 (0.01)*	*11 (0.8)*

Table 7: Accumulation rate of C, N, P in the Cointzio reservoir compared with other tropical reservoirs

Process	Accumulation	Accumulation rate	Source
	$t\ y^{-1}$	$g\ m^{-2}\ y^{-1}$	
Sed_{acc}	$28 \pm 12 \times 10^3$	$7\,800 \pm 3300$	This study
		900	Itezhi-Tezhi large Reservoir in Zambezi River basin (Kunz, et al. 2011)
		320	Pampulha small Reservoir in Brazil (Torres et al. 2007)
		7 700	Global mean in small Reservoirs (< 50 km^2 total area 98 000 km^2 in Harrison et al. 2009) estimated from 6 % retention of global sediment load (12 600 Mt y^{-1}, Syvisky et al. 2005)
		10 000	Global mean in Reservoirs (total area 250 000 km^2 in Harrison et al. 2009) estimated from 20 % retention of total sediment load (12 600 Mt y^{-1}, Syvisky et al. 2005)
C_{acc}	298 ± 128	83 ± 35	This study
		62	Itezhi-Tezhi large Reservoir in Zambezi River basin (Kunz, et al. 2011)
		- 6	Pampulha small Reservoir in Brazil (Torres et al. 2007)
		450	Global mean in Reservoirs estimated from global 0.18 Pg C y^{-1} and global reservoir area of 400 000 km^2 (Cole et al. 2007)
N_{acc}	26 ± 11	7.2 ± 3.1	This study
		14	Valle de Bravo small Reservoir in Mexico (Ramírez-Zierold et al. 2010)
		4	Itezhi-Tezhi large Reservoir in Zambezi River basin (Kunz, et al. 2011)
		11	Global mean (estimation in Kunz et al. 2011 from Beusen et al. 2005 database)
P_{acc}	5 ± 2	1.4 ± 0.5	This study
		5.5	Valle de Bravo small Reservoir in Mexico (Ramírez-Zierold et al. 2010)
		0.8	Itezhi-Tezhi large Reservoir in Zambezi River basin (Kunz et al. 2011)
		1.2	Pampulha small Reservoir in Brazil (Torres et al. 2007)
		3.3	Global mean (estimation in Kunz et al. 2011 from Beusen et al. 2005 database)

NB: mean reservoir area in 2009 of 3.6 km^2 considered for the calculation of accumulation rate

Conclusions of chapter 4

The effects of clay particles from the watershed and the strong influence of watershed-emitted untreated point sources contribute to the high growth of algae, leading to eutrophication of the reservoir and long and intense hypolimnic anoxia. As a result, the water quality decreases with time. Eutrophication represents an issue of concern for most of the lakes and reservoirs in Central Mexico including the Cointzio reservoir. The high accumulation rate of nutrients and carbon was showed in the Cointzio reservoir and this reservoir acts as a "sink" for TSS, nutrients and carbon as well. In order to protect the ecosystem and wildlife in the watershed of Cointzio, it would be important to rapidly adopt some mitigation strategies to treat wastewaters and reduce point source of nutrient loads and keep it at a low level as suggested by our modelling results presented in chapter 5.

CHAPTER 5. EUTROPHICATION OF THE TURBID TROPICAL COINTZIO RESERVOIR: TRENDS AND PROJECTIONS BY THE END OF THE CENTURY

This chapter shows the modelling results of the hydrodynamics and the biogeochemistry in the Cointzio reservoir for the calibration year 2009 and the validation year 2008. The entire mass balance of nutrients and carbon in the reservoir calculated from field data and modelling approach were then estimated. The scenarios of evolution of the water quality in the reservoir under the influence of water level regulation, air temperature rising and nutrients reduction in the coming decades are presented and discussed.

A) Scenarios and projections

1. Effect of water level regulation

A twenty-year historical time series of the water depth was extracted to identify typical dry and wet hydrological years for numerical simulations (Figure 2.6 in chapter 2). The state of reservoir filling on 01st January of a given year was considered to be a relevant indicator of the biogeochemical functioning of the reservoir. This because precipitation and water discharge are almost negligible from January to June (Gratiot et al, 2010; Carlón Allende, 2009), which corresponds to the most critical period in terms of algal growth and chlorophyll *a* blooms. Three different hydrological years were used in the simulations: Target year 2009, a particularly dry year and a particularly wet year selected from the last 20 years timeseries. The observed water depth on 01st January 2009 was at 26m. The year 1990 was considered to represent a critically dry year with a depth of 21 m on 01st January and 1996 a particularly wet year with a depth of 29 m on 01st January. For comparison purposes, the inflows, the outflows and the water quality parameters in the two years (1990 and 1996) were assumed to be the same as the ones of the year 2009 during simulation exercises.

2. Effect of air temperature increase

Global warming is expected to affect lakes and reservoirs dynamics, especially in tropical regions (Inclan et al, 2010) where the mean annual evaporation is generally higher than the precipitation. In the region of Cointzio, climate change is expected to lead to an increase of the mean annual air temperature of 2.5°C and 4.4°C for the decades centered in the year 2060 and 2090, respectively (Gratiot et al, 2010).

Here we assume that the potential increase in air temperature is directly transferred to surface water. This assumption is confirmed by observations (Livingstore & Lotter 1998) and the coupling of global circulation models with hydrological models (Blenckner et al, 2002). To

assess the sole effect of air temperature, which is one consequence of global warming effect, it was further assumed that (i) nutrients input would be the same as the ones of 2009; (ii) nutrients input would be the same as 2009 and changes in other climate parameters, such as wind speed or humidity, are not considered in our analysis. Therefore, we run the model for dry year conditions with an air temperature increase of 2.5°C and 4.4°C corresponding to an increase in reservoir surface temperature by about 1.4°C and 2.4°C as expected for 2060 and 2090 respectively (see linear regression equation in appendix 3).

3. Effect of nutrients reduction

Eutrophication may cause severe water quality problems in the reservoir. It is caused by nutrients loads into surface water bodies and can be minimized by reduction of incoming loads. The field data of nutrients concentration observed downstream of highly populated areas indicate that point sources from domestic waste waters clearly dominated in the Cointzio watershed as opposed to input from agricultural activities where nutrients concentrations were found low (Némery et al, submitted, presented in Chapter 4). Here, some runs were conducted to assess by how much the nutrient loads would have to be reduced to maintain sufficient oxygen content and low chlorophyll a content in the reservoir. In this study, the scenarios of three different nutrients input reductions (50%, 90%, and 100%) were examined.

4. Description of modelling scenarios

The prospective scenarios for water quality assessment of the Cointzio reservoir are described in Table 5.1. These scenarios aim at (i) assessing the long term evolution of the water quality in the reservoir of Cointzio under the influence of water level regulation and global warming and (ii) establishing a management strategy to mitigate eutrophication. The different scenarios were compared with the run of the calibrated model for the year 2009, which will be referred to as the "Present" scenario.

Table 5.1 Summary of scenarios for water quality assessment of the Cointzio reservoir

Scenarios	Description	Parameters used
Present	Target year 2009	Water level H=26 m
P1	Dry year 1990, nutrient inputs 2009	low water level H = 21 m
P2	Wet year 1996, nutrient inputs 2009	high water level H= 29 m
P3	P1 with an increase in air temperature (T_{air}) of 2.5°C	H=21 m and +2.5°C in T_{air}
P4	P1 with an increase in T_{air} of 4.4°C	H=21 m and +4.4°C in T_{air}

P5	P1 with a long term reduction of 50% of nutrient inputs (N,P)	H=21 m, & -50% (N,P)
P6	P1 with a long term reduction of 90% of (N,P) inputs	H=21 m, & -90% (N,P)
P7	P1 with a long term reduction of 100% of (N,P) inputs	H=21 m, & -100% (N,P)
P8	P4 with a long term reduction of 50% of (N,P) inputs	H=21 m, +4.4°C in T_{air} & -50% (N,P)
P9	P4 with a long term reduction of 90% of (N,P) inputs	H=21 m, +4.4°C in T_{air} & -90% (N,P)
P10	P4 with a long term reduction of 100% of (N,P) inputs	H=21 m, +4.4°C in T_{air} & -100% (N,P)

B) Eutrophication of turbid tropical reservoirs: Modelling for the case of Cointzio, Mexico

This part is copied from the paper that was submitted to Ecological Modelling for a Special Issue following the ISEM2013 conference on Ecological Modelling for Ecosystem Sustainability in the context of Global Change. During the conference, the study was presented as an oral presentation.

Eutrophication of turbid tropical reservoirs: Modelling for the case of Cointzio, Mexico

Thuy Kim Phuong Doan[1)], Julien Némery[1)], Martin Schmid[2)], Nicolas Gratiot[1)]

[1)] Univ. Grenoble Alpes, CNRS, IRD, LTHE (UMR5564), 38000 Grenoble, France

[2)] Eawag: Swiss Federal Institute of Aquatic Science and Technology, Surface Waters - Research and Management, CH-6047 - Kastanienbaum, Switzerland

Corresponding author: Thuy Kim Phuong Doan

Tel: +33(0)456520991, Email: kimphuongdhbk@gmail.com; phuong.doan@ujf-grenoble.fr

Abstract

The overall water quality of reservoirs in many regions of Mexico continues to deteriorate. The Cointzio reservoir (capacity 66 Mm^3), located in the Trans-Mexican Volcanic Belt, is no exception. The high content of very fine clay particles and the lack of water treatment plants lead to serious episodes of eutrophication, high level of turbidity and benthic anoxia. During the target year 2009, high phosphate concentrations (up to 0.5 mgP L^{-1}), low Secchi depth (<0.3 m), and high phytoplankton blooms with chlorophyll *a* concentrations of up to 70 µg L^{-1} near the surface were observed. Close to the bottom, anoxic conditions persisted in the hypolimnion during six months.

The present paper aims at examining the ability of vertical one dimensional (1DV) numerical models to reproduce the main biogeochemical cycles and assess scenarios of nutrients (P and N) and eutrophication reduction in the coming decades. The numerical approach developed herein coupled a k-ε mixing model, with a biogeochemical model (Aquasim) for water quality. The k-ε model reproduced nicely the low to moderate temperature stratification which characterizes this turbid reservoir. The Aquasim model was able to reproduce the main patterns of dissolved oxygen (DO), nutrients and chlorophyll *a* during the year 2009. The different simulations pointed out the negative long-term impact of global warming. By the end of the century, an increase of air temperature as high as 4.4°C is expected. When coupled with a low water level, this could lead to critical conditions with a severe depletion of DO and important blooms of chlorophyll *a* (up to 94 µg L^{-1}). Various simulations showed that a drastic reduction of nutrients input (by 90%) would be required to significantly reduce chlorophyll *a* concentrations. If such mitigation measures are adopted, the maximum peak of chlorophyll *a* would reduce significantly, from 94 µg L^{-1} to 40 µg L^{-1}, and the average concentrations in the top 10 m would decrease to 9.5 µg L^{-1} after a ten-year period of efforts, with corresponding positive effect on oxygen concentrations.

To our knowledge, this study provides the first numerical application of k-ε and Aquasim models to simulate high eutrophication levels in a very turbid tropical reservoir. It points out the advantages and limitations of 1DV models and will help stakeholders to adopt appropriate strategies for the management of very turbid tropical reservoirs.

Keywords: Turbid and tropical reservoir, Mexico, eutrophication, biogeochemical modelling, global warming.

1. Introduction

In the XXIst century, pressure on freshwater resources has been increasing considerably, especially in the "tropical world" (Tundisi, 2003). Most lakes, rivers and wetlands are suffering from the input of sediments and nutrients such as nitrogen (N) and phosphorus (P). As a result, the eutrophication of epicontinental waters is progressively extending to tropical water bodies (Alcocer et al, 2010). Besides that, most tropical lakes and reservoirs are situated in developing countries, where there is a chronic lack of financial resources for the establishment of long term and consistent monitoring programs (Von Sperling and Sousa, 2007). As a consequence of limited data availability in tropical regions, the global biogeochemical models are better constrained in temperate regions, and have greater predictive power in economically developed regions (Seitzinger et al, 2010).

Inappropriate disposal of domestic waste, untreated wastewater, and increase of nutrient loads from domestic origin are typical issues of newly industrialized countries. Primitive techniques of farm management, based on forest clearance and combustion of the remaining biomass also cause the influx of sediments and nutrients into natural freshwater tropical systems. As a result of increased nutrient availability, phytoplankton and cyanobacteria can form blooms, causing the release of cyanotoxins. Eutrophication in tropical areas is reflected by increase of algal growth, decrease of water transparency and appearance of a stable oxygen depletion in the hypolimnion (Thomaz & Bini, 2003).

Water quality management has become an increasingly important issue in developing countries and newly industrialized countries, including Mexico. A possible approach to overcome this difficulty is numerical modelling (Chanudet et al, 2012). In the past few years, important advances in principles, concepts and approaches related to water quality management have been achieved. However, there is still a lack of universal methodology for reaching effective management (Gautam et al, 2003).

In general, eutrophication is a kind of water pollution caused by excessive presence of nutrients. In order to prevent or minimize the eutrophication of the water in the reservoir, questions that most often arise with respect to eutrophic conditions include: (i) Can we control eutrophication by limiting key nutrients? (ii) What levels of water quality are acceptable to society? and (iii) Which nutrients limit the maximum algal growth level in the reservoir? (Correll 1998).

In this study, these three questions served as a guideline to assess the biogeochemical cycles taking place in the reservoir of Cointzio. The biogeochemical functioning of the reservoir was simulated to define which factors controlled the water quality in the reservoir. After

calibration on the target year 2009 and validation with the data of 2008, various numerical simulations related to climate changes and mitigation strategies were conducted with the objective of assessing the trophic state of the reservoir in the future. The different scenarios are presented and discussed. Some solutions of rehabilitation are proposed to restore the quality of the water. In the discussion section, results are put in a regional context, with a specific focus on the duration of mitigation plans to get significant water quality improvement for similar reservoirs. The paper ends with some perspectives which could be applied to other similar reservoirs of the region.

2. Study site

The Cointzio reservoir (19.622°N, -101.256°W) is located on the Trans - Mexican Volcanic Belt, at an altitude of 1920 m above sea level. The reservoir drains a volcanic watershed of 627 km^2, where domestic waters are rejected without any treatment. It is an essential source for domestic water supply (20 %) of Morelia city (700 000 inhabitants) and for irrigation. Besides that, it is also used to control flood for Morelia (Figure 1). The reservoir has a maximum depth that does not exceed 29m. It has a surface area of 6 km^2 and a maximum storage capacity of 66 Mm^3. Because there are no waste water treatment plants in the upstream villages and because of high content of very fine clay particles, the water inflow contains high levels of nutrients and sediment (Némery et al, 2009). An extensive field survey has been conducted from 2007 to 2010 with a special focus on the year 2009. This survey revealed that turbidity in the reservoir is high (Secchi < 0.3 m) all year long and chlorophyll *a* concentrations reach values of up to 70 $\mu g\ L^{-1}$ during blooms. Since its construction in 1940, the reservoir has lost 25 % of its storage capacity through siltation (Susperregui et al, 2009).

The climate of the region is sub-humid, characterized by a rainy season from June to September and a dry season the rest of the year. The mean annual rainfall is 810 mm in Morelia, ranging from 400 to 1.100 mm/y (Carlón Allende and Mendoza, 2007; Gratiot et al, 2010). The main river of the watershed is the Rio Grande de Morelia whose source lies about 25 km upstream of the Cointzio reservoir. This is Morelia's most problematic river in terms of silting (some sections were so full of sediment that its natural course changed in places). Water and sediment inflow come almost exclusively from this river, whereas outflow is done through gates opening at the dam. The inflow peaks during five months of the rainy season representing 77% of the water input and 98% of the sediment load (Duvert et al, 2011). The water outflow is concentrated mainly during the end of the dry season, when the agricultural water demand is high. The residence time of the water within the reservoir is about one year.

3. Data and modelling approach

For understanding the biogeochemical cycles within the Cointzio reservoir, monitoring surveys of hydrodynamics and biogeochemistry have been conducted over three years, with a target year in 2009. At the beginning of the project, two extensive measurement campaigns were conducted in December 2005 and May 2006 to check whether lateral effects were playing a role in the hydrodynamics for contrasted conditions. 47 vertical profiles of temperature, turbidity and DO were measured along the longitudinal axis and along five cross sections (data not shown). These two campaigns did not reveal significant lateral heterogeneities and we decided to focus the long term monitoring effort on the temporal variations along the longitudinal axis.

From September 2007 to January 2010, field measurements of temperature, turbidity and meteorological parameters were carried out at a fortnightly to monthly basis along the longitudinal axis of the reservoir (Figure 1). The measurements were systematically done from the dam to the Rio Grande river mouth with a boat. The mean duration of a survey was about 6 hours, beginning in the morning (at about 9:00 AM) and finishing at midafternoon (at about 15:00 PM). The biogeochemical survey was focused on a shorter temporal window from the beginning of 2009 to the beginning of 2010. A multiparameter Hydrolab MS5 probe (Hach Company, Loveland, CO, USA) was used to determine vertical profiles of temperature, turbidity, dissolved oxygen and chlorophyll *a*, at 15 locations, regularly distributed along the longitudinal axis of the reservoir (dashed line). At each station, Secchi depth was measured to evaluate the light attenuation using a Secchi disk. Furthermore, water samples were taken at the deepest point of the reservoir (P27) and at a middle position between the river input and the dam (P6). At these two locations, additional vertical water samples were retrieved from different depths (0, 1, 2, 5, 10, 15, 20 m) and from near the bottom. A 2L Niskin bottle was used for suspended sediment (SS), chlorophyll *a* (μg L^{-1}) and nutrients (PO_4^{3-}, NH_4^+, NO_3^-) analysis. After sampling, water samples were stored in polypropylene flasks at 4°C before analysis. SS was weighed on GF/F Whatman filters (dried at 105°C). Chlorophyll *a* was analyzed after filtering on GF/C Whatman filter using methanol extraction according to Holm-Hansen and Rieman (1978). Nutrients (PO_4^{3-}, NH_4^+, and $NO3^-$) were analyzed with Hach DR/2010 spectrophotometric equipment. Accuracy with standardized methods was evaluated at 10%. A complete description and analysis on these field data are available in Doan et al, 2012 and Némery et al, submitted. In the following, we first present the relevant data and then the modelling approach. A detailed overview of the numerical model and the input data used in this study are given in the supplementary data.

3.1 Model input data

Input requirements for modelling can be divided in four groups, namely (i) the morphological and descriptive data for the reservoir, (ii) meteorological and hydrological data (inflow and outflow), (iii) water quality parameters, and (iv) initial conditions for all the modelled variables. The morphological data consists of cross-sectional areas as a function of elevation of the reservoir. The input data required are wind speed, water surface temperature, shortwave radiation, and the light extinction coefficient which was estimated from Secchi depth. When the water surface temperature was not properly recorded in the reservoir from mid-June to September (sensor malfunction), the reservoir surface temperature was estimated from a linear regression to the air temperature time series (T_{surf}=0.52*T_{air}+9.8, r2=0.84). For the water influx, discharge of the major river is required and its temperature has been measured or estimated from correlations with air temperature. During the high flow period (May-September), the river water temperature was measured with a Vemco minilog TR8k sensor (+0.2°C). The data were collected every week to limit the risk of unrecorded periods. When malfunctioning occurred, a linear regression was fitted to air temperature (T_{river}=0.45*T_{air}+11, r2=0.79) to replace missing data. During the low flow period, the river water depth never exceeded a few centimeters at the outlet of the Cointzio watershed. This led to a good heat exchange between air and water, as revealed by short period of monitoring of air and water temperature. Based on this specific surveys, the river water temperature was deduced from the adjustment of a linear regression with the air temperature (T_{river}=0.28*T_{air}+13, r2=0.82). Likewise, the outflow over the dam through the gates is required. The temperature of the outflow is equal to the simulated water temperature at the outlet depth. The characteristics of the water quality of the inflow were also measured. These include concentrations of DO, nutrients, chlorophyll *a* and particles (XSS or turbidity). Furthermore, phytoplankton biomass and chemical data (DO, and nutrients NO_3^-, NH_4^+, and PO_4^{3-}) are also needed and have been measured in the water column of the reservoir. The quality parameters of the water outflow are model output variables. To initialize the model, initial values of all the model variables, including water quality must be provided.

3.2 Model output

Dissolved oxygen, nutrients, and chlorophyll *a* concentrations were considered to be the most relevant variables of water quality. The distribution of these variables over the vertical water column, and their temporal evolution were used for interpreting the model outputs.

3.3 Modelling approach

All simulations were performed with a combination of two independent models: (1) A slightly adapted version of the buoyancy-extended k-ε model developed by Goudsmit et al, (2002) was used to predict the hydrodynamics and (2) A biogeochemical advection-diffusion-reaction model (Omlin et al, 2001a, 2001b) based on the Aquasim software (Reichert, 1994) was adapted to simulate the biogeochemical cycling in the reservoir.

3.3.1 Physical k-ε model

Vertical turbulent diffusivity $K_z(z)$ was estimated with 30 minutes resolution for the year 2009 using the k-ε model. Two model specific parameters were fitted by the least squares method to reproduce the monthly measured temperature profiles for the calibration year 2009 and they were validated for the year 2008. They are the scaling factor for the wind energy transfer to the internal seiches (α), and a coefficient defining wind drag (C10). The calibrated values of the parameters α and C10 were 0.0025 and 0.001 respectively. The resulting time series of $K_z(z)$ were then used as the input data for the Aquasim biogeochemical model.

3.3.2 Aquasim biogeochemical model

To model reservoir-internal biogeochemical cycles, we adopted the existing model BELAMO (Omlin et al, 2001a, 2001b), which has been successfully applied to various lake and reservoir types (Mieleitner and Reichert, 2006), and the model RES1, a version of BELAMO which has been applied for a tropical reservoir (Kunz et al, 2011). The following main variables were considered: Temperature (T), dissolved phosphate (S_{HPO4}^{3-} in gP m^{-3}), nitrate (S_{NO3}^{-} in gN m^{-3}), ammonium (S_{NH4}^{+} in gN m^{-3}), dissolved oxygen (S_{DO} in gO m^{-3}), chlorophyll *a* (X_{ALG} in g DM m^{-3}), zooplankton (X_{ZOO} in gDM m^{-3}), dead and inert organic matter (X in gDM m^{-3}). In this study, all the units of chlorophyll *a*, zooplankton, and organic matter need to be converted from µg L^{-1} into gDM m^{-3}. This was done by calculating a carbon/chlorophyll *a* ratio of 51 in the Cointzio reservoir (Garnier et al, 1989) and using a carbon/DM ratio of 0.42 (Rodriguez., 2002). The interactions between these variables are described by ten processes: (1) Growth of algae, (2) respiration of algae, (3) death of algae, (4) growth of zooplankton, (5) respiration of zooplankton, (6) death of zooplankton, (7) uptake and release of phosphate, (8) nitrification, (9) aerobic, anaerobic, anoxic mineralization (i.e.: denitrification) within the water column and the sediment surface, and (10) background mineralization (oxidation of reduced substances). The changes in our model, the complete model and the full mathematical descriptions of these interactions are described in the supplementary data.

Several biogeochemical parameters were not measured in the field. Our model calibration was carried out using a heuristic method. The set of calibrated parameters was then carefully compared with values reported in the literature to prevent unrealistic estimates. The half saturation rate for algae growth with respect to phosphate (K_HPO_4_ALG) was calibrated to PO_4^{3-}; nitrification rate (k_nitri_wat_20) was fitted to NH_4^+ and NO_3^-; aerobic (k_miner_aero_20), anoxia (k_miner_anox_20), anaerobic (k_miner_anaero_20) specific mineralization rate at 20°C, and background mineralization rate (k_miner_bg) were fitted to DO. Maximal growth rate of algae (k_gro_ALG_20, k_gro_ALG_N2_20), and maximal growth rate of zooplankton (k_gro_ZOO_20) were fitted to observed $X_{ALG.}$ These are summarized in Table 1 and compared to recent studies of other lakes and reservoirs. Most of them are similar to other studies and within the range found in the literature.

3.4 Modelling scenarios

The prospective scenarios for water quality assessment of the Cointzio reservoir are described in Table 2. These scenarios aim at (i) assessing the long term evolution of the water quality in the reservoir of Cointzio under the influence of water level regulation and global warming and (ii) establishing a management strategy to mitigate the negative effects. The different scenarios were compared with the run of the calibrated model for the year 2009, which will be referred to as the "Present" scenario.

3.4.1. Effect of water level change

A twenty-year historical time series of the water level was extracted to identify typical dry and wet hydrological years for simulation (Figure 2). The state of reservoir filling on 01st January was considered to be a relevant indicator of dry and wet years. Precipitation and water discharge are indeed almost negligible from January to June (Gratiot et al, 2010; Carlón Allende, 2009), which corresponds to the most critical period in terms of algal growth and chlorophyll *a* blooms (shown in the results section, Figure 4).

Three different hydrological years were used in the simulations: Target year 2009, a dry year and a wet year selected from the last 20 years (Figure 2). The observed water level on 01st January 2009 was at 26m. The year 1990 was considered to represent a dry year with a minimum level of 21 m on 01st January and 1996 a wet year with a maximum level of 29 m on 01st January. For comparison purposes, the inflows, the outflows and the water quality parameters in the two years (1990 and 1996) were assumed to be the same as the ones of the year 2009 during simulation exercises. The main limitation of Aquasim is that it automatically generates additional inflow when the outflow is larger than the inflow, and vice versa. This limitation was counterbalanced by the robustness of the model and its

capacity to integrate a large quantity of variables that participate to the biogeochemical cycles. By means of this procedure, the effect of the changing volume of the reservoir from year to year on the mass balance can be taken into account.

3.4.2. Effect of air temperature increase

Global warming is expected to affect lakes and reservoirs dynamics, especially in tropical regions (Inclan et al, 2010) where the mean annual evaporation is generally higher than the precipitation. In the region of Cointzio, climate change is expected to lead to an increase of the mean annual air temperature of 2.5°C and 4.4°C for the decades centered in the year 2060 and 2090, respectively (Gratiot et al, 2010).

To assess the sole effect of air temperature, it was assumed that discharge and nutrients input would be the same as 2009. We decided to focus the projection analysis on the fewer optimist but realistic cases. Therefore, we run the model for dry year conditions with an air temperature increase of 2.5°C and 4.4°C corresponding to an increase in reservoir surface temperature by about 1.4°C and 2.4°C, as expected for 2060 and 2090 respectively.

3.4.3. Reducing eutrophication in the Cointzio reservoir

Eutrophication may cause severe water quality problems in the reservoir. It is caused by nutrients loads into surface water bodies and can be minimized by the mitigation measures (reduction of incoming loads). The field data of maximum Ptot, PO_4^{3-}, and NH_4^+ observed downstream of highly populated areas indicate that point sources from domestic waste waters clearly dominated in the Cointzio watershed as opposed to input from agricultural activities where P and N concentrations were found low (Némery et al, submitted). Here, some runs were conducted to assess by how much the nutrient loads would have to be reduced to maintain sufficient oxygen content and low chlorophyll *a* content in the reservoir. In this study, the scenarios of reducing 50%, 90% and 100% of nutrient inputs were examined.

4. Results

In the following sections we first present results of the hydrodynamic simulations, which serve as boundary conditions for the biogeochemical model. The “Present scenario” is then discussed in order to evaluate the quality of the model before introducing different scenarios.

4.1 Physical k-ε model

We chose to calibrate the model using the data from 2009 and to validate it using the data from 2008, collected at the deepest point of the reservoir (P27). In the validation year 2008 turbidity was lower and the water level was higher than in the calibration year 2009. Figure 3 presents the variation of measured and simulated temperature with time and the difference between observed and simulated results for the years 2009 and 2008.

4.1.1 Model calibration

The top left panels of Figure 3 show the observed temperatures in 2009 with a minimum of 14 °C in January, and a maximum of 23°C in June. The reservoir was stratified during 9 months, from February to October and was vertically mixed, by cooling and wind effect, from the end of October until January. The model reproduces nicely the mixing and stratification periods. With a mean square error of 0.24°C between the simulated and measured temperatures, water temperatures closely followed the measured profiles, indicating that the downward mixing of heat, based on calculated diffusivities in the epi-, meta-, and hypolimnion from the k-ε model were adequately estimated. The maximum difference in temperature was from mid-June to September with a maximum residue of ±1°C which corresponds to the period where missing reservoir surface temperature data was interpolated from correlations with air temperature.

4.1.2 Model validation

Validation consists of testing the model under other meteorological and hydrological conditions. The right panels present observations and simulations of the temperature in 2008 (Figure 3b, d, f). Despite the different hydrological conditions, the model agreed well the data with a mean square error between the simulated and measured temperatures of 0.52°C, and a maximum residue of ±1.5°C.

4.2 Biogeochemical model

4.2.1 Present scenario - Target year 2009

The results of the water quality simulations for the target year 2009 are presented in Figure 4. These simulations were performed with the parameter values given in Table 1. The residues between measurement and simulation of the dissolved oxygen and chlorophyll *a* indicators are shown in Figure 5. The results of the model are in good agreement with DO measurements in 2009 (Figure 4a, b) with a mean square error 1.14 mg L^{-1}. It correctly reproduced the temporal dynamics of the anoxia period and the magnitude of DO concentrations. Most of the residuals between the measured and simulated DO are smaller than ±1 mg L^{-1}, except in April when the model slightly overestimated the oxygen consumption rate in the deep water (Figure 5a). From April to the end of October, DO decreased below 1.0 mg L^{-1} in the whole hypolimnion beneath 10 m depth. At the surface, DO remained high (>6.0 mg L^{-1}) because of oxygen production by photosynthesis and air water exchange (Doan et al, 2012).

Figure 4c, d presents vertical profiles of measured and simulated chlorophyll *a* for the calibration year 2009. The model predictions for chlorophyll *a* concentration are generally

satisfying. It correctly reproduced the time of the first chlorophyll *a* peak in March and its magnitude. However, the arrival of a second bloom in July was not simulated accurately by the model which anticipates the event and overestimates it slightly, as expressed by the large residue between observed and measured chlorophyll *a* (up to -25 μg L^{-1}) in June (Figure 5). The chlorophyll *a* was highest in the top 10 m, with as average concentration of 18.9 μg L^{-1}. Below 10 m depth, light availability strongly limits primary production. From January to April, chlorophyll *a* increased up to 70 μg L^{-1} due to higher light penetration and nutrient availability. During the wet season, the successive flood events supplied a large quantity of SS which reduced Secchi depth to less than 0.2 m. This hindered photosynthesis and chlorophyll *a* dropped below 10 μg L^{-1}.

Phosphate concentration was quite high all year long contributing to important algal production (Figure 4e, f). The PO_4^{3-} concentration increases at the bottom of the reservoir because of the benthic mineralization in the sediment. The time-series showed a clear peak in September - October.

An acceptable result of vertical profiles of measured and simulated NH_4^+ in the target year 2009 was described in Figure 4g, h. The Rio Grande river at the inlet of the reservoir exhibited average ammonium concentration of 0.3 mgN L^{-1}, close to those observed in the reservoir from March to May. The benthic mineralization prevailed from May to October leading to release of NH_4^+ from sediments. As a result, the NH_4^+ concentrations of the hypolimnion increased (> 0.6 mgN L^{-1}) (Doan et al, 2012).

4.2.2 Application to past historical data

P1 scenario – Low water level

In the P1 scenario of the dry year, the chlorophyll *a* is higher and the anoxia period is a little more extended than for the reference year 2009. During the first period, the average chlorophyll *a* is higher (22.9 μg L^{-1}) in the top 10 m, as compared to the year 2009 (18.9 μg L^{-1}) and the highest peak of chlorophyll *a* at surface is 86 μg L^{-1} (Figure 6), compared to 70 μg L^{-1} in the reference year. DO remains high (>6.0 mg L^{-1}) at the surface while the anoxia period occurs at the bottom from April to the end of October. The oxycline depth is 8 m from the surface.

P2 scenario – High water level

The model predicts lower chlorophyll *a* concentrations for the wet year, with peak values of 58 μg L^{-1} (Figure 7). DO decreased below 1.0 mg L^{-1} at the bottom and extended to the whole hypolimnion 10 m depth from the surface. Comparing the simulation results from these three different hydrological years (Figures 5-7), the dry year showed the highest peak

of chlorophyll *a* (86 μg L^{-1}). Thus, this dry condition was chosen to estimate future scenarios (section 4.2.3).

4.2.3 Scenarios under global warming conditions

P3 scenario - Increased air temperature by 2.5°C in 2060

The model results of DO and chlorophyll *a* are presented in Figure 8a, b. The increase of air temperature has a direct effect on the water surface and lead to higher reservoir temperatures. The warming of the water surface positively affects biological processes such as algal growth and decomposition of organic matter but reduces DO solubility in water. Therefore, the maximum peak of chlorophyll *a* increases up to 93 μg L^{-1} and the anoxic layer was thicker, with complete anoxia observed up to 7 m depth compared to 8m for the P1 scenario.

P4 scenario - Increased air temperature by 4.4°C in 2090

The P4 scenario, which simulates an air temperature increase of 4.4°C coupled with minimum water level corresponds to the most critical scenario. As a consequence, the intensity of chlorophyll *a* increases when compared with the target year 2009, as depicted in Figure 8c, d. The mean chlorophyll *a* concentration in the top 10 m was much higher (25 μg L^{-1}) compared with 18.9 μg L^{-1} for 2009. The highest peak of chlorophyll *a* was 94 μg L^{-1} and the duration of the anoxic period in the hypolimnion increases by about 20 days compared for P3 scenario.

4.2.4 Scenarios of nutrients input reduction

Scenarios with 50%, 90%, and 100% nutrient input reductions were simulated using as a starting point both the dry year scenario (P5, P6, and P7) and the future global warming scenario (P8, P9, and P10). The resulting effects on the thickness of the oxycline depth and on the chlorophyll *a* concentration are shown in Figure 9.

Case P1

The oxycline depth was less extended after reducing nutrients input. The anoxic thickness was significantly reduced after two years and remained constant with time. It was below 12 m of depth compared to 8 m for the P1 scenario (Figure 9).

As shown in P5 scenario, a 50% reduction of nutrients input resulted only in a slight decrease in the chlorophyll *a* concentration. In order to see a significant decrease, the nutrients input must be reduced by 90%. This effect occurs quickly within the first 2 years. After 10 years, the maximum peak of chlorophyll *a* concentration reduced from 86 μg L^{-1} to 41 μg L^{-1} and the average concentration in the top 10 m decreased until 7.6 μg L^{-1}. If a reduction of 100% nutrients input could be achieved, it would further improve the water quality with lower concentration of chlorophyll *a* (Figure 9).

Case P4

Concerning the global warming scenario with nutrients input reductions, the oxycline depth was significantly reduced.

Similarly to the case P1, reduction of nutrients input did not have an immediate effect in the Cointzio reservoir. Only after several years, a restoration process of the water quality can take place steadily with time. The reduction of 50% of nutrients input only slightly reduced chlorophyll *a*; the maximum chlorophyll *a* is still high at 78.5 μg L^{-1} after ten years of simulation. After a ten-year reduction of 90% nutrients input, the maximum peak of chlorophyll *a* would be reduced to 40.5 μg L^{-1} and the average chlorophyll *a* concentration in the top 10 m reduced down to 9.5 μg L^{-1}. The maximum peak could be decreased until 29 μg L^{-1} and the average reduced down to 7.3 μg L^{-1} after ten years of 100% reduction (Figure 9) because it still has nutrients released from sediments, as mediated by chemical, physical and biological processes.

5. Discussion

5.1 Biogeochemical analysis of the model for the Cointzio reservoir

The model calculates the DO concentrations as a balance between source and sink terms due to surface aeration, depletion by sediment, consumption by respiration and nitrification, and production by photosynthesis. DO is therefore a key variable that integrates almost all the processes taken into account in the model. Based on the nutrients release and mineralization rates calculated from the model results, we can see that the anoxic, aerobic sediment mineralization and background mineralization are the dominant causes of oxygen depletion in the simulation leading to anoxic conditions at the reservoir bottom (see supplementary data). Two sources of bottom organic matter are: The production of phytoplankton and its sedimentation are dominant during the first period of the year (Figure 4d), the inputs of organic matters with the arrival of hyperpycnal sediment flows prevail from June to October (Doan et al, 2012). The benthic mineralization then leads to the release of nutrients such as phosphorus and ammonia (Figure 4f, h) which contributes to increase the eutrophic state of the reservoir.

After reaching the first maximum peak in March, the chlorophyll *a* was reduced drastically by grazing of zooplankton and then recovered during the following months. The discrepancy between measurements and model may be mitigated if more experimental data points were available to calibrate the ecological model component. As can be seen in Figure 4d, the time series of simulated chlorophyll *a* was very dynamic with significant changes within a few days. However, based on monthly or every three weeks sampling of chlorophyll *a*, it was

difficult to calibrate the phytoplankton model, as sampling just a few days earlier or later could have given different results. Besides that, no input data of zooplankton was available for the model. Moreover, according to Frisk et al, 1999 and our scenarios, the water level is one of the factors in regulating the trophic status of reservoirs. However, we were not able to test this due to the limitation of the Aquasim model of not allowing reservoir level variations. Besides that, the light extinction coefficient influences the time at which the chlorophyll *a* peak concentration occurs and its intensity (Martins et al, 2008). In general, the errors in differences between model scenarios are smaller than the errors in the individual scenarios, because biases tend to be removed by taking the difference between two simulations. In summary, the model was considered to provide satisfying estimates of the chlorophyll *a* dynamics for reservoir management issues.

The results of PO_4^{3-} profiles in Figure 4f show clearly the significant upward flux of PO_4^{3-} released by mineralization from the sediments thus increasing concentrations in the water column. From January to July, PO_4^{3-} concentrations were not only low in the epilimnion, where they were consumed by primary production of algae, but also below in the metalimnion. This is an indication of the significance of PO_4^{3-} uptake by sinking particles. Simulated PO_4^{3-} profiles represent all these effects and agree well with measurements of the year 2009. The deviations between calculation and measurements in the few months of the wet season indicated an underestimation of mixing in the deep hypolimnion.

In general, NH_4^+ in reservoirs may be influenced by atmospheric and riverine inputs, biological uptake, mineralization and nitrification (Dodds 1993). Ammonium concentrations were low in the epilimnion because of uptake by algae. However, the hypolimnetic concentrations of NH_4^+ increased over the course of the stratified period because of mineralization (Figure 4h). These increases coincided with the onset of anoxia in the hypolimnion, but also with a pronounced increase in discharge, and its accompanying suspended sediment load.

5.2 Effect of hydrology and global warming on trophic status

Eutrophication remains a major problem in dry hydrological conditions (Frisk et al, 1999). As shown by our models, the dry year was characterized by high algal blooms (86 $\mu g\ L^{-1}$) that threatened drinking water production. On the basis of the scenarios with application of different hydrological conditions, it can be concluded that the water level is one of the factors regulating the trophic state of the Cointzio reservoir.

From the results of scenarios with global warming effects, chlorophyll *a* in the Cointzio reservoir has been shown to be sensitive to changes in reservoir stratification caused by

global warming. Thus, two scenarios with air temperature increased by 2.5°C and 4.4°C were simulated for the next decades. In the Cointzio reservoir, an air temperature increase of 4.4°C coupled with minimum water level corresponds to the most critical situation (P4 scenario). The increase in air temperature was directly transferred to the surface of the Cointzio reservoir. Higher temperatures will affect biological processes such as increase algal growth and reduce DO concentration in water. The vertical mixing pattern changes significantly with the effect of global warming. With an atmospheric warming of air temperature, temperature gradients increase with time. Following our model results, the scenario with low water level gives bad water quality in the Cointzio reservoir. Meanwhile, the scenario with global warming effect in the future will lead to worst water quality in the reservoir.

5.3 Evaluation of the restoration process of the water quality in the reservoir

Normally, reducing nutrient inputs helps to improve the water quality but there are some exceptions. For example, this did not seem to have an immediate significant effect on the phytoplankton development in the Villerest eutrophic reservoir (Poulin et al, 2004). This also appears to be the case for the Cointzio reservoir. Only after reducing of the nutrients input for several years, a restoration process of the water quality in the Cointzio occurs with time. Two years is the minimum time to have a marked reduction of chlorophyll *a* in the reservoir. It just reduces very lightly after 5 years (Figure 9). This means that 5 years would be the time needed to flush out a maximum amount of nutrients from the system Cointzio. The P release from the model in the global warming scenario for the last year of the simulation, when the reservoir has reached a steady-state, is shown in Table 3. The estimation of P released by all mineralization processes is 1.105 t P y^{-1}. The anaerobic and anoxic mineralization processes in open water are negligible. Thus, the benthic mineralization of organic matter is the most important process explaining P released from sediments. As shown by the P8 scenario, the release of P only reduces slightly after a 50% reduction in nutrients input with the value of 0.867 t P y^{-1} compared to 1.105 t P y^{-1} for the P4 scenario. The P release has a significant decrease when the nutrients input is reduced by 90%. The trend is similar to that seen for chlorophyll *a* (Figure 9). Moreover, P release does not decrease linearly with the reduction in nutrients input, because a large proportion of nutrient is already trapped in clay particles. Moreover, it is not surprising that we need a really large decrease of nutrients input to reduce algal biomass in the Cointzio.

Arruda et al, 1983 estimated that the quantity of organic carbon adsorbed to sediments was over 30 times greater than that available from the phytoplankton in a clay-rich North American reservoir with concentrations of suspended sediments close to 100 mg L^{-1}.

Similarly, in the Cointzio reservoir, there is a lot of clay particles (Acrisols, Luvisols and Andosols) from the watershed discharge into the reservoir so that many nutrients are mineralized directly from these particles. Moreover, the algae production is most probably not limited by nutrients supply, but also by light. Finally, waste water treatment plants should be installed in the villages located upstream of the reservoir to reduce nutrient inputs. Fortunately, most of nutrients pollution levels within the watershed come from domestic sources so it would be feasible to treat this kind of waste water. Special attention should be paid to phosphorus and ammonium removal. While various systems, such as Valle de Bravo (Olvera Viascán et al, 1998) have some comparable morphometric, hydro-meteorological and mineralogical properties, mitigation strategies would not be expected to have significant effects before a period of 5 to 10 years.

6. Conclusions

A physical mixing model using a k-ε scheme and a biogeochemical advection-diffusion-reaction Aquasim model were implemented for the study of the very turbid tropical reservoir of Cointzio in Michoacán, Mexico. This is the first application of a biogeochemical modelling approach in the Trans-Mexican Volcanic Belt. The k-ε model accurately reproduced water temperature profiles and pointed out the low to moderate density stratification which characterizes this turbid environment. The Aquasim biogeochemical model was able to reproduce the main patterns of dissolved oxygen, nutrients and chlorophyll *a* concentrations within the Cointzio reservoir for the target year 2009. The set of parameters obtained after calibration was reasonable in comparison with the range of parameter values found in the literature. The present study has shown how a calibrated model can be used to help water resources management. The model allowed investigating the progress of restoration from several water quality indicators and in global warming context. Here, we focused on chlorophyll *a* and dissolved oxygen, which were the two main indicators concerned by reservoir water management. The following conclusions can be drawn:

In order to assess the future evolution of the trophic state of tropical reservoirs, it is important to consider the climatic conditions (Bravo-Inclan et al, 2010). In this study, the scenarios were designed for predicting the long term effect of global warming, without neglecting the natural variation between dry and wet hydrological year at a decadal scale. The scenario that coupled a dry hydrological year with a 4.4°C increase of the air temperature revealed enhance significantly the eutrophication of the Cointzio reservoir with the maximum peak of chlorophyll *a* up to 94 $\mu g\ L^{-1}$.

In terms of mitigation strategies, results of the study show that a short term response to risks of chlorophyll *a* blooms consists in maintaining a sufficiently high water level in the reservoir. A far more benefit strategy consists in reducing nutrients input into the reservoir. Generally, the strategies in nutrient inputs control are successful to improve the water quality in term of dissolved oxygen level and phytoplankton development in reservoirs. However, in the case of the Cointzio reservoir, we need a really large decrease of nutrients input to reduce algal biomass due to a lot of clay particles coming to the reservoir and the nutrients input is very high which are far from nutrient limitation. Moreover, the positive effect of reduction of nutrients input on the phytoplankton development is not immediate because time is needed to flush out the nutrients, mineralized directly from particles, accumulated in the suspension and benthic layers. As shown by our model, it was characterized by high algal blooms (78 μg L^{-1}) that threatened drinking water production, even after the implementation of drastic programs of point source reduction up to 50% of the present loading. The reduction in nutrients input by 90% would improve the water quality in the reservoir, reducing the maximum peak of chlorophyll *a* from 94 μg L^{-1} to 40 μg L^{-1} and the average concentration in the top 10 m decreased until 9.5 μg L^{-1} after 5 years. The depth of anoxic conditions decreases from 7 m to 11 m. This scenario could be realistic if we compare it to other study with a point source reduction down to 85% (Garnier et al, 2005). Five years would be the time needed to flush out a maximum amount of nutrients from the system.

The challenge for the Cointzio reservoir management is to reduce the nutrient load and keep it at a low level because the ongoing global warming is likely to deteriorate the water quality of the reservoir. From a managing point of view, if the direct sources of nutrients have been significantly reduced by the implantation of several water treatment plants in the surrounding watershed, it also would be necessary to worry the diffuse sources of nutrients in order to reach better water quality.

Acknowledgements

This study was performed at the Laboratory of Transfers Hydrology and Environment (LTHE), Grenoble, France in the framework of the European Research project DESIRE (2007-2011) and the French ANR Research project STREAMS (2008-2010). The assistance of all the individuals participating in this program, financed by the ANR STREAMS project and the DESIRE European project, is gratefully acknowledged. Thuy Kim Phuong Doan is recipient of a fellowship from the Vietnamese government. We also thank Marie Paule Bonnet for fruitful advice in early model implementation and Jean Gagnon for revision of the English manuscript.

References

Alcocer, J., Bernal-Brooks, F., 2010. Limnology in Mexico, Hydrobiologia. 644, 15-68.

Arruda, J. A., Marzolf, G. R., Faulk, R. T., 1983. The role of suspended sediments in the nutrition of zooplankton in turbid reservoirs. Journal of Ecology. 64, 1225-1235.

Bansal, M. K., 1976. Nitrification in natural streams. Journal of the Water Pollution Control Federation. 48, 2380-2393.

Bonnet, M. P., Poulin, M., Devaux, J., 2000. Numerical modelling of thermal stratification in a lake reservoir. Methodology and case study. Aquatic Sciences. 62, 105-124.

Bravo-Inclan, L. A., Saldana-Fabela, M. P., Sanchez-Chavez, J. J., 2008. Long-term eutrophication diagnosis of a high altitude body of water, Zimapan Reservoir, Mexico. Water Science and Technology. 57, 1843-1849.

Carlón Allende, T., Mendoza, M. E., 2007. Análisis hidrometeorológico de las estaciones de la cuenca del lago de Cuitzeo, Investigaciones Geográficas, Boletín del Instituto de Geografía, UNAM. 63, 56–76.

Chanudet, V., Fabre, V., Kaaij. T. V. D., 2012. Application of a three–dimensional hydrodynamic model to the Nam Theun 2 Reservoir (Lao PDR). Journal of Great Lakes Research. 38, 260-269.

Chen, C. W., Orlob, G. T., 1975. Ecological Simulation of Aquatic Environments, in Systems Analysis and Simulation in Ecology, Vol. 3, B. C Pattern (ed.), Academic Press, New York, N. Y; 476-588.

Collins, C. D., Wlosinski, J. H., 1983. Coefficients for Use in the U.S. Army Corps of Engineers Reservoir Model, CE-QUA-R1. U.S. Army Corps of Engineers, Waterways Experiments Station, Vicksburg, Mississippi.

Correll, D. L., 1998. The Role of Phosphorus in the Eutrophication of Receiving Waters: A Review. Journal of Environment Quality. 27, 261-273.

Denman, K. L., 2003. Modelling planktonic ecosystems: parameterizing complexity. Progress in Oceanography. 57, 429–452.

Doan, T. K. P., Wendling, V., Bonnet, M. P., Némery, J., Gratiot, N., 2012. Impact of high turbidity on the hydrodynamic and biogeochemical functioning of tropical reservoirs: The case study of Cointzio, Mexico. 4th International Conference on Estuaries and Coasts, (October). 1, 231–238.

Dodds, W. K., 1993. What control levels of dissolved phosphate and ammonium in surface waters? Aquatic Sciences. 55, 132–142.

Duvert, C., Gratiot, N., Némery, J., Burgos, A., Navratil, O., 2011. Sub-daily variability of suspended sediment fluxes in small mountainous catchments – implications for community based river monitoring. Hydrology and Earth System Sciences. 15, 703–713.

Frisk, T., Kaipainen, H., Malve, O., 1999. Modelling phytoplankton dynamics of the eutrophic Lake Võrtsjärv, Estonia, Hydrobiologia. 414, 59-69.

Garnier, J., Blanc, P., Benest, D., 1989. Estimating a Carbon/Chlorophyll ratio in Nannoplankton (Creteil Lake, S-E Paris, France), Water Resources Bulletin. 25, 751-754.

Garnier, J., Némery, J., Billen, G., Théry, S., 2005. Nutrient dynamics and control of eutrophication in the Marne River system: Modelling the role of exchangeable phosphorus. Journal of Hydrology. 304, 397-412.

Gautam, A. P., Webb, E., Shivakotia, G. P., Zoebisch, M. A., 2003. Land use dynamics and landscape change pattern in a mountain watershed in Nepal. Agriculture, Ecosystems and Environment. 99, 83–96.

Goudsmit, G.-H., Burchard, H., Peeters, F., Wüest, A., 2002. Application of k-ε turbulence models to enclosed basins: The role of internal seiches. Journal of Geophysical Research. 107, 3230-3243.

Gratiot, N., Duvert, C., Collet, L., Vinson, D., 2010. Increase in surface runoff in the central mountains of Mexico: lessons from the past and predictive scenario for the next century, Hydrology and Earth System Sciences. 14, 291–300.

Holm-Hansen, O., Riemann, B., 1978. Chlorophyll *a* determination: improvements in methodology. Oikos. 30, 438-447.

Jørgensen, S.E (ed.) 1979. Handbook of Environmental data and Ecological Parameters. International Society for Ecological Modelling.

Jørgensen, S.E., Nielsen, S.N., & Mejer, H. (1995) Emergy, environ, exergy and ecological modelling. Ecological Modelling, 77, 99-109.

Jørgensen, S.E., Ray, S., Berec, L., Straskraba, M., 2002. Improved calibration of an eutrophication model by use of the size variation due to succession. Ecological Modelling. 153, 269–277.

Kunz, M. J., Wüest, A., Wehrli, B., Landert, J., Senn, D. B., 2011. Impact of a large tropical reservoir on riverine transport of sediment, carbon, and nutrients to downstream wetlands. Water Resources Research. 47, 1-16.

Martins, G., Ribeiro, D. C., Pacheco, D., Cruz, J. V., Cunha, R., Gonçalves, V., Nogueira, R., 2008. Prospective scenarios for water quality and ecological status in Lake Sete Cidades (Portugal): The integration of mathematical modelling in decision processes. Applied Geochemistry. 23, 2171–2181.

Matzinger, A., Schmid, M., Sturm, M., Wüest, A., 2007. Eutrophication of ancient Lake Ohrid: Global warming amplifies detrimental effects of increased nutrient inputs. Limnology and Oceanography. 52, 338–353.

Mieleitner, J., Reichert, P., 2006. Analysis of the transferability of a biogeochemical lake model to lakes of different trophic state. Ecological Modelling. 194, 49–61.

Némery, J., Alvarado, R., Gratiot, N., Duvert, C., Mahé, F., Duwig, C., Bonnet, M. P., Prat, C., Esteves, M., Abstract number: H53D-0958. Biogeochemical characterization of the Cointzio reservoir (Morelia, Mexico) and identification of a watershed-dependent cycling of nutrients. AGU Fall Meeting, San Francisco, 14-18 December 2009.

Némery, J., Gratiot, N., Doan, T. K. P., Duvert, C., Alvarado, R., 2013. Biogeochemical mass balances in a turbid tropical reservoir and identification of a watershed-dependent cycling of nutrients. Aquatic Sciences. Submitted.

Omlin, M., Reichert, P., Forster, R., 2001a. Biogeochemical model of Lake Zürich: Model equations and results. Ecological Modelling. 141, 77–103.

Omlin, M., Brun, R., Reichert, P., 2001b. Biogeochemical model of Lake Zürich: sensitivity, identifiability and uncertainty analysis. Ecological Modelling. 141, 105–123.

Orlob 1983. Mathematical modelling of water quality: Streams, lakes, and reservoirs. Wiley (Chichester West Sussex and New York) 518 pp.

Olvera-Viascán, V., Bravo-Inclán, L., Sánchez-Chávez, J., 1998. Aquatic ecology and management assessment in Valle de Bravo reservoir and its watershed. Aquatic Ecosystem Health & Management. 1, 277–290.

O'Connor, D. J., Mancini, J. L., Guerriero, J. R., 1981. Evaluation of Factors Influencing the Temporal Variation of dissolved oxygen in the New York Bight, PHASE II. Manhattan College, Bronx, New York.

Poulin, M., Bonnet, M.-P., 2004. Dylem-1D: a 1D physical and biochemical model for planktonic succession, nutrients and oxygen cycling. Application to a hyper-eutrophic, Ecological Modelling. 180, 317-344.

Rubio, M., 1998. Dinámica del cambio de la cobertura y del uso de los suelos en la microcuenca de Atécuaro (Michoacán, México), Una perspectiva desde las ciencias ambientales, PhD thesis, Univ. Michoacana de San Nicolás de Hidalgo, Univ. Aut. Barcelona, 253 pp.

Rodriguez, A., Final Report for 2001 Activity Memorandum of Understanding ECT/FG/MMM/97.012, July 2002.

Scavia, D., Park, R. A., 1976. Documentation of Selected Constructs and Parameter Values in the Aquatic Model CLEANER. Ecological Modelling. 2, 33-58.

Seitzinger, S. P., et al, (2010). Global river nutrient export: A scenario analysis of past and future trend. Global Biogeochemical Cycles. 24, 1-16.

Smith, D. J., 1978. Water quality for River –Reservoir Systems (technical report). U.S Army Corps of Engineers (Hydrologic Engineering Center), Davis, CA.

Susperregui, A. S., Gratiot, N., Michel, E., Christian, P., 2009. A preliminary hydrosedimentary view of a highly turbid, tropical, manmade lake: Cointzio Reservoir (Michoacán, Mexico). Lakes & Reservoirs: Research & Management. 14, 31-39.

Thomaz, S. M., Bini, L. M., 2003. Ecologia e Maneojo de Macrófitas Aquáticas, Editora da Universidade Estadual de Maringá, 342 pp.

Tundisi, J. G., 2003. Água no Século XXI: enfrentando a escassez. São Carlos: Rima; IIE, 248 pp in Restoration and Management of Tropical Eutrophic Lakes, Mallapureddi Vikram Reddy (ed.). Science Publishers, Inc, 271-274.

Von Sperling, E., Sousa, A. D., 2007. Long-term monitoring and proposed diffuse pollution control of a tropical reservoir. Water Science and Technology. 55, 161-166.

Figure legends:

Figure 1. Map of the Cointzio reservoir, and localization of sampling sites. 16 vertical profiles were realized along the longitudinal axis (dashed line).

Figure 2 Time series of the water levels in the Cointzio reservoir.

Figure 3. Time evolution of the temperature in 2009 (left panels) and 2008 (right panels). The top map is obtained with the measured temperature, the middle one with the simulated one. The bottom one depicts the residues Tmea-Tsim.

Figure 4. Vertical profiles of measured (left panels) and simulated (right panels) DO, chlorophyll *a*, PO_4^{3-}, NH_4^+ at P27 of the Cointzio reservoir in 2009.

Figure 5. The residues between measurement and simulation of DO and chlorophyll *a* in 2009.

Figure 6. Simulation of DO and chlorophyll *a* under the dry year conditions (P1 scenario).

Figure 7. Simulation of DO and chlorophyll *a* under the wet year conditions (P2 scenario).

Figure 8. DO and chlorophyll *a* in increasing air temperature of 2.5°C and 4.4°C (P3 and P4 scenarios).

Figure 9. The results of DO and chlorophyll *a* for the case P1 (left panels) with three different reduction in nutrients input (P5, P6, and P7 scenarios) and the case P4 (right panels) for the scenarios P8, P9, and P10 during a ten-year period. The top figure is obtained with the oxycline position, the middle one with the maximum peak of chlorophyll *a*. The bottom one depicts the mean chlorophyll *a* in the top 10 m.

Table legends:

Table 1. Literature values and main parameters of the biogeochemical model compared to other published applications of the same model. See supplementary data for definitions of parameters.

Table 2. Summary of scenarios for water and ecological quality assessment of the Cointzio reservoir.

Table 3. P release in the global warming scenario for the last year of the simulation with the nutrient-reduction scenarios P8 and P9.

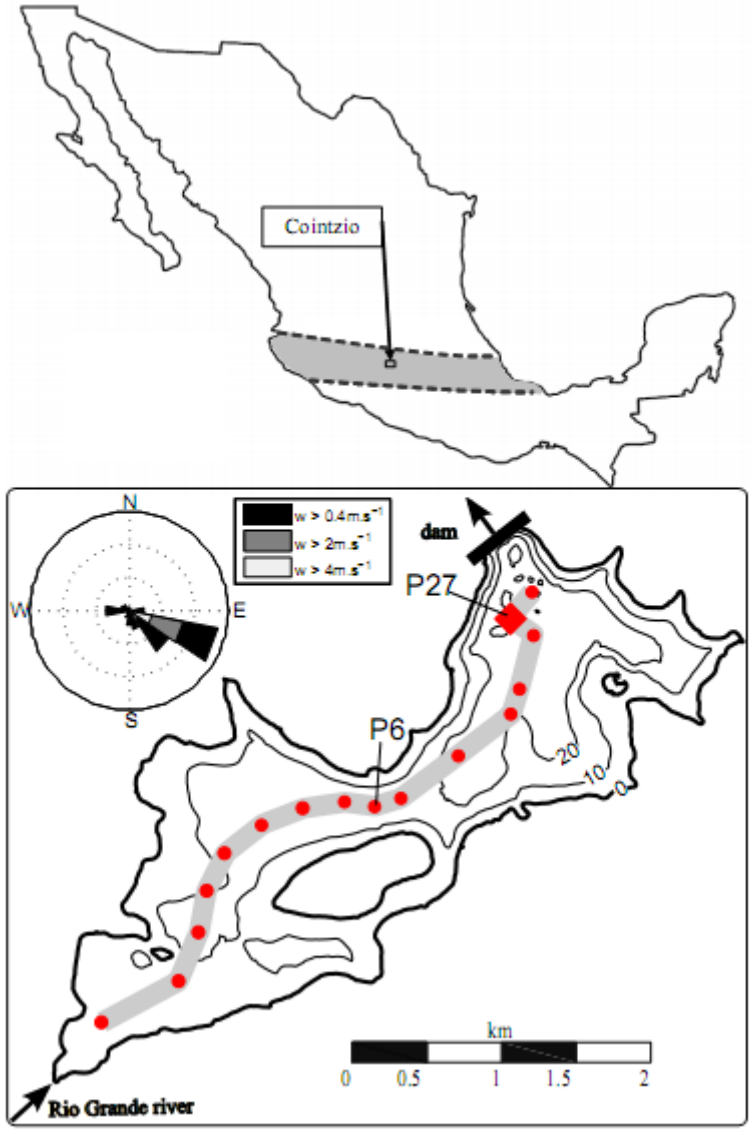

Figure 1: Map of the Cointzio reservoir, and localization of sampling sites. 16 vertical profiles were realized along the longitudinal axis (dashed line)

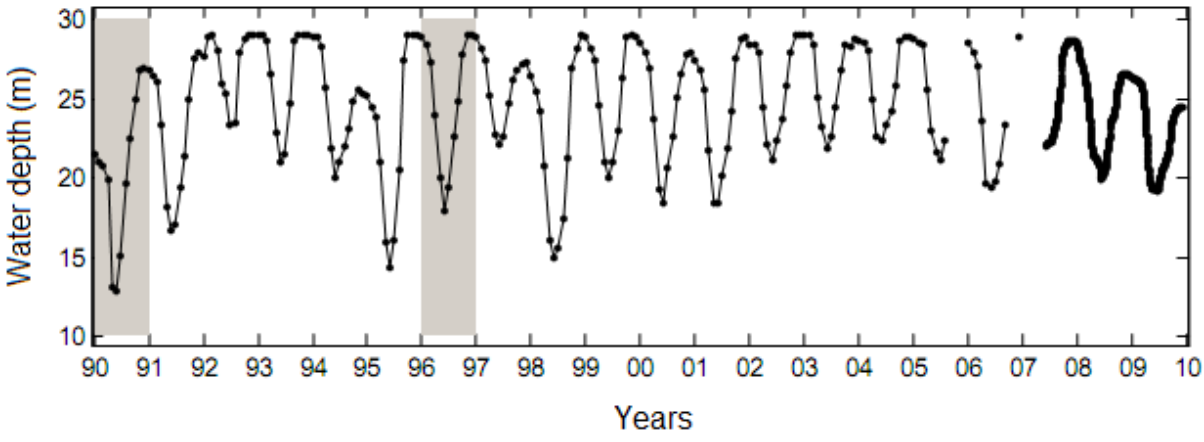

Figure 2: Time series of the water depths in the Cointzio reservoir

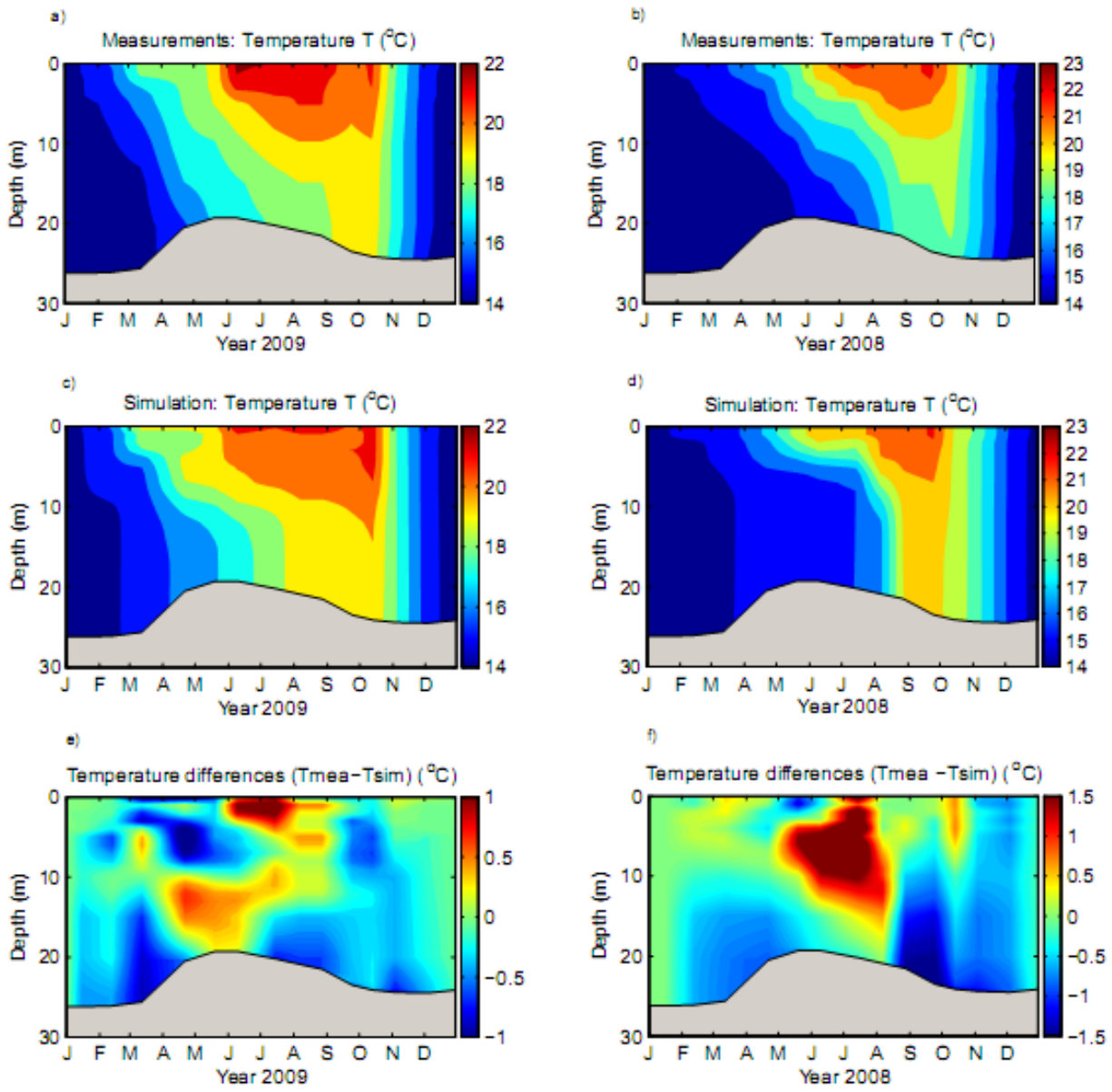

Figure 3: Time evolution of the temperature in 2009 (left panels) and 2008 (right panels). The top map is obtained with the measured temperature, the middle one with the simulated one. The bottom one depicts the residues Tmea-Tsim

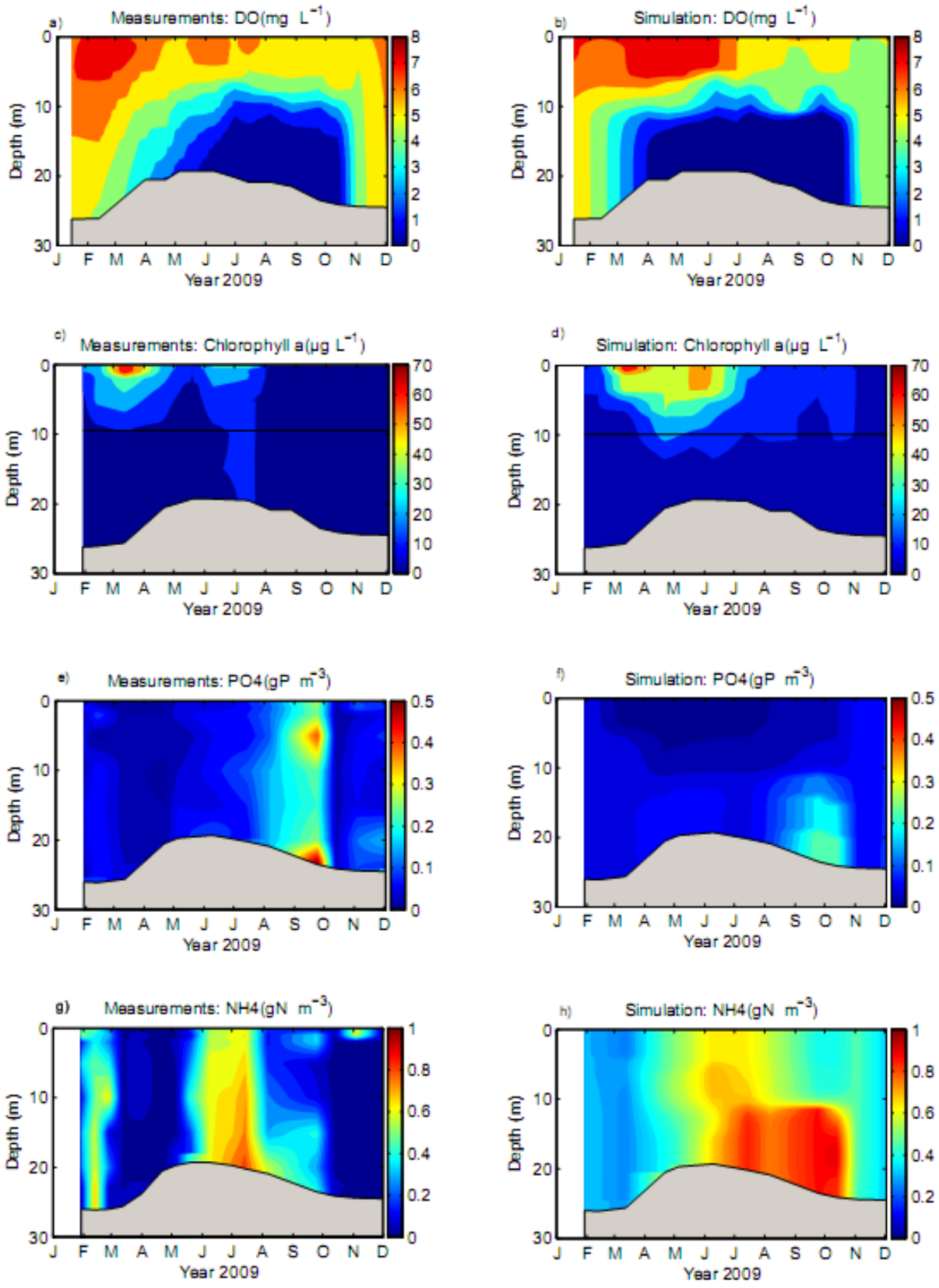

Figure 4: Vertical profiles of measured (left panels) and simulated (right panels) DO, chlorophyll a, PO_4^{3-}, NH_4^+ at P27 of the Cointzio reservoir in 2009

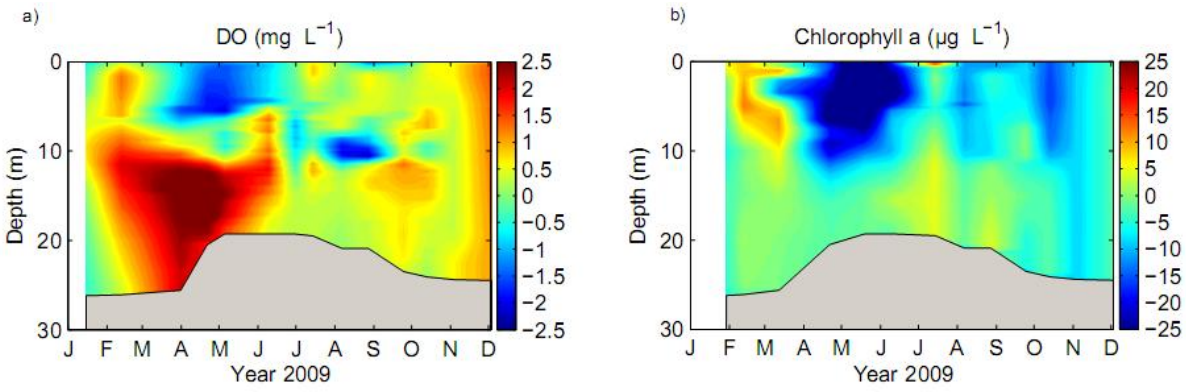

Figure 5: The residues between measurement and simulation of DO and chlorophyll a in 2009

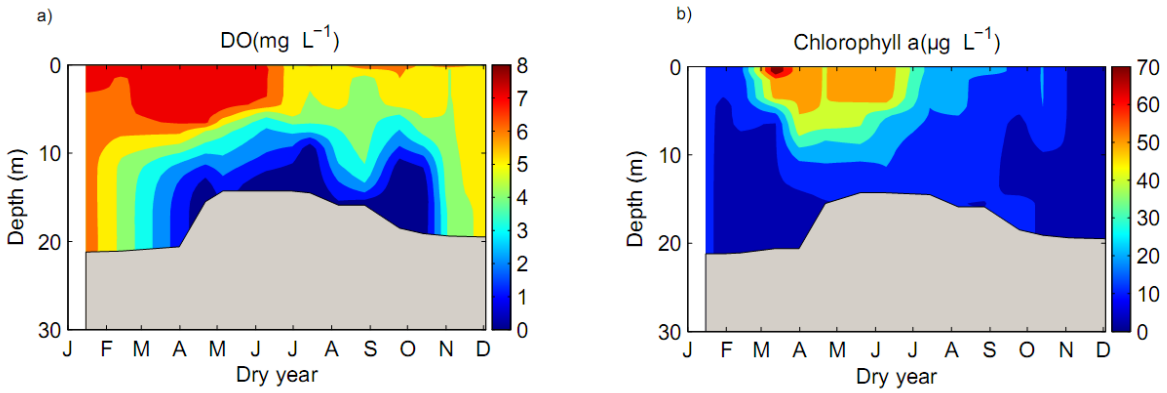

Figure 6: Simulation of DO and chlorophyll a under the dry year conditions (P1 scenario)

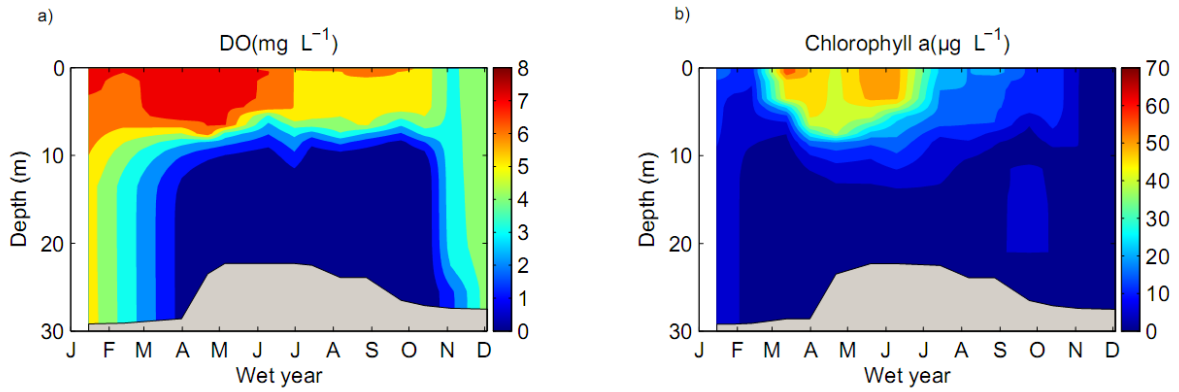

Figure 7: Simulation of DO and chlorophyll a under the wet year conditions (P2 scenario)

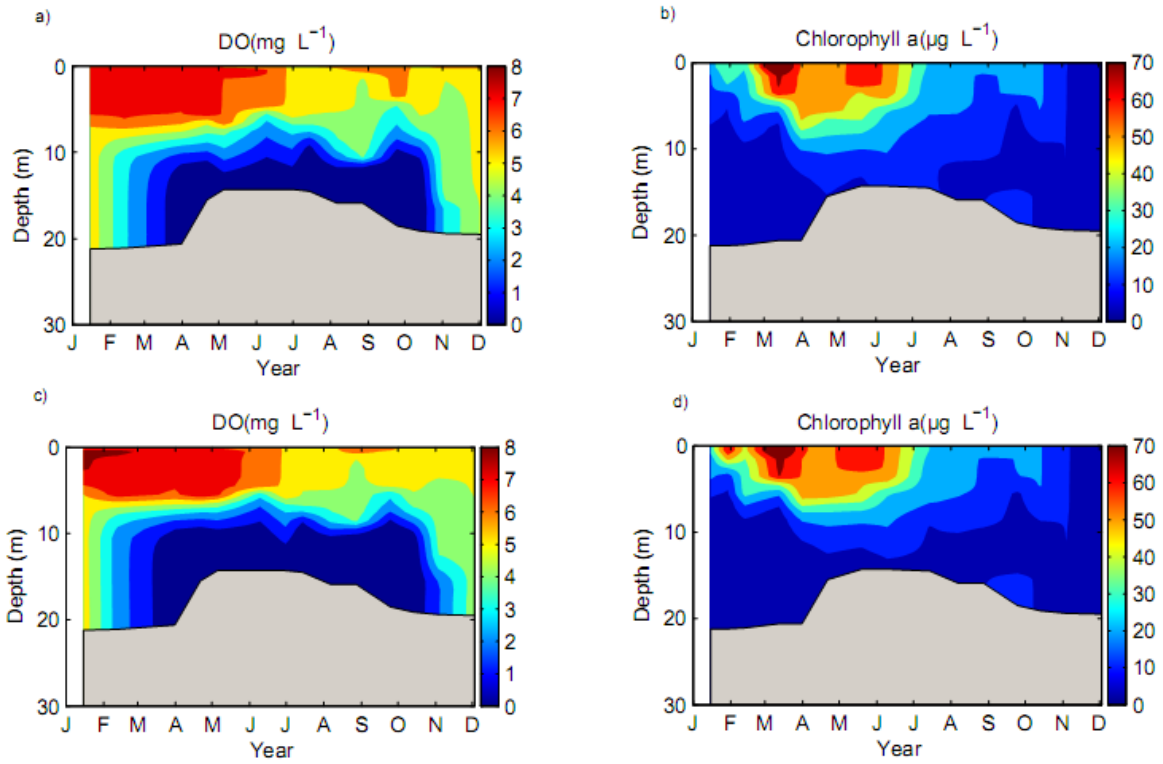

Figure 8: DO and chlorophyll a in increasing air temperature of 2.5°C and 4.4°C (P3 and P4 scenarios)

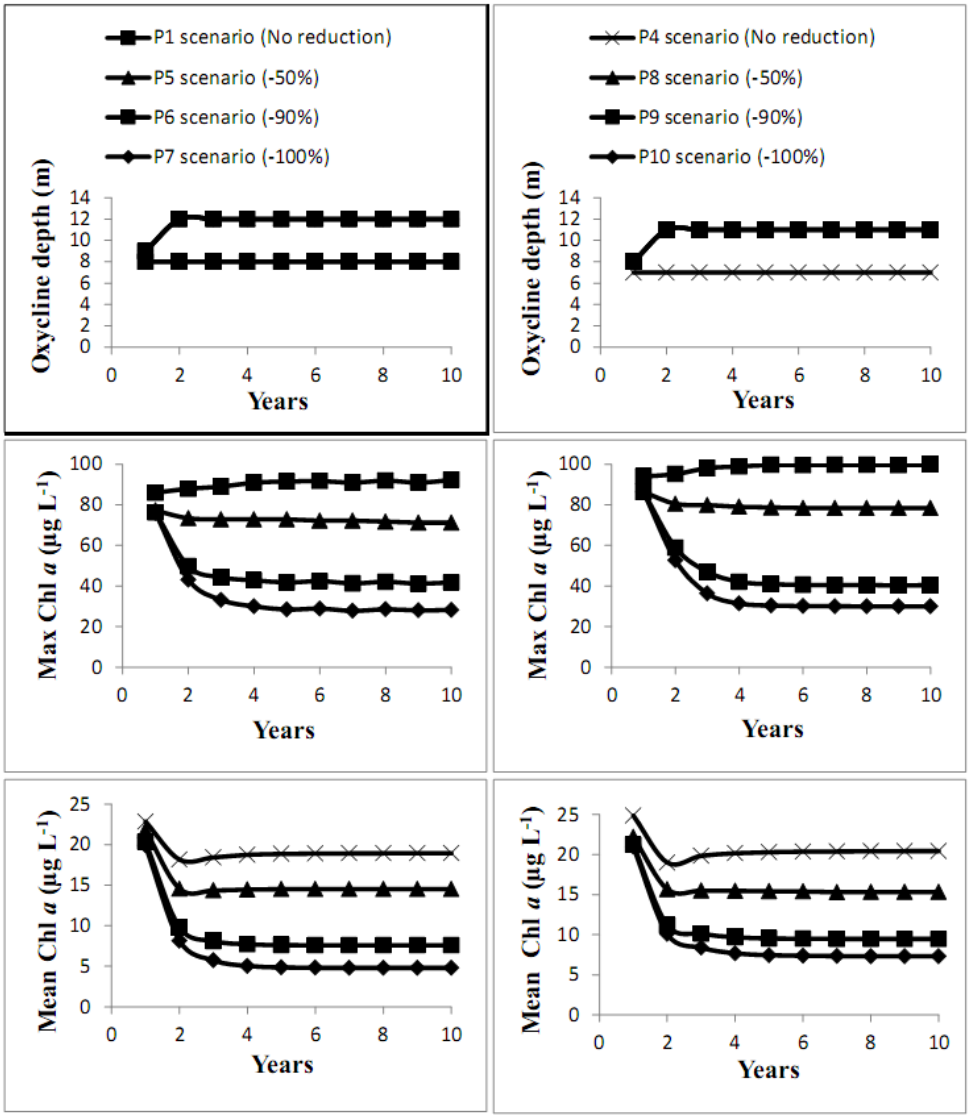

Figure 9: The results of DO and chlorophyll a for the case P1

Table 1: Literature values and main parameters of the biogeochemical model compared to other published applications of the same model. See supplementary data for definitions of parameters.

Parameters	**Units**	**Cointzio reservoir** (This study)	**Lake Zürich** (Omlin et al., 2001)	**Lakes Walensee/ Zürich/ Greifensee** (Mieleitner & Reichert, 2006)	**Itezhi –Tezhi reservoir** (Kunz et al., 2011)	**Lake Ohrid** (Matzinger et al., 2007b)	**Other literature values and ranges**
k_gro_ALG_20[a]	d^{-1}	1.2	1.1	1.6	1.1[c]	1.88	0.58-3[1]
k_gro_ALG_N2_20[a]	d^{-1}	0.85	-	-	0.25	-	
k_gro_ZOO_20[a]	$gDM^{-1}m^3d^{-1}$	0.001	0.3	0.4	0.25[c]	3.47	0.15-0.25[2]
k_death_ALG_20[a]	d^{-1}	0.03	0.03	0.03	0.01[d]	0.03	0.03[3]
k_death_ZOO_20[a]	d^{-1}	0.1	0.029	0.01/0.035/0.11	0.1[d]	0.029	0.003-0.155[4]
k_resp_ALG_20	d^{-1}	0.05	0.05	0.05	0.05[c]	0.05	0.05-0.15[5]
k_resp_ZOO_20	d^{-1}	0.003	0.003	0.003	0.003[c]	0.003	0.001-0.11[6]
k_nitri_wat_20[a]	$gN^{-1}m^3d^{-1}$	0.05	0.1	0.1	0.1	-	0.03-0.25[7]
k_miner_aero_20[a]	d^{-1}	0.1	0.01	0.005	0.1	0.008	
k_miner_anox_20[a]	d^{-1}	0.01	0.01	0.005	0.01	-	
k_miner_anaero_20[a]	d^{-1}	0.001	-	0.0005	0.001	-	
k_miner_bg[a]	d^{-1}	0.1	-	-	0.1	-	
K_HPO4_ALG	gPm^{-3}	0.0007	0.0019	0.0005	0.002	0.0019	
K_I_ALG	Wm^{-2}	34.32	34.32	10[b]	34.32	-	
S_HPO4_crit	gPm^{-3}	0.0042	0.0042	0.004	0.004	0.004	
DeltaS_HPO4	gPm^{-3}	0.0013	0.0013	0.0013	0.0013	0.0013	
k_upt	$m^4gDM^{-1}d^{-1}$	1200	1200	30[b]	1200	1200	

Cointzio reservoir: Turbid tropical eutrophic reservoir

Lake Zürich: Mesotrophic temperate lake

Lakes Walensee/ Zürich/ Greifensee: Temperate lakes (Walensee is oligotrophic, Greifensee is eutrophic)

Itezhi –Tezhi reservoir : Tropical eutrophic reservoir

[a] Parameters fitted during the calibration of the Cointzio reservoir

[b] Large change in meaning due to modification of the formulations

[c] Kunz et al., 2011 adapted from Omlin et al., 2001

[d] Kunz et al., 2011 adapted from Mieleitner and Reichert., 2006

[1] Jørgensen (1979); [2]Chen & Orlob (1975); [3]Scavia et al., 1976

[4] Collins & Wlosinski (1983); [5]O'Connor et al., (1981); [6]Smith (1978); [7]Bansal (1976)

Table 2: Summary of scenarios for water and ecological quality assessment of the Cointzio reservoir.

Scenarios	Description	Parameters used
Present	Target year 2009	Water level H=26 m
P1	Dry year 1990, nutrient inputs 2009	low water level H = 21 m
P2	Wet year 1996, nutrient inputs 2009	high water level H= 29 m
P3	P1 with an increase in air temperature (T_{air}) of 2.5°C	H=21 m and +2.5°C in T_{air}
P4	P1 with an increase in T_{air} of 4.4°C	H=21 m and +4.4°C in T_{air}
P5	P1 with a long term reduction of 50% of nutrient inputs (N,P)	H=21 m, & -50% (N,P)
P6	P1 with a long term reduction of 90% of (N,P) inputs	H=21 m, & -90% (N,P)
P7	P1 with a long term reduction of 100% of (N,P) inputs	H=21 m, & -100% (N,P)
P8	P4 with a long term reduction of 50% of (N,P) inputs	H=21 m, +4.4°C in T_{air} & -50% (N,P)
P9	P4 with a long term reduction of 90% of (N,P) inputs	H=21 m, +4.4°C in T_{air} & -90% (N,P)
P10	P4 with a long term reduction of 100% of (N,P) inputs	H=21 m, +4.4°C in T_{air} & -100% (N,P)

Table 3: P release in the global warming scenario for the last year of the simulation with the nutrient-reduction scenarios P8 and P9.

Scenarios / **P releases (t P y^{-1})**	**P4 (No reduction)**	**P8 (-50%)**	**P9 (-90%)**
Aerobic mineralization at sediment surface	0.486	0.421	0.223
Anoxic mineralization at sediment surface	0.216	0.081	0.014
Anaerobic mineralization at sediment surface	0.170	0.167	0.082
Aerobic mineralization in water column	0.22	0.191	0.104
Anoxic mineralization in water column	0.0058	0.003	0.0004
Anaerobic mineralization in water column	0.00047	0.00045	0.00023
Total mineralization processes	**1.105**	**0.867**	**0.425**

C) Biogeochemical mass balance in the turbid tropical reservoir of Cointzio, Mexico: Field data and modelling approach

1. Introduction

Biogeochemical budgets (C, N and P) are major concerns for management of highly eutrophic reservoirs (Hart et al, 2002), particularly in tropical systems. In the case of reservoirs with anoxic hypolimnia, internal nutrient loads from sediment release can become a significant term of nutrient budgets, as outlined previously by Nürnberg (1984) and Jensen et al, (1992). In the case of P, it is relatively well known that its release depends on P sedimentation and retention capacity of sediments (Gächter & Wehrli 1998, Prairie et al, 2001). However, the budgets for nitrogen in reservoirs should be different from those observed for phosphorus because of the numerous biological processes involved (e.g., denitrification, N_2 fixation, nitrification) (Wetzel, 2001). Lewis (2002) suggested that N is largely denitrified, and poorly stored in sediments of tropical lakes. The goals of this section are (i) to identify and estimate the main processes involved in nutrients release and carbon removal and (ii) complete the annual mass balance in the reservoir using modelling results.

2. Results

2.1 Mineralization rates in the Cointzio reservoir

Table 5.2 Mineralization rates in the water column and at the sediment surface for the target year 2009

Mineralization rates	**g O_2 m^{-3} d**
Aerobic mineralization in water column	0.15
Anoxic mineralization in water column (denitrification)	8.34E-03 ~ 0
Anaerobic mineralization in water column (mineralization in the absence of DO and NO_3^-)	2.34E-04 ~ 0
Aerobic mineralization at sediment surface	1.95
Anoxic mineralization at sediment surface (denitrification)	7.55
Anaerobic mineralization at sediment surface	0.88

The numerical simulations undertaken have shown that the mineralization rates at sediments are presumably much higher than the mineralization rates in the water column (Doan et al, 2014). In the reservoir of Cointzio, the benthic mineralization of organic matter is believed to be the predominant factor explaining nutrients released from sediments (Table 5.2).

2.2 Temporal variability of benthic mineralization processes

Organic matter (OM) undergoes mineralization through settling in the water column and then the process of mineralization continues after it is deposited in sediments (Kunz et al, 2011). Since the Cointzio reservoir is heavily influenced by seasonal variation of OM inputs, the mineralization rates dominate during the anoxic period from May to October (nearly ~100 % of annual mineralization) (Figure 5.1). This is mainly due to accumulation of OM from inputs and from dead algae sink as discussed in the previous section (chapter 4).

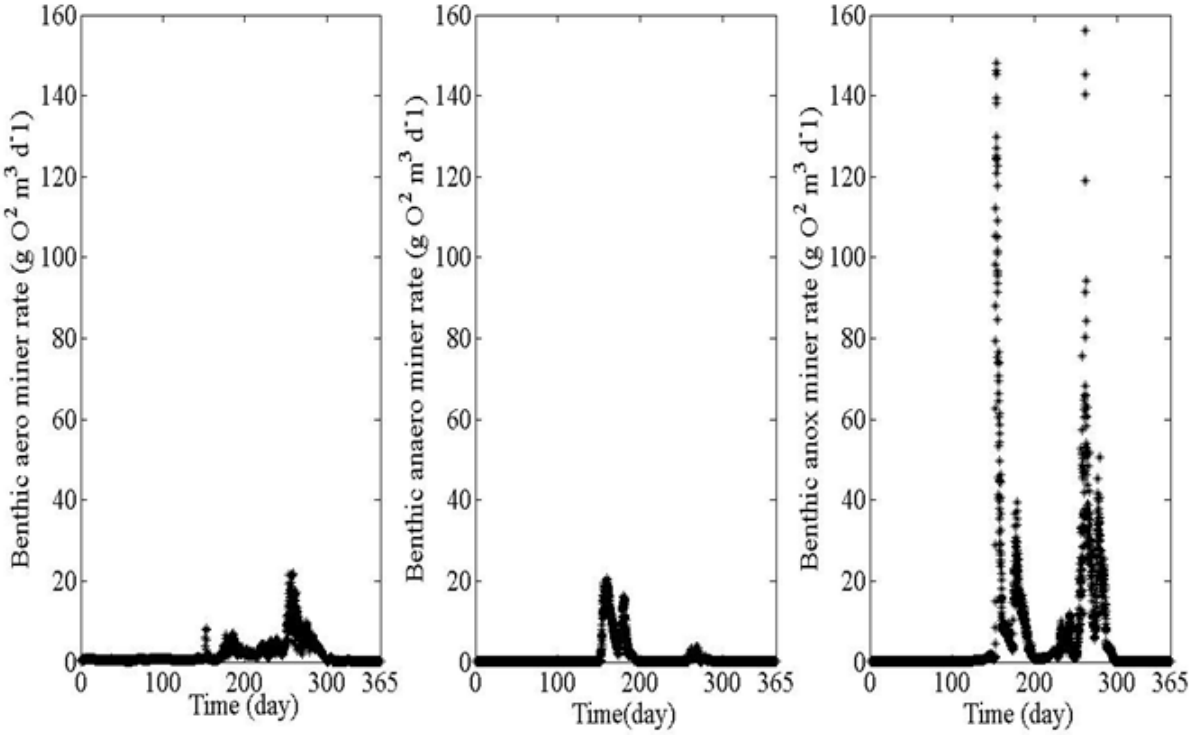

Figure 5.1 Temporal variability of a) benthic aerobic mineralization b) benthic anaerobic mineralization and c) benthic anoxic mineralization rates at the deepest point of the Cointzio reservoir in 2009

2.3 Nutrients releases and N_2 removal

Dissolved inorganic nitrogen (DIN**)** and soluble reactive phosphorus (SRP) are usually released during mineralization, either directly by settling of material through the water column, or by diffusion from bed sediments (Kunz et al, 2011). The total release of DIN and SRP estimated from the model during the stratified period from mid-February to October are 20.1 t N y^{-1} and 2.2 t P y^{-1} respectively. They are lower than the Redfield-derived estimates of 27.01 t N y^{-1} and 3.74 t P y^{-1} (Table 5.3). The Redfield calculation of N and P release was obtained by applying the ratio C:N = 5.68 and C:P = 41 (Redfield et al, 1966). The N_2 removal was calculated from the anoxic benthic mineralization (denitrification) as 80.7 t N y^{-1} and was much higher than N release from sediments in the Cointzio reservoir (20.1 t N y^{-1}).

Table 5.3 The model estimations of nutrient releases and N2 and carbon removal in the Cointzio reservoir for the target year 2009

Nutrient releases	**N release (t N y^{-1})**		**P release (t P y^{-1})**		**C removal (t C y^{-1})**
Methods of calculation	Modelling approach	Redfield-derived estimation	Modelling approach	Redfield-derived estimation	Modelling approach
Aerobic mineralization in water column	0.08	0.28	0.25	0.32	12.95
Aerobic mineralization in sediments	3.49	4.09	0.42	0.57	23.26
Anoxic mineralization in sediments (denitrification)	15.50 80,7 (N_2)	18.20	1.42	2.52	103.36
Anaerobic mineralization in sediments	1.13	2.45	0.12	0.34	13.9 (CH_4)
Total mineralization processes	**20.1** **80.7 (N_2)**	**27.02**	**2.22**	**3.74**	**153.5**

2.4 The mass balance of C, N, P in the Cointzio reservoir

C, N, P fluxes and accumulation were obtained from field data in 2009 (see chapter 4) and nutrients release and C removal were estimated from the model to obtain the C, N, P mass balance (Figure 5.2).

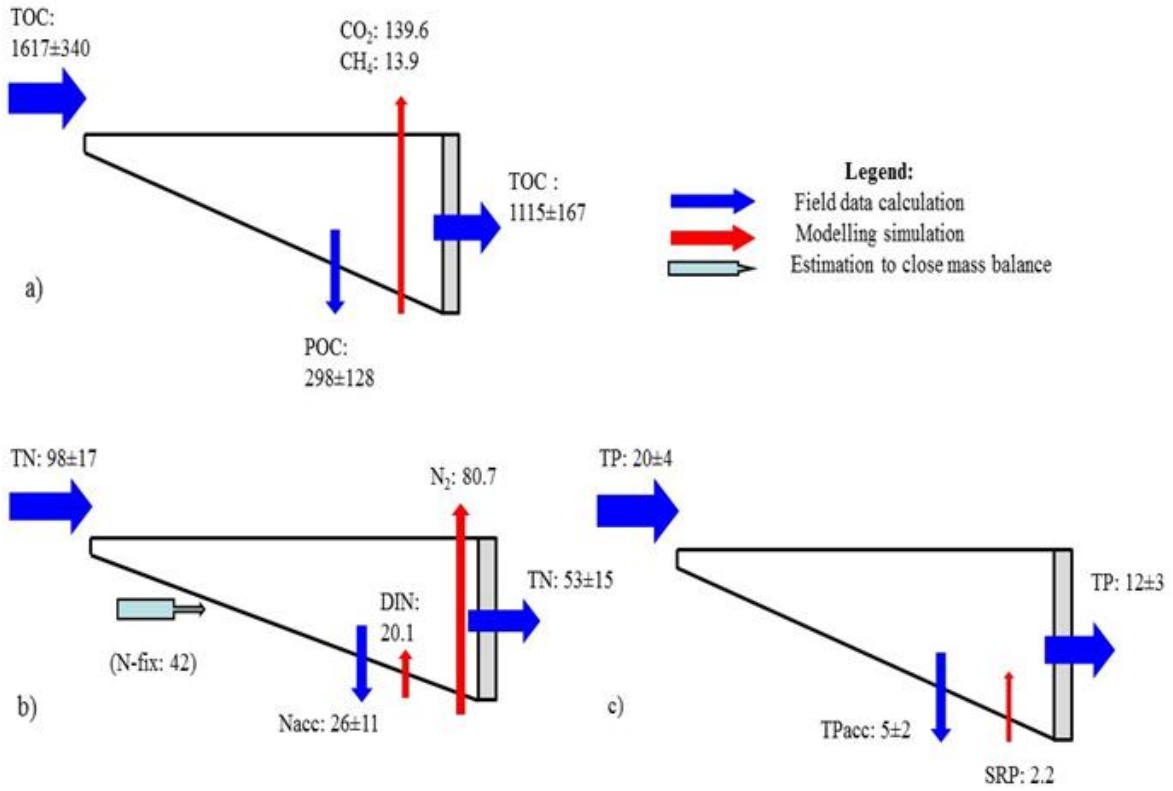

Figure 5.2 C, N, P mass balance in the Cointzio reservoir (fluxes are in t y^{-1})

2.4.1 Carbon retention and removal

Total organic carbon (TOC) input was 1617 ± 340 t C y^{-1} against a TOC output of 1115 ± 167 t C y^{-1}. The particulate organic carbon (POC) accumulation was estimated at 298 ± 128t C y^{-1} based on sediment deposition and organic carbon content of sediments within the reservoir (see detailed calculation in Tables 5 and 7 of chapter 4). The C removal by all mineralization processes calculated from the model is 153.5 t C y^{-1} (Table 5.3). As shown from the Figure 5.1, the anaerobic benthic mineralization (methanization) occurred during the anoxic period from May to October. The release of C as CH_4 was estimated at 13.9 t C y^{-1}. This means that C removal would be 90% as CO_2 and 10% as CH_4 (Figure 5.2a).

2.4.2 Nitrogen removal

Total nitrogen (TN) input was 98 ±17.2 t N y^{-1} in opposition to 53 ± 15 t N y^{-1} in the output. N accumulation (Nacc) was estimated as 26 ± 11 t N y^{-1} (see chapter 4). N is either lost to

sediments by burial or to the atmosphere through denitrification. The N_2 removal estimation from the anoxic benthic mineralization (denitrification) was 80.7 t N y^{-1} corresponding to 22.4 g m^{-2} y^{-1} which was compared to 6 g m^2 y^{-1} of the Itezhi-Tezhi Reservoir (Kunz et al, 2011). The total release of DIN from the model during the stratified period of the reservoir was 20.1 t N y^{-1} (Table 4.3).

The N mass balance in the Cointzio reservoir is: $TN_{in} + TN_{fix} + TN_{release} = TN_{out} + TN_{acc} + TN_{denit}$

Where TN_{in} = TN input, TN_{fix} = TN fixation, $TN_{release}$ = TN release

TN_{out} = TN output, TN_{acc} =TN accumulation and TN_{denit} =TN denitrification

We have: 98 t N y^{-1} + TNfix? + 20,1 t N y^{-1} = 53 t N y^{-1} + 26 t N y^{-1} + 80,7 t N y^{-1}

Besides of N input from the Rio Grande de Morelia River led to an availability of N for phytoplankton growth in the Cointzio reservoir, there was an additional input of DIN (20.1 t N y-1) becoming available for phytoplankton growth via the mineralization of OM, N limiting conditions prevailed.

The differences in the nitrogen budget in this case may be explained by the nitrogen fixing by cyanobacteria since cyanobacteria (*Oscillatoria lacustris)* were identified as the dominant species in the Cointzio reservoir (López-López & Dávalos-Lind, 1998). This confirms the N fixation would be important in the Cointzio reservoir which is similar with the study of Henry et al, (1999) for the Jurumirim tropical reservoir in Brazil.

Consequently, N fixation could be considered as an important process in the tropical Cointzio reservoir, with fixed N that was estimated about 42 t N y^{-1} to close the N mass balance (Figure 5.2b). Based on the mass balance of N, this result further supports the interpretation that N fixation is a quantitatively important process in tropical reservoirs. Fixation of atmospheric N2 can account for 6–82% of the N input to eutrophic tropical systems (Howarth et al, 1988).

2.4.3 Phosphorus retention

Input of total phosphorus (TP) was 20 ± 4.4 t P y^{-1} against 12 ± 2.7 t P y^{-1} of TP output. Based on the mean total particulate phosphorus (TPP) in dry season, P accumulation (Pacc) was estimated at 5 ± 2 t P y^{-1}. The estimation of SRP released by all mineralization processes from the model during the stratified period was 2.2 t P y^{-1} (Figure 5.2c).

The P mass balance in the Cointzio reservoir: $TP_{in} + TP_{release} = TP_{out} + TP_{sed}$

Where TP_{in} = TP input, $TP_{release}$ = TP release, TP_{out} = TP output, and TP_{sed} = TP sedimentation.

Therefore, we have

20 ± 4 t P y^{-1} + 2.2 t P y^{-1} = 12 ± 3 t P y^{-1} + 5 ± 2 t P y^{-1}

3. Conclusions

In summary, the values of the entire mass balance of nutrients and carbon estimated from field data calculation and modelling approach are at equilibrium. The analysis indicates that the benthic mineralizations are the dominant processes explaining the nutrients release. Especially the anoxic benthic mineralization (denitrification), with the production of N_2 (81 t N y^{-1}), should be an important process explaining the mass balance of nitrogen in the Cointzio reservoir that was identical with the study of Duff & Triska, (1990) for aquatic ecosystems. N fixation should be a quantitatively important process in tropical Cointzio reservoir that was concluded for eutrophic tropical systems (Howarth et al, 1988).

This is the first implementation of a biogeochemical model applied to a highly productive reservoir in the TMVB in order to estimate the mass balance of nutrients and carbon. This study showed that the Cointzio reservoir is acting as a "sink" for nitrogen and phosphorus that have similar properties in shallow and eutrophic tropical reservoirs (Straskraba et al, 1995).

Conclusions of chapter 5

The vertical one - dimensional (1DV) numerical models (Aquasim biogeochemical model coupled with k-ε mixing model) were applied to reproduce the main biogeochemical cycles in the Cointzio reservoir and to assess scenarios of nutrients (P and N) and eutrophication reduction in the coming decades. The k-ε model accurately reproduced water temperature profiles for the calibration year 2009 and the validation year 2008. The Aquasim biogeochemical model was able to reproduce the main patterns of dissolved oxygen, nutrients and chlorophyll *a* concentrations within the Cointzio reservoir for the target year 2009. The different simulations pointed out the negative long - term effects of eutrophication under dry conditions and global warming. Large nutrient reduction is required to improve the trophic state of the Cointzio reservoir. If measures are not taken to mitigate eutrophication, extensive algal blooms such as the ones reported by the local newspapers in the spring 2014 will occur more and more frequently, with some critical consequences for the lake ecosystem, its aquatic life and the water potabilization.

In order to complete the mass balance of nutrients and carbon in the reservoir, the model was used to calculate the nutrients release and carbon removal. The entire mass balance of nutrients and carbon calculated from field data and estimated from modelling approach are at equilibrium in general. In-out and internal mass balances in this study showed that the Cointzio reservoir clearly acts as a "trap" for TSS, C, N and P.

CONCLUSIONS & PERSPECTIVES

This study provides a critical analysis of the biogeochemical functioning of a turbid tropical reservoir located on the Trans - Mexican Volcanic Belt in Mexico. It is based on an original compilation of some historical sources (since 1940) and some field surveys conducted from 2007 to 2010. Apart from the direct analysis of data series, the compilation was used for further water quality modelling.

The principal objective of the present thesis focuses on pluri-annual estimation of the biogeochemical cycles in the Cointzio reservoir. The results of the hydrodynamic field measurements did not reveal significant lateral heterogeneities. Thus it was decided to focus the long term monitoring efforts on the temporal variations along the longitudinal axis. Besides that, the vertical profiles of water quality variables from the biogeochemical field measurements realized fortnightly at the deepest point and the middle of the reservoir confirmed that longitudinal gradients were negligible for long term applications. Considering, the difficulties to integrate all the parameters playing a role in the dynamic of the reservoir, and the ones corresponding to input and output fluxes, it was decided to develop a 1DV modelling approach.

Within the watershed of the Cointzio reservoir, eight sampling sites were surveyed on a monthly basis in 2009 to identify the hot spots of pollution emission. The results of our study indicated that point sources from domestic wastewater clearly dominated the dynamics of the reservoir while diffuse sources were of secondary importance. Nutrient pollutions mainly originated from the most populated villages located upstream of the reservoir since wastewaters were not treated in these municipalities. The analytical results for the samples taken from the inlet of the Cointzio reservoir indicated that the water drained by the Rio Grande de Morelia River was of poor quality. The water taken from this river gave high values especially for total P (0.38 ± 0.23 mg L^{-1}), P-PO_4^{3-} (0.11 ± 0.07 mg L^{-1}), NH_4^+ (0.15 ± 0.10 mg L^{-1}) and TSS (2220 ± 1559 mg L^{-1}), which indicated a significant input of nutrients to the reservoir. The watershed of Cointzio was principally subjected to the erosion of clay particles (Acrisols, Luvisols and Andosols) that discharged into the reservoir so that a large amount of phosphorus was adsorbed directly from these particles. These led to high levels of turbidity (Secchi depth < 30 cm), serious episodes of eutrophication (up to 70 µg chl. a L^{-1}), and long hypolimnic anoxia (from May to October) in the water column. Eutrophication represents an issue of concern for most of the lakes and reservoirs in Central Mexico. In the case of the Cointzio reservoir, this issue is especially critical as an important part of the water

stored is used for drinking water supply. Point sources nutrient reduction should be a water management priority for the reservoir in the upcoming years.

Based on intensive field measurements in 2009 within the reservoir, we did an integrated study in order to assess internal cycling and to establish biogeochemical (TSS, C, N, P) mass balance in the reservoir. In-out and internal mass balances showed that the Cointzio reservoir was an efficient trap for TSS, C, N and P. The large difference between TSS inputs and outputs was explained by a large amount of TSS deposition (89-92 %), as evidenced for the three years 2007, 2008, and 2009. The reservoir acted as a sink for TSS. Sediment trapping is a key issue for the management of the Cointzio reservoir since it has already lost 25 % of its initial storage capacity. Total organic carbon (TOC) input was 1617±340 t C y^{-1} against a TOC output of 1115±170 t C y^{-1}. The particulate organic carbon (POC) accumulation was estimated at 298±130 t C y^{-1} based on sediment deposition and organic carbon content of sediments within the reservoir. According to the nutrients estimated in sediments (collected at during the wet season and the dry season), mineralization of OM revealed to be the most important process for explaining nutrients release from sediments. These results have been presented in chapter 4.

To complete field data analyses we examined the ability of vertical one - dimensional (1DV) numerical models (Aquasim biogeochemical model coupled with k-ε mixing model) to reproduce the main biogeochemical cycles in the Cointzio reservoir and assess scenarios of nutrients (P and N) and eutrophication reduction in the coming decades. The model was used to identify and estimate the main processes involved in nutrients release and carbon removal. The entire mass balance of nutrients and carbon in the reservoir was also estimated.

The k-ε model reproduced nicely the vertical mixing that takes place from the end of October until January and the stratified period that begins in February and lasts until October. With a mean square error of 0.24°C between the simulated and measured temperatures, water temperatures closely followed the measured profiles. After the calibration of the scaling factor for the wind energy transfer to the internal seiches (α), and the wind drag coefficient (C10), the vertical turbulent diffusivity Kz(z) was estimated with a time step of 30 minutes. The resulting time series of Kz(z) were then used as the input data for the Aquasim biogeochemical model. The Aquasim model was able to reproduce the main patterns of DO, nutrients and chlorophyll *a* concentrations within the Cointzio reservoir for the target year 2009. The set of parameters obtained after calibration was reasonable in comparison with the range of parameter values found in the literature.

In Chapter 5 scenarios were designed for predicting the long term effect of global warming, without neglecting the natural variation of the hydrological cycle at a decadal scale (dry and wet years). The different simulations pointed out the negative long-term impact of air temperature rising. By the end of the century, an increase of air temperature as high as 4.4°C is expected from global warming in the region. The scenario that coupled a dry hydrological year with a 4.4°C increase of the air temperature led to an exacerbated eutrophication with peaks of chlorophyll *a* up to 94 μg L^{-1} and with a severe depletion of DO. In order to assess by how much the nutrient loads would have to be reduced to maintain oxic conditions and low contents of chlorophyll *a*, some scenarios of reduction of 50%, 90% and 100% in the nutrient inputs were examined. Tests with the three different nutrient input reductions were simulated for both the dry year scenario and the global warming scenario. Generally, the strategies in nutrient inputs control are successful to improve the water quality in term of DO level and phytoplankton development in reservoirs. In the case of the Cointzio reservoir, the results of numerical simulation showed that a large reduction of the nutrients input would be required to reduce significantly the quantity of algal biomass and the concentration of chlorophyll *a*. Moreover, the positive effect of reduction of the nutrients input on the phytoplankton development is not immediate and will be observed after a few years. This time is needed to flush out the nutrients, mineralized directly from particles, accumulated in the water column and the benthic layer of the reservoir. If such mitigation measures were adopted, the maximum peak of chlorophyll *a* would reduce significantly, from 94 μg L^{-1} to 40 μg L^{-1}, and the average concentrations in the top 10 m would decrease to 9.5 μg L^{-1} after a five-year period of efforts. The depth of the anoxic layer would have a large decrease, with a positive effect on the ecosystem. After the period of five years the model predicts a stabilization of the biogeochemical cycles.

In order to confirm this result, the model was used to calculate the entire mass balance of nutrients and carbon in the reservoir and to estimate P release in the global warming scenarios. All the mineralization rates acting in the water column and in the sediment of the reservoir were estimated from the model. The model estimation of the entire mass balance of nutrients and carbon are at equilibrium. The analysis indicates that the nutrient release occurs during the anoxic period from May to October and is dominated by the benthic mineralization. The release of P only reduces slightly after a 50% reduction in nutrients input but it has a large decrease when the nutrients input is reduced by 90%. Therefore, a 90% decrease of nutrients input is needed to reduce chlorophyll *a* concentrations in the Cointzio reservoir. The challenge for the Cointzio reservoir management is to reduce the nutrient load to balance the negative

effects of ongoing global warming. Air temperature increase is likely to deteriorate the water quality of the reservoir. Waste water treatment plants should be installed in the villages located upstream of the reservoir to reduce nutrient inputs. Fortunately, most of nutrients pollution levels within the watershed come from domestic sources so it would be feasible to treat this kind of waste water. Special attention should be paid to phosphorus and ammonium removal.

Based on our study of the turbid, hollow type, tropical reservoir of Cointzio, some guidelines can be addressed regarding the advantages and limitations of Aquasim model. First, Aquasim model has an open structure that can be modified to integrate new processes which are suitable for a specific case. The user of the Aquasim model is free in specifying any set of state variables and transformation processes to be active within the compartments. Moreover, the model is able to perform simulations, sensitivity analyses and parameter estimations using measured data. These features make the Aquasim model a very useful research tool. The Aquasim model is also divided into two different parts: Physical and biogeochemical parts that make easier to do modelling simulation. In addition, since 2011 the Aquasim model is free and open software which makes it is very relevant for developing countries. Besides that, Aquasim model has restrictions that we should consider. For instance, the Aquasim version considered in this work does not allow variable surface water levels. The software automatically generates additional inflow when the outflow is larger than the inflow, and vice versa. Therefore, we have to use an average lake level. In addition, with the current version of the Aquasim model, the wind stress is always considered to be in the same direction; therefore wind speeds can result in buildup of unrealistically strong currents leading to stronger vertical mixing. Furthermore, for reservoirs that are very turbid, the simulation of light attenuation may present some difficulties. In the case of the Cointzio reservoir, these physical features (high wind and extreme turbidity) are gathered all year long. Our study shows that the physical Aquasim module fails in reproducing vertical profiles of temperature and an excessive water mixing was simulated all year long. Therefore, the k-ε model was considered to predict the seasonal development of temperature stratification and turbulent diffusivity for the Cointzio reservoir. These above limitations were counter balanced by the robustness of the Aquasim model and its capacity to integrate a large quantity of variables that participate to the biogeochemical cycles. As a mixed strategy, the simulations of biogeochemical cycles in the Cointzio reservoir were performed by using two independent models: (i) the k-ε model for the physical modelling of the lake and (ii) the Aquasim model for the simulation of the biogeochemical cycles. In our study we considered a one vertical dimension (1DV) since the horizontal and longitudinal gradients are negligible for long term

applications in the Cointzio reservoir. In the case of another large reservoirs, two-dimensional (2D) and three-dimensional (3D) models should probably be applied, e.g. Hydrodynamic and Water quality Model CE-QUAL-W2 (Portland State University, United States).

At the end of this study, we identify three main perspectives of our work:

1) First, the computation of internal processes indicated that the benthic mineralizations are the dominant processes explaining the nutrients release in the Cointzio reservoir. However, in this study, sediment compartment as described by Omlin et al, 2001a was replaced by sediment-water interface because of lacking data in sediment layers. Some further field investigations would be particularly useful to provide measure of biogeochemical fluxes at the interface between bottom sediments and the water column. Such information could be implemented in the model, as an explicit sediment compartment to add mineralization processes in sediment layers.
2) Secondly, it would be interesting to apply a similar strategy of survey (monitoring and modelling) on other systems exhibiting comparable characteristics. This very turbid, "hollow type", tropical reservoir has been surveyed extensively during about three years. These field measurements and the numerical simulations revealed that the reservoir of Cointzio remains poorly stratified all year long. This functioning is attributed to the coupled effects of high wind and extreme turbidity. It would be interesting to evaluate if this functioning is site specific, regional, or if it can attribute to many wind swept turbid reservoirs.
3) A last perspective of this work concerns operational issues. In order to predict the further trends of water quality in the Cointzio reservoir under the development of socio-economic activities and climate changes, it is important to establish a master plan that will take into account human and climate related indicators in Michoacán, Mexico in the upcoming years or next decade. Among the variables that significantly affect the functioning of the reservoir of Cointzio are river temperature, waste water discharges and concentrations, outflows, air temperature, relative humidity, atmospheric pressure, etc. Some estimations of these variables could give realistic scenarios of simulations particularly useful to predict the future of the Cointzio reservoir.

This study provides a good example of the behaviour of a small tropical reservoir under intense human pressure and it may help stakeholders to adopt appropriate strategies for the management of very turbid, "hollow type", tropical reservoirs. The results of this study could

be applied to other turbid tropical reservoirs in the world including Vietnam. Indeed Vietnam, where I was born, is a Southeast Asian tropical country, which is located downstream of some major rivers, and thus has a vast river network. Although the quality of upstream river water is generally good, the downstream sections of major rivers reveal poor water quality, and most of the lakes and canals in urban areas have become sewage sinks. The main causes of water pollution in Vietnam are the weakness in wastewater management and the lack of civic awareness (source from http://www.studymode.com/essays/Juny-1288503.html). Therefore, water quality management has become an increasingly important and more difficult issue in tropical systems including Mexico or Vietnam.

REFERENCES

A

Abril, G., Richard S., and Guérin F., (2006). In situ measurements of dissolved gases (CO2 and CH4) in a wide range of concentrations in a tropical reservoir using an equilibrator, Science of the Total Environment. 354: 246-251.

Alcocer, J., Bernal-Brooks, F., (2010). Limnology in Mexico, Hydrobiologia. 644: 15-68.

Alcocer, J., A. Lugo, E. Escobar, M. R. Sánchez & G. Vilaclara., (2000). Water column stratification and its implications in the tropical warm monomictic lake Alchichica, Puebla, Mexico. Verhandlungen der internationalen Vereinigung für theoretische und angewandte Limnologie. 27: 3166–3169.

Alcocer, J. & Escobar E., (1993). Morphometric characteristics of six Mexican coastal lakes related to productivity. Revista de biologia tropical. 41(2): 171-179. SCI 0.107

Al-Kharabsheh A. and Ta'any R. (2003). Influence of urbanization on water quality deterioration during drought periods at South Jordan. Journal of Arid Environments. 53: 619-630.

Allende T. C., Mendoza M. E., López Granados E. M., Morales Manilla LM (2009) Hydrogeographical Regionalisation: An Approach for Evaluating the Effects of Land Cover Change in Watersheds. A Case Study in the Cuitzeo Lake Watershed, Central Mexico. Water Resources Management. 23:2587–2603.

Alvarado-Villanueva R, Salles N., Ortega-Murillo M. R., Némery J,. Gratiot N., Hermandez-Morales R., (2010). Distribucion vertical del fitoplancton, durante la epoca de secas en la presa de Cointzio, Michoacan. SOMPAC 25 (XVI Reunión Nacional y IX Internacional de la Sociedad Mexicana de Planctología A. C. –SOMPAC-), 27-30 April. Lapaz Mexico.

American Public Health Association (APHA) (1995). Standard methods for the examination of water and wastewater. In: Greenburg AE, Clesceri LS, Eaton AD (eds) 20th edn. American Public Health Association, Washington, DC

Anderson, E. R., (1954). Energy budget studies. In: Waterloss investigations: Lake Hefner Studies, Geological Survey Professional Paper (United States). 269: 71-118.

Araujo, M., Costa, M. F, Aureliano, J. T. & Silva, M. A., (2008). Mathematical modelling of hydrodynamics and water quality in a tropical reservoir, northeast Brazil. Brazilian Journal of Aquatic Science And Technology. 12(1):19-30.

Arruda, J. A., Marzolf, G. R., Faulk, R. T., (1983). The role of suspended sediments in the nutrition of zooplankton in turbid reservoirs. Journal of Ecology. 64: 1225-1235.

Arredondo-Figueroa, J. L. & Aguilar C., (1987). Bosquejo histórico de las investigaciones limnológicas realizadas enlagos mexicanos, con especial énfasis en su ictiofauna. In Gómez, S. & V. Arenas (eds), Contribuciones en Hidrobiología. Universidad Nacional Autónoma de México, México: 91–133.

Aspila K.I, Agemian H., Chau A. S. Y., (1976). A semi-automated method for the determination of inorganic, organic and total phosphate in sediments. Analytica chimica acta. 101:187–197.

Avila Garcia P., (2006). Water, society and environment in the history of one Mexican city. Environment and Urbanization. 8: 129-140 doi: 10.1177/0956247806063969.

B

Batalla R. J., (2003). Sediment deficit in rivers caused by dams and instream gravel mining. A review with examples from NE Spain. Cuaternario y Geomorfologiá 17 (3-4): 79-9.

Barros, N.; Cole, J. J.; Tranvik, L. J.; Prairie, Y. T.; Bastviken, D.; Huszar, V. L. M.; Del Giorgio, P. & Roland, F., (2011). Carbon emission from hydroelectric reservoirs linked to reservoir age and latitude. Nature Geoscience, 4: 593-596.

Bansal, M. K., (1976). Nitrification in natural streams. Journal of the Water Pollution Control Federation. 48: 2380-2393.

Bauer, K., Seiler, W., Giehl, H., (1979). CO-produktion höherer pflanzen an natürlichen standorten, Z. Pflanzenphysiol., CAS, Web of Science. 94: 219–230.

Barbour, C. D., (1973). A biogeographical history of Chirostoma (Pisces: Atherinidae): a species flock from the Mexican Plateau. COPEIA 3: 533–556.

Bassols, A., (1977). Recursos Naturales de México. Nuestro Tiempo, México.

Beattie Peter (2010). The Burrill Report. http://www.burrillreport.com/article-the_world%e2%80%99s_tropical_zone_%e2%80%93_rich_beauty_rare_opportunity.html

Beck, M. B. (1987). "Water quality modeling: A review of the analysis of uncertainty," Water Resources Research. 23(8): 1393-1442.

Berrera Camacho G., Bravo Espinosa M., (2009). La planificación del territorio, gestión de recursos o gestión de conflictos. El Caso de Cointzio, Michoacán CONACYT report.

Billen G, Garnier J, Némery J, Sebilo M, Sferratore A, Barles S, Benoit P, Benoît M (2007). A long-term view of nutrient transfers through the Seine river continuum. Science of the Total Environment. 375: 80–97

Bonnet, M. P., Poulin, M., Devaux, J., (2000). Numerical modelling of thermal stratification in a lake reservoir. Methodology and case study. Aquatic Sciences. 62: 105-124.

Boorman D. B. (2003). Climate, Hydrochemistry and Economics of Surface-water Systems (CHESS): Adding a European dimension to the catchment modelling experience developed under LOIS. Science of the Total Environment. 314-316: 411-437.

Bouraoui F., Grizzetti B. (2014). Modelling mitigation options to reduce diffuse nitrogen water pollution from agriculture. Science of the Total Environment 468–469:1267–1277

Bowen, I. S., (1926). The ratio of heat losses by conduction and by evaporation from any water surface. Physical Review. 27: 779-787.

Bosch N. S., Allan J. D., (2008). The influence of impoundments on nutrient budgets in two catchments of Southeastern Michigan. Biogeochemistry. 87:325–338

Bravo-Inclan, L. A., Saldana-Fabela, M. P., Sanchez-Chavez, J. J., (2008). Long-term eutrophication diagnosis of a high altitude body of water, Zimapan Reservoir, Mexico. Water Science and Technology. 57: 1843-1849.

Bravo-Inclán L. A., Olvera-Viascán V., Sánchez-Chávez J. J., Saldaña-Fabela P., Tomasini-Ortiz A. C., (2010). Trophic state assessment in warm-water tropical lakes and reservoirs of the central region of Mexico in Van Bochove EPA, Vanrolleghem PA, Chambers G, Thériault B. Novotná and Burkart MR (eds.) Issues and Solutions to Diffuse Pollution: 14th International Conference of the IWA Diffuse Pollution Specialist Group, DIPCON 2010 Québec CANADA 495pp.

Bravo-Espinosa M, Mendoza ME, Medina-Orozco L, Prat C, García-Oliva F, López-Granados E., (2009). Runoff, soil loss, and nutrient depletion under traditional and alternative cropping systems in the Transmexican Volcanic Belt, Central Mexico. Land Degrad Develop 20(6):640-653.

Burford M. A., Green S. A., Cook A. J., Johnson S. A., Kerr J. G., O'Brien K. R., (2012). Sources and fate of nutrients in a subtropical reservoir. Aquatic Science. 74:179–190 doi 10.1007/s00027-011-0209-4

Burchard, H., and H. Baumert, (1995). On the performance of a mixed-layer model based on the k-ε turbulence model, Journal of Geophysical Research. 100: 8523– 8540.

C

Canfield, D. E., Hoyer M. V., (1988). The eutrophication of Lake Qkeechobee, In G. Redfield (Editor), Lake Reservoire Management. 4: 91-100.

Carlón Allende, T., Mendoza, M. E., (2007). Análisis hidrometeorológico de las estaciones de la cuenca del lago de Cuitzeo, Investigaciones Geográficas, Boletín del Instituto de Geografía, UNAM. 63: 56–76.

Cerro Pelón (Ejido Capulín, Estado de México), (1996). Memorias del 1o. Simposio sobre protección en Areas Naturales Protegidas, 18-20 diciembre. Valle de Bravo. PROFEPA, México.

Conagua, Semarnat. *Estadísticas del Agua en México*. Edición (2007). Conagua. México.

[CNA] Comisión Nacional del Agua, (2008). Estadísticas del Agua en México [Water statistics in Mexico]. México (DF).

[CNA] Comisión Nacional del Agua, (2006). Estadísticas del Agua en México. Secretaría del Medio Ambientey Recursos Naturales, México.

Chacón Torres A., (1993). Lake Pátzcuaro, Mexico: watershed and water quality deterioration in a tropical high-altitude Latin American lake. Lake and Reservoir Management. 8: 37–47.

Chacón-Torres A., Rosas-Monge C., (2008) Water quality characteristics of a high altitude oligotrophic Mexican lake. Aquatic Ecosystem Health & Management. 1: 237–243.

Chanudet, V., Fabre, V., Kaaij. T. V. D., (2012). Application of a three–dimensional hydrodynamic model to the Nam Theun 2 Reservoir (Lao PDR). Journal of Great Lakes Research. 38: 260-269.

Chanudet V., Descloux S., Harby A., Sundt H., Brakstad B. H. H. O., Serça D., Guérin F., (2011). Gross CO_2 and CH_4 emissions from the Nam Ngum and Nam Leuk sub-tropical reservoirs in Lao PDR. Science Total Environnement. 409:5382–5391.

Chávez, M. & G. Vilaclara, (1992). Datos para la regionalización limnológica mexicana. Paper Pres. I Encuentro de Limnólogos Iberoamericanos, Sevilla, August 14–20.

Chen, C. W., Orlob, G. T., (1975). Ecological Simulation of Aquatic Environments, in: Pattern, B. C. (ed.), Systems Analysis and Simulation in Ecology. 3: 476-588.

Chuco T. D., (2003). Dynamic integrated modelling of basic water quality and fate and effect of organic contaminants in rivers, PhD thesis.

Clarke, E. H., Haverkamp ,J. A. & Chapman, W. (1985). Eroding soils: The off-farm impacts. The Conservation Foundation, Washington, D.C.

Cole J. J., Prairie Y. T., Caraco N. F., McDowell W. H., Tranvik L. J., Striegl R. G., Duarte C. M., Kortelainen P., Downing J. A., Middelburg J. J., (2007). Plumbing the global carbon cycle: Integrating inland waters into the terrestrial carbon budget. Ecosystems. 10:172–185.

Collins, C. D., Wlosinski, J. H., (1983). Coefficients for Use in the U.S. Army Corps of Engineers Reservoir Model, CE-QUA-R1. U.S. Army Corps of Engineers, Waterways Experiments Station, Vicksburg, Mississippi.

Conley, D. J., Paerl, H.W., Howarth, R.W., Boesch, D.F., Seitzinger, S.P., Havens, H.E., Lancelot, Ch.,Likens, G.E., (2009). Controlling eutrophication: nitrogen and phosphorus. Science. 223, 114-115.

Correll, D. L., (1998). The Role of Phosphorus in the Eutrophication of Receiving Waters: A Review. Journal of Environment Quality. 27, 261-273.

Cosgrove, William J. and Rijsberman Frank R. (2000). World Water Vision: Making Water Everybody's Business. Eartscan Publications, London.

Covaleda S., Gallardo J. F., Garcıá-Oliva F., Kirchmann H., Prat C., Bravo M., Etchevers J. D., (2011). Land-use effects on the distribution of soil organic carbon within particle-size

fractions of volcanic soils in the Transmexican Volcanic Belt (Mexico). Soil Use and Management. 27:186–194.

Coynel A., Etcheber H., Abril G., Maneux E., Dumas J., Hurtrez J. E., (2005) Contribution of small mountainous rivers to particulate organic carbon input in the Bay of Biscay. Biogeochemistry. 74:151–171.

D

Dang T. H, Coynel A, Orange D, Blanc G, Etcheber H, Le L. A, (2010). Long term monitoring (1960–2008) of the river-sediment transport in the Red River Watershed (Vietnam): temporal variability and dam-reservoir impact. Science Total Environnement. 408:4654–4664.

Dawson J. C. C, Tetzlaff D, Speed M, Hrachowitz M, Soulsby C, (2011). Seasonal controls on DOC dynamics in nested upland catchments in NE Scotland. Hydrological Processes. 25:164 –1658.

De Anda J, Shear H, Maniak U, Riedel G (2011) Phosphates in Lake Chapala, Mexico. Lakes and Reservoirs: Research and Management. 6: 313–321

De Boer, D. H., Froehlich, W., Mizuyama, T., and Pietroniro, A. (2003). Preface, in: Erosion prediction in ungauged basins (PUBs): integrating methods and techniques, de Boer, D. H., Froehlich,W., Mizuyama, T., and Pietroniro, A. (Eds.), Proceedings of the Sapporo Symposium, Dec 2003, The International Association of Hydrological Sciences Publication, 279: V–VII.

Demarty, M., Bastien J., Tremblay A., Hesslein R. H., and Gill R. (2009). Greenhouse gas emissions from boreal reservoirs in Manitoba and Quebec, Canada, Environnement Science Technology. 43(23): 8905–8915, doi:10.1021/es8035658.

Denman, K. L., (2003). Modelling planktonic ecosystems: parameterizing complexity. Progress in Oceanography. 57: 429–452.

Deksissa, T., Meirlaen, J., Ashton, P. & Vanrolleghem, P. (2004). Simplifying dynamic river water quality modelling: A case study of inorganic nitrogen dynamics in the Crocodile River (South Africa). Water Air and Soil Pollution, 155(1-4):303{320. ISSN 0049-6979.

Doan, T. K. P., Wendling, V., Bonnet, M. P., Némery, J., Gratiot, N., (2012). Impact of high turbidity on the hydrodynamic and biogeochemical functioning of tropical reservoirs: The case study of Cointzio, Mexico. 4th International Conference on Estuaries and Coasts, (October). 1: 231–238.

Doan T. K. P., Némery J., Gratiot N., Schmid M., (2013). Eutrophication of turbid tropical reservoirs: Modelling for the case of Cointzio, Mexico. 19th ISEM Conference - Ecological Modelling for Ecosystem Sustainability. Toulouse (France), 28-31 oct.

Doan T. K. P., Némery J., Gratiot N., Schmid M., (2014). Biogeochemical mass balance in the turbid tropical reservoir of Cointzio, Mexico: Field data and modelling approach. European Geosciences UnionGeneral Assembly Vienna, Austria, 27 April – 02 May.

Doan T. K. P., Némery J., Schmid M., Gratiot N.,. Eutrophication of turbid tropical reservoirs: Modelling for the case of Cointzio, Mexico. Ecological Modelling, under review.
Dodds, W. K., (1993). What control levels of dissolved phosphate and ammonium in surface waters? Aquatic Sciences. 55: 132–142.

Dokulil, M. T. (1994). Environmental control of phytoplankton productivity in turbulent turbid systems. Hydrobiologia. 289: 65–72.

Donohue, I., and Molinos, J. G. (2009). Impacts of increased sediment loads on the ecology of lakes. Biological Reviews of the Cambridge Philosophical Society 84: 517–531.

Dos Santos, M.A.; Rosa, L.P.; Sikar, B.; Sikar, E. & Dos Santos, E.O. (2006). Gross greenhouse gas fluxes from hydro-power reservoir compared to thermo-power plants. Energy Policy, 34: 481-488.

Downing, J. A., McClain, M., Twilley, R., Melack, J.M., Elser, J., Rabalais, N. N., Lewis Jr., W., Turner, M., Corredor, R.E., Soto, J., Yanez-Arancibia, D., Kopaska, A., Howarth, J.A.R.W., (1999). The impact of accelerating land–use change on the N-cycle of tropical aquatic ecosystems; Current conditions and projected changes. Biogeochemistry. 46: 109-148.

Dumont, E., Harrison, J. A., Kroeze, C., Bakker, E. J., and Seitzinger, S. P. (2005). Global distribution and sources of dissolved inorganic nitrogen export to the coastal zone: results from a spatially explicit, global model. Global Biogeochemical Cycles. 19(4): GB4S02.

Duff J. H. and Triska F. J., (1990). Denitrification in sediments from hyporheic zone adjacent to a small forest stream. Canadian Journal of Fisheries and Aquatic Sciences. 47:1140-1147.

Duvert C., Gratiot N., Evrard O., Navratil O., Némery J., Prat C., Esteves M., (2010). Drivers of erosion and suspended sediment transport in three headwater catchments. Geomorphology. 123(3-4):243-256.

Duvert, C., Gratiot, N., Némery, J., Burgos, A., Navratil, O., (2011). Sub-daily variability of suspended sediment fluxes in small mountainous catchments – implications for community based river monitoring. Hydrology and Earth System Sciences. 15: 703–713.

E

Etcheber H., Taillez A., Abril G., Garnier J., Servais P., Moatar F., and Commarieu M. V., (2007). Particulate organic carbon in the estuarine turbidity maxima of the Gironde, Loire and Seine estuaries: origin and lability, Hydrobiology. 588: 245–259.

Evrard O., Poulenard J., Némery J., Ayrault S., Gratiot N., Duvert C., Prat C., Lefèvre I., Bonté P., Esteves M., (2013). Tracing sediment sources in a tropical highland catchment of central Mexico by using conventional and alternative fingerprinting methods. Hydrological Processes. 27: 911-922 doi: 10.1002/hyp.9421.

F

Fang, X. and Stefan, H. G. (1996). Long-term lake water temperature and ice cover simulations/measurements. Cold Regions Science and Technology. 24: 289–304.

[FAO] Food and Agriculture Organization, (1998). La Pesca Continental. FAO Orientaciones Técnicas para la Pesca Responsable.

[FAO] Food and Agriculture Organization, (2006). Global Forest Resources Assessment 2005: Progress towards Sustainable Forest Management.

Falkenmark, M. and Lindh. G. (1993). "Water and Economic Development". In P.H. Gleick, ed. Water in Crisis: A Guide to the World's Fresh Water Resources. Oxford Univesity Press, New York, USA. Oxford University Press: 80-91.

Ferrari L., Orozco-Esquivel T., Manea V., Manea M., (2012). The dynamic history of the Trans-Mexican Volcanic Belt and the Mexico subduction zone. Tectonophysics 522–523: 122–149.

Flipo N., Even S., Poulin M., Thery S., Ledoux E., (2007). Modeling nitrate fluxes at the catchment scale using the integrated tool CAWAQS. Science Total Environnement. 375(1-3): 69-79.

Finger, D., Schmid, M., & Wüest, A., (2007). Comparing effects of oligotrophication and upstream hydropower dams on plankton and productivity in perialpine lakes. Water Resources Research. 43:1-18.

Frisk, T., Kaipainen, H., Malve, O., (1999). Modelling phytoplankton dynamics of the eutrophic Lake Võrtsjärv, Estonia, Hydrobiologia. 414: 59-69.

Friedl G., Wüest A., (2002). Disrupting biogeochemical cycles – Consequences of damming. Aquatic Science. 64:55-65.

G

Gardner W. S., Cavaletto J. F., Bootsma, H. A, Lavrentyev P. J., and Troncone F. (1998). Nitrogen cycling rates and light effects in tropical Lake Maracaibo, Venezuela. Limnology and Oceanography. 43: 1814-1825.

Garnier, J., Blanc, P., Benest, D., (1989). Estimating a Carbon/Chlorophyll ratio in Nannoplankton (Creteil Lake, S-E Paris, France), Water Resources Bulletin. 25: 751-754.

Garnier J., Leporcq B., Sanchez N. & Philippon X., (1999). Biogeochemical mass-balances (C, N, P, Si) in three large reservoirs of the Seine Basin (France). Biogeochemistry. 47:119–146.

Garnier, J., Némery, J., Billen, G., Théry, S., (2005). Nutrient dynamics and control of eutrophication in the Marne River system: Modelling the role of exchangeable phosphorus. Journal of Hydrology. 304: 397-412.

Gautam, A. P., Webb, E., Shivakotia, G. P., Zoebisch, M. A., (2003). Land use dynamics and landscape change pattern in a mountain watershed in Nepal. Agriculture, Ecosystems and Environment. 99: 83–96.

García, M. A., (1982). Los recursos hidraúlicos. In López, M. (ed.), El Medio Ambiente en México: Temas, Problemas y Alternativas. Fondo de Cultura Económica, México. 92–109.

García, E., (1988). Modificaciones al Sistema de Clasificación Climática de Köppen. P. imprenta, México.

García-Calderón, J. L. & G. De la Lanza, (2002). Las aguas Epicontinentales de México. In García-Calderón, J. L. & G. De la Lanza (eds), Lagos y Presas de México. AGT Editor, Mexico SA. 5–34.

Gächter, R. and Wehrli, B. (1998). Ten years of artificial mixing and oxygenation: No effect on the internal phosphorus loading of two eutrophic lakes. Environnemental Science & Technology. 32: 3659–3665.

Giles, J. (2006). Methane quashes green credentials of hydropower. Nature 444(7119): 524-525.

Gloor, M., Wüest A., and Imboden D., (2000). Dynamics of mixed bottom boundary layers in a stratified, natural water basin, Journal of Geophysical Research. 105: 8629–8646.

Goudsmit, G.-H., Burchard, H., Peeters, F., Wüest, A., (2002). Application of k-ε turbulence models to enclosed basins: The role of internal seiches. Journal of Geophysical Research. 107: 3230-3243.

Gratiot, N., Duvert, C., Collet, L., Vinson, D., (2010). Increase in surface runoff in the central mountains of Mexico: lessons from the past and predictive scenario for the next century, Hydrology and Earth System Sciences. 14: 291–300.

Grayson, R. B., and Blöschl G., (2000), Summary of pattern comparison and concluding remarks, in Spatial Patterns in Catchment Hydrology: Observations and Modeling, Grayson R. B., Blöschl G. (eds). Cambridge University Press: Cambridge, UK; 355–367.

Great Lakes Water Quality Agreement | The Clean Water Act | Great Lakes | US EPA (1978).[On line].
Available: http://www.epa.gov/greatlakes/glwqa/1978/annex.html.

Guérin F., Abril G., Richard S., Burban B., Reynouard C., Seyler P., Delmas R. (2006). Methane and carbon dioxide emissions from tropical reservoirs: significance of downstream rivers. Geophysical Research Letters. 33:L21407. doi:10.1029/2006GL027929.

Guérin F., Abril G., de Junet A., Bonnet M. P. (2008). Anaerobic decomposition of tropical soils and plant material: implication for the CO_2 and CH_4 budget of the Petit Saut Reservoir. Applied Geochemistry. 23:2272–83.

Guenther, M. & Bozelli, R., (2004). Effects of inorganic turbidity on the phytoplankton of an Amazonian Lake impacted by bauxite tailings. Hydrobiologia 511: 151–159.

Gupta, H., Kao, S.J., Dai, M. (2012). The role of mega dams in reducing sediment fluxes: A case study of large Asian rivers. Journal of Hydrology. 464–465: 447–458

H

Hambright, K. D. and Zohary T. (2000). Phytoplankton species diversity control through competitive exclusion and physical disturbances. Limnology and Oceanography. 45: 110-122.

Hamilton, D. P., Schladow, S. G., (1997). Prediction of water quality in lakes and reservoirs. Part I - Model description. Ecological Modelling. 96: 91–110.

Harrison J. A., Maranger R. J., Alexander R. B., Giblin A. E., Jacinthe P. A., Mayorga E., Seitzinger S. P., Sobota D. J., Wollheim W. M. (2009). The regional and global significance of nitrogen removal in lakes and reservoirs. Biogeochemistry. 93:143–157.

Hart, B. T., Dok, W. V., & Djuangsih, N. (2002). Nutrient budget for Saguling reservoir, West Java Indonesia. Water Research, 36: 2152–2160.

Henderson–Sellers B., (1986). Calculating the surface energy balance for lake and reservoir modeling: a review. Reviews of Geophysics. 24: 625–649.

Henry, R., Santos, A. A. N. & Camargo, Y. R., (1999). Transporte de sólidos suspensos, N e P Total pelos Rios Paranapanema e Taquari e uma avaliação de sua exportação na Represa de Jurumirim (São Paulo, Brasil). In: Henry, R. (ed.) Ecologia de reservatórios: estrutura, função e aspectos sociais. FAPESP, FUNDIBIO, Botucatu. p.687-710.

Howarth R. W., Marino R. and Cole. J. J. (1988). Nitrogen fixation in freshwater, estuarine, and marine ecosystems. 1. Rates and importance. Limnology and Oceanography. 33: 669–687.

Holas J., Holas M. & Chour V., (1999). Pollution by phosphorus and nitrogen in water streams feeding the Zelivka drinking water reservoir. Water Science Technology. 39:207-214.

Holm-Hansen, O., Riemann, B., (1978). Chlorophyll a determination: improvements in methodology. Oikos. 30: 438-447.

Hope D, Billett M. F., Cresser M. S. (1997). Exports of organic carbon in two river systems in NE Scotland. Journal of Hydrology.193: 61–82.

Hupfer, M., Gächter, R., Giovanoli, R., (1995). Transformation of phosphorus species in settling seston and during early sediment diagenesis. Aquatic Sciences. 57: 305–324.

Hutchinson, G. E., (1975). A Treatise on Limnology, Vol. 1: Geography, Physics and Chemistry. John Wiley, New York, USA.

I

Imboden, D. M. & W¨uest, A., (1995), Mixing mechanisms in lakes, in A. Lerman, D. M. Imboden & J. R. Gateds, 'Physics and Chemistry of Lakes', Springer Verlag, pp. 83–138.

INEGI (Instituto Nacional de Estadística, Geografía e Informática), (1995). Estadísticas del Medio Ambiente. México.

INEGI (Instituto Nacional de Estadística, Geografía e Informaticá), (1996). Anuario Estadístico del Estado de Mexico. [Anuario statistics of the State of Mexico]. México. Spanish.

INEGI (Instituto Nacional de Estadística, Geografía e Informaticá), (2006): Conteo de Población y Vivienda, Resultados definitivos, Sistema Nacional de Información Estadística y Geografica, México.

J

Jensen, H. S., Kristensen P., Jeppesen E., and Skytthe A. (1992). Iron: phosphorus ratio in surface sediment as an indicator of phosphate release from aerobic sediments in shallow lakes. Hydrobiologia 235/236: 731–743.

Jørgensen, S. E (ed.) (1979). Handbook of Environmental data and Ecological Parameters. International Society for Ecological Modelling.

Jørgensen S. E., Jorgensen, L. A., Nielsen, S. N., (1991). Handbook of Ecological Parameters and Ecotoxicology, Elsevier.

Jørgensen, S.E., Nielsen, S.N., Mejer, 1995. Emergy, environ, exergy and ecological modelling. Ecological Modellling. 77, 99–109.

Jørgensen, S. E., Ray, S., Berec, L., Straskraba, M., (2002). Improved calibration of an eutrophication model by use of the size variation due to succession. Ecological Modelling. 153: 269–277.

Jørgensen, S. E & Bendoricchio, G. (2001). Fundametal Ecological Modelling. Elsevier

K

Kantoush, S. A., and T. Sumi, A. Kubota, and T. Suzuki., (2010). The impacts of sediment replenishment below dams on flow behavior and bed morphology of river channel and river mouth. First International Conference, Alexandria, Egypt, 6-10 March.

Kalff, J. and Watson K., (1986). Phytoplankton and its dynamics in two tropical lakes. A tropical and temperate zone comparision. Hydrobiologia 138: 161-176.

Kennedy R. H., Tundisi J. G., Straškrábová V., Lind O. T., Hejzlar J., (2003). Reservoirs and the limnologist's growing role in sustainable water resource management Hydrobiology. 504: xi–xii.

Kemenes, A.; Forsberg, B. R. & Melack, J. M. (2007). Methane release below a tropical hydroelectric dam. Geophysical Research Letters. 34: 0094-8276

Kiirikki, M., Inkala, A., Kuosa, H., Pitkänen, H., Kuusisto, M., and Sarkkula, J., (2001). Evaluating the effects of nutrient load reductions on the biomass of toxic nitrogen-fixing cyanobacteria in the Gulf of Finland, Baltic Sea, Boreal Environmental Research . 6: 131-146.

Kondolf, G. M., (1997). Hungry water: Effect of dams and gravel mining on river channels. Environmental Management, 21 (4): 533-551.

Kunz, M. J., Anselmetti, F. S., Wüest A., Wehrli B., Vollenweider A., Thuring S., and Senn D. B. (2011). Sediment accumulation and carbon, nitrogen, and phosphorus deposition in the large tropical reservoir Lake Kariba (Zambia/Zimbabwe). Journal of Geophysical Research. 116: G03003. doi: 10.1029/2010JG001538.

Kunz, M. J., Wüest, A., Wehrli, B., Landert, J., Senn, D. B., (2011). Impact of a large tropical reservoir on riverine transport of sediment, carbon, and nutrients to downstream wetlands. Water Resources Research. 47: 1-16.

L

Lal, R. (2001). Soil degradation by erosion. Land Degradation & Development 12 : 519–539.

Laws E. A. (1993). Aquatic pollution: An introductory Text. 2nd edition, John Wiley and Sons, INC, New York.

Lewis Jr W. M (1974). Primary production in the plankton community of a tropical lake. Ecological Monographs.

Lewis Jr W. M. (1987). Tropical limnology. Annual Review of Ecology and Systematics. 18: 159-184.

Lewis Jr W. M. (1996). Tropical lakes: how latitude makes a difference. Perspectives in tropical limnology. 43-64.

Lewis Jr W. M. (2000). Basis for the protection and management of tropical lakes. Lake and Reservoir Management. 5: 35–48.

Lehner B., Döll P., (2004) Development and validation of a global database of lakes reservoirs and wetlands. Journal of Hydrology. 296:1–22.

Lewis W. M., (2002). Estimation of background nitrogen yields for North America by use of benchmark watersheds. Biogeochemistry 57–58: 375–385.

Livingstone, D. M., and Imboden D. M. (1989), Annual heat balance and equilibrium temperature of Lake Aegeri, Switzerland, Aquatic Science. 51(4), 351–369, doi:10.1007/BF00877177

Ligon, F. K., Dietrich W. E. and Trush. W. J., (1995). Downstream ecological effects of dams: a geomorphic perspective, Bioscience. 45(3): 183-192.

Lind, O. T., Doyle, R., Vodopich, D. S., Trotter, B. G., Limon, J. G. and Davalos-Lind, L. (1992). Clay turbidity: regulation of phytoplankton production in a large, nutrient-rich tropical lake. Limnology and Oceanography. 37(3): 549-565.

López López E., Dávalos-Lind L., (1998). Algal growth potential and nutrient limitation in a tropical river-reservoir system of the Central Plateau, Mexico. Aquatic Ecosystem Health & Management. 1:345-351.

López-García, J., Manzo-Delgado, L. L. & Nava-Soria, P. (1996). Capacidad de carga, ecoturismo y desarrollo sustentable en la Reserva Especial de la Biósfera "Mariposa Monarca", Santuario.

López-Granados E., Mendoza M. E., González D. I., (2013) Linking geomorphologic knowledge, RS and GIS techniques for analyzing land cover and land use change: a multitemporal study in the Cointzio watershed, Mexico. Ambi Água –An Interdisciplinary Journal of Applied Science 8(1):18-37 doi: 10.4136/ambi-agua.956.

López-Granados, E. M., Bocco, G., Mendoza, M. E., Velázquez, A., and Aguirre-Rivera, J. R. (2006): Peasant emigration and land-use change at the watershed level: A GIS-based approach in Central Mexico, Agricultural Systems. 90: 62–78.

López-Granados, E. M., Bocco, G., and Mendoza, M. E. (2001): Predicción del cambio de cobertura y uso del suelo, El caso de la ciudad de Morelia, Investigaciones Geográficas, Boletín del Instituto de Geografía, UNAM. 45: 56–76.

M

Martins, G., Ribeiro, D. C., Pacheco, D., Cruz, J. V., Cunha, R., Gonçalves, V., Nogueira, R., (2008). Prospective scenarios for water quality and ecological status in Lake Sete Cidades (Portugal): The integration of mathematical modelling in decision processes. Applied Geochemistry. 23: 2171–2181.

Matzinger, A., Pieters, R., Ashley, K. I., Lawrence, G. A., Wüest, A., (2007a). Effects of impoundment on nutrient availability and productivity in lakes, Limnology Oceanography. 52: 2629–2640.

Matzinger, A., Schmid, M., Sturm, M., Wüest, A., (2007b). Eutrophication of ancient Lake Ohrid: Global warming amplifies detrimental effects of increased nutrient inputs, Limnology Oceanography. 52: 338–353.

Matzinger, A., Schmid, M., Sturm, M., Wüest, A., (2007). Eutrophication of ancient Lake Ohrid: Global warming amplifies detrimental effects of increased nutrient inputs, Limnology Oceanography. 52: 338–353.

Maneux E., Probst J. L., Veyssy E., Etcheber H. (2001) Assessment of dam trapping efficiency from water residence time: application to fluvial sediment transport in the Adour, Dordogne and Garonne river basins (France). Water Resources Research. 37: 801–811.

Mendoza M, Granado E. L., Gratiot N, Arnaud F, Magand O, Prat C, Esteves M. (2013). Relationships between land cover, land use change and erosion-sedimentation processes at

the watershed level: A multitemporal study in the Cointzio watershed, Mexico. 8th IAG conference on Geomorphology 27-31 August. Paris, France.

Mendoza, M. E. and Lopez-Granados, E. M. (2007). Caracterizacíon f ísico-geográfica de la subcuenca de Cointzio, Michoacan: informacíon básica para el manejo integrado de cuencas, in: Bases Metodologicas para el Manejo Integrado de Cuencas Hidrológicas, edited by: Sánchez- Brito, C., Fragoso-Tirado, E., and Bravo-Espinoza, M., Libro Técnico INIFAP.

Mengis, M., Gächter, R., Wehrli, B., (1997). Nitrogen elimination in two deep eutrophic lakes. Limnology Oceanography. 42: 1530–1543.

Mijangos Carro M., Izurieta Dávila J., Gómez Balandra A., López R. H., Huerto Delgadillo R., Sánchez Chávez J., Bravo Inclán L., (2008) Importance of diffuse pollution control in the Patzcuaro Lake Basin in Mexico. Water Technology. 58(11):2179–2186 doi:10.2166/wst.2008.820

Mieleitner, J., Reichert, P., (2006). Analysis of the transferability of a biogeochemical lake model to lakes of different trophic state. Ecological Modelling. 194: 49–61.

Mieleitner, J., Reichert P., (2008). Modelling functional groups of phytoplankton in three lakes of different trophic state. Ecological Modelling. 211: 279-291.

Morán, D. J., (1986). Breve revisión sobre la evolución tectónicade México. Revista de la Unión Geofísica Mexicana. 25: 9–38.

Morales, D. (2007). Michoacán ha perdido 70% de aguas superficiales en los últimos 100 anos, La Jornada Michoacán, 25 November.

Mulder, T., & Alexander, J. (2001). The physical character of subaqueous sedimentary density currents and their deposits. Sedimentology. 48: 269–299.

Murphy J., Riley J. P., (1962). A modified single solution method for the determination of phosphate in natural waters. Analytica Chimica Acta. 27: 31– 36.

N

Nelson, S. A. & Sánchez-Rubio G., (1986). Trans Mexican Volcanic Belt Field Guide. Volcanology Division of the Geological Association of Canada & Instituto de Geología, Universidad Nacional Autónoma de México, México.

Newcombe, C. P. and MacDonald, D. D. (1991). Effects of suspended sediments of aquatic ecosystems. North American Journal of Fisheries Management. 11: 72-82.

Némery J, Garnier J, (2007). Origin and fate of phosphorus in the Seine watershed (France): The agricultural and hydrographic P budget. JGR- Biogeosciences. 112: G03012, doi: 10.1029/2006JG000331.

Némery, J., Alvarado, R., Gratiot, N., Duvert, C., Mahé, F., Duwig, C., Bonnet, M. P., Prat, C., Esteves, M., (2009). Abstract number: H53D-0958. Biogeochemical characterization of

the Cointzio reservoir (Morelia, Mexico) and identification of a watershed-dependent cycling of nutrients. AGU Fall Meeting, San Francisco. 14-18 December.

Némery, J., Gratiot, N., Doan, T. K. P., Duvert, C., Alvarado, R.,. Carbon, phosphorus, nitrogen and sediment retention in a turbid tropical reservoir. Aquatic Sciences. Will be submitted.

Némery J., Mano V., Coynel A., Etcheber H., Moatar F., Meybeck M., Belleudy P. & Poirel A., (2013). Carbon and suspended sediment transport in an impounded alpine river (Isère, France). Hydrological Processes. 27: 2498-2508; DOI: 10.1002/hyp.9387.

Nurnberg, G. K. (1984). The prediction of internal phosphorus load in lakes with anoxic hypolimnia. Limnololy & Oceanography. 29: 111–124.

O

O'Connor, D. J., Mancini, J. L., Guerriero, J. R., (1981). Evaluation of Factors Influencing the Temporal Variation of dissolved oxygen in the New York Bight, PHASE II. Manhattan College, Bronx, New York.

Octavio, K.A., Jirka, G.H. and Harleman, D.R.F., (1977). Vertical transport mechanisms in lakes and reservoirs. Techn. Rep. 227, Ralph M. Parsons Laboratory, Mass. Inst. Technology, Cambridge, MA, 131pp.

Omlin, M., Reichert, P., Forster, R., (2001a). Biogeochemical model of Lake Zürich: Model equations and results. Ecological Modelling. 141: 77–103.

Omlin, M., Brun, R., Reichert, P., (2001b). Biogeochemical model of Lake Zürich: sensitivity, identifiability and uncertainty analysis. Ecological Modelling. 141: 105–123.

Orlob (1983). Mathematical modelling of water quality: Streams, lakes, and reservoirs. Wiley (Chichester West Sussex and New York). 518 pp.

Olvera-Viascán, V., Bravo-Inclán, L., Sánchez-Chávez, J., (1998). Aquatic ecology and management assessment in Valle de Bravo reservoir and its watershed. Aquatic Ecosystem Health & Management. 1: 277–290.

Ooapas (2007). Organismo Operador de Agua Potable de Morelia. Evaluation socioeconomic del saneamiento de aguas residuals de Morelia (http://www.shcp.gob.mx/EGRESOS/ppi/Proyec_hidraulicos/saneamiento_morelia.pdf).

Ortiz-Ávila, T. (2009): Estrategia interinstitucional para el quehacer ambiental municipal en Michoacan: experiencias y propuestas de la Unidad de Vinculación del CIEco, Conference, Centro de Investigaciones en Ecosistemas, UNAM Campus Morelia, Mexico, April.

P

Padisàk, J. (1994). Identification of relevant time scales in non-equilibrium community dynamics. Conclusions from phytoplankton surveys. New Zealand. Journal of Ecology. 18: 169-176.

Parkhill,K. L. & Gulliver, J. S., (2002). Effect of inorganic sediment on whole-stream productivity. Hydrobiologia. 472: 5–17.

Parfitt R. L., Clayden B. (1991). Andisols - the development of a new order in Soil Taxonomy. Geoderma. 49: 181-198.

Park H. K, Byeon M. S., Shin Y. N., Jung D. I., (2009). Sources and spatial and temporal characteristics of organic carbon in two large reservoirs with contrasting hydrologic characteristics. Water Resources Research. 45:W11418.

Petts, G. E., (1984). Impounded River: Perspectives for Ecological Management, John Wiley & Sons, Chichester, United Kingdom, 326pp.

Petzold, L., (1983). A description of DASSL: A differential/algebraic system solver. In:Stepleman, R.E. (Ed.), Scientific Computing. IMACS/North-Holland, Amsterdam, pp. 65–68.

Pinto-Coelho R. M. (2000). Fundamentos em Ecologia. Artes Médicas, Porto Alegre. 252p.

Pimentel D., Harvey C., Resosudarmo P., Sinclair K., Kurz D., McNair M., Crist S., Shpritz L., Fitton L., Saffouri R., et Blair R. (1995). Environmental and Economic Costs of Soil Erosion and Conservation Benefits. Science. 267(520): 1117-1123, févr.

Poulin, M., Bonnet, M.-P., (2004). Dylem-1D: a 1D physical and biochemical model for planktonic succession, nutrients and oxygen cycling. Application to a hyper-eutrophic, Ecological Modelling. 180: 317-344.

Poulenard, J., Podwojewski, P., Janeau, J. L., and Collinet, J. (2001): Runoff and soil erosion under rainfall simulation of Andisols from the Ecuadorian Páramo: effect of tillage and burning, Catena. 45: 185–207.

Poff, N. L., Allan J. D., Bain M. B., Karr J. R., Prestegaard K. L., Richter B. D., Sparks R. E., and Stromberg J. C., (1997). The natural flow regime: A paradigm for river conservation and restoration, Bioscience. 47(11): 769-784.

Prairie, Y. T., de Montigny, C., Del Giorgio, P. A., (2001). Anaerobic phosphorus release from sediments: a paradigm revisited. Verh. Int. Ver. Limnol. 27: 4013–4020.

Q

Quinton J. N., Govers G., Van Oost K., Bardgett R., (2010). The impact of agricultural soil erosion on biogeochemical cycling. Nature Geosci 3: 311-314.

R

Ramírez-Zierold J. A., Merino-Ibarra M., Monroy-Ríos E., Olson M., Castillo F. S., Gallegos M. E., Vilaclara G. (2010). Changing water, phosphorus and nitrogen budgets for Valle de Bravo reservoir, water supply for Mexico City Metropolitan Area. Lake Reservoir Management. 26:23–34.

Ramírez-Olvera MA, Díaz-Argüero M, López-López E (2004) Planktonic Crustacean Assemblages in a System of three reservoirs in the Mexican Central Plateau: Seasonal and Spatial Patterns. Journal of Freshwater Ecology.19(1):25-34.

Rãdoane M., Rãdoane N., (2005). Dams, sediment sources and reservoir silting in Romania. Science of the Total Environment. 71(1-2):112–125.

Redfield, A. C., Ketchum, B., Richars, F., (1966). The influence of organism on the composition of seawater. In: Hill, M. (Ed.), The Sea, vol. 2. Wiley Interscience, New York.

Ryding, S.O., Rast. W., (1989). The Control of Eutrophication of Lakes and Reservoirs. UNESCO and Parthenon Publishing Group, Paris, pp. 38-49.

Regnier P., Friedlingstein P., Ciais, P., Mackenzie F. T., Gruber N., Janssens I. A., Laruelle G. G., Lauerwald R., Luyssaert S., Andersson A. J., Arndt S., Arnosti C., Borges A. V., Dale A. W., Gallego-Sala A., Goddéris Y., Goossens N., Hartmann J., Heinze C., Ilyina T., Joos F., LaRowe D. E., Leifeld J., Meysman F. J. R., Munhoven G., Raymond P. A., Spahni R., Suntharalingam, Thullner M., (2013). Anthropogenic perturbation of the carbon fluxes from land to ocean. Nature Geosci 6: doi: 10.1038/NGEO1830.

Reichert, P., (1994). AQUASIM – a tool for simulation and data analysis of aquatic systems. Water Science and Technology. 30: 21–30.

Reichert, P., (1998). AQUASIM 2.0 — User Manual. Technica report, Swiss Federal Institute for Environmental Scienc and Technology (EAWAG), Dubendorf, Switzerland.

Reichert, P., et al, (2001). River water quality model no. 1 (RWQM1): II. Biochemical process equations. Water Science Technol. 43, 11–30.

Robertson, R. A. & Colletti, J. P. (1994). Off-site impacts of soil erosion on recreation: the case of Lake Rock Reservoir in central Iowa. Journal of Soil and Water Conservation. 49: 576–581.

Robertson G. P., Coleman D. C., Bledsoe C. S., Sollins P. (1999). Standard soil methods for long-term ecological research. Oxford University Press: New York Oxford; 480p.

Rodriguez, A., Final Report for 2001 activity. Memorandum of Understanding ECT/FG/MMM/97.012, July.

Rodi, W., (1984). Turbulence models and their application in hydrodynamics—A state of the art review, University of Karlsruhe, Karlsruhe, Germany.

Roland, F.; Vidal, L. O.; Pacheco, F. S.; Barros, N. O.; Assireu, A.; Ometto, J.; Cimbleris, A. C. P. & Cole, J. J. (2010). Variability of carbon dioxide flux from tropical (Cerrado) hydroelectric reservoirs. Aquatic Sciences, 72(3): 283-293.

Rosas I, Velasco A, Belmont R, Baez A, Martínez A (1993) The algal community as an indicator of trophic status in Lake Patzcuaro, Mexico. Environmental Pollution. 80: 255–264.

Rubio, M., (1998). Dinámica del cambio de la cobertura y del uso de los suelos en la microcuenca de Atécuaro (Michoacán, México), Una perspectiva desde las ciencias ambientales, PhD thesis, Univ. Michoacana de San Nicolás de Hidalgo, Univ. Aut. Barcelona, 253 pp.

S

Salas H. J., Martino P. (1991). A simplified phosphorus trophic state model for warm-water tropical lakes. Water Research. 25(3): 341–350.

Scavia, D., Park, R. A., (1976). Documentation of Selected Constructs and Parameter Values in the Aquatic Model CLEANER. Ecological Modelling. 2: 33-58.

Schmid M., Andreas L., Wüest A., Halbwachs M., Tanyileke G. (2003). Development and sensitivity analysis of a model for assessing stratification and safety of Lake Nyos during artificial degassing. Ocean Dynamics. 53: 288–301 DOI 10.1007/s10236-003-0032-0.

Schwilch G., Hessel R., Verzandvoort S. (Eds) (2012). DESIRE for greener land. Options for sustainable land management in drylands. Publishers University of Bern - CDE, Alterra, Wageningen UR and ISRIC - World Soil Information WOCATFAO. pp 250.

Schindler D. W. (1977). Evolution of phosphorus limitation in lakes: Natural mechanisms compensate for deficiences of nitrogen and carbon in eutrophied lakes. Science. 195: 260-262.

Seitzinger S. P., Mayorga E., Kroeze C., Bouwman A. F., Beusen A. H. W., Billen G., Van Drecht G., Dumont E., Fekete B. M., Garnier J., and Harrison J. A. (2010). Global river nutrient export: A scenario analysis of past and future trend. Global Biogeochemical Cycles. 24: 1-16.

Sepulveda-Jauregui A., Hoyos-Santillan J., Gutierrez-Mendieta F. J., Torres-Alvarado R., Dendooven L., Thalasso F., (2013). The impact of anthropogenic pollution on limnological characteristics of a subtropical highland reservoir "Lago de Guadalupe", Mexico. Knowledge and management of aquatic ecosystems. 410:04 doi: 10.1051/kmae/2013059.

SEDESOL (Secretaría de Desarrollo Social), (1993). México. Informe de la Situación Actual General en Materia de Equilibrio Ecológico y Protección al Ambiente 1991–1992. Secretaría de Desarrollo Social, Instituto Nacional de Ecología, México.

SEMARNAT (Secretaría de Medio Ambiente y Recursos Naturales), (2002). Norma Oficial Mexicana NOM-059-ECOL-2001, Protección Ambiental-Especies Nativas de México de Flora y Fauna Silvestres – Categorías de Riesgo y Especificaciones para su Inclusión, Exclusióno Cambio – Lista de Especies en Riesgo. Diario Oficial, 6 de Marzo, 2002.

Sherman B. S., Ford P. F., Hatton P., Whittington J., Green D., Baldwin D., Oliver R. L., Shiel R., van Berkel J., Beckett R., Grey L., Maher W., (2001). The Chaffey Dam Story – Final report to the CRC for Freshwater Ecology. Canberra, Australia.

Smith, D. J., (1978). Water quality for River –Reservoir Systems (technical report). U.S Army Corps of Engineers (Hydrologic Engineering Center), Davis, CA.

SRH (Secretaría de Recursos Hidraúlicos), (1976). Atlas del Agua de la República Mexicana. México.

St. Louis, V. L.; Kelly, C. A.; Duchemin, E.; Rudd, J. W. M. and Rosenberg, D. M. (2000). Reservoir surfaces as sources of greenhouse gases to the atmosphere: A global estimate. BioScience. 50(9): 766-775.

Straskraba M., Dostalkova I., Heijzlar J. & Vyhnalek V., (1995). The effect of reservoirs on phosphorus concentration. Internationale Revue der gesamten Hydrobiologie. 80:403-413.

Sugimura Y. and Suzuki Y. (1988). A high temperature catalytic oxidation method for non - volatile dissolved organic carbon in seawater by direct injection of a liquid sample. Marine Chemistry. 24: 105-131.

Susperregui A. S. (2008). Caractérisation hydro-sédimentaire des retenues de Cointzio et d'Umécuaro (Michoacán, Mexique) comme indicateur du fonctionnement érosif du bassin versant. Phd Thesis Grenoble University. pp 289.

Susperregui A. S., Gratiot N., Esteves M., Prat C., (2009). A preliminary hydrosedimentary view of a highly turbid tropical, manmade lake: Cointzio Reservoir (Michoacán, Mexico). Lakes and Reservoirs: Research and Management. 14: 31–39.

Svendsen L. M., Redsdorf A., Nørnberg P., (1993). Comparison of methods for analysis of organic and inorganic phosphorus in river sediment. Water Research. 27:77– 83.

Syvitski J. P. M., Vörösmarty J. V., Kettner A. J., Green P., (2005). Impacts of humans on the load of terrestrial sediments to the global coastal ocean. Science. 308: 376–380.

Sweers, H. E., (1976). A nomogram to estimate the heat-exchange coefficient at the air-water interface as a function of wind speed and temperature; a critical survey of some literature. Journal of Hydrology. 30: 375-401.

T

Teodoru, C. R., Prairie Y. T., and del Giorgio P. A. (2011), Spatial heterogeneity of surface CO2 fluxes in a newly created Eastmain-1 reservoir in northern Québec, Canada, Ecosystems, 14(1): 28–46, doi:10.1007/s10021-010-9393-7.

Thomaz, S. M., Bini, L. M., (2003). Ecologia e Maneojo de Macrófitas Aquáticas, Editora da Universidade Estadual de Maringá, 342 pp.

Thouvenot M, Billen G, Garnier J (2007) Modelling nutrient exchange at the sediment–water interface of river systems. Journal of Hydrology. 341:55–78.

Thornton, K. W., (1990). Perspectives in reservoir limnology. In Thornton, K. W., B. L. Kimmel & F. E. Payne (eds), Reservoir Limnology: Ecological Perspectives. Wiley, New York: 1–13.

Toledo, V. M., Carabias J., Toledo C. & González-Pacheco, C. (1989). La Producción Rural en México: Alternativas Ecológicas. Prensas de Ciencias, UNAM y Fundación Universo Ventiuno. Colección Medio Ambiente 6, México.

Torres-Orozco, R. E., Jiménez-Sierra C. and Pérez-Rojas A. (1996). Some limnological features of three lakes from Mexican neotropics, Hydrobiologia, 341: 91-99.

Torres I. C, Resck R. P, Pinto-Coelho R. M., (2007). Mass balance estimation of nitrogen, carbon, phosphorus and total suspended solids in the urban eutrophic, Pampulha reservoir, Brazil. Acta Limnologica Brasiliensia. 19:79-91.

Tranvik L. J., Downing J. A., Cotner J. B., Loiselle S. A., Striegl R. G., Ballatore T. J., Dillon P., Finlay K., Fortino K., Knoll L. B., Kortelainen P. L., Kutser T., Larsen S., Laurion I., Leech D. M., McCallister S. L., McKnight D. M., Melack J. M., Overholt E., Porter J. A., Prairie Y., Renwick W. H., Roland F., Sherman B. S., Schindler D. W., Sobek S., Tremblay A., Vanni M. J., Verschoor A. M., von Wachenfeldt E., Weyhenmeyera G. A., (2009). Lakes and reservoirs as regulators of carbon cycling and climate. Limnology Oceanography. 54(6): 2298–2314.

Tundisi, J. G., (2003). Água no Século XXI: enfrentando a escassez. São Carlos: Rima; IIE, 248 pp in Restoration and Management of Tropical Eutrophic Lakes, Mallapureddi Vikram Reddy (ed.). Science Publishers, Inc, 271-274.

U

Ujang, Z. and Buckley, C. (2002). Promoting sustainable industry through Waste Minimisation Club. Water Science and Technology. 46(9), 1–10.

USEPA (2000). National Water Quality Inventory. Report EPA-841-R-02-001, EPA Office of Water, Washington D.C.

Ulrich, M., (1991). Modeling of chemicals in lakes—Development and application of user-friendly simulation software (MASAS and CHEMSEE) on personal computers, Ph.D. thesis, Eidgenössische Technische Hochschule Zürich.

V

Vaccari D. A., (2009). Phosphorus famine: The threat to our food supply. Scientific American, June, p. 36.

Velázquez, L. & Ordaz, A., (1992). Provincias hidrogeológicas de México. Ingeniería Hidraúlica en México. 7: 36–55.

Venegas, S. S., Herrera J. J. & Maciel, R. (1985). Algunas características de la Faja Volcánica Mexicana y de susrecursos geotérmicos. Geofísica Internacional. 24: 47–81.

Verhoff F. H., Yaksich S. M., Melfi D. A., (1980). River nutrient and chemical transport estimates. Environmental and Engineering Geology Division. 10: 591–608.

Vidal, J., Valero M. & Rangel, R. (1985). Frontera Acuícola, Comisión del Plan Nacional Hidraúlico. SARH, México.

Vörösmarty J. V., Meybeck M., Fekete B., Sharma K., Green P., Syvitski J. P. M., (2003) Anthropogenic sediment retention: major global impact from registered river impoundments. Global and Planetary Change. 39(1-2): 169–190.

Von Sperling, E., Sousa, A. D., (2007). Long-term monitoring and proposed diffuse pollution control of a tropical reservoir. Water Science and Technology. 55: 161-166.

Y

Young W. J., Marston F. M. & Davis J. R., (1996). Nutrient exports and land use in Australian catchments. Journal of Environmental Management. 47:165-183.

W

Walling D. E., Webb W., (1985). Estimating the discharge of contaminants to coastal waters by rivers: some cautionary comments. Marine Pollution Bulletin. 16(12): 488 – 492.

Walling, D. E., Owens, P. N., Carter, J., Leeks, G. J. L., Lewis, S., Meharg, A. A. & Wright , J. (2003). Storage of sediment-associated nutrients and contaminants in river channel and floodplain systems. Applied Geochemistry. 18: 195–220.

Water Framework Directive, 2000/60/EC (2000). Establishing a framework for community action in the field of water policy (OJ (2000) L327/1).

Whalen, S. C., Chalfant, B. B., Fischer, E. N., Fortino, K. A. & Hershey, A. E. (2006). Comparative influence of resuspended glacial sediment on physicochemical characteristics and primary production in two arctic lakes. Aquatic Sciences. 68, 65–77.

Williams, G. P., and Wolman, M. G. (1984). Downstream effects of dams on alluvial rivers, Geological Survey Professional Paper. 1286, 83 pp.

Wilcock, P. R., Barta, A. F., Shea, C. C. et al., (1996). Observations of flow and sediment entrainment on a large gravel-bed river, Water Resources Research. 32: 2897-2910.

Welch, E. B. and Jacoby J. M., (2004). Pollutant Effects in Freshwater, Applied Limnology, 3rd Edition. Spon Press, London.

Wendling V. (2011). Hydrodynamique sédimantaire de la retenue de Cointzio (Michoacan, Mexique). Master's thesis.

Wetzel R. G., (2001). Limnology: Lake and River Ecosystems, 3rd Edition, 1006 pp, Academic, San Diego, Calif.

Wüest, A., Lorke, A., (2003). Small - Scale Hydrodynamics in Lakes. Annual Review of Fluid Mechanics. 35: 373–412.

APPENDIX

Appendix 1. Investigation results of priorities of municipalities in Michoacán, Mexico

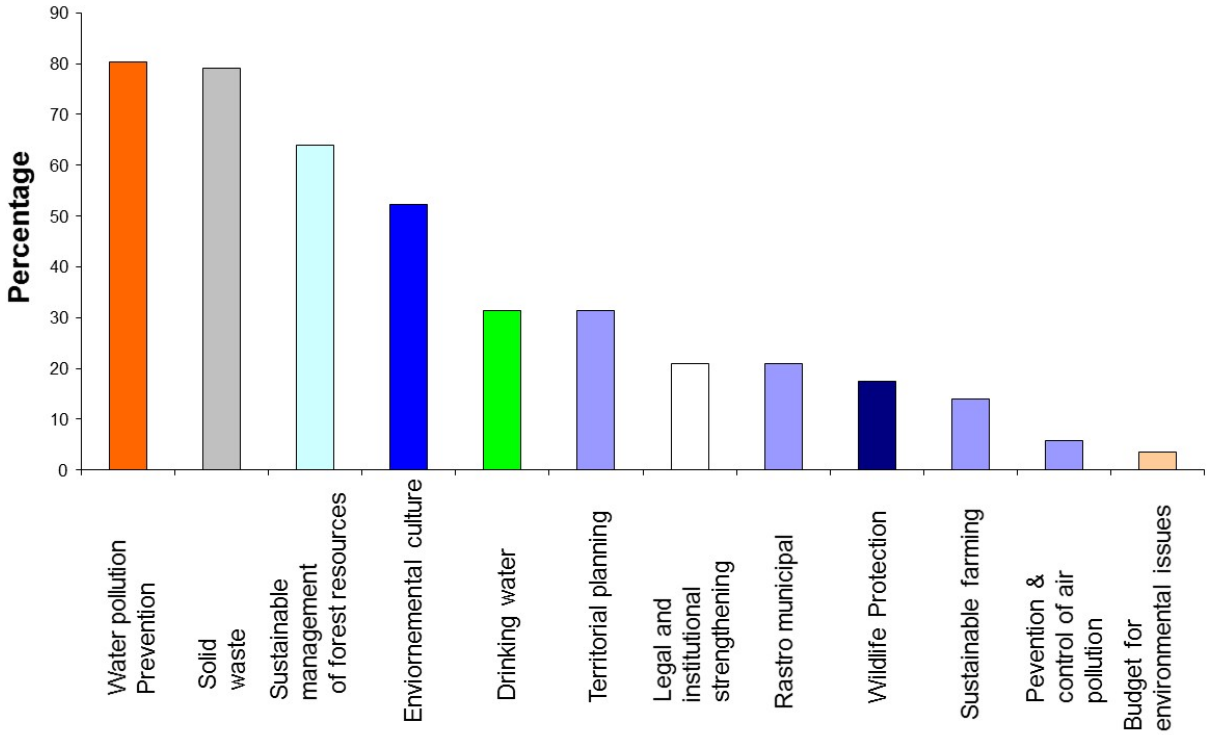

Accoring to the investigation results of municipalities priorities in Michoacán, Mexico, there was up to 80% of the Michoacán's population wishing to prevent water pollution in the Cointzio reservoir.

Appendix 2. Instrumentations and strategy of monitoring data in the Cointzio reservoir

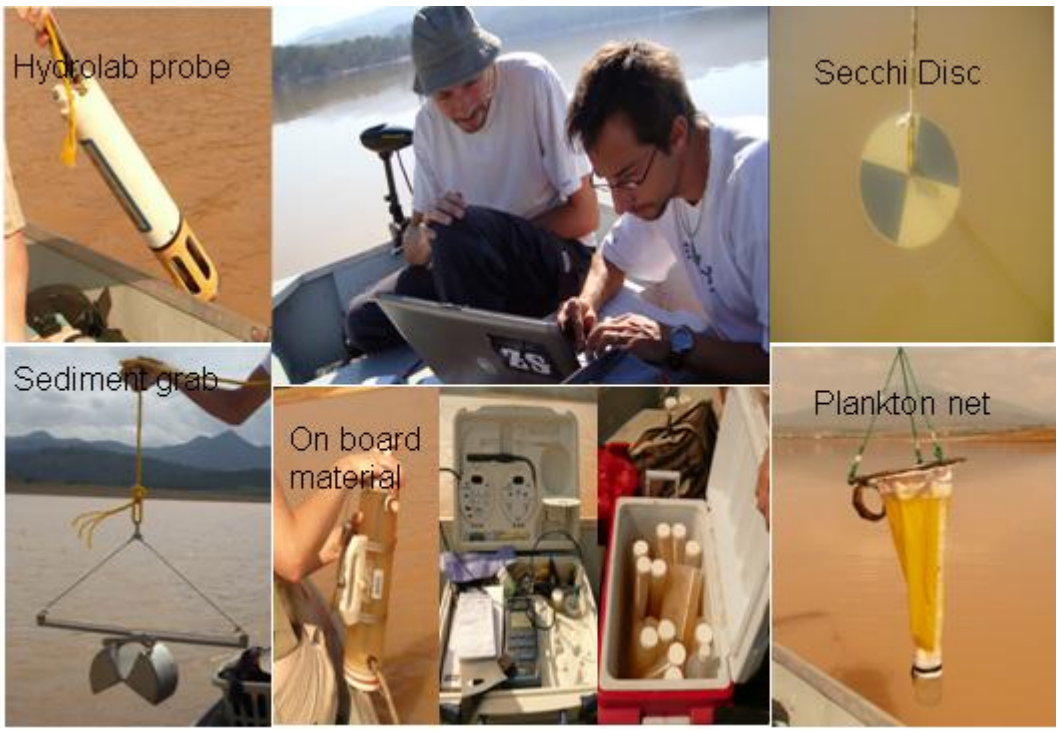

Appendix 3. Interpolated (pink colour) and measured (blue colour) surface temperature in 2009

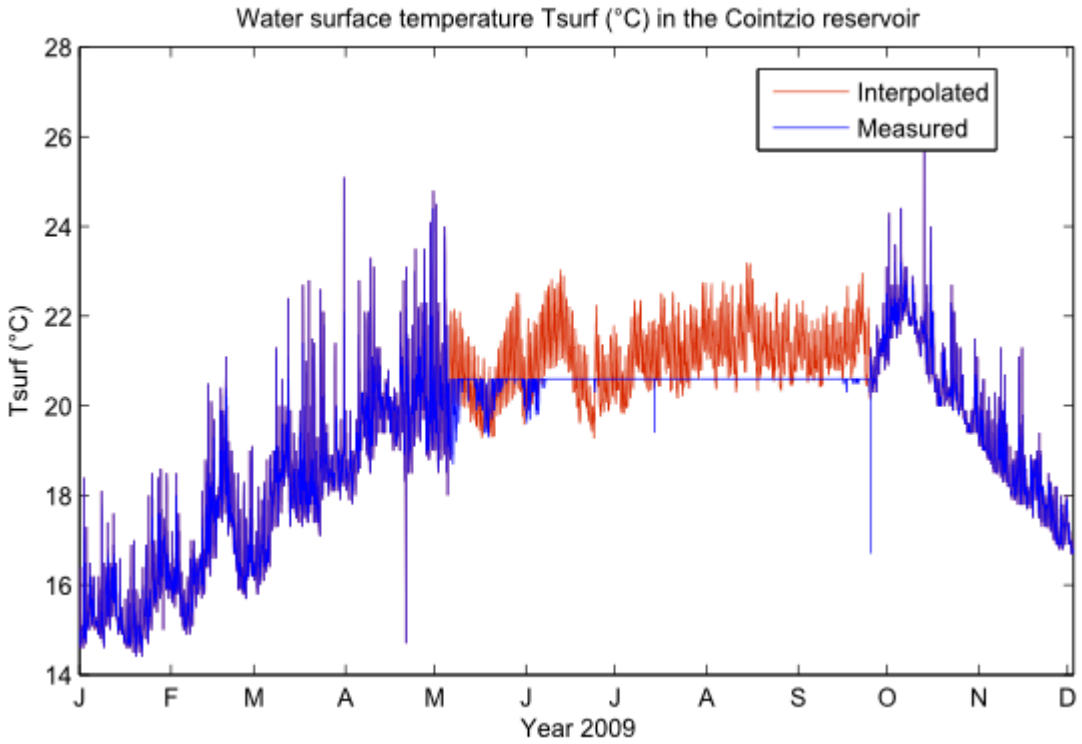

The reservoir surface temperature was estimated from a linear regression to the air temperature time series by the equation: $T_{surf} = 0.52*T_{air}+9.8$, r2=0.84.

Appendix 4. Linear regression between MES (mg L^{-1}) and Turbidity (NTU) from measurements data in the Cointzio reservoir

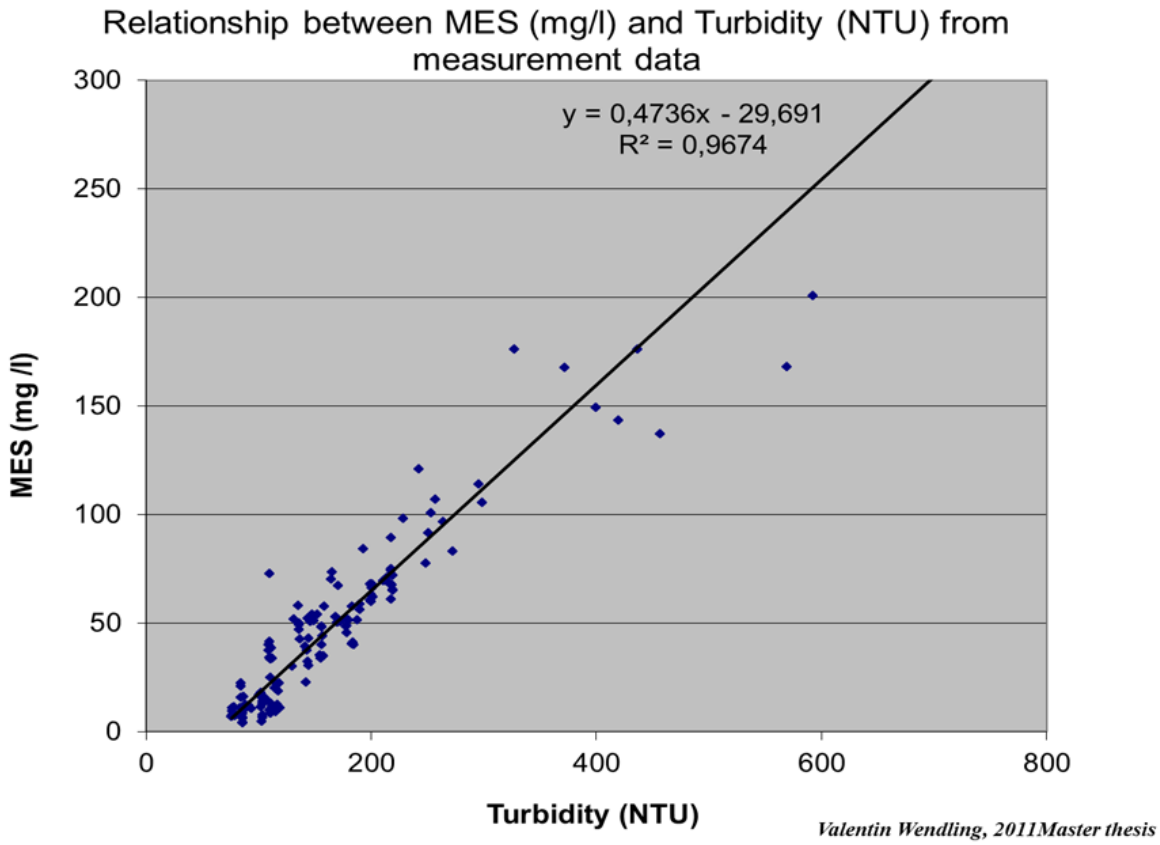

Appendix 5. Regression equations between chlorophyll a (µg L^{-1}) and chlorophyll a (volts)

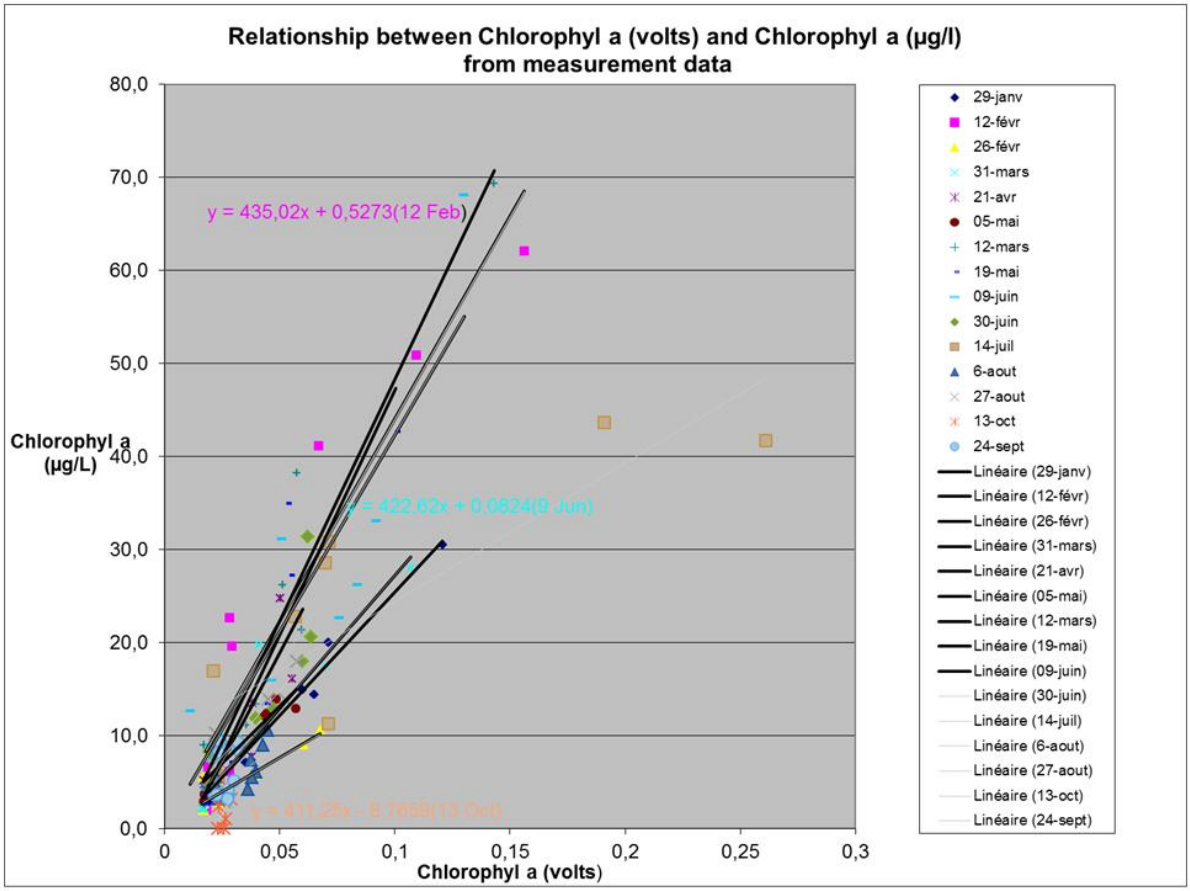

Appendix 6. The ratio between C and chlorophyll a in the Cointzio reservoir

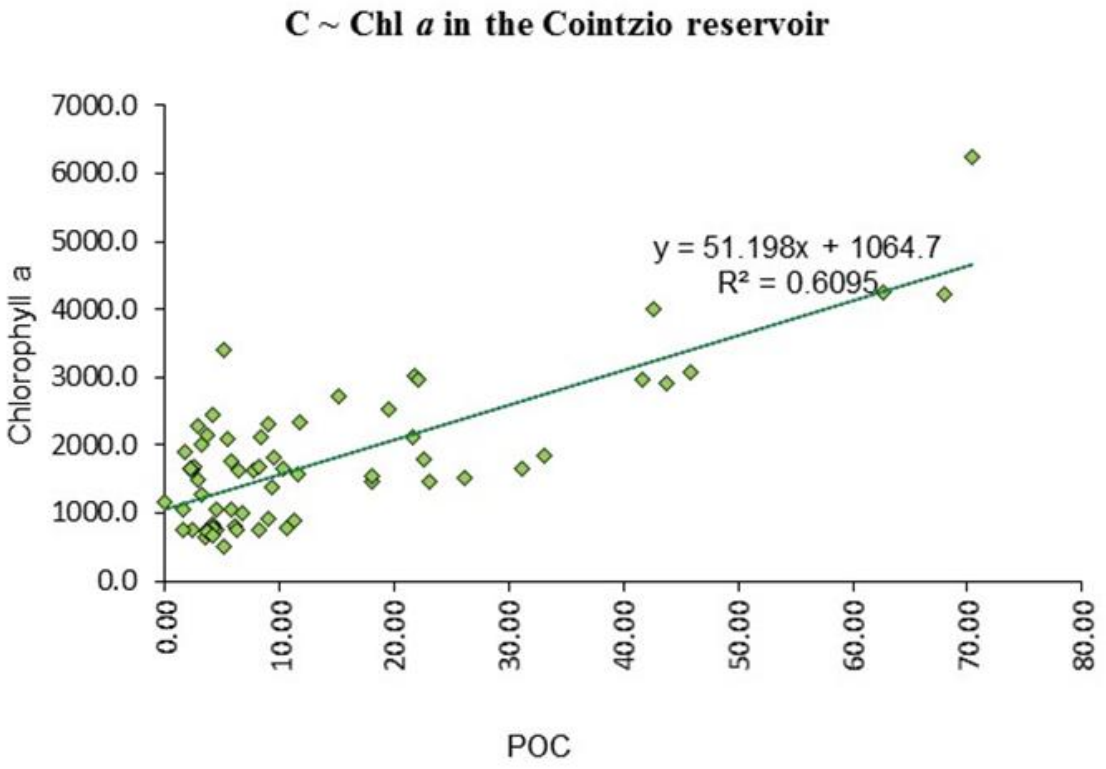

Appendix 7. The resulting time series of vertical turbulent diffusivity obtained from the physical k-epsilon model

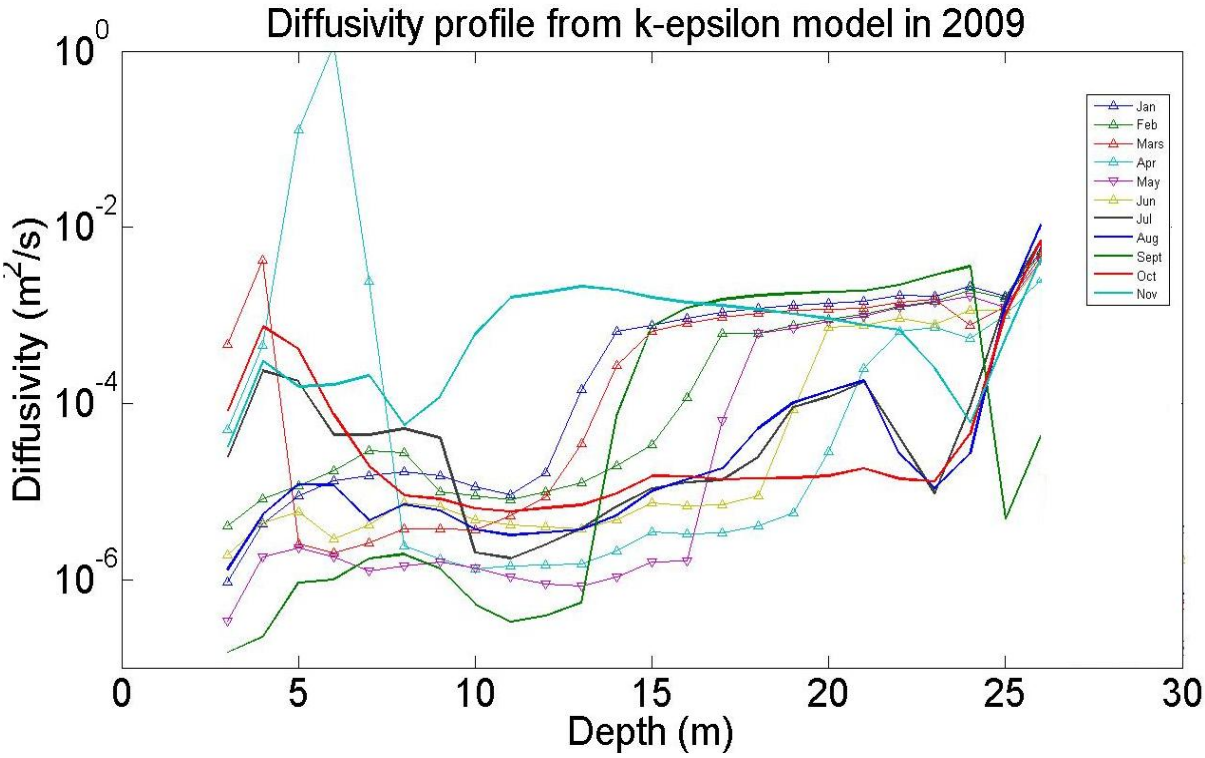

ABSTRACT

The overall water quality of lakes and reservoirs continues to deteriorate in many regions of Mexico. The Cointzio reservoir, located in the southern part of the Mexican Central Plateau on the Trans-Mexican Volcanic Belt (TMVB), is no exception. This turbid tropical reservoir behaves as a warm monomictic water body (area = 6 km^2, capacity 66 Mm^3, residence time ~ 1 year). It is strategic for the drinking water supply of the city of Morelia, capital of the state of Michoacán, and for downstream irrigation during the dry season. The reservoir is threatened by sediments accumulation and nutrients originating from untreated waters in the upstream watershed. The high content of very fine clay particles and the lack of water treatment plants lead to serious episodes of eutrophication (up to 70 µg chl. a L^{-1}), high levels of turbidity (Secchi depth < 30 cm) and seasonal periods of anoxia (from May to October).

Based on intensive field measurements in 2009 (sampling in the watershed, deposited sediment, water vertical profiles, reservoir inflow and outflow) we presented an integrated study of the hydrodynamics and biogeochemical functioning of the Cointzio reservoir. Water column measurements of temperature, TSS, DO, chlorophyll *a*, carbon and nutrients undertaken during the year 2009 were used to assess internal cycling in the reservoir.

To complete field data analyses we examined the ability of some vertical one dimensional (1DV) numerical models (Aquasim biogeochemical model coupled with k-ε mixing model) in order to (i) reproduce the main biogeochemical cycles in the Cointzio reservoir and (ii) assess scenarios of nutrients (P and N) and eutrophication reduction in the coming decades. The k-ε model reproduced nicely the low to moderate temperature stratification which characterizes this turbid reservoir. The Aquasim model was able to reproduce the main patterns of DO, nutrients and chlorophyll *a* during the year 2009. The different simulations pointed out the negative long-term impact of global warming. By the end of the century (2090), an increase of air temperature as high as 4.4°C was predicted from Global Circulation Models. When coupled with a dry hydrological year, this scenario could lead to critical conditions with a severe depletion of DO and important blooms of chlorophyll *a* (up to 94 µg L^{-1}). Various simulations showed that a drastic reduction of nutrients input (by 90%) would be required to significantly reduce chlorophyll *a* concentrations. If such mitigation measures are adopted, the maximum peak of chlorophyll *a* would reduce significantly, from 94 µg L^{-1} to 40 µg L^{-1}after a five-year period of efforts.

To our knowledge, this study provides the first numerical application of k-ε and Aquasim models to simulate high eutrophication levels in a very turbid tropical reservoir.

Keywords: Mexico, tropical reservoirs, eutrophication, turbid, modelling, nutrients mass balance